Quenching H_2O_2 Residuals Using Granular Activated Carbon: Effect of pH and Biodegradation

By

Anmol Ratna Singh

Thesis submitted in conformity with the requirements
for degree of Masters in Applied Sciences (MASc.)

Graduate Department of Civil Engineering
University of Toronto

Quenching H_2O_2 Residuals Using Granular Activated Carbon: Effect of pH and Biodegradation

Anmol Ratna Singh

Master of Applied Science Degree

Department of Civil Engineering

University of Toronto

Abstract

This thesis has two parts:

Part I

Residual H_2O_2, dissolved oxygen and pH data were observed for quenching of H_2O_2 by virgin, 1 year and 2 years old GAC in pilot columns. All GACs completely quenched 4 mg/L of H_2O_2 but not 10 mg/L H_2O_2. Active reaction sites in the columns were concentrated near the top for virgin and middle for aged GAC.

Part II

Pseudo first order reaction constant, k, for H_2O_2 quenching was measured for six different GACs, at three different age levels, in the pH range: 6.50 - 12.50. We observed a marked increase in k values above pH 11.00.

H_2O_2 quenching by sand showed an increase from ~5% to ~10% in k value and from ~3% to ~10% in percentage quenching between week 3 and week 10 of bench scale experiments suggesting that biofilm was able to induce H_2O_2 quenching ability in an otherwise inert media.

Acknowledgements

I would like to thank University of Toronto for providing me this wonderful opportunity to learn about the field of Civil Engineering and complete a M.A.Sc. degree.

I would also like to thank my supervisor Dr. Arash Zamyadi for his continuous guidance throughout my masters program. I would like to express my gratitude to my friends who have always been an encouraging influence during my studies. Lastly I would like to thank my family for their unconditional support and blessings.

Table of Contents

List of Figures

List of Tables

1. Research objectives and organization of chapters

1.1 Objective

The objective of this study was to gain insight about the quenching reaction of H_2O_2 by granular activated carbon (GAC). Ageing of Centaur GAC due to quenching of hydrogen peroxide (H_2O_2) was examined in the first part of the thesis. In the second part of the study, pH dependence of quenching reaction and biofilm formation on GAC and sand media surface was studied.

1.2 Organization of chapters

There are two research chapters in this thesis:

Chapter 2

- Pilot-scale study of service life of GAC on the basis of its ability to quench H_2O_2.
- Lorne Park water treatment plant in Mississauga, Ontario (Canada) has full-scale GAC contactors to periodically quench H_2O_2. These contactors include GAC that are 1 or 2 years old. We collected core samples from the full-scale GAC contactors, inserted them into pilot columns and then spiked them with H_2O_2 to monitor H_2O_2 concentration as a function of depth. To understand ageing of Centaur due to quenching of H_2O_2, we investigated residual H_2O_2 concentration, dissolved oxygen and pH profiles on the basis of depth of GAC in the pilot column and their change with continuously increasing bed volumes of water passing through the pilot columns.

Chapter 3

- Study of kinetic reaction constant k for bench scale setup of six different GACs at six different values of pH. Three types of aged GACs were used in the experiment: virgin, ageing by water matrix containing NOM, and ageing by water matrix containing NOM + H_2O_2 ageing.
- Biofilm growth on the surface of GAC and sand was investigated for a bench scale setup.
- Kinetic reaction constant k, quenched percentage of H_2O_2 and ATP values for biofilm were studied.

2. Assessing service life of GAC using pilot scale testing

2.1 Abstract

Quenching reaction between H_2O_2 and Centaur granular activated carbon (GAC) was examined in a pilot scale setup. 128 cm long glass columns with 4 ports at heights of 25, 50, 75 and 100 cm from the top were used for the experiments. The height of the column was modelled after the depth of the GAC bed contactor at the Lorne Park water treatment plant in Mississauga, Ontario. Residual H_2O_2, dissolved oxygen (DO) and pH data were measured at each port for three types of GAC: virgin, 1 year, and 2 years old. Two inlet H_2O_2 concentrations of 4 mg/L and 10 mg/L were used. The experiment was conducted continuously for 7 days. One set of observations was taken every day, with each day equivalent to ~350 bed volumes.

Virgin GAC was seen to be better at quenching H_2O_2 than aged GAC. Neither virgin GAC nor aged GAC were able to completely quench 10 mg/L H_2O_2, however, both were able to completely quench 4 mg/L of H_2O_2. pH and DO proved that active reaction sites were concentrated near the top and middle of the column for virgin GAC. Similar reactive sites continued until the lower end of the column for aged GAC proving that reaction sites at the top had been eliminated.

2.2 Introduction

The Lorne Park drinking water treatment plant in the region of Peel provides drinking water to the adjoining population of Mississauga (Ontario, Canada). It employs granular activated carbon contactors (GACCs) to quench excess H_2O_2 residuals after advanced oxidation process involving UV irradiation. The advanced oxidation process is a part of its treatment train to prevent the occurrence of taste and odor compounds in tap water. Quenching of H_2O_2 by GACC is the last treatment process before chlorination therefore it is very important that the process achieves its goals definitively. In case of inadequate quenching of H_2O_2 by GACC, H_2O_2 being an oxidizing agent will react with chlorine. It is important to understand that it is mandated by law to have a specific amount of chlorine in the treated water reaching the public. In the backdrop of these circumstances, quenching of H_2O_2 by GAC assumes importance in the overall treatment train of drinking water treatment plants.

GAC has been known to act as a catalyst in the decomposition of H_2O_2 (Khalil et al., 2001) and has been used in a number of drinking water treatment plants due to its ability to quench H_2O_2 (Cotton et al.., 2010). Two major theories have been put forward for quenching mechanism of hydrogen peroxide by GAC (Kurniawan et al., 2009 and Bach et al., 2011). The hypothesis by Kurniawan et al. (2009) is given as follows:

$$AC + H_2O_2 \rightarrow AC^+ + OH^- + \bullet OH \qquad \textbf{Equation 1. 1}$$

$$AC^+ \rightarrow AC + H^+ + \bullet OOH \qquad \textbf{Equation 1. 2}$$

The •OOH and •OH would combine to give H_2O and O_2 thus completing the decomposition process. The second hypothesis by Bach et al. (2011) is given as follows:

$$H_2O_2 \rightleftharpoons H^+ + HO_2^- \quad (pK_a = 11.75) \qquad \textbf{Equation 1. 3}$$

$$AC - OH + H^+HO_2^- \rightarrow AC - OOH + H_2O \qquad \textbf{Equation 1. 4}$$

$$AC - OOH + H_2O_2 \rightarrow AC - OH + O_2 + H_2O \qquad \textbf{Equation 1. 5}$$

We can observe that both the mechanisms involve use of H^+ ion and formation of oxygen gas.

Despite the use of GACCs in treatment plant operations, factors affecting service life of GACCs are mostly unknown. Taking into consideration the reaction mechanism and energetics of decomposition of H_2O_2 we decided to investigate hydrogen peroxide quenching by GAC by analyzing the following three reaction parameters in a pilot scale experimental setup:

- Residual H_2O_2 concentration in reacting water
- Dissolved oxygen in reacting water aliquots and its comparison with dissolved oxygen of water (containing H_2O_2) entering the system
- pH of reacting water aliquots and its comparison with pH of water (containing H_2O_2) entering the system.

2.3 Materials and methods

2.3.1 Pilot-scale setup of columns

The pilot scale setup at Lorne park drinking water treatment plant consisted of three vertical glass columns. Height of columns was 128 cm, as the columns were modeled after full-scale GAC media contactors which had a depth of 128 cm. Each of the three columns had a different age of Centaur GAC – virgin, one year and two years in operation. GAC from respective contactors containing one and two year old GAC was removed from the contactors and transferred into columns using a Wilson sampler. The sampler allows removal of GAC from the contactor while maintaining its properties based on stratification. Lorne park GAC contactors have an empty bed contact time of 4.12 minutes. To keep our results as similar to the existing facility as possible, we used an EBCT of 4.12 minutes for our columns experiments. Besides inlet and outlet, each column had four ports for sampling at depths of 25cm, 50 cm, 75 cm and 100 cm. Inflowing water into the columns consisted of ultra-filter membrane permeate, while the waste was allowed to flow into a waste tank at the plant.

2.3.2 Description of quenching, dissolved oxygen and pH profile

There were two tests conducted on three different kinds of GACs – virgin, operationally active for one and operationally active for two years. The general procedure was to measure different GAC parameters at two different concentrations of H_2O_2 – 4 mg/L and 10 mg/L. This concentration of H_2O_2 was added to the water from membrane permeate tanks of the drinking water treatment plant at Lorne Park. Measured GAC parameters include residual H_2O_2 concentration in the column as a function of depth, dissolved oxygen in the GAC column as a function of depth and pH in the column as a function of depth. Depth profiles for these parameters were observed using outflow from the four ports and also from the inlet and outlet points. Water was allowed to flow continuously with one observation taken every day at a fixed time over a course of 7 days. This allowed us to compile data at seven different bed volumes, with one day being an equivalent of roughly 350 bed volumes of water.

Measurement of H_2O_2 residuals was done using the ferric thiocyanate method (Wells, 1984). The method involves use of ammonium thiocyanate + ferrous ion solution in vacu-vials. When these vacu-vials are exposed to H_2O_2 solution, ferrous oxidizes to ferric combining with thiocyanate to form coloured ferric thiocyanate as shown below:

$$\mathbf{2}\,[\boldsymbol{NH^{4+}}\,\boldsymbol{S^{-}-C\equiv N}] \rightleftharpoons\ \mathbf{2}\,\boldsymbol{NH_3}+\mathbf{2}\,\boldsymbol{H^{+}(aq)}+\mathbf{2}\,[\boldsymbol{S^{-}-C\equiv N}] \qquad \textbf{Equation 1. 6}$$

$$\mathbf{2}\,\boldsymbol{Fe^{2+}}+\ \boldsymbol{H_2O_2}+\mathbf{2}\,\boldsymbol{H^{+}(aq)}\ \rightarrow \mathbf{2}\,\boldsymbol{Fe^{3+}}+\mathbf{2}\,\boldsymbol{H_2O} \qquad \textbf{Equation 1. 7}$$

$$\boldsymbol{Fe^{3+}}+\ \mathbf{6}\,[\boldsymbol{S^{-}-C\equiv N}]\rightarrow[\boldsymbol{Fe(SCN)_6}]^{\boldsymbol{3-}}\ (\boldsymbol{Red\ coloured}) \qquad \textbf{Equation 1. 8}$$

Absorbance of ferric thiocyanate at a wavelength of 470 nm is proportional to the concentration of H_2O_2 in solution.

The formula used was:

$$\boldsymbol{H_2O_2\left(in\ \frac{mg}{L}\right) = 4.39\ \times Abs.(at\ 470\ nm) - 0.03} \qquad \textbf{Equation 1. 9}$$

On partially breaking the nib of the vacu-vial solution in a solution, liquid gets drawn into the vacu-vial due to suction. Colourless ammonium ferro-thiocyanate solution inside the vacu-vials converts into red coloured ferric thiocyanate if H_2O_2 is present in the tested solution. Absorbance of this red coloured ferric thiocyanate at 470 nm on a spectrophotometer gives us the concentration of H_2O_2. We used a mobile spectrophotometer for our analysis.

Measurement of dissolved oxygen was done using electrochemical dissolved oxygen sensing technique (American Public Health Association 1998) using a dissolved oxygen probe. pH was measured using a standard pH meter.

2.4 Results and discussion

2.4.1 Effect of column height on H_2O_2 quenching by GAC

H_2O_2 quenching by virgin, 1 and 2 year old GAC for inlet H_2O_2 = 4 mg/L and 10 mg/L is shown in Figure 1 and Figure 2 respectively

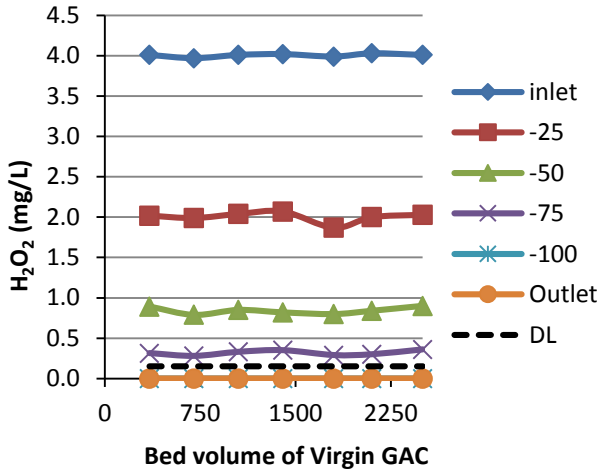

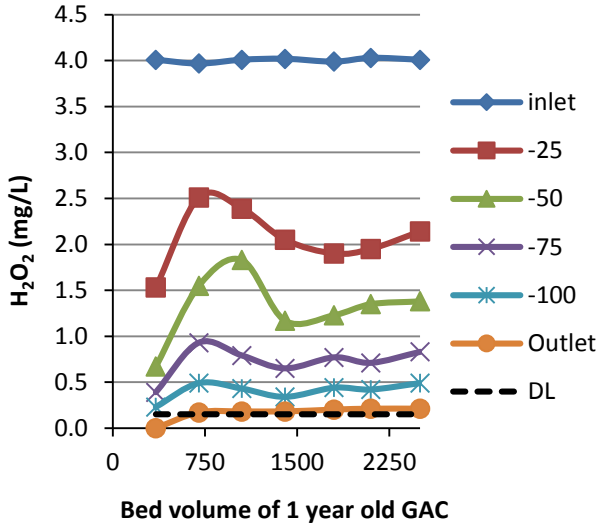

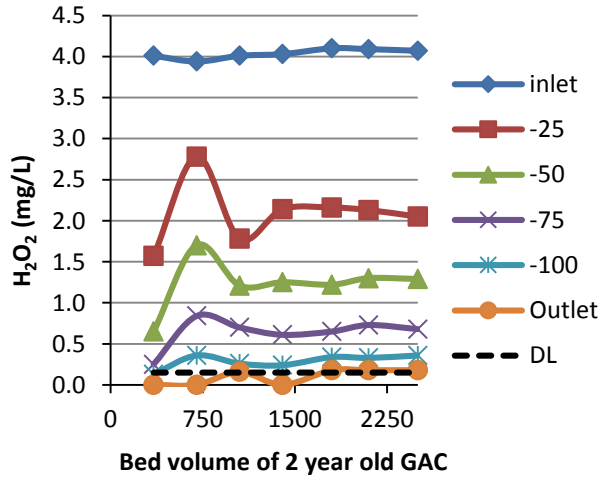

Figure 1: H_2O_2 quenching by virgin, 1 and 2 year old GAC. Inlet H_2O_2 = 4 mg/L

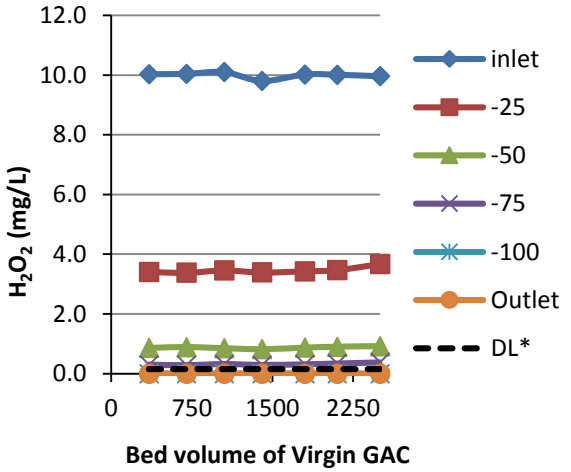

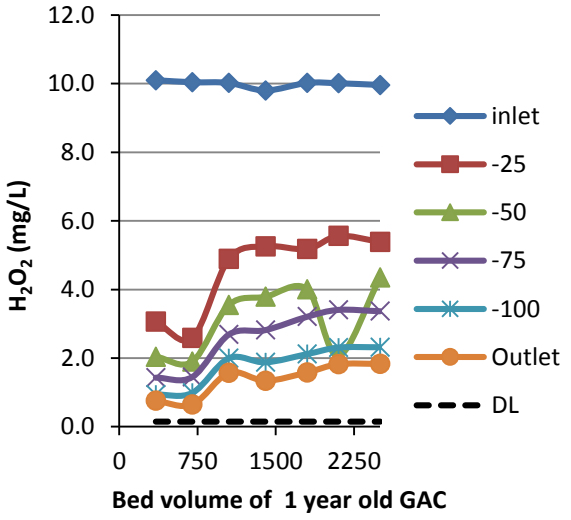

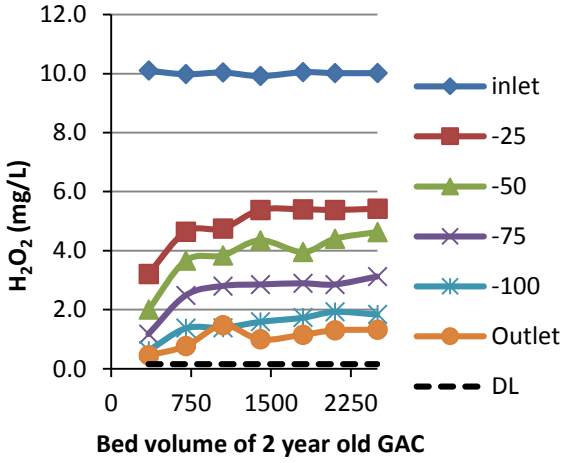

Figure 2: H_2O_2 quenching by virgin, 1 and 2 year old GAC. Inlet H_2O_2 = 10 mg/L

DL in Figure 1and Figure 2 denotes detection limit. The trend lines for GACs with inlet = 4 mg/L of H_2O_2 showed very consistent behavior where amount of H_2O_2 left at 25 cm < 50 cm < 75 cm < outlet. This was expected as H_2O_2 would be quenched more with increasing depth of the column. We were able to observe a peak formation at around 750 bed volumes region of the graph for the outlets at depth of 25 cm and 50 cm. We also observed that the peak became more prominent as we moved from virgin to one year old to two year old GAC. The decreasing quenching ability of GAC between 0 and 750 bed volumes, which is the crest of the peak, points to the fact that the GAC media near the top of the column was exhausted with usage and became less capable of quenching H_2O_2. The rising quenching ability of the GAC between 750 and 1000 bed volumes, which is the trough of the peak, could point to the onset of biofilm growth on the GAC. However, since biological activity was not measured in the GACs, we are not in a position to make a conclusive statement on the growth of biofilm here. The observation may even indicate a measurement error.

Trend lines for GACs with inlet = 10 mg/L H_2O_2 also show very consistent patterns. Again, concentration of H_2O_2 can be seen to decrease continuously with increasing depth of GAC media. The climbing graphs in one and two year old GAC prove that H_2O_2 quenching ability of GAC decreases with time. Another important observation for one and two year old GACs is that the final H_2O_2 concentration at the outlet is not very close to 0 but close to 2 mg/L. This proves that old GACs may not be adequate to quench H_2O_2 residuals from advanced oxidation processes if applied H_2O_2 concentrations happen to be as high as 10 mg/L. However, lower H_2O_2 concentrations of 4 mg/L can be easily handled by GAC which is operationally even two years old.

On comparing the 4 mg/L and 10 mg/L graphs we observed that GAC quenching 10 mg/L of H_2O_2 had higher concentration of H_2O_2 at all ports as compared to the values obtained at similar ports for GAC quenching 4 mg/L H_2O_2.

It is visible that quenching ability of virgin GAC is much more than that of 1 year and 2 year old GAC. It is noteworthy that 1 and 2 year old GAC have very similar quenching ability. In order to reach H_2O_2 concentration of 0.5 mg/L down from 4 mg/L at inlet, virgin GAC requires somewhere between 50 – 75 cm of GAC bed depth while 1 and 2 year old GACs require somewhere between 75 – 100 cm of GAC bed depth.

2.4.2 Effect of column height on dissolved oxygen profile of H_2O_2 quenching by GAC

The DO profile for virgin, 1 and 2 year old GAC for inlet H_2O_2 = 4 mg/L and 10 mg/L is shown in Figure 3 and Figure 4 respectively.

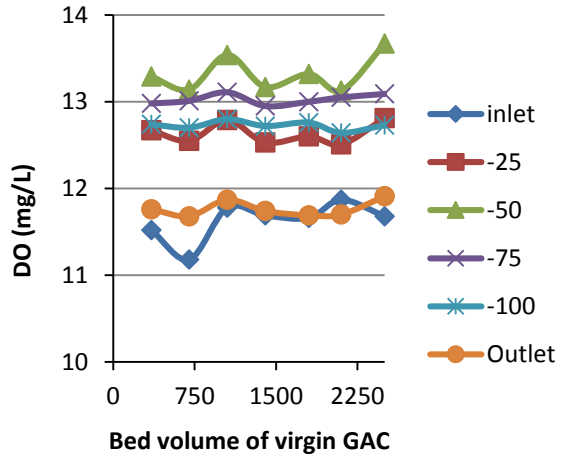

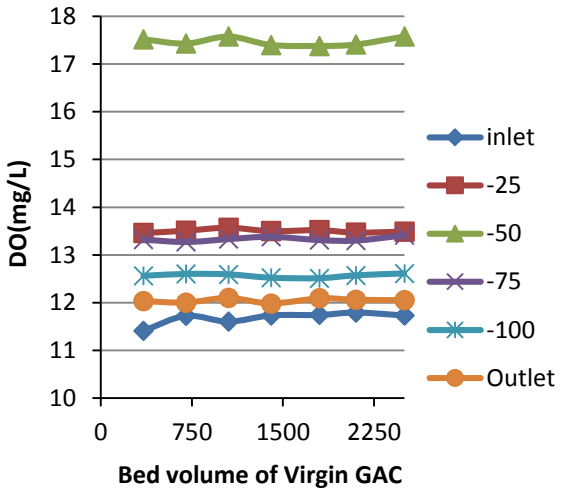

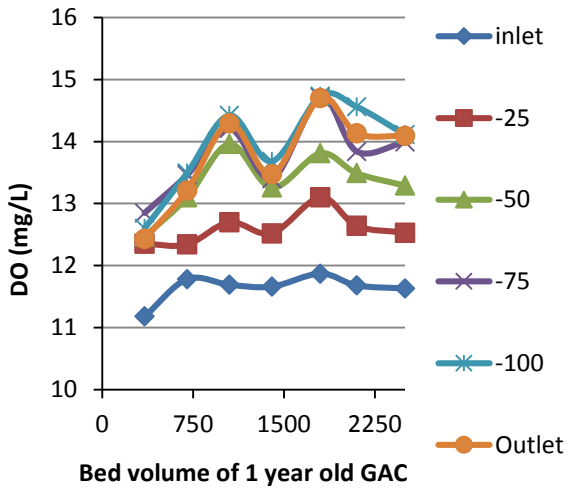

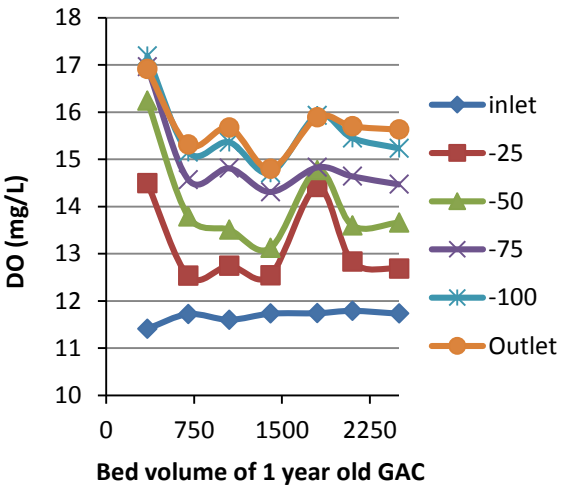

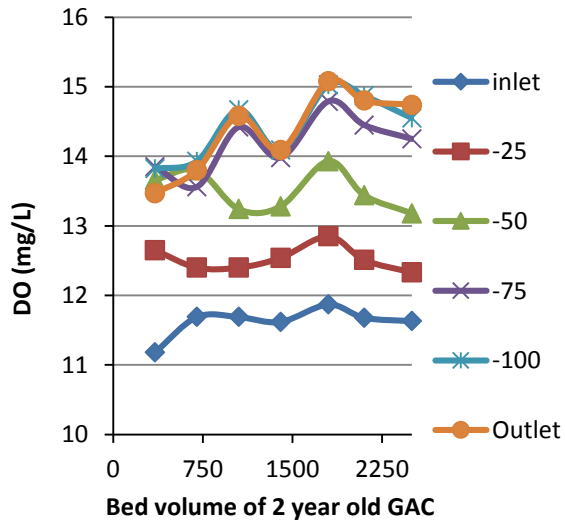

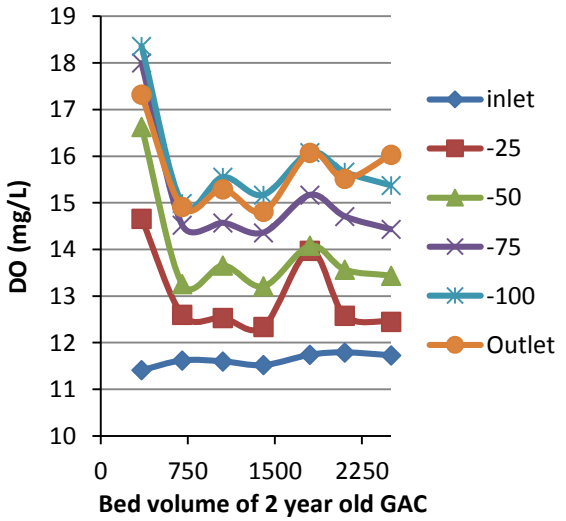

Figure 3: DO profile for virgin, 1 and 2 year old GAC. Inlet H_2O_2 = 4 mg/L

Figure 4: DO profile for virgin, 1 and 2 year old GAC. Inlet H_2O_2 = 10 mg/L

Figure 3 and Figure 4 show dissolved oxygen (DO) values obtained at the outlet ports of the columns containing GAC. As oxygen is a by-product of H_2O_2 quenching, it is an indirect measure of quenching activity. The DO probe used in our experiment was capable of measuring oxygen bubbles only qualitatively. However, oxygen dissolved in water was measured quantitatively. The saturation concentration of oxygen at 10^oC, which was the temperature while conducting the experiment, is 11.27 mg/L. As all values in Figure 3 and Figure 4 are above 11.27, they point to the presence of oxygen bubbles.

In case of inlet H_2O_2 = 4 mg/L we saw that one year old GAC and two year old GAC trends were similar, however, they were different as compared to the trends in virgin GAC graph. The basic difference was that in virgin GAC we see high DO levels around the top of the column while in old GACs we saw high DO levels around the bottom of the column. This observation points to the fact that as GAC ages, the sites of quenching reaction shift to the more reactive depths of the GAC volume.

In case of H_2O_2 = 10 mg/L we saw very similar trends as those in case of inlet H_2O_2 = 4 mg/L. The observation of quenching reaction moving to deeper active sites of GAC held true for inlet H_2O_2 = 10 mg/L as well. We observed very high DO values during the first few bed volumes for all ports of the columns. This was because when a high concentration of H_2O_2 was made to come into contact with the GAC it was actively quenched by the reactive sites. However as the reactive sites got spent, intensity of reaction decreased. This resulted in a decrease of the observed DO levels.

When we compared observations with inlet H_2O_2 = 4 mg/L with the observations for inlet H_2O_2 = 10 mg/L we were able to observe few differences. Firstly, the variability for DO levels observed for inlet H_2O_2 = 4 mg/L case was much lower than in case of inlet H_2O_2 = 10 mg/L. Secondly, the DO levels at all ports were substantially higher for inlet H_2O_2 = 10 mg/L case as more H_2O_2 requires more quenching, hence higher observed DO levels. Lastly, the DO levels were seen to be highest for the first few bed volumes for GAC with inlet H_2O_2 = 10 mg/L, while, for GAC with inlet H_2O_2 = 4 mg/L similar DO levels were lowest. This could point towards growing biofilm. With increasing biofilm the intensity of quenching reaction would increase resulting in higher DO levels. However, lack of growth of biofilm would result in continuously decreasing DO levels with increasing bed volumes. As no formal testing of the presence of biofilm was done, we cannot be certain about the reason for maxima and minima of individual trend lines.

2.4.3 Effect of column height on pH profile of H_2O_2 quenching by GAC

pH profile for virgin, 1 and 2 year old GAC for nlet H_2O_2 = 4 mg/L and 10 mg/L is shown in Figure 5 and Figure 6 respectively.

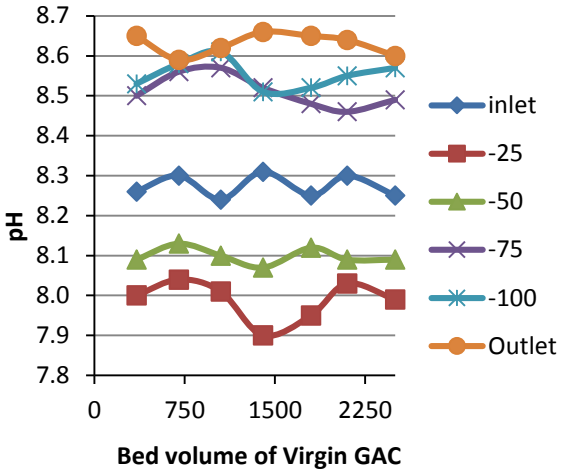

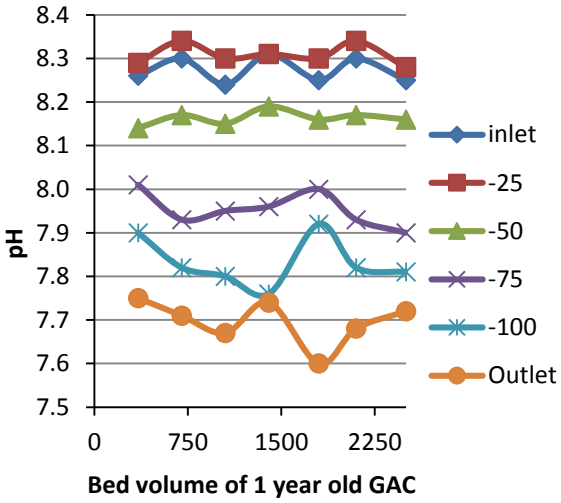

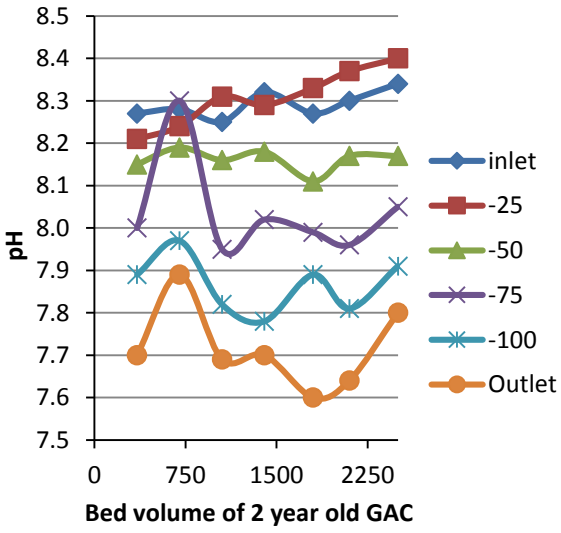

Figure 5: pH profile for virgin, 1 and 2 year old GAC. Inlet H_2O_2 = 4 mg/L

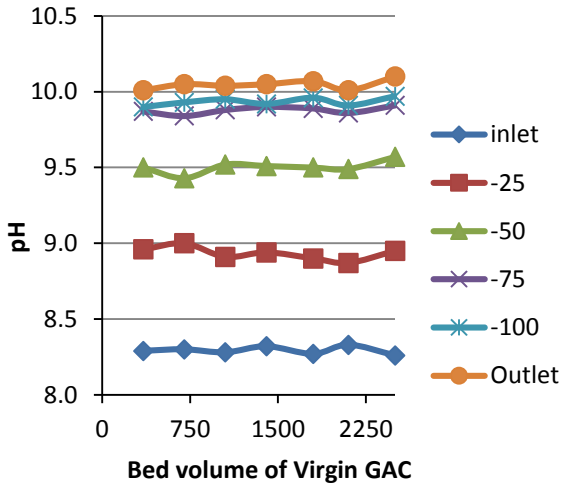

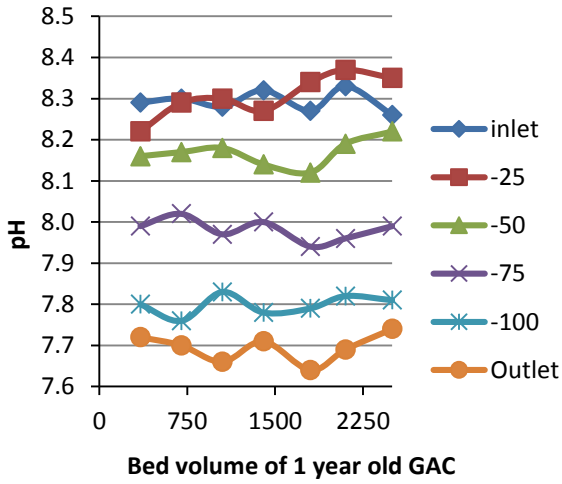

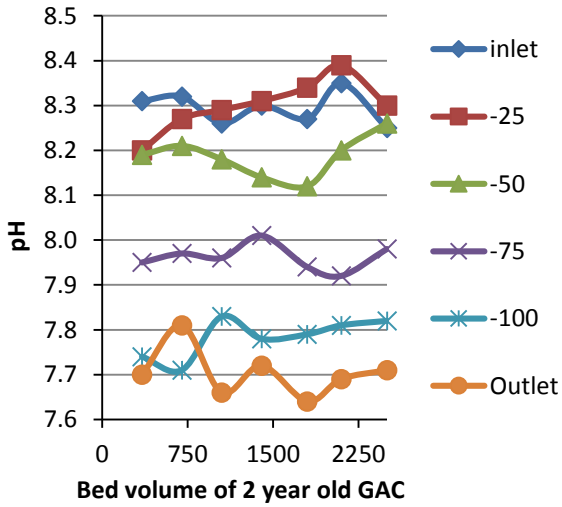

Figure 6: pH profile for virgin, 1 and 2 year old GAC. Inlet H_2O_2 = 10 mg/L

Figure 5 depicts pH trends in virgin, 1 year old and 2 year old GAC with inlet H_2O_2 = 4 mg/L. Our observations on the study of pH pointed towards a shift in trend lines as we moved from virgin GAC to aged GAC. The virgin GAC pH trend lines showed lowest pH values for aliquots taken at ports around the top of the column. While the aged GAC pH trend lines show lowest pH values for aliquots taken at the lower end of the column. The reaction of H_2O_2 with GAC results in release of H^+ ions, therefore more active site of quenching reaction tend to have the lower pH. With this information, we can clearly state that the observations in Figure 5 point to the fact that with increasing age of GAC the actual site of quenching reaction moves towards more reactive sites in GAC which occur at increasingly greater depths with the passage of time.

Figure 6 depicts pH trends in virgin, 1 year old and 2 year old GAC with inlet H_2O_2 = 10 mg/L. All the trends for inlet H_2O_2 = 4 mg/L hold true for inlet H_2O_2 = 10 mg/L case too. An important observation in the inlet H_2O_2 = 10 mg/L case is that the graph for virgin GAC exhibits remarkably high pH values. This observation points to low intensity of quenching reaction for virgin GAC at all port depths as quenching of H_2O_2 on the surface of GAC results in release of H^+ ion. A probable explanation for this observation could be that the reaction intensity was highest somewhere between inlet and the first port at a depth of 25 cm. However, as there were no observations made before the inlet and the first port at 25 cm, it is hard to zero in on the exact cause behind this behavior of virgin GAC.

A comparison of respective pH values for inlet H_2O_2 = 4 mg/L case and inlet H_2O_2 = 10 mg/L case pointed to the difference in pH trends of virgin GAC. Virgin GAC in case of inlet H_2O_2 = 10 mg/L showed markedly higher values when compared with inlet H_2O_2 = 4 mg/L. The reason for this observation could be attributed to the high intensity of quenching reaction between inlet and the first port. However, as the first port of observation was at 25 cm, we cannot say anything conclusively about this observation.

2.4.4 Comparison of quenched H_2O_2 between virgin, 1 and 2 years (operationally) old GAC

A comparison of H_2O_2 quenching between virgin, 1 year old and 2 year old GAC with inlet H_2O_2 = 4 mg/L and 10 mg/L can be seen in Figure 7 and Figure 8 respectively.

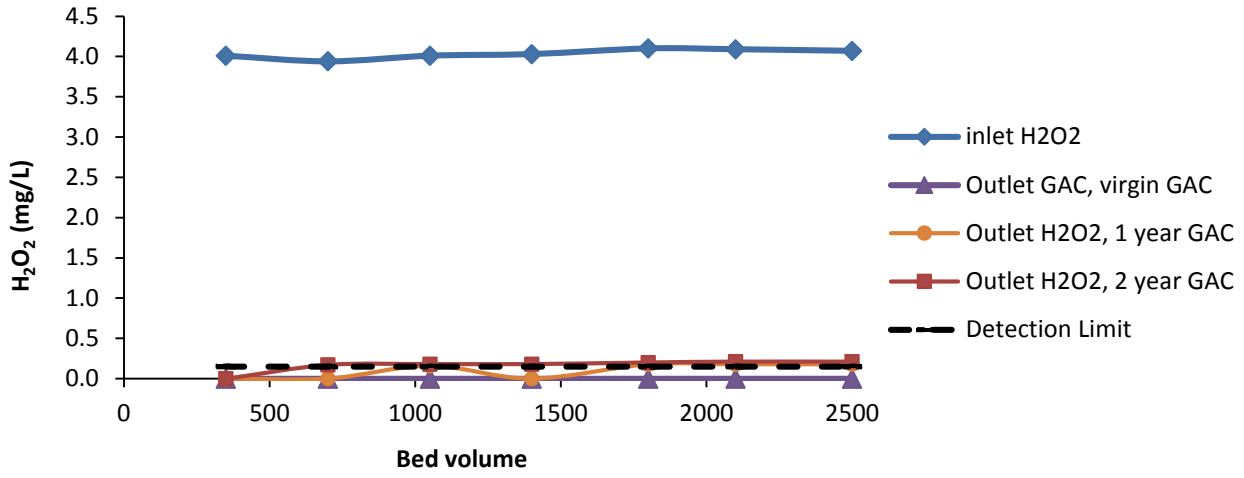

Figure 7: Comparison of H_2O_2 quenching between virgin, 1 year old and 2 year old GAC with inlet H_2O_2 = 4 mg/L

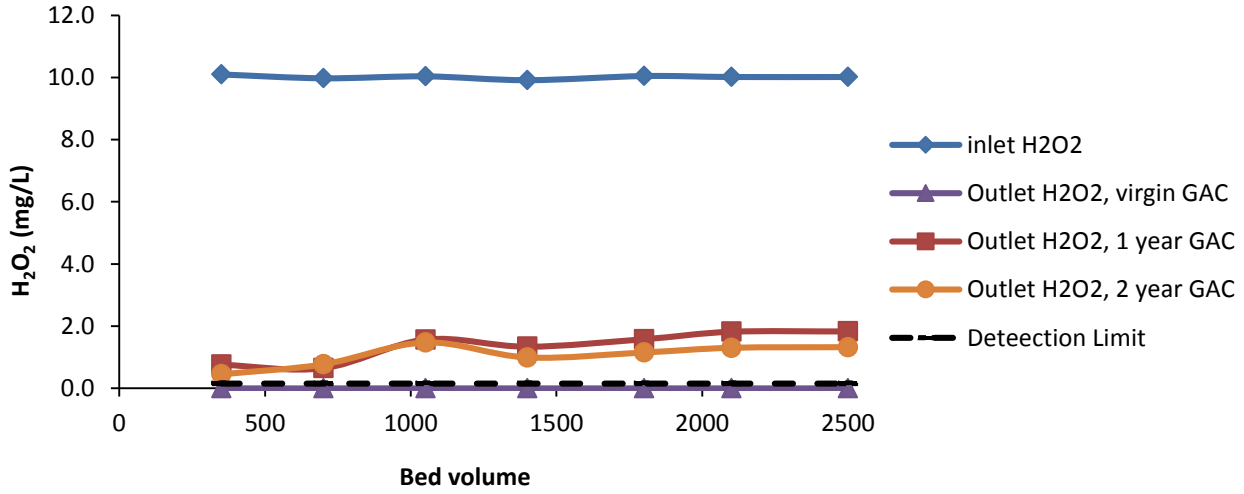

Figure 8: Comparison of H_2O_2 quenching between virgin, 1 year old and 2 year old GAC with inlet H_2O_2 = 10 mg/L

Trend lines of outlet port H_2O_2 concentration for virgin and aged GAC were different for the case where inlet H_2O_2 was 10 mg/L (Figure 8). Aged GAC was not able to fully quench H_2O_2 with H_2O_2 residuals remaining around 2 mg/L for higher bed volumes. This proves that quenching capacity of GAC decreases with time.

There was a marked similarity between trend lines of GAC aged by one year and GAC aged for two years. Both the graphs followed each other very closely.

2.4.5 Comparison of dissolved oxygen for H_2O_2 quenching by GAC between virgin, 1 and 2 years (operationally) old GAC

A comparison of dissolved oxygen at outlet between virgin, 1 year old and 2 year old GAC with inlet H_2O_2 = 4 mg/L and 10 mg/L is shown in Figure 9 and Figure 10 respectively.

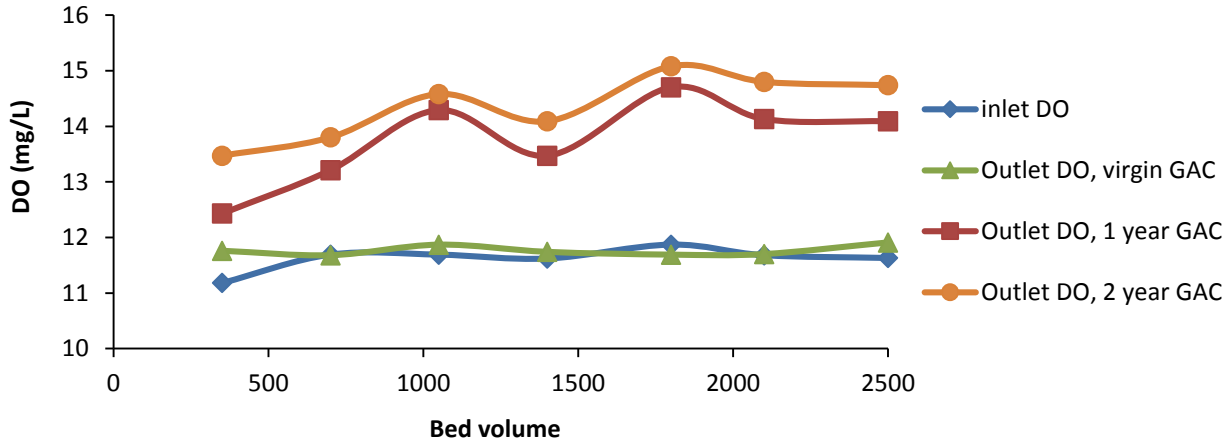

Figure 9: Comparison of dissolved oxygen at outlet between virgin, 1 year old and 2 year old GAC with inlet H_2O_2 = 4 mg/L

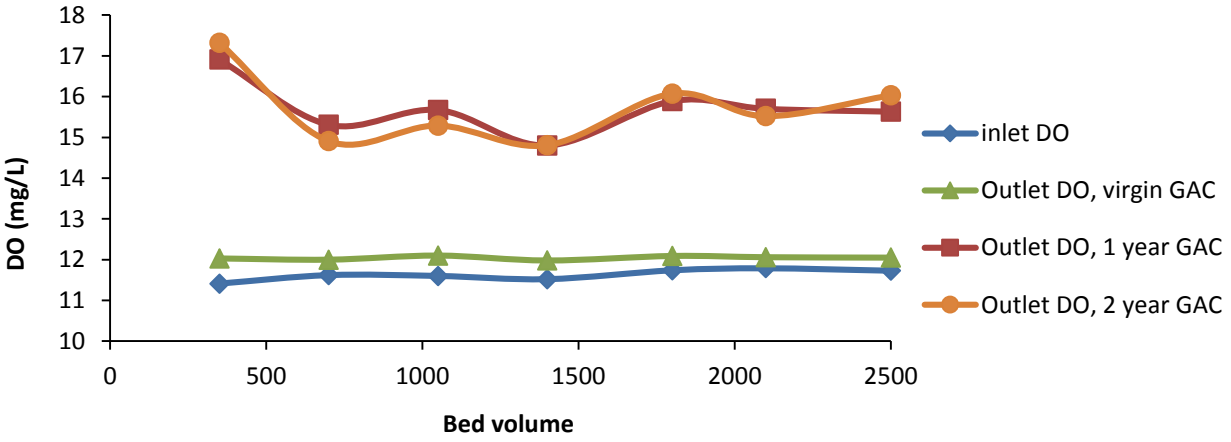

Figure 10: Comparison of dissolved oxygen at outlet between virgin, 1 year old and 2 year old GAC with inlet H_2O_2 = 10 mg/L

Trend lines for dissolved oxygen levels at outlet port for virgin, 1 year and 2 year old GAC for inlet H_2O_2 concentrations = 4 mg/L and 10 mg/L were observed (Figure 9 and Figure 10). Behavior of 1 year aged and 2 year aged GAC was very similar for both inlet H_2O_2 concentrations. However, behaviour of virgin GAC was starkly different when compared with 1 year and 2 year old GAC. Virgin GAC exhibited a lower concentration of DO, very similar to inlet DO concentration, at the outlet indicating that the major reaction sites for quenching exist in

the initial depths of GAC for virgin GAC. This observation points to the fact that deeper portions of the GAC get involved in quenching as the surface reaction sites of ageing GAC get spent.

2.4.6 Comparison of pH for H_2O_2 quenching by GAC between virgin, 1 and 2 years (operationally) old GAC

Comparison of pH at outlet between virgin, 1 year old and 2 year old GAC with inlet H_2O_2 = 4 mg/L and 10 mg/L is shown in Figure 11 and Figure 12 respectively.

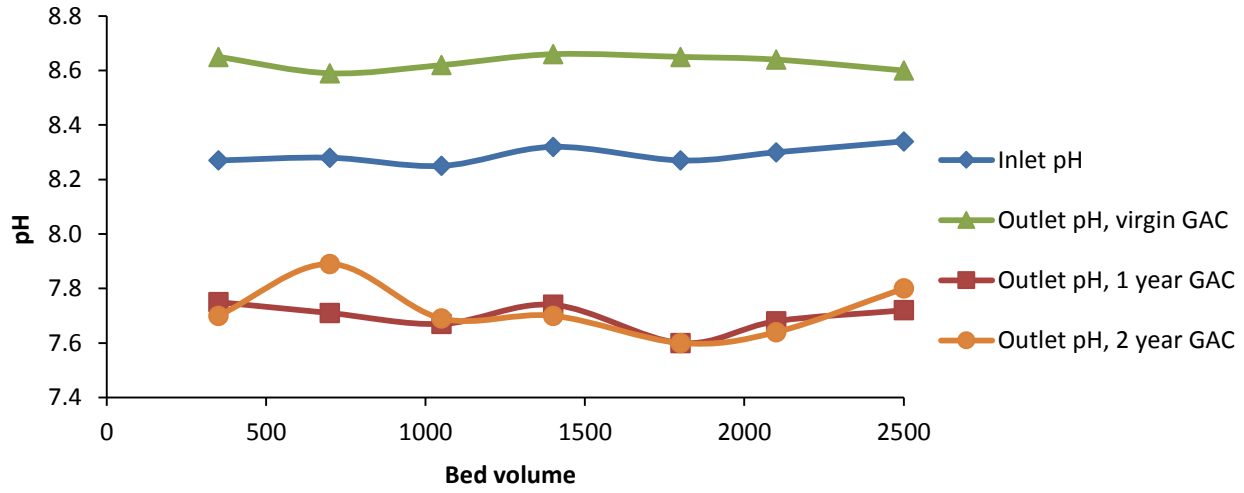

Figure 11: Comparison of pH at outlet between virgin, 1 year old and 2 year old GAC with inlet H_2O_2 = 4 mg/L

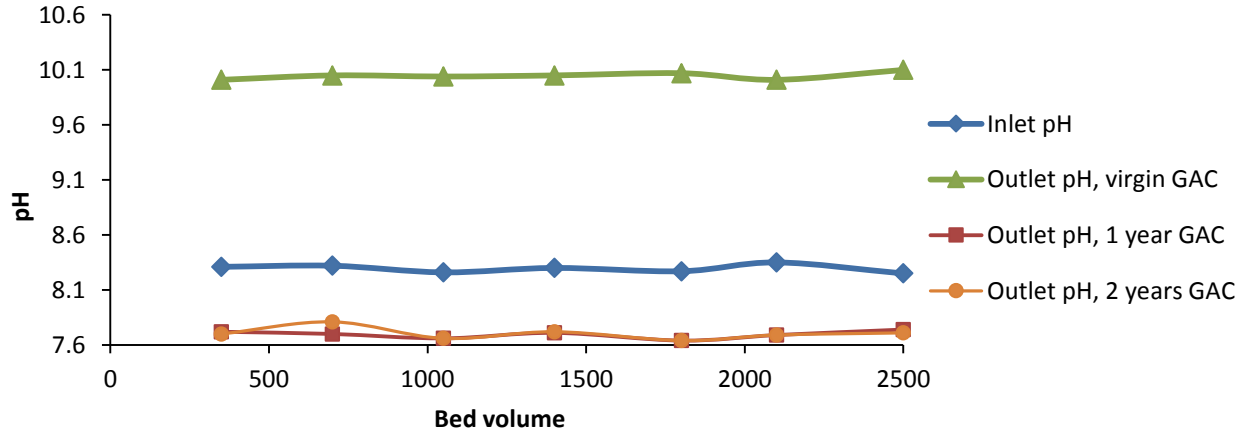

Figure 12: Comparison of pH at outlet between virgin, 1 year old and 2 year old GAC with inlet H_2O_2 = 10 mg/L

Graphs of pH profile at outlet port for virgin, 1 year old and 2 year old GAC exhibited uniform behavior except for virgin GAC with 10 mg/L as inlet H_2O_2 concentration. Aged GAC showed lower pH values than pH at inlet or pH for virgin GAC. This proves that H_2O_2 was quenched actively near the outlet port in case of aged GAC as quenching reaction results in production of H^+ ion. Higher pH values at outlet port in case virgin GAC denote lack of quenching activity near the outlet region. This proves that in case of virgin GAC most of the quenching happens near the top the column or the top surface of a GAC contact bed.

2.5 Conclusion and recommendations for future work

The experiments performed on GAC centaur in pilot columns setup in Lorne Park drinking water treatment plant unambiguously point to the fact that virgin GAC was better at quenching H_2O_2 residuals as compared to one year and two year old GAC. Results for virgin GAC were quite different from aged GACs, however, the two forms of aged GACs – one year old and two year old showed surprisingly similar trends in all aspects of measured quenching reaction parameters viz. residual H_2O_2 concentration, dissolved oxygen (DO) concentration and pH value. In case of virgin GAC, reaction sites were concentrated towards the top portion of the column. While, data from one and two year old GAC points to more reaction sites in the middle and the lower portion of the column as most of the reaction sites at the top had been spent with age. The column was analogous to a GAC bed contactor with top portion of the column signifying the exposed top surface of the GAC bed and the middle and bottom portion of the column being same as the deeper unexposed portions of GAC bed.

Quenching reaction involving 10 mg/L of H_2O_2 resulted in 0 mg/L H_2O_2 residuals in case of virgin GAC. However, one year old and two year old GAC had residual H_2O_2 concentrations in the range of 0.5 mg/L to 2 mg/L, for the applied empty bed contact time (EBCT) of 4.1 minutes. This is of significance for treatment plants using GAC to quench H_2O_2 as quenching percentage varied between 80% and 95% for high concentration H_2O_2 dose.

There are a number of areas which need to be explored in the quenching of H_2O_2 by GAC:

- Maximum possible concentration of H_2O_2 that can be quenched by a particular GAC as a function of the age of GAC and empty bed contact time (EBCT)
- Continuous pilot project involving monitoring of residual H_2O_2, dissolved oxygen (DO) and pH measurements continuously for at least two years to gain understanding about ageing of GAC and deactivation of its reactive sites
- More accurate dissolved oxygen measurement technique which would allow quantitative measurement of bubble + dissolved form of oxygen
- Analysis of exhausted GAC surface with virgin GAC surface can give us important information about the reaction mechanism of the quenching process between H_2O_2 and GAC.

2.6 References

Aguinaco, A., Pocostales, J.P. , García-Araya, J.F., and Beltran, F.J., 2011. Decomposition of hydrogen peroxide in the pesence of activated carbons with different characteristics. Journal of Chemical Technology & Biotechnology.

Alasri, A., Roques, C. and Michel, G. , 1992. Bactericidal Properties of Peracetic Acid and Hydrogen Peroxide, Alone and in Combination, Chlorine and Formaldehyde Against . Bacterial Water Strains 38, no. 7: 635.

Alvárez, P.M., García-Araya , J.F., Beltrán, F.J., Giráldez, I., Jaramillo, J., Gómez-Serrano, V., 2006. The influence of various factors on aqueous ozone decomposition by granular activated carbons and the development of a mechanistic approach. Carbon 44 (14): 3102–3112.

American Public Health Association, American Water Works Association, Water Environmental Federation, APHA-AWWA-WEF, 1998. Standard Methods for the Examination of Water and Wastewater . Washington D.C.

Bach, A., and Semiat, R., 2011. The role of activated carbon as a catalyst in GAC/iron oxide/H2O2 oxidation process. Desalination. 273 (1) .

Bielski, B.H.J., Cabelli, D.E., Arudi, R.L., and Ross, A.B., 1985. Reactivity of HO2 / O2(-) radicals in aqueous solution. (J Phys Chem Ref Data) 14(4):1041–100.

Buxton, G.V., Greenstock, C.L., Helman, W.P., and Ross, A.B., 1988. Critical review of rate constants for reactions of hydrated electrons, hydrogen atoms and hydroxyl radicals (HO./O.-) in aqueous solution. J Phys Chem Ref Data, 17(2):513–886 ed.

Calgon-Carbon. Centaur HSL 8X20, 2011. Pittsburgh: Calgon Carbon.

Calgon-Carbon. Filtrasorb 300, 2012. Pittsburgh: Calgon Carbon.

Calgon-Carbon. TN-5 8X30, 2011. Pittsburgh: Calgon Carbon.

Campbell, J.E., and Kimmick, R.L., 1966. Effect of 3% Hydrogen Peroxide on viability of Serratia Marcescens. (Journal Bacteriology) 91:3:925.

Castro, C.S., Oliveira, L.C.A., and Guerreiro, M.C., 2009. Effect of hydrogen treatment on the catalytic activity of iron oxide based materials dispersed over activated carbon: investigations toward hydrogen peroxide decomposition. Catalysis Letters.

Cotton, C., Jousset, S., Linden, K., and Collins, J., 2010. Applying UV-AOP at an existing WTP: effects on disinfection strategy and DBP formation. (AWWA WQTC).

Crittenden, J.C., Hu, S., Hand, J.W., Green, S.A., 1999. A kinetic model for H2O2/ UV process in a completely mixed batch reactor. Water Research 33(10): 2315.

Dotson, A., Corwin, C., Rowley, C., Downs, M. and Linden, K., 2010. Dynamic bench-scale quenching of H2O2 by GAC. AWWA WQTC (AWWA WQTC).

Elliot, A.J., and Buxton, G.V., 1992. Temperature dependence of the reactions OH + O2(-) and OH + HO2 in water upto 200 degrees celcius. Faraday Trans .

Evans, M.G., and Uri, N., 1949. The dissociation constant of hydrogen peroxide and electron afficnity of HO2 radical. Trans Faraday Society: 224-230.

Gogate, P.R., and Pandit, A.B., 2004. A review of imperative technologies for wastewater treatment I: oxidation technologies at ambient conditions. Adv Environ Res.

Gomes, H.T., Miranda, S.M., Sampaio, M.J., Silva, A.M.T., and Faria, J.L., 2010. Activated carbons treated with sulphuric acid: catalysts forcatalytic wet peroxide oxidation. Catal Today, 151(1-2): 153 - 8 ed.

Granular activated carbon used as catalyst or catalyst support, 1987. Calgon Carbon Corporation.

Hage, R., and Lienke, A., 2006 Applications of transition-metal catalysts to textile and wood-pulp bleaching. Angew Chem Int Ed.

Huang, H.H., Lu, M.C., Chen, J.N., Lee, C.T., 2003. Catalytic decomposition of hydrogen peroxide and 4-chlorophenol in the presence of modified activated carbons. Chemosphere 51 , no. 9: 935–943.

Ingle, J. D. J., Crouch, S. R., 1988. Spectrochemical Analysis. New Jersey: Prentice Hall.

Khalil, L.B., Girgis, B.S., and Tawfik, T.A., 2001. Decomposition of H2O2 on activated carbon obtained from olive stones. Journal of Chemical Technology and Biotechnology.

Klassem, N., Marchington, D., McGowan, H., 1994. H2O2 determination by I3(-) method and by KMnO4 titration. 66, 2921-2925.

Koppenol, W.H., Butler, J., and Van Leeuwen, J.W., 1978. The Haber-Weiss cycle. Photochemistry Photobiology, 28(4–5):655–8 ed.

Krejci, D., Woschnak, A., Scharlemann, C., Ponweiser, C., 2011. Hydrogen Peroxide Decomposition for Micro Propulsion: Simulation and Experimental Verification. ASEE.

Kurniawan, T.A., and Lo, W.H., 2009. Removal of refractory compounds from stable landfill leachate using an integrated H2O2 oxidation treatment and GAC adsorption treatment. Water Research 43, no. 16: 4079 - 4091.

Lee, H.J., Ho, M.R., Bhuwan, M., Hsu, C.Y., Huang, M.S., Peng, H.L., Chang, H.Y., 2010. Enhancing ATP-based bacteria and biofilm detection by enzymatic pyrophosphate regeneration. Analytical Biochemistry.

Lucking, F., Koser, H., Jank, M., and Ritter, A, 1998. Iron powder, graphite and activated carbon as catalysts for the oxidation of 4- chlorophenol with hydrogen peroxide in aqueous solution. Water Res, 32(9):2607–14. ed.

Jans, U., and Hoigné, J., 1998. Activated carbon and carbon black catalyzed transformation of aqueous ozone into OH-radicals. Ozone: Science & Engineering. The Journal of the International Ozone Association 20: 67-90.

Jones, C.W., 1999. Application of Hydrogen Peroxide and Derivatives. The Royal Society of Chemistry.

Lide, Dr. C.R.C., 2006. Handbook of Chemistry and Physics. Boca Raton, FL: CRC Press, Taylor and Francis Group.

Linden, K.G., Mohseni, M., 2014. Comprehensive Water Quality and Purification, Advanced Oxidation Processes: Applications in Drinking Water Treatment. Earth Systems and Environmental Science.

Linden, K.G., Sharpless, C.M., Andrews, S.A., Atasi, K.Z., Korategere, V., and Stefan, M., 2005. Innovative UV Technologies to Oxidize Organic and Organoleptic Chemicals. London UK: IWA Publishing.

Li, J., 2013. Quenching H2O2 Residuals After UV/ H2O2 Drinking Water Treatment Using Granular Activated Carbon. Toronto.

McKay, G., Sjelin, B., Chagnon, M., Ishida, K.B., Mezyk, S.B., 2013. Kinetic study of the reactions between chloramine disinfectants and hydrogen peroxide: temperature dependence and reaction mechanism. Chemosphere 92 (11): 1417–1422.

Michaud, J.P., 1991. A citizen's guide to understanding and monitoring lakes and streams. Vol. 1. Department of Ecology publications office.

National Institute for Occupational Safety and Health (NIOSH), 2010, Revised March 2012. NIOSH pocket guide to chemical hazards: hydrogen peroxide.

Norit. GAC 300, 2013. Billerica: Norit.

Norit. Hydrodarco 3000, 2013. Billerica: Norit.

Ontario, Legislative Assembly of. Safe Drinking Water Act 2002. (Govt. of Ontario) 2002.

Philippe, S., and Figueiredo, J.L., 2009. Carbon Materials for Catalysis. Wiley.

Raffellini, S., Schenk, M., Guerrero, S., and Alzamora, S.M., 2011. Kinetics of Escherichia coli inactivation employing hydrogen peroxide at varying temperatures, pH and concentration. (Food Control) 22(6):920-32.

Rebeiro, R.S., Silva, A.M.T., Figueiredo, J.L., Faria, J.L., and Gomes, H.T., 2012. The influence of stucture and surface chemistry of carbon materials on the decomposition of hydrogen peroxide. Elsevier.

Rey, A., Zazo, J.A., Casas, J.A., Bahamonde, A. and Rodriguez, J.J., 2011. Influence of the structural and surface characteristics of activated carbon on the catalytic decomposition of hydrogen peroxide. Applied Catalysis A, General 402, 146–155 ed.

Robinson, R.A., and Stokes, R.H., 1968. Electrolyte solution. London: Butterworths.

Schlegel, H.G., 1977. Aeration without Air: Oxygen supply by hydrogen peroxide. Biotechnology Bioengineering.

Skibinski, B., Müller, S., Uhl, W., 2009. Removal of free and combined chlorine at GAC surfaces and impact on pool water quality. Swimming Pool & Spa International Conference. London: PWTAG.

Suidan, M.T., Sneyink, V.L., Schmitz, R.A., 1977. Reduction of aqueous free chlorine with granular activated carbon-pH and temperature effects. Environmental Science & Technology 11 (8): 785-789.

Urfer, D., Huck, P.M., 1997. Effect of Hydrogen Peroxide on Biologically Active Filters. Ozone Science and Engineering.

USATSDR. 2011. Medical Management guideleines for hydrogen peroxide. Atlanta, US.

Watts, M.J., Hofmann, R., Rosenfeldt, E.J. Low-pressure UV/Cl2 for advanced oxidation of taste and odor. Journal American Water Works Association, n.d.: 104(1), 47-48.

Weinstein, J., and Bielski, B.H.J., 1979. Kinetics of the interaction of perhydroxy and superoxide radicals with hydrogen peroxide, the Haber Weiss reaction. (Junior American Chemial Society) 101(1):58–62.

Wells, A.F., 1984. Structural Inorganic Chemistry. Oxford, U.K.: Oxford University Press.

3. Effect of pH, water matrix and biofilm on quenching of H_2O_2 by GAC

3.1 Abstract

Quenching reaction between H_2O_2 and GAC was examined at bench-scale. The pseudo first order reaction constant k for the quenching reaction was calculated at six different values of pH: 6.50, 7.00, 8.50, 11.00, 11.75 and 12.50, and for six different GACs: ADCAT, Centaur, F-300, Norit GAC-300, HD-3000 and TN-5. Each GAC had been exposed to three different types of ageing: virgin, exposed to 45000 bed volumes of natural organic matter (NOM) and exposed to 45000 bed volumes of NOM + H_2O_2. Results suggested that virgin GAC was faster at quenching H_2O_2 as compared to aged GAC. Both types of aged GACs quenched H_2O_2 at almost similar rates. There was a marked increase in the rate of quenching beyond a pH value of 11.00 with virgin GAC showing a sharper rise than aged GACs.

Biofilm growth and its effect on quenching ability of virgin GAC Centaur and sand (inert media) was investigated for a duration of 10 weeks by performing bench-scale experiments. Reaction rates showed an increase between week 3 and week 10 suggesting a positive influence of biofilm on the quenching ability of GAC. Sand showed an increase from ~5% to ~10% in reaction constant k values between week 3 and week 10 suggesting that biofilm growth had induced a quenching ability in an otherwise inert media like sand.

3.2 Introduction

3.2.1 Reaction constant k in quenching reaction

The quenching reaction of H_2O_2 by GAC is an important step in the treatment train of water treatment facilities which make use of H_2O_2 in advanced oxidation process. Characterization of reaction mechanism for the quenching process has been an active point of debate between researchers (Aguinaco et al., 2011, Rey et al., 2011 and Khalil et al., 2001). To investigate this question of reaction mechanism as well as the related question of service life of GAC we studied existing literature on the quenching process (Bach et al., 2011, Kurniawan et al., 2009 and Krejci, 2011).

Literature review redirected us to focus on three parameters which we considered to be fundamentally important in the quenching reaction: final H_2O_2 concentration left after quenching, dissolved oxygen (DO) in solution during quenching and pH of the solution undergoing the quenching process. Analysis of data obtained for these three parameters have been discussed in the first part of this thesis. All the three parameters were found to be linked to the quenching reaction. While final H_2O_2 concentration left after quenching was directly related to the quenching reaction, pH, DO was found to give important, although similar, information about the quenching reaction. In a way, pH and DO were found to have all qualities required for acting as indirect channels of gaining information about the reaction mechanism of quenching reaction. We concluded from the study that detailed analysis of any one of these parameters could provide us very useful information for the quenching process. pH was finally chosen as the parameter for detailed study as it was easiest to measure and control in an experimental setting. DO was rejected as they faced some fundamental short-comings. In case of dissolved oxygen, the DO probe was found to be capable of only qualitative measurement of oxygen bubbles. This prevented us from going forward with any experimental plan based on quantitative analysis of dissolved oxygen.

The rate of quenching reaction between H_2O_2 and GAC had been studied by (Bach et al., 2011) and (Kurniawan et al., 2009) and they showed that the quenching reaction was a redox chemical reaction rather than a reaction involving physical adsorption. Modelling the quenching reaction, with non-organic water matrix, on first order kinetics had yielded high correlation values > 0.99 to a number of research groups (Huang et al., 2003, Kurniawan et al., 2009 and Rey et al., 2011). Two different reaction mechanism of quenching have been proposed by two different research groups (Kurniawan et al., 2009 and Bach et al., 2011) The hypothesis by Kurniawan et al., 2009 is given as follows:

$$\mathbf{AC + H_2O_2 \rightarrow AC^+ + OH^- + \bullet OH} \qquad \textbf{Equation 2. 1}$$

$$\mathbf{AC^+ \rightarrow AC + H^+ + \bullet OOH} \qquad \textbf{Equation 2. 2}$$

Here AC = activated carbon (granular or powdered)

The •OOH and •OH would combine to give H_2O and O_2 thus completing the decomposition process. The second hypothesis by Bach et al., 2011 is given as follows:

$$\mathbf{H_2O_2 \rightleftharpoons H^+ + HO_2^- \quad (pK_a = 11.75)} \qquad \textbf{Equation 2. 3}$$

$$\mathbf{AC-OH + H^+HO_2^- \rightarrow AC-OOH + H_2O} \qquad \textbf{Equation 2. 4}$$

$$\mathbf{AC-OOH + H_2O_2 \rightarrow AC-OH + O_2 + H_2O} \qquad \textbf{Equation 2. 5}$$

Here AC = activated carbon (granular or powdered)

We can observe that both the mechanisms involve use of H^+ ion and HO_2^- or HO_2•.

With all of this available information on quenching reaction we decided on an experimental plan incorporating a parameter signifying quenching – reaction constant k, and another parameter which was closely connected to reaction mechanism – pH of reacting solution.

According to the reaction mechanisms proposed by Kurniawan et al., 2009 and Bach et al., 2011 the only intermediate chemical species which seemed to be involved in the reaction process besides GAC, was HO_2^-. Therefore we proposed a hypothesis where we stated that if the reaction mechanism was fundamentally dependent on HO_2^-, we will observe proportional increase in reaction constant k. To test this hypothesis, we decided to control the pH as pH is a surrogate to HO_2^- ion concentration in quenching reaction. The basis of this statement is borne out of the fact that H_2O_2 being an acid always remains in equilibrium with HO_2^- and H^+ according to Equation 2.3.

Furthermore, in order to understand the general principles governing the quenching reaction we decided to test our hypothesis on different types of GAC. We stood to gain two basic advantages out of this construct. Firstly, analysis of more data would have allowed us to find common trends in quenching behavior of GACs. Secondly, it is a good scientific practice to review results based on varied sources, it eliminates exceptions to a large degree. To implement this experimental plan we used six different GACs which were commonly in use in the water treatment industry: ADCAT, Centaur, F-300, Norit GAC-300, HD-3000 and TN-5. Their surface characteristics and other physical and chemical properties relevant to quenching reaction are discussed in Table 2.

Use of different virgin GACs at different pH values would have, in essence, given us only a snapshot of the quenching mechanism in the early life of GAC. However, GAC in real life remains new only for a very short duration in its life span. To counter this imbalance in our experimental plan we decided to investigate all six GACs with different types of surface characteristics induced by ageing due to exposure to a specific form of water matrices. We decided on two types of aged GACs - GAC aged with natural organic matter (NOM) which occurs commonly in natural lake and river water, and GAC aged with NOM + H_2O_2 which would be the case for GAC in a GAC bed contactor in a water treatment plant. The third type of surface

was chosen to be unaltered virgin GAC. Finally, virgin, NOM aged and NOM + H_2O_2 aged GAC were decided as reactant media for testing our hypothesis.

Given the materials and defined reactant conditions for our hypothesis, we needed to find concentration of HO_2^- ion over a range of pH values and obtain k values for H_2O_2 quenching by GAC at those given pH values. If the k values from the reaction are found to increase proportionally with HO_2^- then our hypothesis will be true and HO_2^- will prove to be a fundamentally important factor in the quenching reaction mechanism. However, if the k values are found to be independent of HO_2^- ion concentration then our hypothesis will prove to be false.

To test our hypothesis six pH values were selected: 6.50, 7.00, 8.50, 11.00, 11.75 and 12.50. pH values around 11.75, which is also the pK_a of hydrogen peroxide (Evans et al., 1949), were chosen so that we may be able to understand the effect of high HO_2^- ion concentration on k values. Criteria for selecting lower pH values around 7.00 was based on observing effect on k value of the quenching process at pH values which are observed commonly at treatment facilities.

HO_2^- ion concentration at different pH values were calculated as follows:

Assuming initial concentration of H_2O_2 to be 'a' moles/litre:

$$H_2O_2 \rightleftharpoons HO_2^- + H^+$$

a - x x 10^{-pH} (concentrations at equilibrium)

(x = equilibrium concentration of HO_2^-)

$$K_a = \frac{x \times 10^{-pH}}{a - x} \qquad \textbf{Equation 2. 6}$$

$$\frac{a-x}{x} = \frac{10^{-pH}}{K_a} \qquad \textbf{Equation 2. 7}$$

$$\frac{a}{x} = \frac{10^{-pH}}{K_a} + 1 \qquad \textbf{Equation 2. 8}$$

$$x = \frac{a}{1 + \frac{10^{-pH}}{K_a}} \quad (K_a = 10^{-11.75}) \qquad \textbf{Equation 2. 9}$$

Table 1: Concentration of species at different pH values

pH	HO_2^- conc. (x) as a function of $[H_2O_2]_o$ – initial concentration of H_2O_2	Ratio of HO_2^- at any pH to HO_2^- at pH 6.5
6.50	5.62×10^{-6} $[H_2O_2]_o$	1.00
7.00	1.78×10^{-5} $[H_2O_2]_o$	3.17
8.50	5.62×10^{-4} $[H_2O_2]_o$	100.00
11.00	0.15 $[H_2O_2]_o$	2.69×10^4
11.75	0.50 $[H_2O_2]_o$	8.90×10^4
12.50	0.85 $[H_2O_2]_o$	1.51×10^5

3.2.2 Biofilm growth

The topic of biofilm growth on GAC is new to the field of GAC chemistry in terms of H_2O_2 quenching. Not a lot of literature is available on this topic. As a result information available on the subject area is very basic. Alasri et al., 1992 and Urfer et al., 1997 had investigated biofilm growth on granular activated carbon (GAC). Subsequently, they were able to point to changing H_2O_2 quenching ability of GAC due to biofilm growth.

With the use of GAC bed contactors in the drinking water treatment plants and their continuous exposure to water matrix with some concentration of bio-nutrients biofilm formation on GAC beds is a natural phenomenon. As the GAC bed contactors are mostly placed before chlorination process, bacteria colonies can thrive on the GAC beds. However, their runaway growth is inhibited due to presence of oxidizing agents such as H_2O_2 in water which passes over GAC beds. Also the fact that there is a continuous flow and no stagnation of water over the GAC beds results in inhibition of high amount of growth on GAC beds.

The first part of the thesis where we observed important parameters of quenching process like residual H_2O_2 concentration, dissolved oxygen concentration and pH of H_2O_2 solution undergoing quenching in presence of GAC. In the trend lines of all these parameters there were certain peaks and troughs which could not be explained on the basis of continuous ageing or exhaustion behavior of GAC. The observations pointed to some external effect which was affecting the quenching process besides GAC and H_2O_2 concentration.

Keeping the above in mind, we designed a bench-scale experimental setup in which we provided GAC with favourable growth conditions for biological growth - high nutrients, zero flow and open to atmospheric oxygen. We kept the GAC at different H_2O_2 concentrations of 0.0 mg/L, 0.5 mg/L, 1.0 mg/L, 3.0 mg/L, 5.0 mg/L and 10 mg/L to mimic water matrices encountered by GAC beds in different treatment plants. Along with GAC, we also used brown sand with defined characteristics - uniformity coefficient (UC) < 2.1 and effective size (ES) in the range of 0.8 - 1.0 mm, and kept it at the same H_2O_2 concentrations as GAC. Our hypothesis was to test the

contribution of biofilm to quenching H_2O_2 by GAC. If biofilm growth was a major contributor to quenching H_2O_2 in aged GAC, then with sufficient growth of biofilm on sand we should be able to see similar amount of quenching between biofilm covered sand and biofilm covered GAC. Observations showing similar quenching results for sand and GAC would prove our hypothesis to be correct, else our hypothesis would stand rejected.

3.3 Materials and methods

The properties of GAC used in the bench scale test for analyzing first order kinetic reaction constant k for quenching reaction between H_2O_2 and GAC are listed in Table 2. Information was compiled using product release from companies and works of Li et al., 2013.

Table 2: GAC properties

GAC Type	Relative Density (g/mL)	Iodine No. (mg/g)	Moisture (% by wt)	Effective Size (mm)	Uniformity Coefficient	US Sieve Size	Manufacturer
HD 3000	0.38	500	8	0.7 – 0.9	2.1 (max)	8X30	Norit
Centaur	0.53	1044	4	0.8 – 1.0	2.1 (max)	8X30	Calgon
F-300	0.56	900	2	0.8 – 1.0	2.1 (max)	8X30	Calgon
GAC-300	0.52	900	2	0.8 – 1.0	2.1 (max)	8X30	Norit
ADCAT	0.485	956	2	0.8 – 1.0	2.1 (max)	8X30	Carbotech
TN-5	0.60	861	2	0.8 – 1.0	2.1 (max)	8X30	Calgon

3.3.1 Bench-scale setup for analyzing effects of pH on kinetics

The general procedure for these bench-scale experiments was to conduct continuously-stirred batch reactor tests in which the rate of H_2O_2 decay in the presence of a fixed amount of GAC was monitored. H_2O_2 decay was always observed to follow pseudo first-order kinetics (data presented in Appendix A), so a first-order decay coefficient, k, was obtained from each test. The decay tests were carried out over a period of five hours, with the concentration of hydrogen peroxide measured every hour. Each test was done in duplicate to ascertain the reproducibility and precision of the method. An experimental control was also conducted in the absence of GAC, to confirm that there was negligible loss of hydrogen peroxide.

In each test, one litre bottles were filled with 490 (±2) mL of water, 10 (± 1) mL of 50 mM buffer and 0.25 (± 0.005) g of GAC. To initiate the reaction, 50 (±0.5) µl of 30% (w/w) hydrogen peroxide was injected into the GAC+water+buffer solution. The reaction bottle was

then put into an orbital shaker assembly, with an rpm value of 180, for the full duration of the experiment. This ensured good contact between the entire solution of H_2O_2 and the GAC particles. At the end of every hour, the reaction bottle was removed from the shaker assembly and an aliquot of the solution was removed to measure hydrogen peroxide concentration.

3.3.2 Description of kinetic reaction constant calculation

Measurement of hydrogen peroxide was done by iodometric method (Klassem et al., 1994). In this method, a solution of potassium iodide was made to react with hydrogen peroxide resulting in the formation of tri-iodide (I_3^-). The tri-iodide ion quantitatively absorbs light at 351 nm, according to the Beer-Lambert law (Ingle et al., 1988):

Absorbance = k x C x L **Equation 2. 10**

Here k = molar absorptivity ($26450\ M^{-1}m^{-1}$)
C = concentration of the absorber (mg/L)
L = path length traversed by the light, 1 cm

Absorbance was measured using a spectrophotometer, details are provided in Appendix C

$$[H_2O_2] = A_{351} \times \frac{Total\ Volume}{Sample\ Volume} \times 34.01 \frac{g}{mol} \times 1000 \frac{mg}{g} \div 26450\ M^{-1}\ m^{-1} \quad \textbf{Equation 2. 11}$$

$[H_2O_2]$ = concentration of $[H_2O_2]$ in mg/L. A_{351} = absorbance of H_2O_2 solution at 351 nm.

The reaction between H_2O_2 and GAC was evaluated at six different pH values: 6.50, 7.00, 8.50, 11.00, 11.75, and 12.50. The lower pH values were selected to predict the quenching process at pH values that are most commonly observed at treatment facilities. pH values around 11.75 were selected as this is the pK_a of hydrogen peroxide (Evans and Uri 1949), and it was desired to determine if the species of H_2O_2 (i.e. HO_2^-) might affect its decomposition rate. The buffers used to adjust pH were as shown in Table 3 (next page).

Table 3: Buffers

pH	Buffer
6.50	KH_2PO_4 (100 ml of 0.2M soln.) + NaOH (27.8 of 0.2M soln.) + 72.2 ml water
7.00	KH_2PO_4 (100 ml of 0.2M soln.) + NaOH (58.2 ml of 0.2M soln.) + 41.8 ml water
8.50	$Na_2B_4O_7.10H_2O$ (100 ml of 0.05M soln.) + HCl (30.4 ml of 0.2M soln.) + 69.6 ml water
11.00	Na_2HPO_4 (100 ml of 0.1 M) + NaOH (8.2 ml of 0.2M) + 91.8 ml water
11.75	Na_2HPO_4 (100 ml of 0.1 M) + NaOH (35.1 ml of 0.2M) + 64.9 ml water
12.50	KCl (50 ml of 0.2 M) + NaOH (40.8 ml of 0.2M) + 59.2 ml water

All experiments were conducted at a temp of 22^0C. Individual graphs (Appendix A) from which each k value point was obtained point conclusively to a first order reaction between H_2O_2 and GAC. Truth of this statement is borne by the fact that modelling kinetic reaction data points on first order kinetics gives us a correlation value > 0.99 for every k value (Appendix A). And this was true for the full range of pH values from 6.5 to 12.5.

3.3.3 Bench –scale setup for analyzing biofilm effects

The bench-scale setup for analyzing biofilm effects consisted of 12 standalone containers. Six containers held 2 dm^3 (2 litres volume) of virgin GAC Centaur from GAC contactor bed of a treatment plant at six different ambient H_2O_2 concentrations of 0.0 mg/L, 0.5 mg/L, 1.0 mg/L, 3 mg/L, 5.0 mg/L and 10.0 mg/L. The objective was to model the container environment after the conditions of a GAC bed which continuously remains in contact with water containing H_2O_2 residuals from advanced oxidation processes. The remaining six containers contained 2 dm^3 (2 litres volume) brown sand with uniformity coefficient (UC) < 2.1 and effective size (UC) in the range of 0.8 - 1.0 mm at the same ambient concentrations of H_2O_2 as GAC. Each of the containers contained the media (GAC or sand) immersed in 2L of water at a given concentration of H_2O_2. The containers were kept in a lab open to atmosphere. Temperature of the lab was maintained at 22ºC by the HVAC system. Water in the containers was replaced on every third day with de-chlorinated tap water. De-chlorination was achieved by keeping the tap water in a closed vessel for 24 hours. We tested stored water for chlorine by injecting it with 10 mg/L of H_2O_2 and measuring its concentration after 15 minutes. We regularly found no change in the concentration of H_2O_2 in that time. This indicated the absence of chlorine and chlorine related oxidizing agents in the water. Appropriate amount of H_2O_2 was injected into containers filled with GAC, three times a day in order to keep the concentration of H_2O_2 close to the labelled ambient H_2O_2 concentration of the GAC container (0.0 or 0.5 or 1.0 or 3.0 or 5.0 or 10.0 mg/L) as H_2O_2 is continuously quenched by the GAC. Since sand does not quench GAC, appropriate H_2O_2 injections in sand containers were made only while refilling the container with fresh water. Water in each container was fortified with carbon, nitrogen and phosphorus in the ratio 15:5:1 (Urfer et al., 1997) to act as food for bacterial biofilm. Fortification was applied to the containers on alternate days. Details of chemicals used for fortification are given in Table 4**.**

Table 4: Chemicals used for fortification of water

Carbon	Nitrogen	Phosphorus
Formaldehyde – 100.00 ug/L	Sodium Nitrate – 614.08 ug/L	Dipotassium hydrogen phosphate – 113.55 ug/L
Glyoxal – 30.00 ug/L		
Acetic acid – 300.00 ug/L		
Formic acid – 400.00 ug/L		
Oxalic acid – 200.00 ug/L		
Total C = 303.43 ug/L	**Total N = 101.14 ug/L**	**Total P = 20.23 ug/L**

With this setup, we went forward to grow biofilm and test quenching behavior under the influence of biofilm for both sand and GAC.

3.3.4 Description of reaction constant -k, quenching percentage and ATP value calculations

Kinetic reaction tests, quenching reaction tests and ATP tests were conducted on media from all containers at the start of the experiment (week 0), after 3 weeks and at the end of 10 weeks from the start of the experiment. Kinetic reaction tests were conducted in the same way as stated in section 3.3.1

Quenching reaction tests made use of a glass column. The column was filled with 50 ml of the media. We used an empty bed contact time (EBCT) of 4.12 minutes, to model our experiment after the GAC contactor beds at the Lorne park drinking water treatment plant. A pump applying a flow of $\frac{Media\ Volume}{EBCT} = \frac{50}{4.12} \approx 12\ \frac{ml}{min}$ was used to conduct the quenching reaction. H_2O_2 concentration was measured using vacu-vials which work on the principle of ferric thiocyanate. The method is explained in section 3.3.2. ATP measurements were performed using the Luciferase assay method. The DSA test kit utilizes a 10-minute dilution-based analysis to measure a parameter called Total ATP. To perform this test we first find a calibration value by adding 100 uL of Luminase to 100 uL of Ultrachek 1 and finding the relative light unit (RLU) value of this 200 uL solution on a Lumimeter. After calculating the calibration value we move onto sample preparation. In step1 we measure close to 1 g of media in a plastic tube. Then we add 5 ml of ultralyse 7 solution to the media and allow it to incubate for 5 minutes. This releases any ATP from alive or dead cells in the sample. Next we dilute the interferences by adding 1 ml of the media sample to 9 ml of Ultralute. Finally we add 100 uL of the sample to 100 uL of

Luminase and find out the relative light units (RLU) value of the 200 uL solution via a Lumimeter.

The calculations involved were: $$\mathbf{ATP}\left(\frac{\mathbf{pg}}{\mathbf{g}}\right) = \frac{RLU_{tATP}}{RLU_{UC1}} \times \frac{\mathbf{50000}}{m_{sample}}$$ **Equation 2. 12**

In this way kinetic reaction constant – k, H_2O_2 quenching percentage and ATP values were calculated for GAC and sand media kept in all of the twelve containers at different H_2O_2 concentrations.

3.4 Results and discussion

3.4.1 Effect of pH on quenching hydrogen peroxide by virgin GAC

pH dependence of kinetic reaction constant k for virgin GACs is shown in Figure 13 (next page).

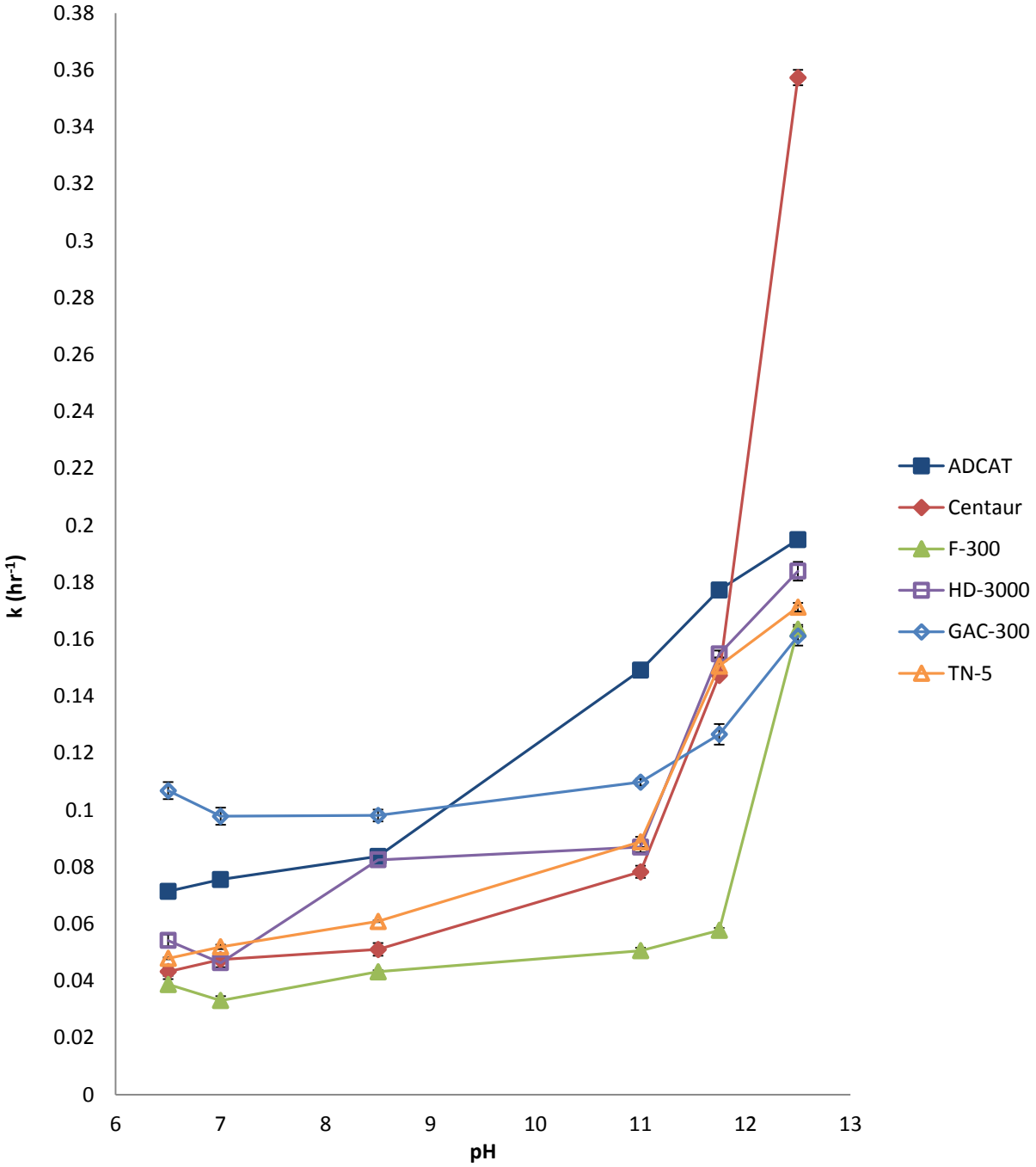

Figure 13: pH dependence of kinetic reaction constant for virgin GACs

Figure 13 depicts kinetic reaction constant for quenching reaction of H_2O_2 by virgin GACs. The plotted values were average values of duplicates. It can be observed from Figure 13 that error bars which denote individual values of duplicates are small and in good agreement. There are no controls shown in Figure 13 as they were different for each GAC. All information on controls is available in the individual k value graphs in Appendix A.

According to our hypothesis k value of GAC should have changed by five orders of magnitude between pH 6.5 and pH 12.5 (Table 1). However, we saw almost constant values of k between pH 6.50 and 11.00. Beyond pH 11.00 we saw a marked increase in k for every GAC. The increase is minimal when compared to the projected values of Table 1. Change in k value between pH 6.50 and pH 12.50 varied between 1.51 for Norit GAC-300 to 8.27 times for Centaur. This proved that the hypothesis is incorrect. Subject to further investigation, increase in k values beyond pH 11.00 might point to a change in reaction mechanism or a change in the surface characteristics of GAC with pH.

3.4.2 Effect of pH on quenching hydrogen peroxide by GAC aged with NOM

pH dependence of kinetic reaction constant for GACs aged with 45000 bed volumes of water containing NOM is shown in Figure 14.

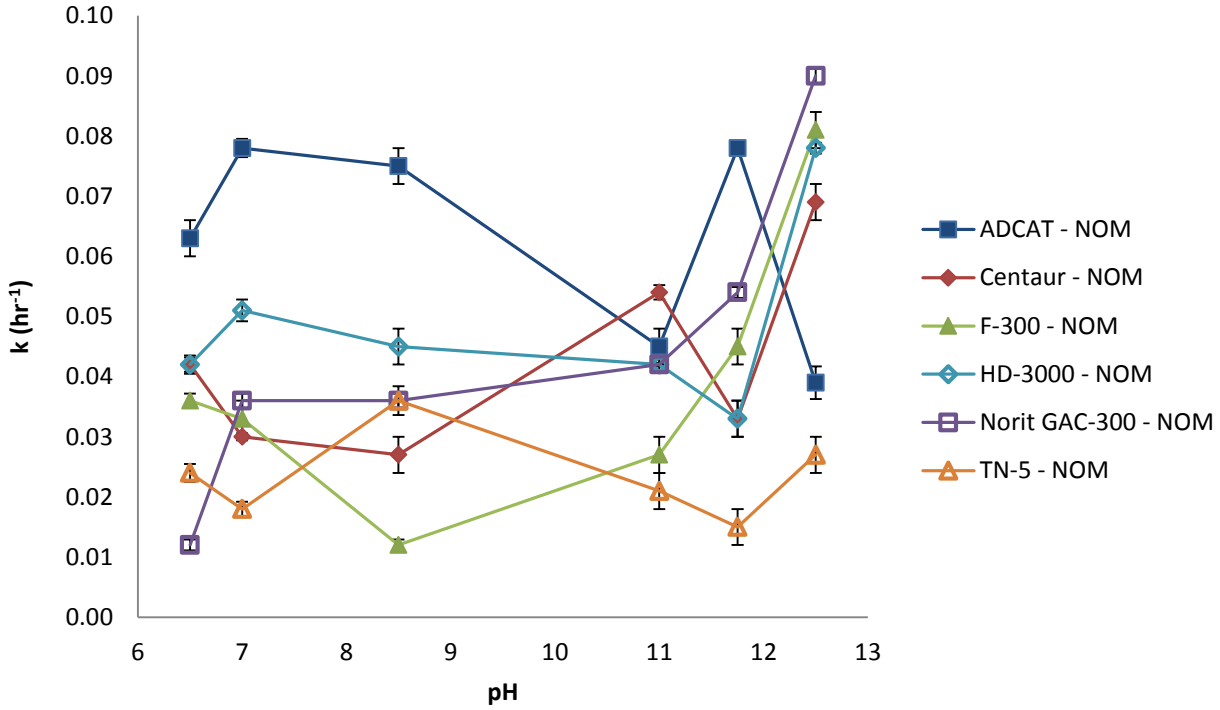

Figure 14: pH dependence of kinetic reaction constant for GACs aged with 45000 bed volumes of water containing NOM

Average k values of kinetic reaction of GACs aged with 45000 bed volumes of water containing NOM exhibited non-uniform behaviour against pH. All GACs except ADCAT showed an increase in k value beyond pH 11.75. Variation between k values for different GACs was smallest at pH 11.00.

All k value points in the above graph were obtained from individual graphs shown in Appendix A. Overall, the variation between duplicates was more in Figure 14 as compared to Figure 13. This

was expected as different samples of aged GAC taken for quenching experiment can contain slightly different amounts of biofilm growth and other varying surface characteristics. Ageing is expected to decrease uniformity of factory manufactured GAC. Controls are not shown in the above graph as they were different for every GAC. Controls for individual k values are shown in Appendix A.

3.4.3 Effect of pH on quenching hydrogen peroxide by GAC aged with NOM + H_2O_2

pH dependence of kinetic reaction constant for GACs aged with 45000 bed volumes of water containing NOM + H_2O_2 is shown in Figure 15.

Figure 15

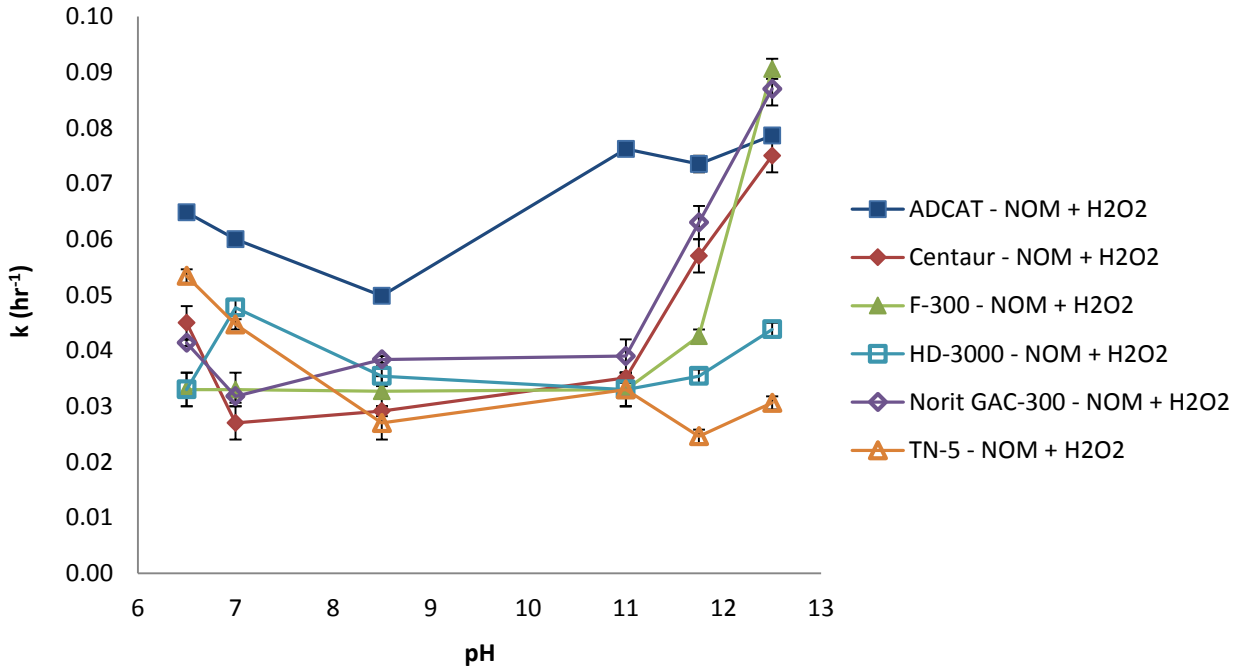

Figure 15: pH dependence of kinetic reaction constant for GACs aged with 45000 bed volumes of water containing NOM + H_2O_2

Reaction constant values k for H_2O_2 reacting with different GACs aged with 45000 bed volumes of water containing NOM and H_2O_2 in Figure 15 exhibited uniformity at pH 8.50 and pH 11.00. ADCAT was a marked exception with higher and more randomly changing k values as compared to other GACs. The k values appear to be steady at pH of 8.50 and 11.00, after which they tend to increase (except for TN-5). Unlike others, TN-5 showed a decline in k values beyond pH 11.00. Subject to further verification, this could point to a different level of biofilm growth in TN-5, which would change the reaction mechanism of quenching reaction between H_2O_2 and GACTN-5TN-5 leading to slow-down of the reaction hence smaller k value. Variation between duplicates was highest for Centaur in the above graph. This fact pointed to greater level of non-uniformity in surface characteristics of Centaur in comparison with other GACs. Controls for individual k value experiments are shown in single k value graphs in Appendix A.

3.4.4 Comparison of kinetic reaction constant for virgin GAC, GAC aged with NOM and GAC aged with NOM + H_2O_2 at different pH values

Comparison of Virgin GAC, GAC aged with 45000 bed volumes of water containing NOM and GAC aged with 45000 bed volumes of water containing NOM+H_2O_2 is shown in Figure 16 (next page).

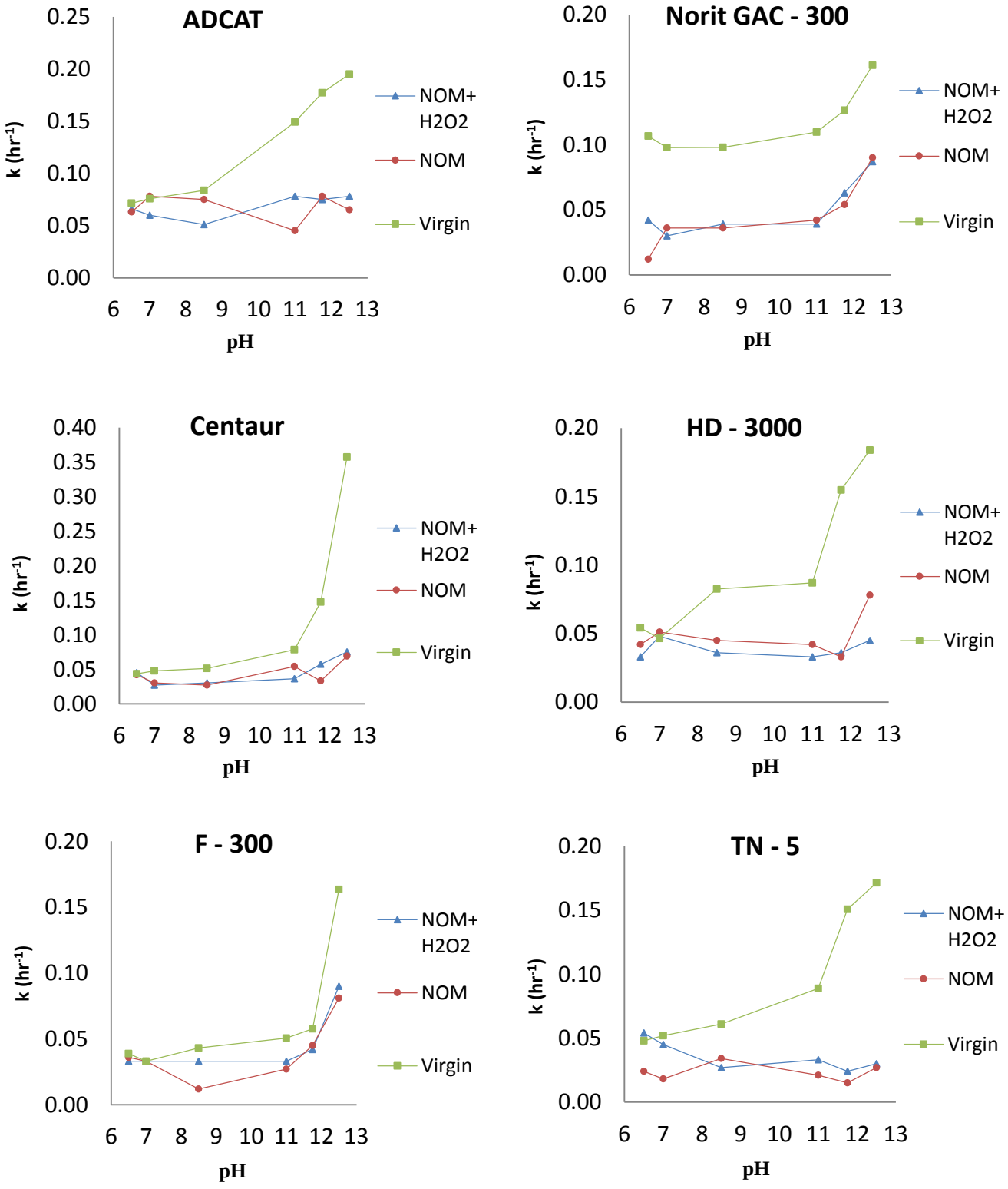

Figure 16: Comparison of Virgin GAC, GAC aged with 45000 bed volumes of water containing NOM and GAC aged with 45000 bed volumes of water containing$NOM+H_2O_2$

Comparison of k value graphs of virgin GAC, GAC aged with 45000 bed volumes of NOM and GAC aged with 45000 bed volumes of NOM + H_2O_2 in Figure 16 showed a general trend where virgin GAC exhibits higher k values than GAC aged with NOM and GAC aged with NOM + H_2O_2. This trend continued until the pH value of 11.00 beyond which the difference became more conspicuous. With the exception of Norit GAC-300, we observed that the k values of virgin GACs, GACs aged with NOM and GACs aged with NOM + H_2O_2 were very similar around neutral pH value of 7.00 and is true to a considerable degree up until the pH value of 9.00. This is of significance for drinking water treatment plants employing GAC for removing H_2O_2 used in advanced oxidation process as most treatment plants tend to obtain water from sources whose pH is within the range 6.50 – 9.00 (Michaud 1991). Given that the k value for quenching reaction between H_2O_2 and GAC were similar between pH 6.50 and pH 9.00 we can say that age of GAC is not a big factor in H_2O_2 quenching rate of GAC.

Chemical industries using GAC can take advantage of the fact that ability of GAC to quench H_2O_2 increases with pH and rises sharply beyond pH 11.00. It is important to note, however, that pH sensitivity of kinetic reaction constant of H_2O_2 quenching by GAC decreased with operational age of GAC.

Error bars in the above graphs are not shown to give a clear depiction of data in Figure 16, however they are shown individually in Figure 13, Figure 14 and Figure 15. Comparison between duplicates and controls for individual k values can be found in Appendix A.

3.4.5 Variation in reaction constant – k of GAC and sand due to biofilm growth

Variation of reaction constant (k) for GAC Centaur and sand is shown in Figure 17 (next page).

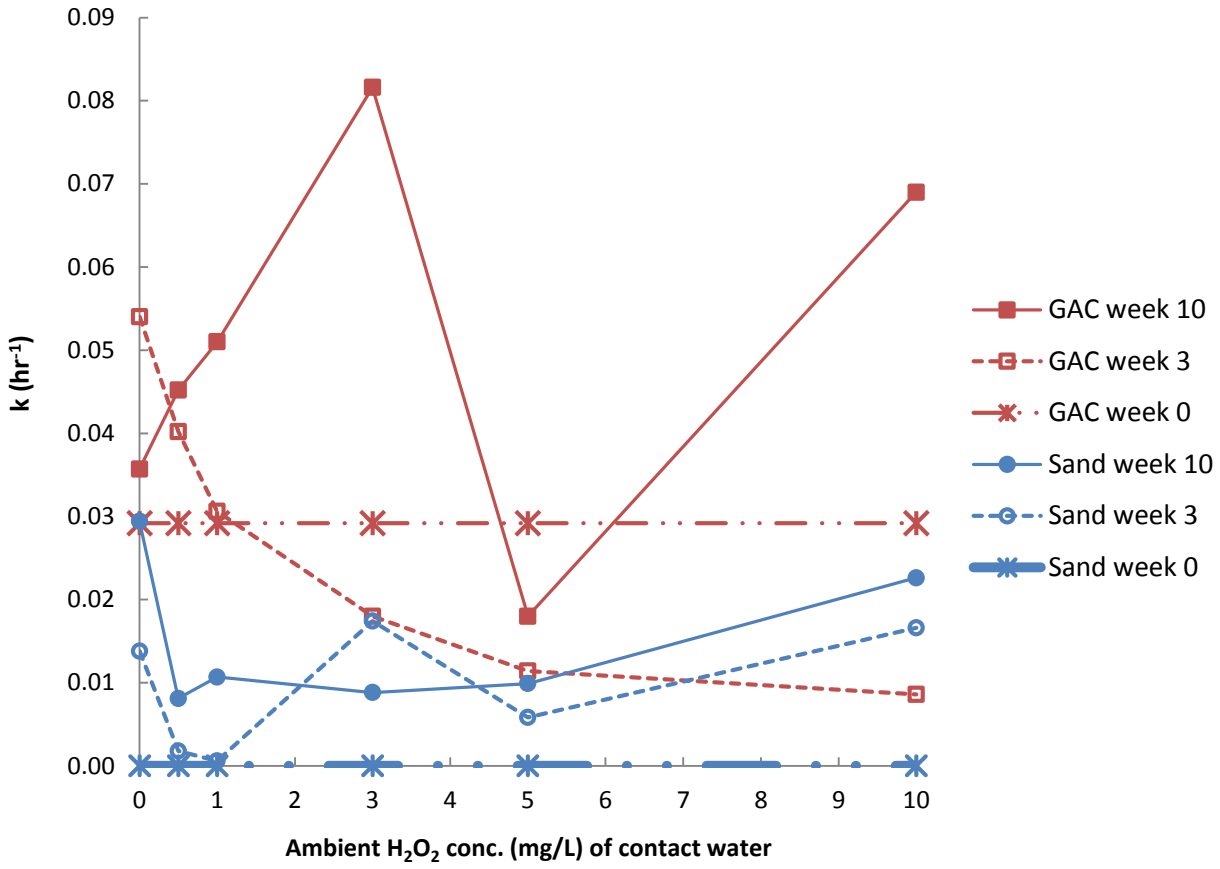

Figure 17: Variation of reaction constant (k) of GAC Centaur and sand

The graph for k value of quenching reaction between GAC Centaur and sand showed non-uniform variation. However, there were some important observations which could be derived by analyzing relative k values. At same ambient H_2O_2 concentrations k values for GAC and sand analyzed during week 10 were higher than respective k values observed in week 3. This suggested that k values increased with growing biofilm. K value at 0 mg/L of ambient H_2O_2 concentration for GAC and k value at 3 mg/L of ambient H_2O_2 concentration of contact water for sand were exceptions. More extensive and longer duration experiments need to be conducted to investigate these trends in more detail.

3.4.6 Variation in quenching percentage of H_2O_2 due to biofilm growth

Variation of quenching ability of GAC and sand for H_2O_2 is shown in Figure 18 (next page).

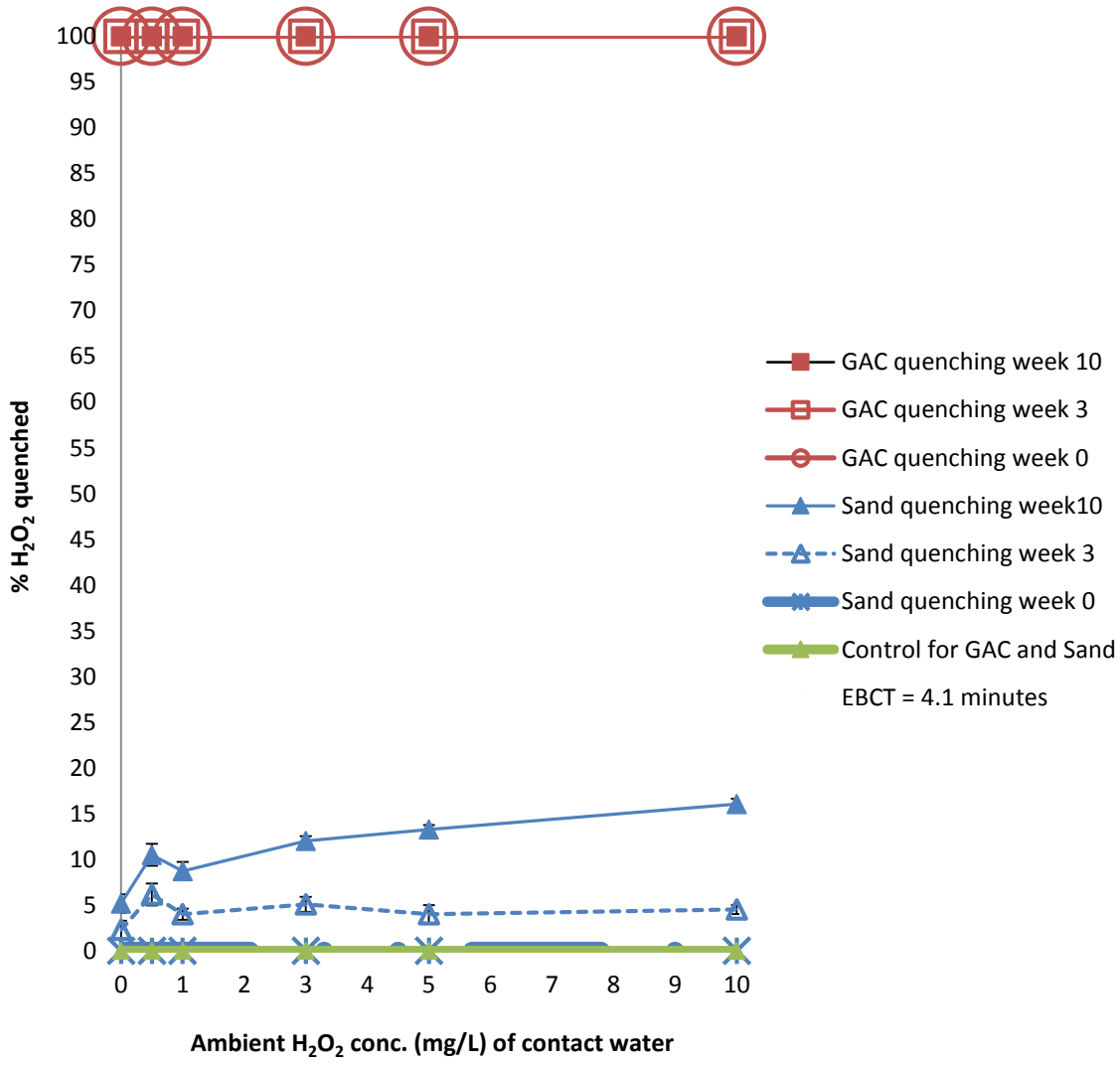

Figure 18: Variation of quenching ability of GAC and sand for H_2O_2

Time variation of H_2O_2 quenching by sand and GAC is shown in Figure 18. The empty bed contact time for the experiment was chosen to be same as the empty bed contact time at Lorne Park drinking water treatment plant – 4.12 minutes. Initial concentration of H_2O_2 was 10 mg/L. It is clear from the graph that GAC from week 0 through week 10 were able to quench 100% of the H_2O_2. This means that under normal operational conditions GAC in a drinking water treatment plant can quench 100% of H_2O_2 residual from the advance oxidation process which is roughly in the range of 0.5 mg/L to 5 mg/L (K. G. Linden 2014).

The quenching behavior of sand gave us important information about the correlation between quenching capacity and biofilm. We observed increase in quenching ability of sand with time. This suggests that biofilm growth clearly creates H_2O_2 quenching ability in sand, which is otherwise non-reactive with H_2O_2 - percentage of quenched H_2O_2 was 0 in week 0. Also, as the

trend line for week 3 was below that for week 10, we can conclude that quenching ability increases with growth of biofilm.

Error bars in Figure 18 showed small variation between duplicates. All controls in the graph showed 0 or close to 0 quenching of H_2O_2 by GAC and sand.

3.4.7 Variation in ATP values of GAC and sand due to biofilm growth

Variation of ATP for GAC Centaur and sand due to biofilm is shown in Figure 19.

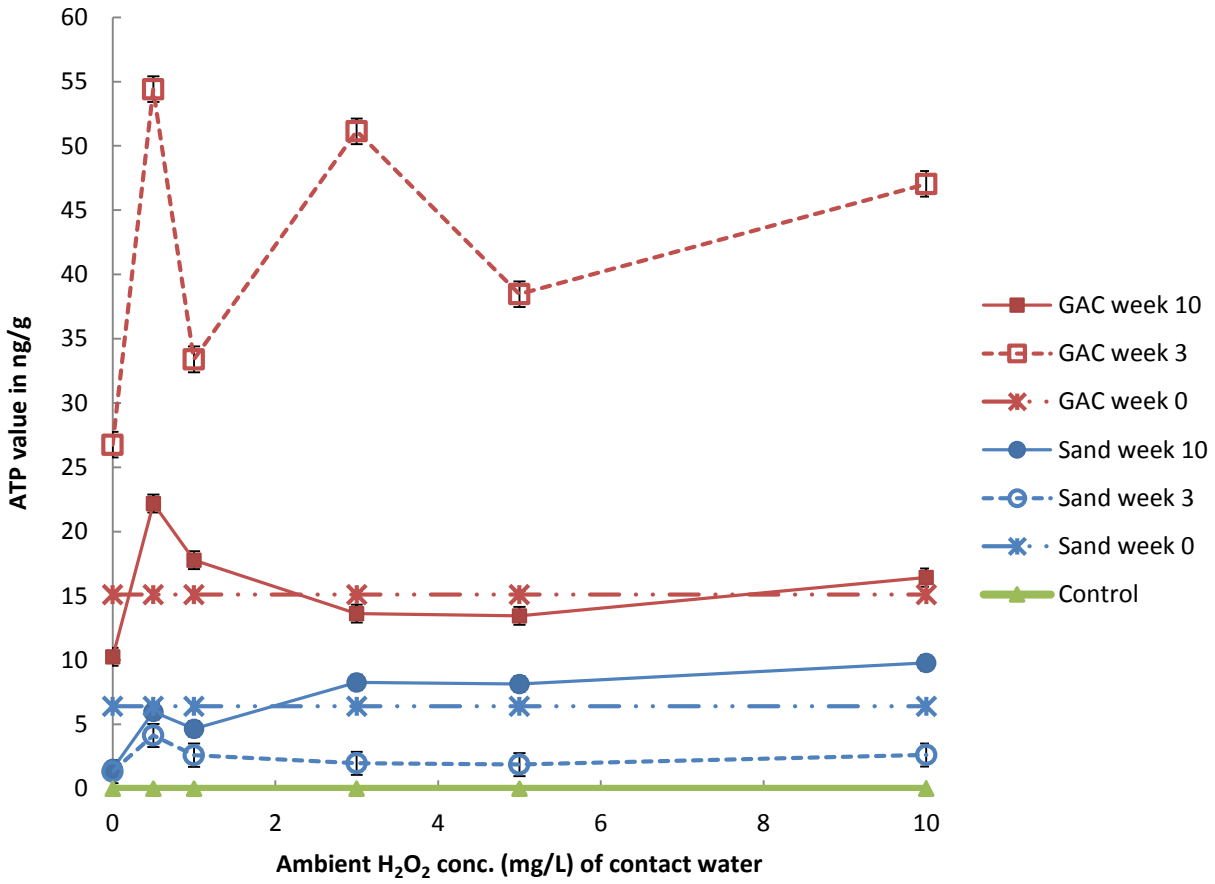

Figure 19: Variation of ATP for GAC Centaur and sand due to biofilm

Figure 19 shows the variation of ATP for GAC Centaur and sand due to biofilm growth. On the X axis is the ambient H_2O_2 concentration in which the GAC and sand were kept immersed for the duration of the experiment.

The above graph does not give any conclusive information about the state of bio-film on sand or GAC because ATP values below 100 ng/g point to dormant or very small amount of biologically active bacteria (Hui-Ju Lee 2010). The above graph inconclusively proves that there was very

limited biological growth on the GAC in the 10 week period in which the GAC was kept immersed in water containing a certain concentration of H_2O_2.

However, there are a few important observations that can be derived from Figure 19 for GAC. The ATP value for GAC kept at 0 mg/L was always the lowest amongst all other data points of the set, however, ATP value for GAC kept in 0.5 mg/L H_2O_2 was the highest. This indicates that a small concentration of H_2O_2 is the best dosage to promote growth of biofilm on GAC (Daniel Urfer 1997). The trend line for ATP values for week 10 was higher than the trend line for week 3. This proves that there was biological growth on GAC between week 3 and week 10.

Behavior of sand in the above graph was quite different from GAC. Sand showed almost constant ATP value with increasing concentration of H_2O_2, between 3 mg/L and 10 mg/L H_2O_2. This conveys that biofilm growth on sand or any non-adsorbing and non-reactive media is not affected with higher concentration of H_2O_2 in the range of 3 mg/L H_2O_2 to 10 mg/L H_2O_2. ATP values for sand in week 10 were higher than in week 3. This again proves that there was non-zero biofilm growth between week 3 and week 10.

The error bars depict deviation between the ATP values of duplicates. A small difference as was observed for GAC and sand. This underlines consistency in the observed data. Control values for GAC and sand gave ATP observations equalling 0.

3.5 Conclusion and recommendations for future work

3.5.1 Reaction constant value - k

We studied the kinetic reaction constant for quenching reaction of H_2O_2 by six different GACs - ADCAT, Centaur, F-300, HD-3000, Norit GAC-300 and TN-5 at six different pH values - 6.50, 7.00, 8.50, 11.00, 11.75 and 12.50. We observed that k values for virgin GACs, GACs aged with 45000 bed volumes of water containing NOM and GACs aged with 45000 bed volumes of water containing NOM + H_2O_2 exhibited very similar behavior between pH values of 6.50 and 8.50, with only a couple of exceptions in the form of Norit GAC – 300 and HD-3000. This proves that rate of quenching with the pH range of 6.50 to 8.50 is pretty much independent of the age of GAC (unless GAC is totally exhausted). It was also observed that NOM aged and NOM + H_2O_2 aged GAC showed very similar trends in k value for the full range of pH values.

Beyond the pH value of 11.00 a majority of the aged GACs and all of the virgin GACs showed a sharp rise in k value. Our hypothesis that k value was dependent on HO_2^- concentration turned out to be wrong as the k value did not increase in proportion to increase in HO_2^- concentration with pH for any of the GACs. This observation may actually point towards a change in reaction mechanism or change in surface characteristics of the GAC beyond pH 11.00. The fact that k value for virgin GAC increases swiftly beyond pH 11.00 could be of use in an industry using

virgin GAC as reducing agent for H_2O_2 as its rate of reducing H_2O_2. It is important to mention here that the rise in k value of aged GACs beyond pH value of 11.00 was not as sharp as that for virgin GAC proving that sensitivity of k value of GAC against pH (beyond pH 11.00) decreases with its age.

In the subject area of pH dependence of reaction constant k for quenching reaction of H_2O_2 by GAC there are a number of questions which need further research:

- Analysis of k value trends below pH 6.50, between pH 8.50 and 11.00 and beyond pH value of 12.50. It may give us useful information about the quenching reaction mechanism.
- Replication of k value experiments using different buffers than the ones used in this study to find out if there was any interference due to buffers
- K value trend analysis of same GACs aged by very different water matrices
- K value analysis at H_2O_2 concentrations higher than 100 mg/L to see if quenching rates of GAC are dependent on H_2O_2 concentration
- pH dependence of k value for GAC which are close to full exhaustion, and whether k value trends for such GAC exhibit a rise in k value beyond pH 11.00

3.5.2 Biofilm growth

Experiments involving biofilm growth gave us important information related to quenching of H_2O_2 by GAC Centaur as well as sand. Biofilm related experiments were done in three parts – kinetic reactions, quenching reactions and ATP reactions at three different timelines of week 0, week 3 and week 10. Our hypothesis that biofilm growth is a contributor to quenching of H_2O_2 by GAC or any inert media like sand came out to be true. However, further investigations need to be done to figure out the actual percentage contribution of biofilm to the quenching process.

An important conclusion from biofilm experiments was that biofilm growth, on an otherwise un-reactive media - sand, was able to induce H_2O_2 quenching capacity in the media. This statement is based on sand observations which showed increasing H_2O_2 quenching percentages from week 3 to week 10 and also increasing k value between week 3 and week 10. ATP values, however, did not increase, between week 0 and week 10, to levels that anything conclusive about biofilm growth could be stated. In conclusion, we can state with a high level of confidence that it is hard to justify increasing k value and higher quenching percentages if we discount growth of biofilm on sand. Therefore, in all probability, biofilm was established on sand which had contributed positively to quenching H_2O_2.

In case of GAC, the increase in observed k values between week 3 and week 10 does point towards growing biofilm. The H_2O_2 quenching percentage for GAC in week 0, week 3 and week 10 was 100% which meant that the quenching experiments were basically redundant. ATP values

changed over a small range which means that nothing conclusive can be stated about biofilm growth on GAC. However, with changing increasing k values between week 0 and week 10, we can say that a small amount of biofilm growth did take place on the GAC which enhanced the H_2O_2 quenching ability of GAC.

The field of biofilm growth on drinking water filter media is open to a number of investigations:

- Investigation of methods other than ATP value analysis to establish biofilm growth on filter media
- Use of continuous flow reactors instead of static water containers (as used in this study) to model biofilm growth in actual GAC beds in treatment plants
- Comparative studies on methods which can be employed to enhance biofilm growth
- Finding appropriate seed bacteria, which would grow into a biofilm that can mimic bio-colonies on GAC beds in treatment plants
- Characterization of bacteria involved in the eco-system in bio-colonies in GAC beds of treatment plants

3.6 References

Aguinaco, A., Pocostales, J.P. , García-Araya, J.F., and Beltran, F.J., 2011. Decomposition of hydrogen peroxide in the pesence of activated carbons with different characteristics. Journal of Chemical Technology & Biotechnology.

Alasri, A., Roques, C. and Michel, G. , 1992. Bactericidal Properties of Peracetic Acid and Hydrogen Peroxide, Alone and in Combination, Chlorine and Formaldehyde Against . Bacterial Water Strains 38, no. 7: 635.

Alvárez, P.M., García-Araya , J.F., Beltrán, F.J., Giráldez, I., Jaramillo, J., Gómez-Serrano, V., 2006. The influence of various factors on aqueous ozone decomposition by granular activated carbons and the development of a mechanistic approach. Carbon 44 (14): 3102–3112.

American Public Health Association, American Water Works Association, Water Environmental Federation, APHA-AWWA-WEF, 1998. Standard Methods for the Examination of Water and Wastewater . Washington D.C.

Bach, A., and Semiat, R., 2011. The role of activated carbon as a catalyst in GAC/iron oxide/H2O2 oxidation process. Desalination. 273 (1) .

Bielski, B.H.J., Cabelli, D.E., Arudi, R.L., and Ross, A.B., 1985. Reactivity of HO2 / O2(-) radicals in aqueous solution. (J Phys Chem Ref Data) 14(4):1041–100.

Buxton, G.V., Greenstock, C.L., Helman, W.P., and Ross, A.B., 1988. Critical review of rate constants for reactions of hydrated electrons, hydrogen atoms and hydroxyl radicals (HO./O.-) in aqueous solution. J Phys Chem Ref Data, 17(2):513–886 ed.

Calgon-Carbon. Centaur HSL 8X20, 2011. Pittsburgh: Calgon Carbon.

Calgon-Carbon. Filtrasorb 300, 2012. Pittsburgh: Calgon Carbon.

Calgon-Carbon. TN-5 8X30, 2011. Pittsburgh: Calgon Carbon.

Campbell, J.E., and Kimmick, R.L., 1966. Effect of 3% Hydrogen Peroxide on viability of Serratia Marcescens. (Journal Bacteriology) 91:3:925.

Castro, C.S., Oliveira, L.C.A., and Guerreiro, M.C., 2009. Effect of hydrogen treatment on the catalytic activity of iron oxide based materials dispersed over activated carbon: investigations toward hydrogen peroxide decomposition. Catalysis Letters.

Cotton, C., Jousset, S., Linden, K., and Collins, J., 2010. Applying UV-AOP at an existing WTP: effects on disinfection strategy and DBP formation. (AWWA WQTC).

Crittenden, J.C., Hu, S., Hand, J.W., Green, S.A., 1999. A kinetic model for H2O2/ UV process in a completely mixed batch reactor. Water Research 33(10): 2315.

Dotson, A., Corwin, C., Rowley, C., Downs, M. and Linden, K., 2010. Dynamic bench-scale quenching of H2O2 by GAC. AWWA WQTC (AWWA WQTC).

Elliot, A.J., and Buxton, G.V., 1992. Temperature dependence of the reactions OH + O2(-) and OH + HO2 in water upto 200 degrees celcius. Faraday Trans .

Evans, M.G., and Uri, N., 1949. The dissociation constant of hydrogen peroxide and electron afficnity of HO2 radical. Trans Faraday Society: 224-230.

Gogate, P.R., and Pandit, A.B., 2004. A review of imperative technologies for wastewater treatment I: oxidation technologies at ambient conditions. Adv Environ Res.

Gomes, H.T., Miranda, S.M., Sampaio, M.J., Silva, A.M.T., and Faria, J.L., 2010. Activated carbons treated with sulphuric acid: catalysts forcatalytic wet peroxide oxidation. Catal Today, 151(1-2): 153 - 8 ed.

Granular activated carbon used as catalyst or catalyst support, 1987. Calgon Carbon Corporation.

Hage, R., and Lienke, A., 2006 Applications of transition-metal catalysts to textile and wood-pulp bleaching. Angew Chem Int Ed.

Huang, H.H., Lu, M.C., Chen, J.N., Lee, C.T., 2003. Catalytic decomposition of hydrogen peroxide and 4-chlorophenol in the presence of modified activated carbons. Chemosphere 51 , no. 9: 935–943.

Ingle, J. D. J., Crouch, S. R., 1988. Spectrochemical Analysis. New Jersey: Prentice Hall.

Khalil, L.B., Girgis, B.S., and Tawfik, T.A., 2001. Decomposition of H2O2 on activated carbon obtained from olive stones. Journal of Chemical Technology and Biotechnology.

Klassem, N., Marchington, D., McGowan, H., 1994. H2O2 determination by I3(-) method and by KMnO4 titration. 66, 2921-2925.

Koppenol, W.H., Butler, J., and Van Leeuwen, J.W., 1978. The Haber-Weiss cycle. Photochemistry Photobiology, 28(4–5):655–8 ed.

Krejci, D., Woschnak, A., Scharlemann, C., Ponweiser, C., 2011. Hydrogen Peroxide Decomposition for Micro Propulsion: Simulation and Experimental Verification. ASEE.

Kurniawan, T.A., and Lo, W.H., 2009. Removal of refractory compounds from stable landfill leachate using an integrated H2O2 oxidation treatment and GAC adsorption treatment. Water Research 43, no. 16: 4079 - 4091.

Lee, H.J., Ho, M.R., Bhuwan, M., Hsu, C.Y., Huang, M.S., Peng, H.L., Chang, H.Y., 2010. Enhancing ATP-based bacteria and biofilm detection by enzymatic pyrophosphate regeneration. Analytical Biochemistry.

Lucking, F., Koser, H., Jank, M., and Ritter, A, 1998. Iron powder, graphite and activated carbon as catalysts for the oxidation of 4- chlorophenol with hydrogen peroxide in aqueous solution. Water Res, 32(9):2607–14. ed.

Jans, U., and Hoigné, J., 1998. Activated carbon and carbon black catalyzed transformation of aqueous ozone into OH-radicals. Ozone: Science & Engineering. The Journal of the International Ozone Association 20: 67-90.

Jones, C.W., 1999. Application of Hydrogen Peroxide and Derivatives. The Royal Society of Chemistry.

Lide, Dr. C.R.C., 2006. Handbook of Chemistry and Physics. Boca Raton, FL: CRC Press, Taylor and Francis Group.

Linden, K.G., Mohseni, M., 2014. Comprehensive Water Quality and Purification, Advanced Oxidation Processes: Applications in Drinking Water Treatment. Earth Systems and Environmental Science.

Linden, K.G., Sharpless, C.M., Andrews, S.A., Atasi, K.Z., Korategere, V., and Stefan, M., 2005. Innovative UV Technologies to Oxidize Organic and Organoleptic Chemicals. London UK: IWA Publishing.

Li, J., 2013. Quenching H2O2 Residuals After UV/ H2O2 Drinking Water Treatment Using Granular Activated Carbon. Toronto.

McKay, G., Sjelin, B., Chagnon, M., Ishida, K.B., Mezyk, S.B., 2013. Kinetic study of the reactions between chloramine disinfectants and hydrogen peroxide: temperature dependence and reaction mechanism. Chemosphere 92 (11): 1417–1422.

Michaud, J.P., 1991. A citizen's guide to understanding and monitoring lakes and streams. Vol. 1. Department of Ecology publications office.

National Institute for Occupational Safety and Health (NIOSH), 2010, Revised March 2012. NIOSH pocket guide to chemical hazards: hydrogen peroxide.

Norit. GAC 300, 2013. Billerica: Norit.

Norit. Hydrodarco 3000, 2013. Billerica: Norit.

Ontario, Legislative Assembly of. Safe Drinking Water Act 2002. (Govt. of Ontario) 2002.

Philippe, S., and Figueiredo, J.L., 2009. Carbon Materials for Catalysis. Wiley.

Raffellini, S., Schenk, M., Guerrero, S., and Alzamora, S.M., 2011. Kinetics of Escherichia coli inactivation employing hydrogen peroxide at varying temperatures, pH and concentration. (Food Control) 22(6):920-32.

Rebeiro, R.S., Silva, A.M.T., Figueiredo, J.L., Faria, J.L., and Gomes, H.T., 2012. The influence of stucture and surface chemistry of carbon materials on the decomposition of hydrogen peroxide. Elsevier.

Rey, A., Zazo, J.A., Casas, J.A., Bahamonde, A. and Rodriguez, J.J., 2011. Influence of the structural and surface characteristics of activated carbon on the catalytic decomposition of hydrogen peroxide. Applied Catalysis A, General 402, 146–155 ed.

Robinson, R.A., and Stokes, R.H., 1968. Electrolyte solution. London: Butterworths.

Schlegel, H.G., 1977. Aeration without Air: Oxygen supply by hydrogen peroxide. Biotechnology Bioengineering.

Skibinski, B., Müller, S., Uhl, W., 2009. Removal of free and combined chlorine at GAC surfaces and impact on pool water quality. Swimming Pool & Spa International Conference. London: PWTAG.

Suidan, M.T., Sneyink, V.L., Schmitz, R.A., 1977. Reduction of aqueous free chlorine with granular activated carbon-pH and temperature effects. Environmental Science & Technology 11 (8): 785-789.

Urfer, D., Huck, P.M., 1997. Effect of Hydrogen Peroxide on Biologically Active Filters. Ozone Science and Engineering.

USATSDR. 2011. Medical Management guideleines for hydrogen peroxide. Atlanta, US.

Watts, M.J., Hofmann, R., Rosenfeldt, E.J. Low-pressure UV/Cl2 for advanced oxidation of taste and odor. Journal American Water Works Association, n.d.: 104(1), 47-48.

Weinstein, J., and Bielski, B.H.J., 1979. Kinetics of the interaction of perhydroxy and superoxide radicals with hydrogen peroxide, the Haber Weiss reaction. (Junior American Chemial Society) 101(1):58–62.

Wells, A.F., 1984. Structural Inorganic Chemistry. Oxford, U.K.: Oxford University Press.

Appendix A

A.1.1 K values of Virgin ADCAT

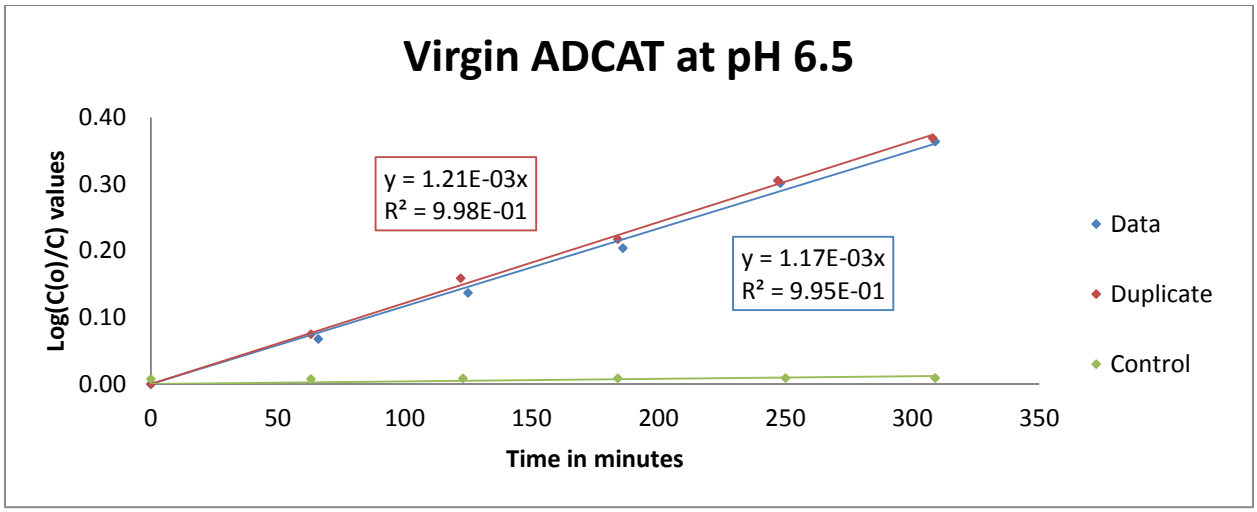

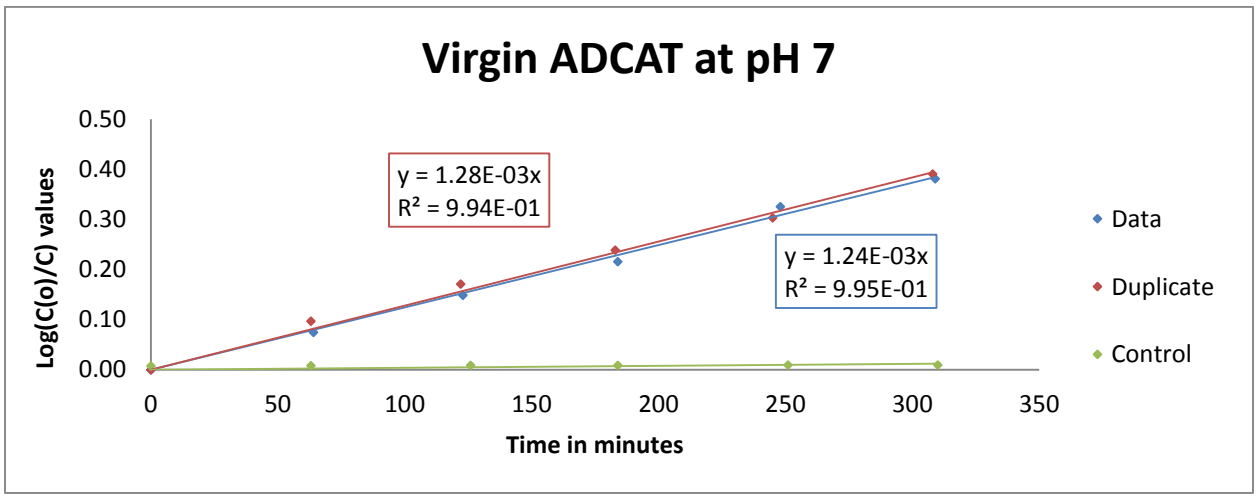

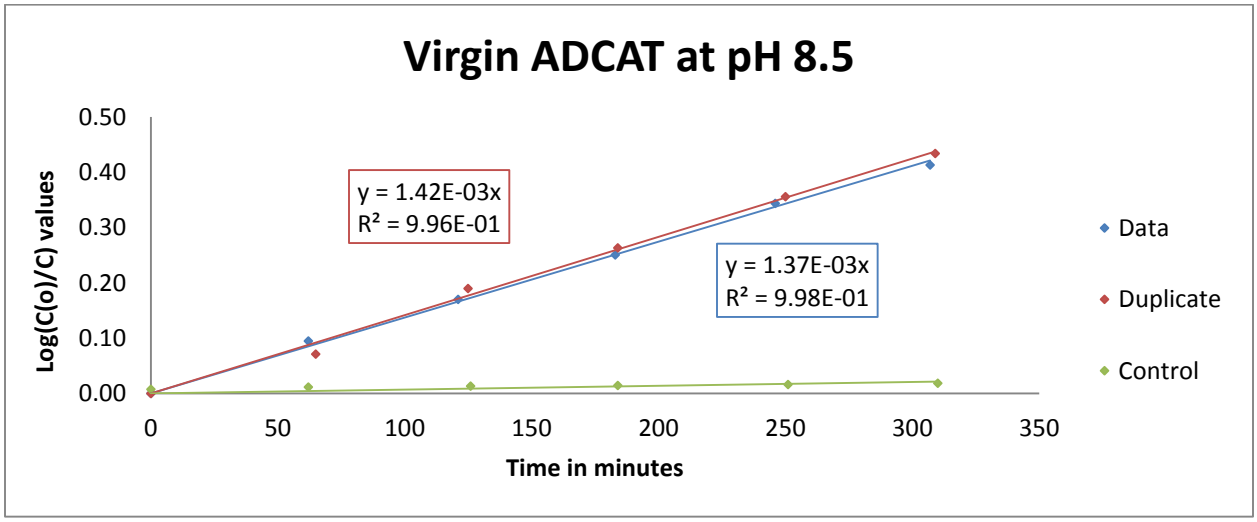

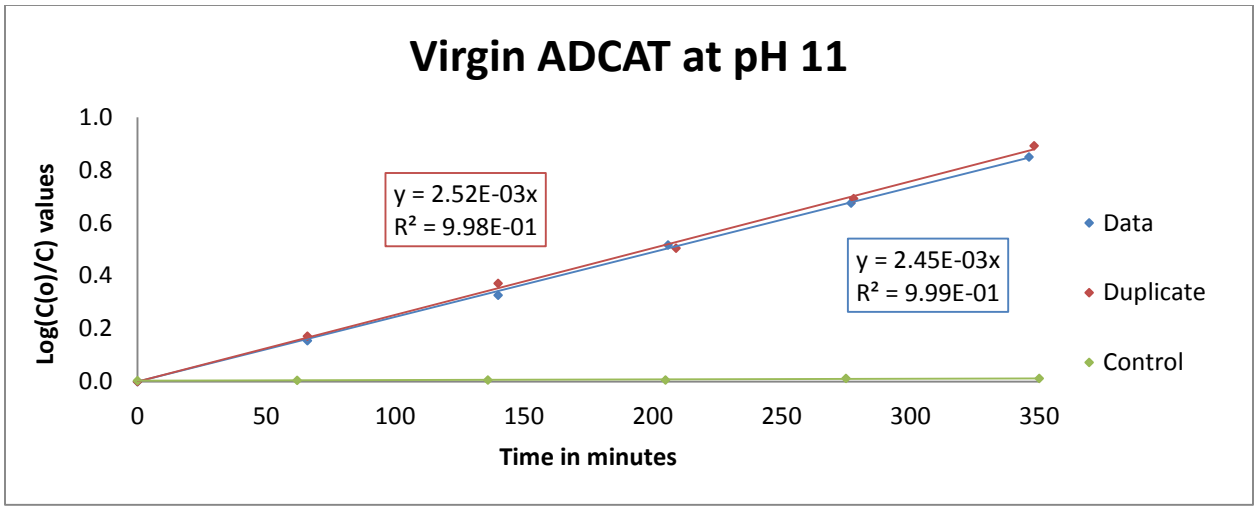
Virgin ADCAT at pH 11
Log(C(o)/C) values
1.0
0.8
0.6
0.4
0.2
0.0
y = 2.52E-03x
R² = 9.98E-01
y = 2.45E-03x
R² = 9.99E-01
0
50
100
150
200
250
300
350
Time in minutes
Data
Duplicate
Control

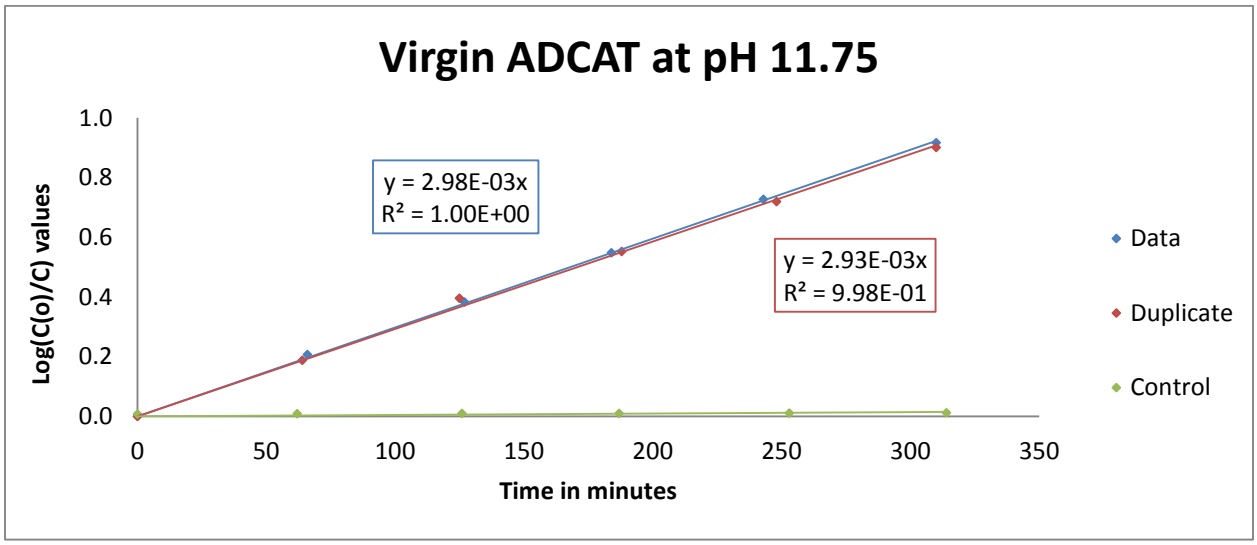
Virgin ADCAT at pH 11.75
Log(C(o)/C) values
1.0
0.8
0.6
0.4
0.2
0.0
y = 2.98E-03x
R² = 1.00E+00
y = 2.93E-03x
R² = 9.98E-01
0
50
100
150
200
250
300
350
Time in minutes
Data
Duplicate
Control

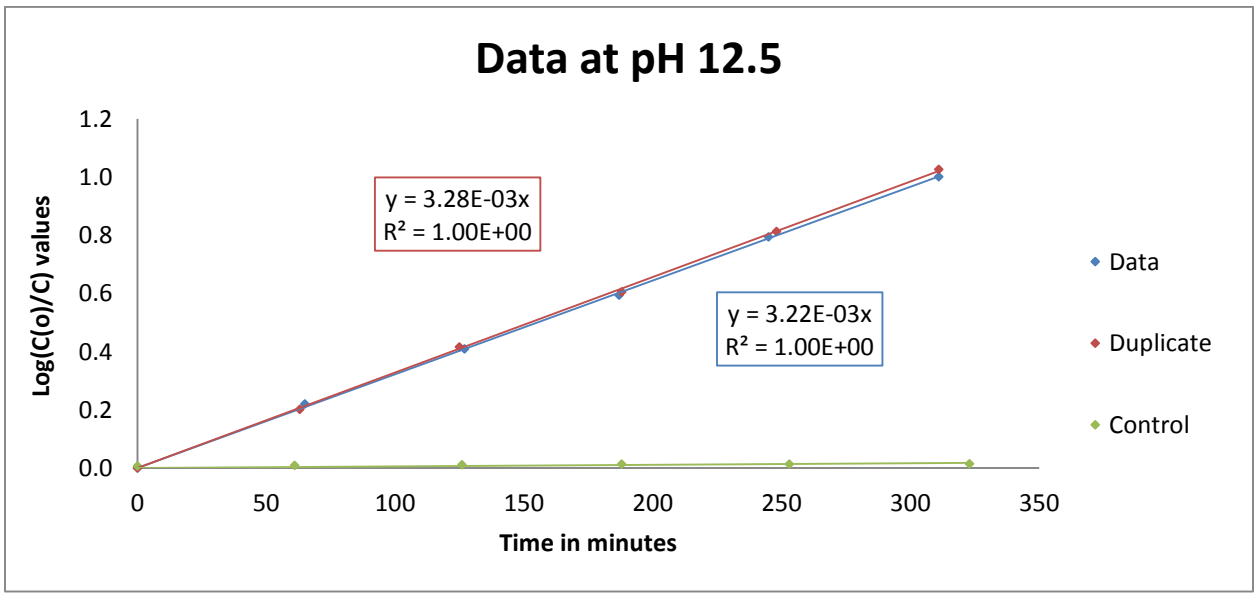
Data at pH 12.5
Log(C(o)/C) values
1.2
1.0
0.8
0.6
0.4
0.2
0.0
y = 3.28E-03x
R² = 1.00E+00
y = 3.22E-03x
R² = 1.00E+00
0
50
100
150
200
250
300
350
Time in minutes
Data
Duplicate
Control

A.1.2 K values of ADCAT aged with NOM

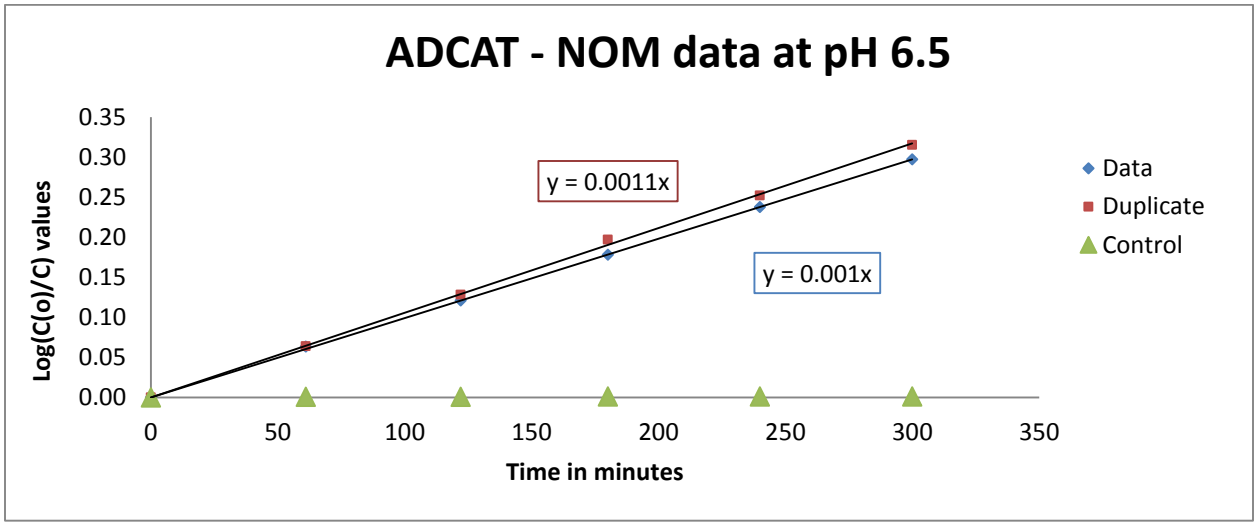

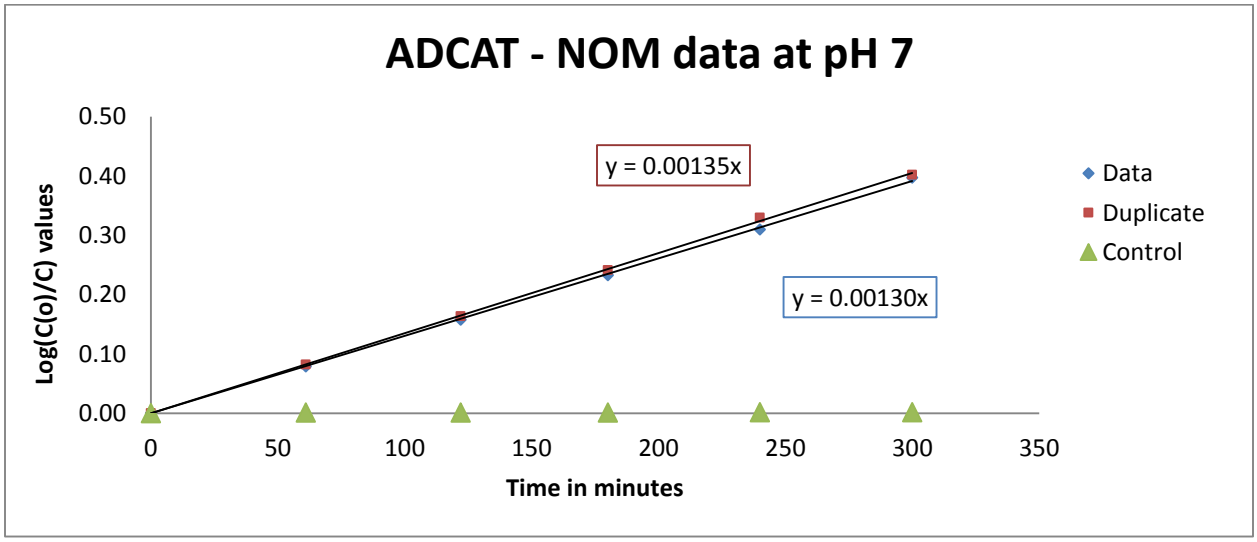

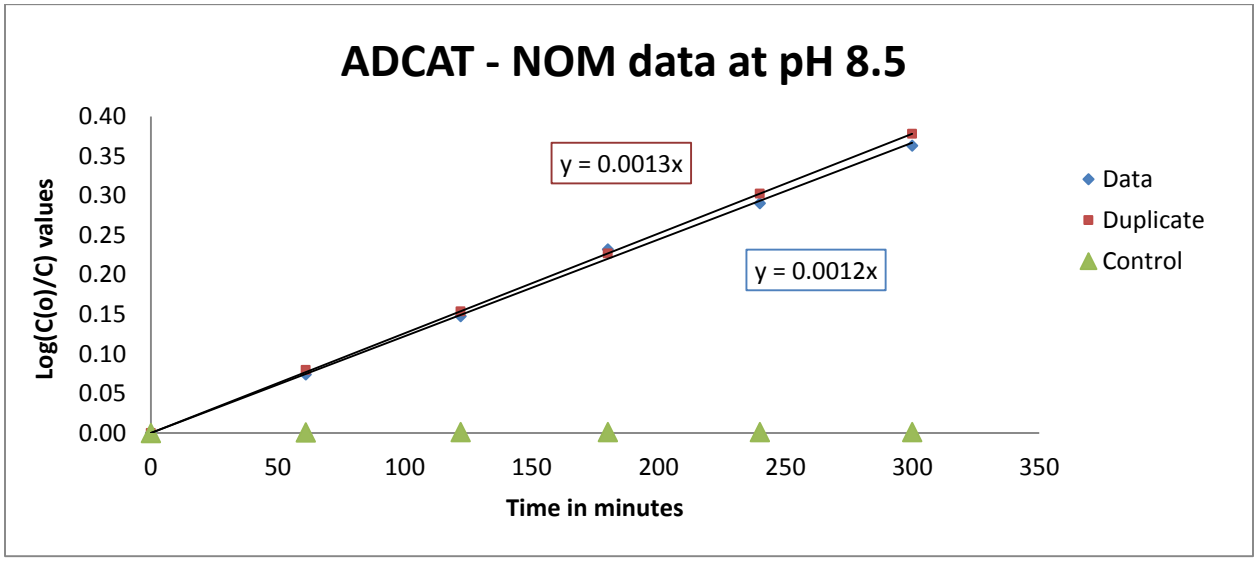

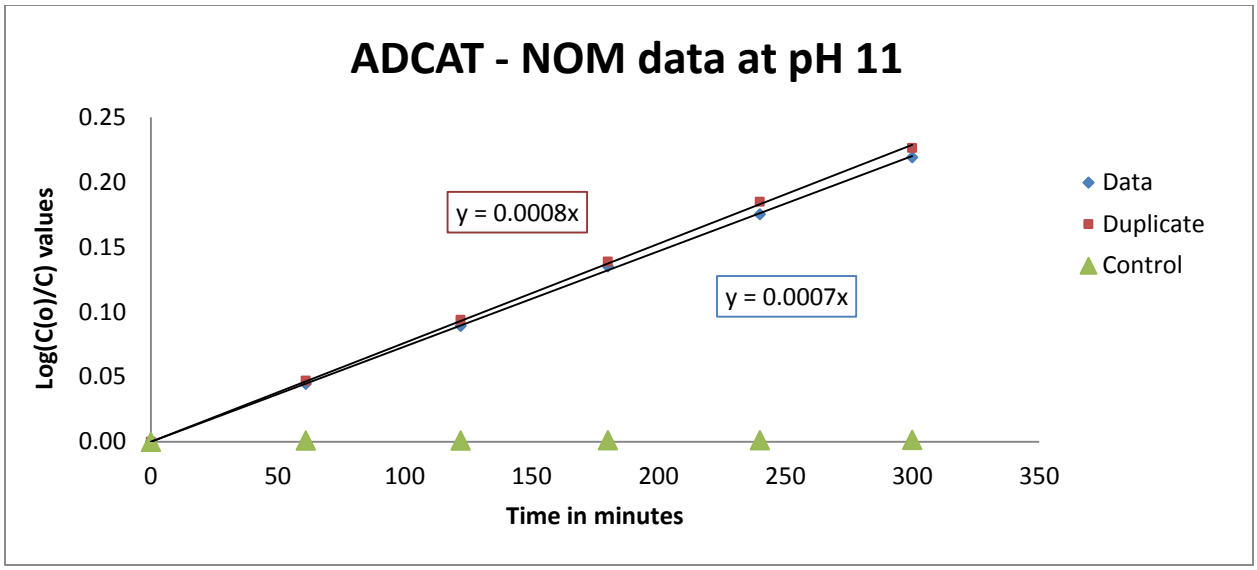
ADCAT - NOM data at pH 11
Log(C(o)/C) values
0.25
0.20
0.15
0.10
0.05
0.00
y = 0.0008x
y = 0.0007x
Data
Duplicate
Control
0
50
100
150
200
250
300
350
Time in minutes

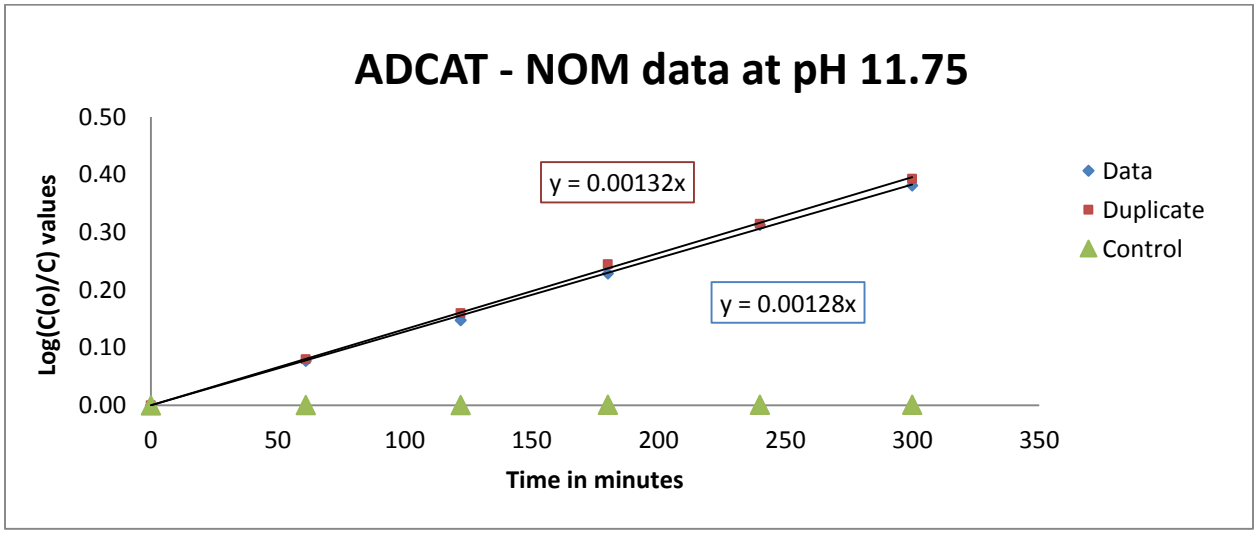
ADCAT - NOM data at pH 11.75
Log(C(o)/C) values
0.50
0.40
0.30
0.20
0.10
0.00
y = 0.00132x
y = 0.00128x
Data
Duplicate
Control
0
50
100
150
200
250
300
350
Time in minutes

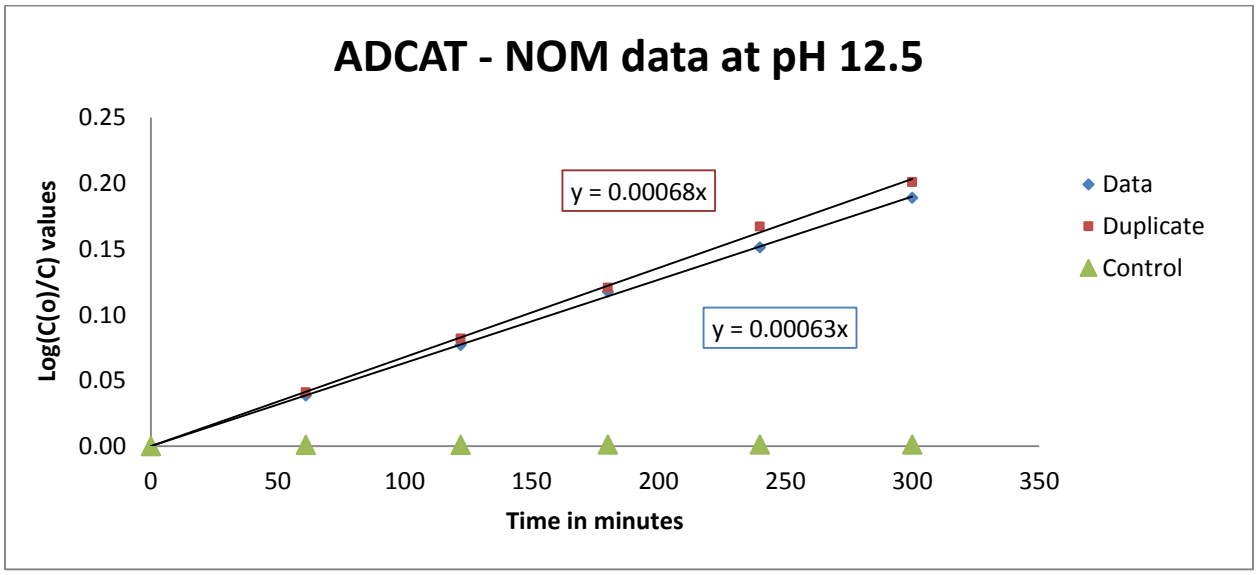
ADCAT - NOM data at pH 12.5
Log(C(o)/C) values
0.25
0.20
0.15
0.10
0.05
0.00
y = 0.00068x
y = 0.00063x
Data
Duplicate
Control
0
50
100
150
200
250
300
350
Time in minutes

A.1.3 K values of ADCAT aged with NOM + H2O2

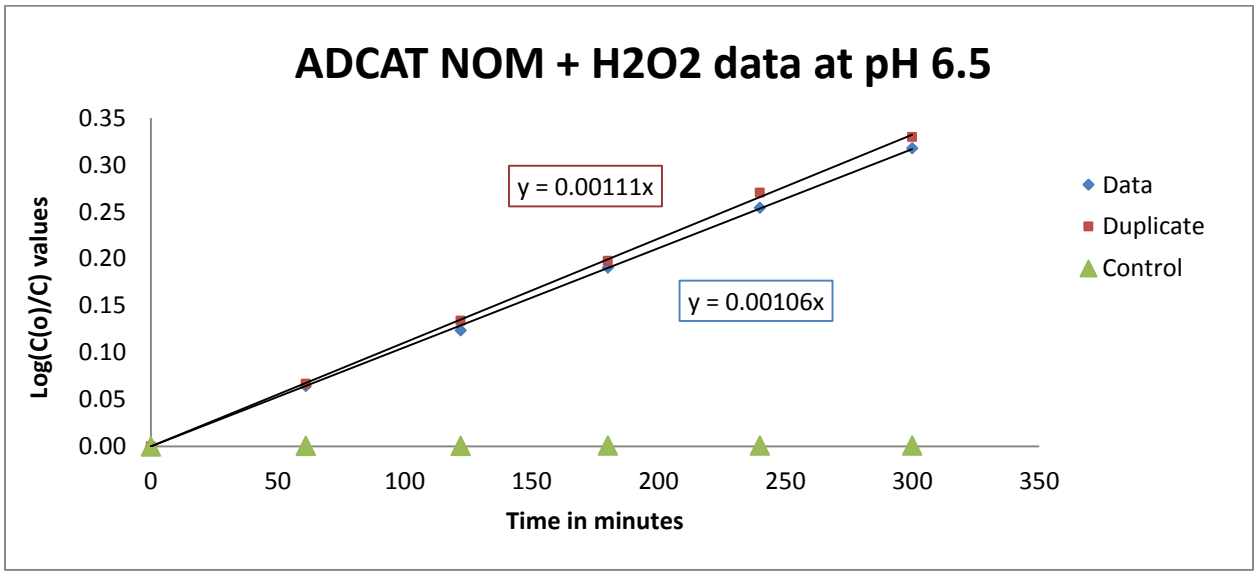

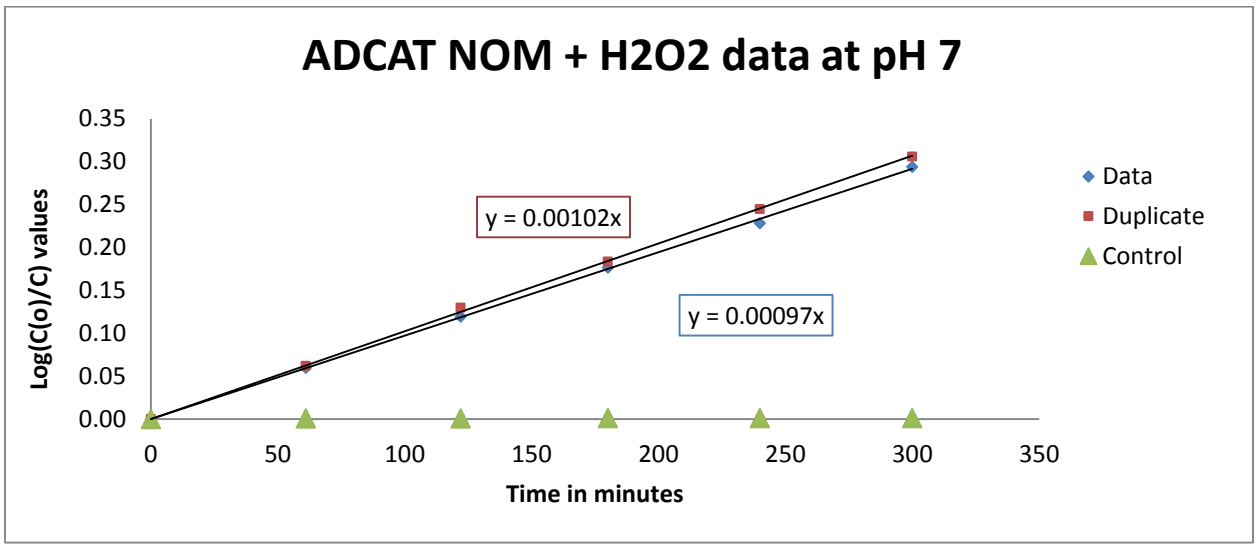

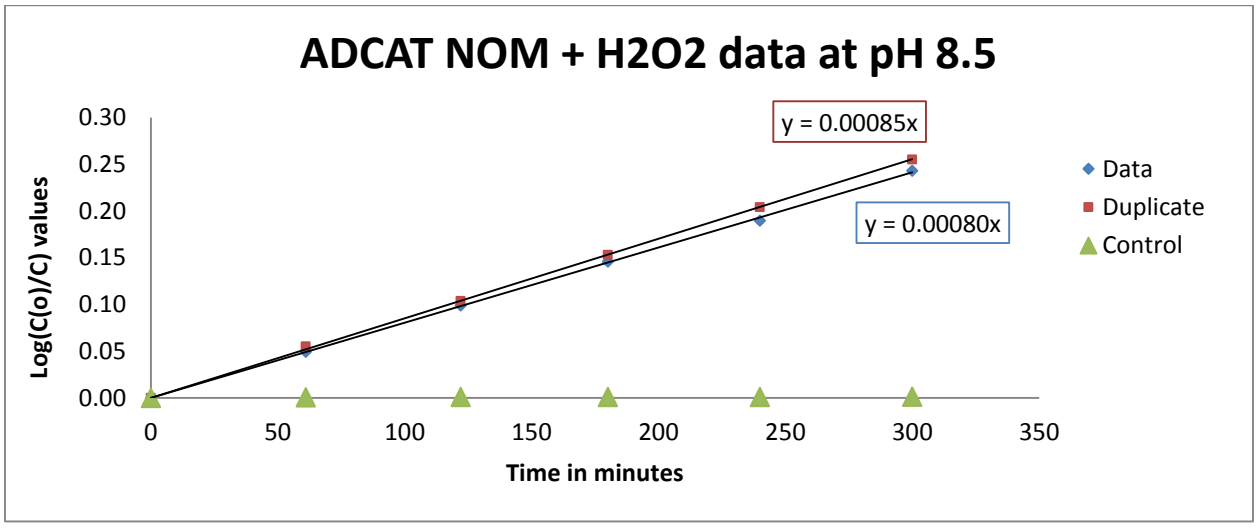

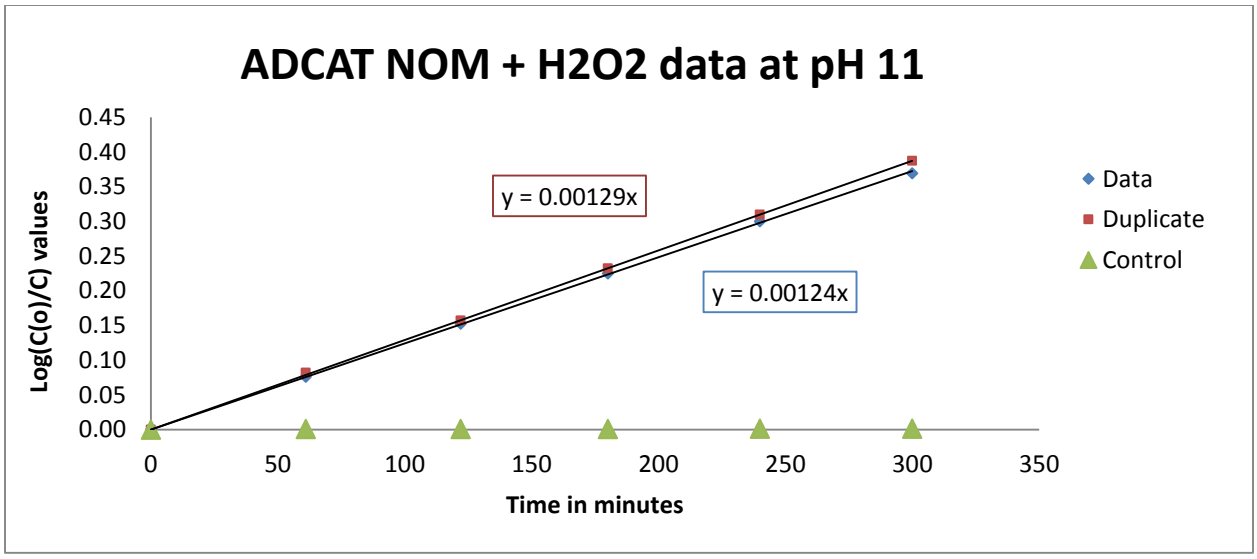
ADCAT NOM + H2O2 data at pH 11
Log(C(o)/C) values
0.45
0.40
0.35
0.30
0.25
0.20
0.15
0.10
0.05
0.00
y = 0.00129x
y = 0.00124x
Data
Duplicate
Control
0
50
100
150
200
250
300
350
Time in minutes

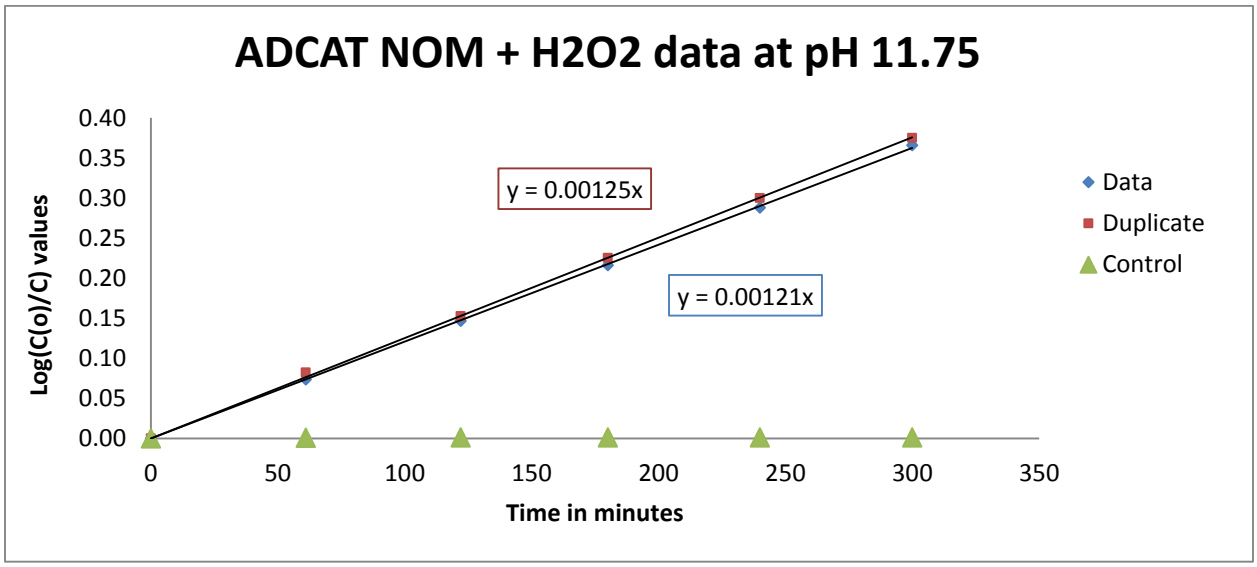
ADCAT NOM + H2O2 data at pH 11.75
Log(C(o)/C) values
0.40
0.35
0.30
0.25
0.20
0.15
0.10
0.05
0.00
y = 0.00125x
y = 0.00121x
Data
Duplicate
Control
0
50
100
150
200
250
300
350
Time in minutes

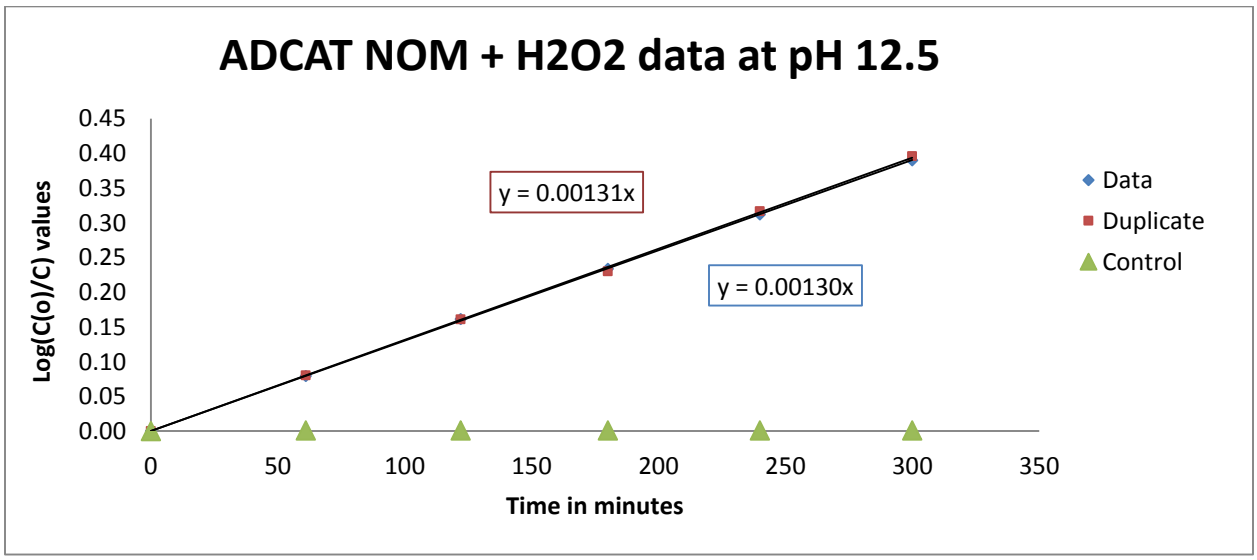
ADCAT NOM + H2O2 data at pH 12.5
Log(C(o)/C) values
0.45
0.40
0.35
0.30
0.25
0.20
0.15
0.10
0.05
0.00
y = 0.00131x
y = 0.00130x
Data
Duplicate
Control
0
50
100
150
200
250
300
350
Time in minutes

A.2.1 K values of Virgin Centaur

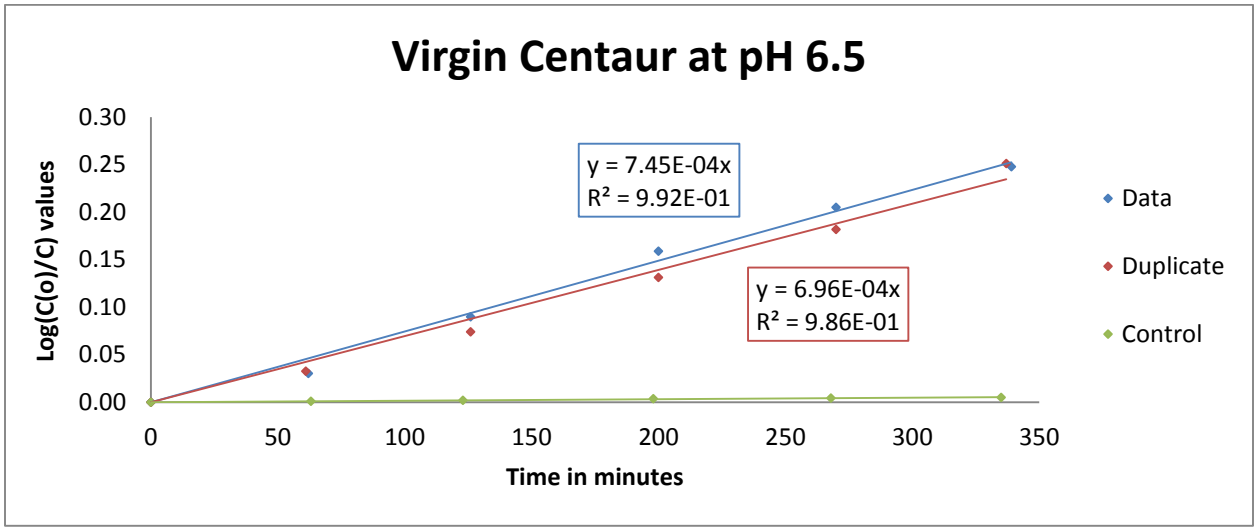

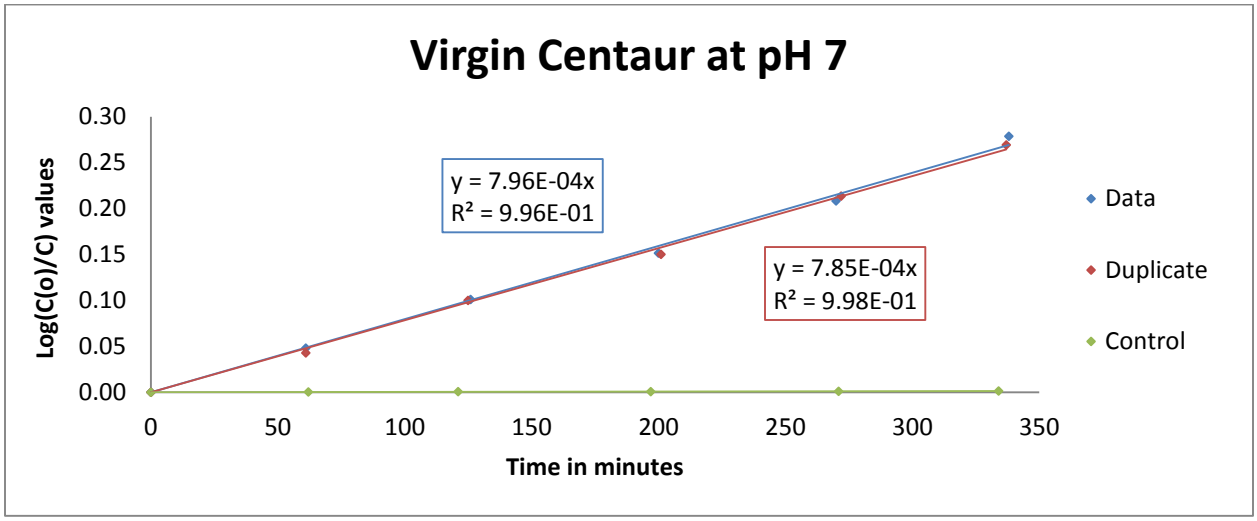

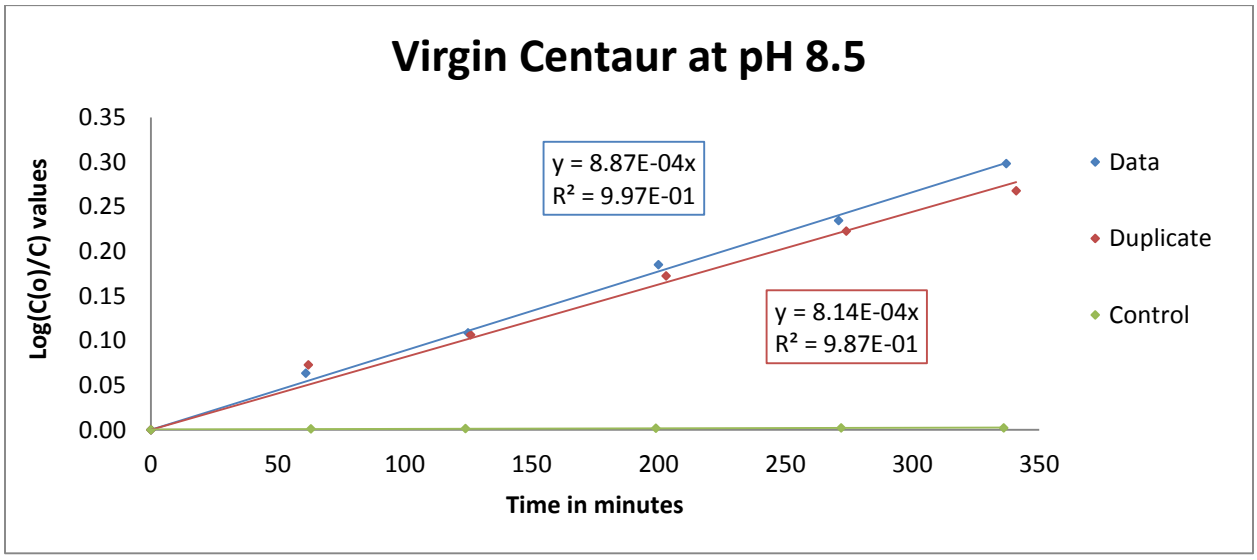

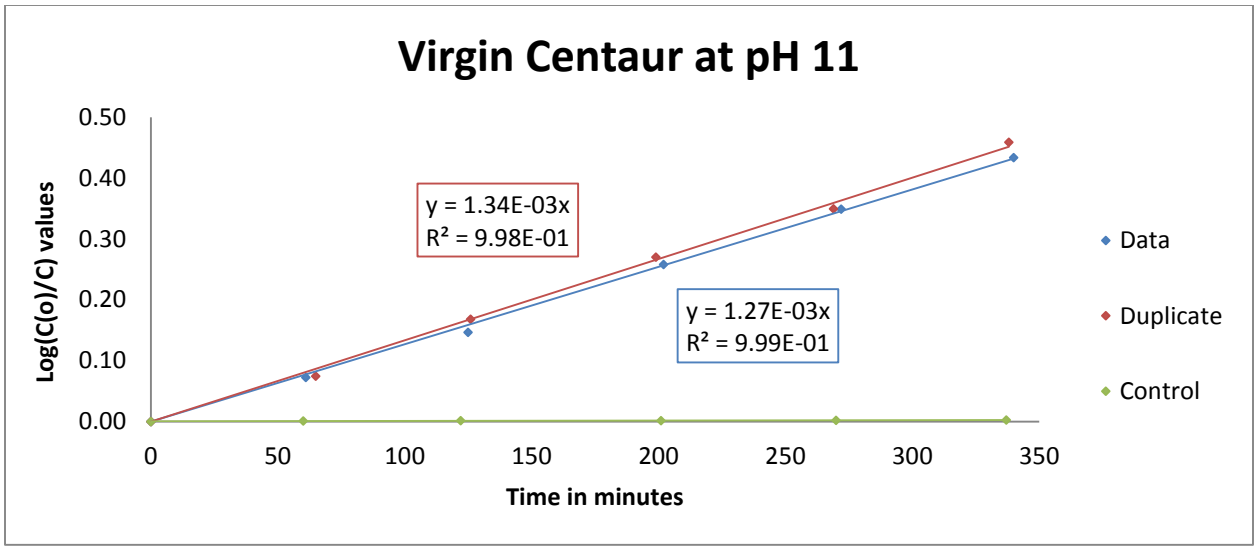
Virgin Centaur at pH 11
Log(C(o)/C) values
0.50
0.40
0.30
0.20
0.10
0.00
0
50
100
150
200
250
300
350
Time in minutes
y = 1.34E-03x
R² = 9.98E-01
y = 1.27E-03x
R² = 9.99E-01
Data
Duplicate
Control

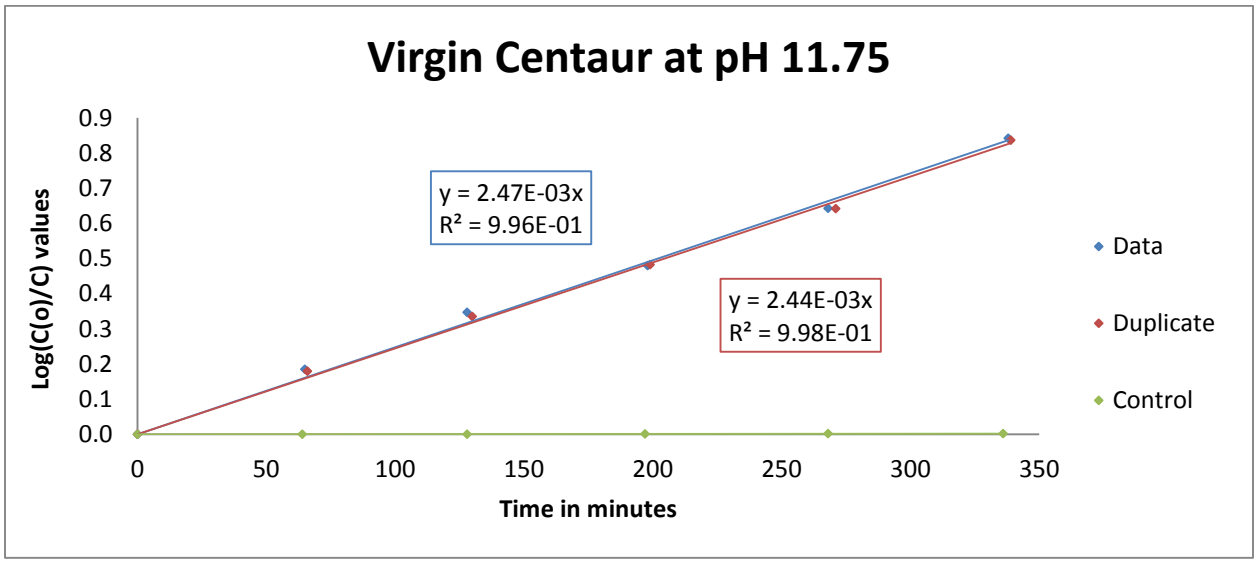
Virgin Centaur at pH 11.75
Log(C(o)/C) values
0.9
0.8
0.7
0.6
0.5
0.4
0.3
0.2
0.1
0.0
0
50
100
150
200
250
300
350
Time in minutes
y = 2.47E-03x
R² = 9.96E-01
y = 2.44E-03x
R² = 9.98E-01
Data
Duplicate
Control

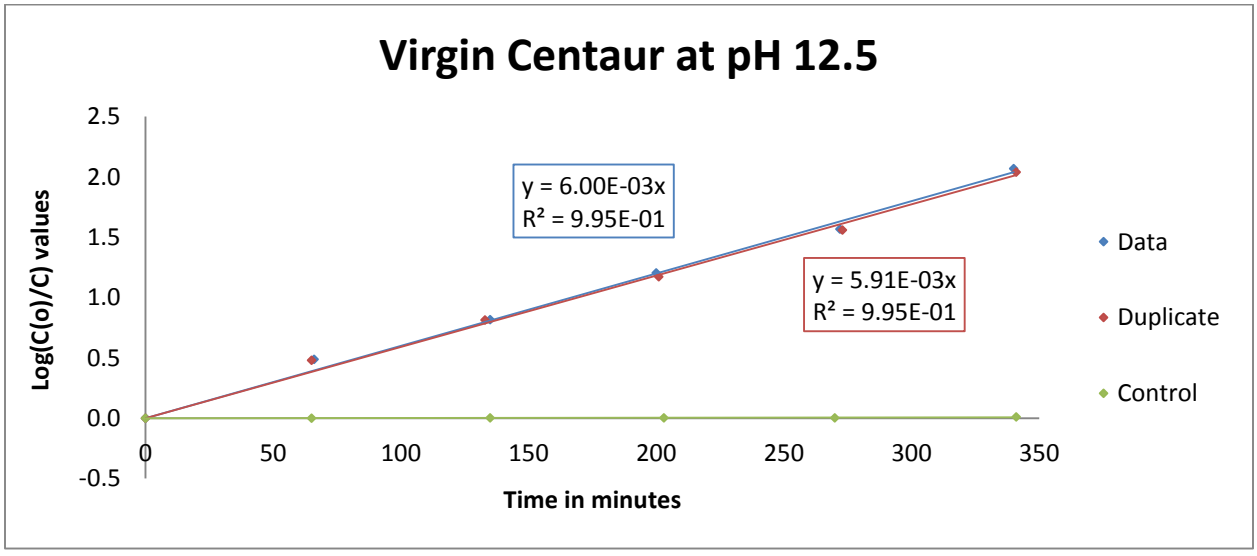
Virgin Centaur at pH 12.5
Log(C(o)/C) values
2.5
2.0
1.5
1.0
0.5
0.0
-0.5
0
50
100
150
200
250
300
350
Time in minutes
y = 6.00E-03x
R² = 9.95E-01
y = 5.91E-03x
R² = 9.95E-01
Data
Duplicate
Control

A.2.2 K values of Centaur aged with NOM

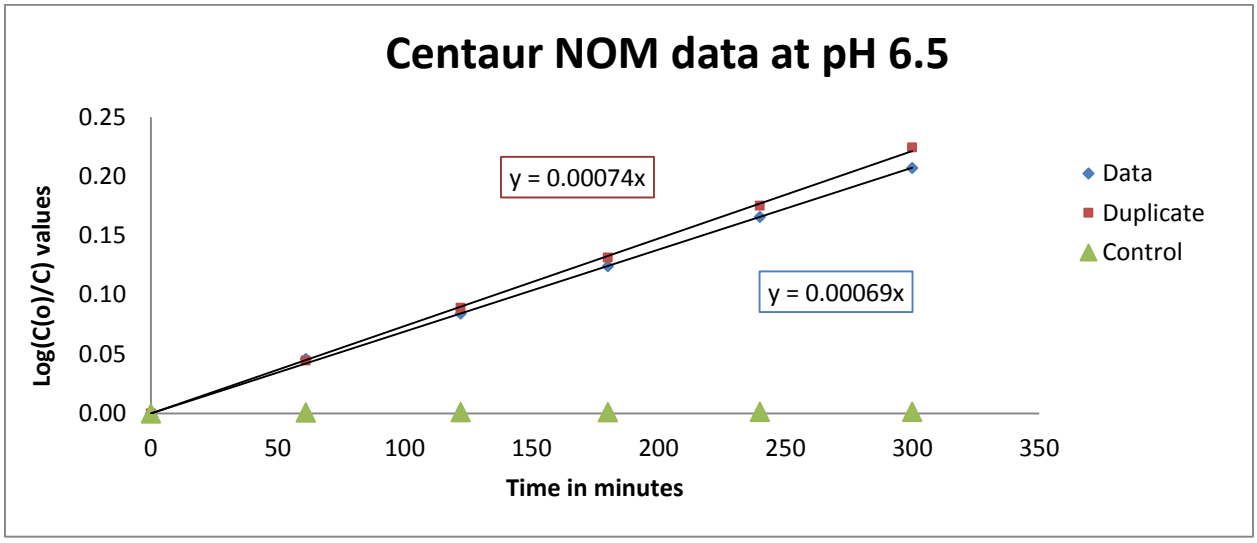

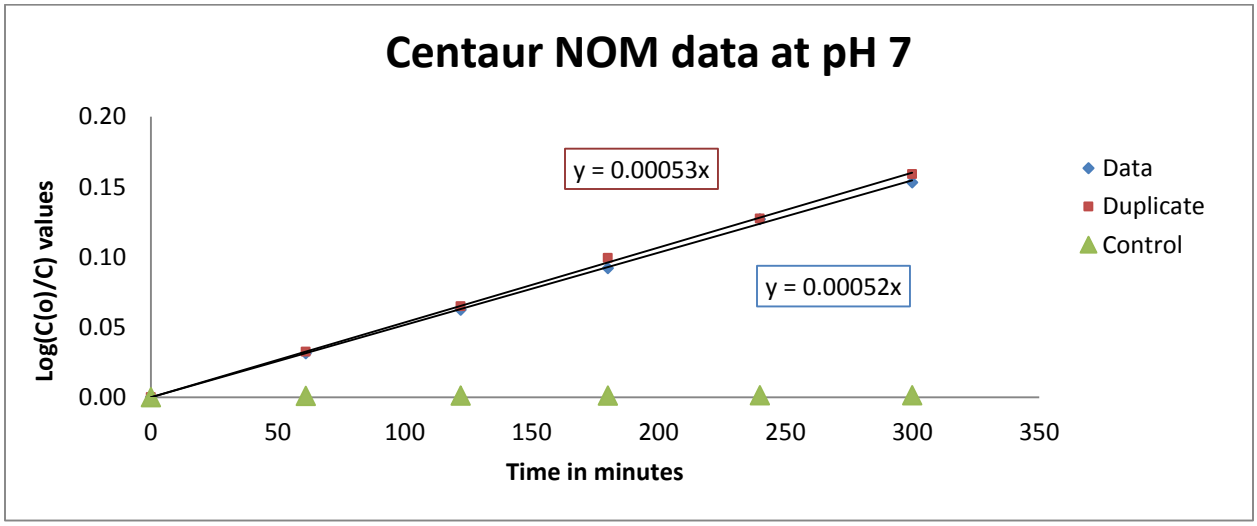

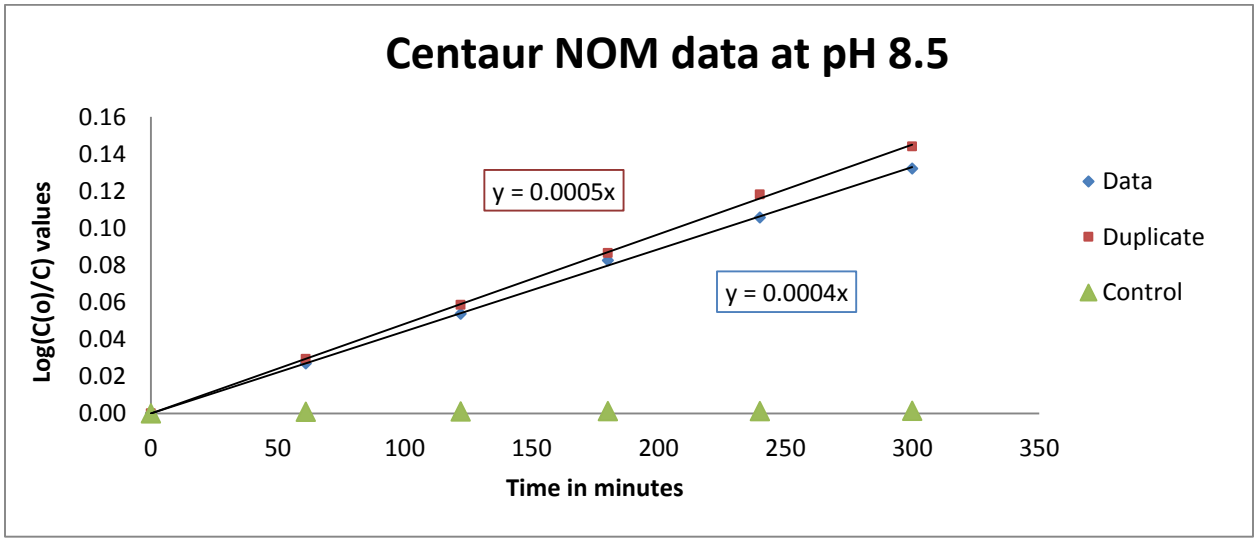

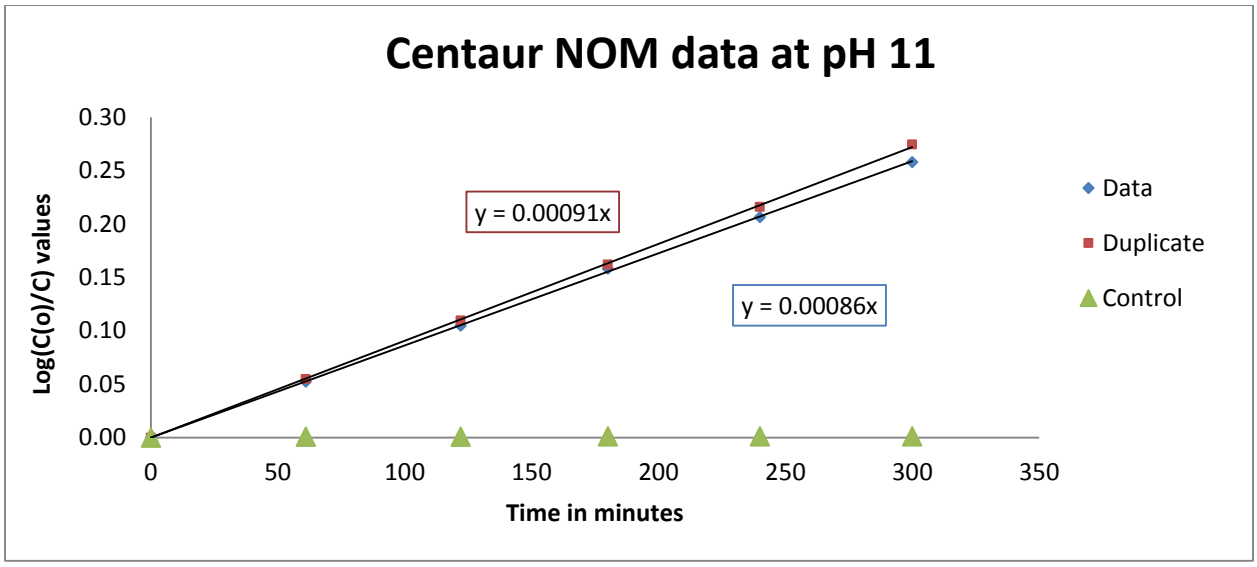
Centaur NOM data at pH 11
Log(C(o)/C) values
0.30
0.25
0.20
0.15
0.10
0.05
0.00
y = 0.00091x
y = 0.00086x
0
50
100
150
200
250
300
350
Time in minutes
Data
Duplicate
Control

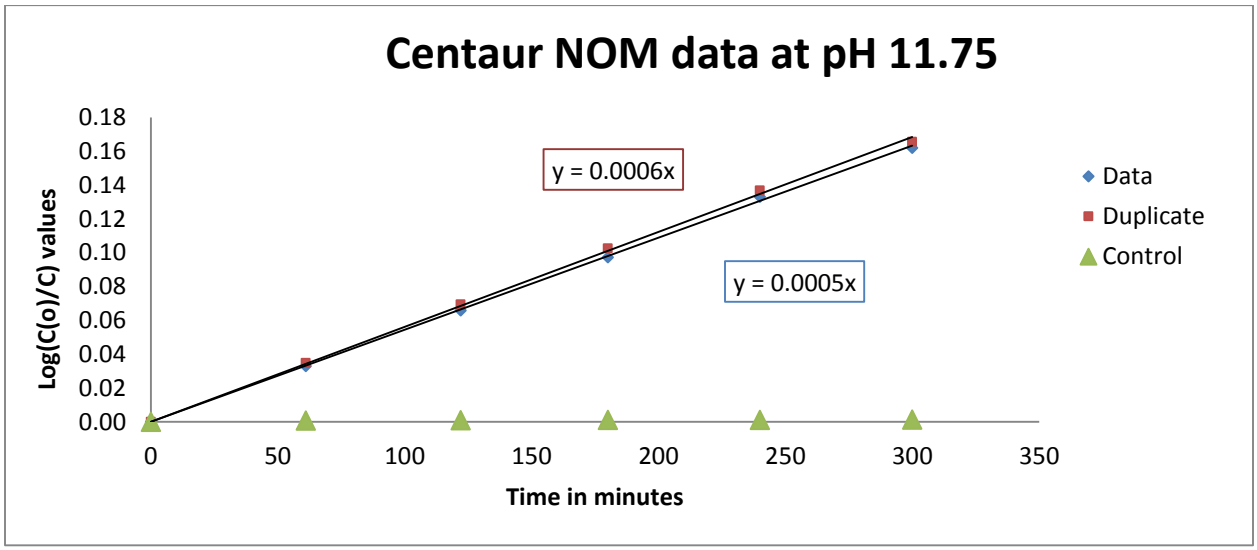
Centaur NOM data at pH 11.75
Log(C(o)/C) values
0.18
0.16
0.14
0.12
0.10
0.08
0.06
0.04
0.02
0.00
y = 0.0006x
y = 0.0005x
0
50
100
150
200
250
300
350
Time in minutes
Data
Duplicate
Control

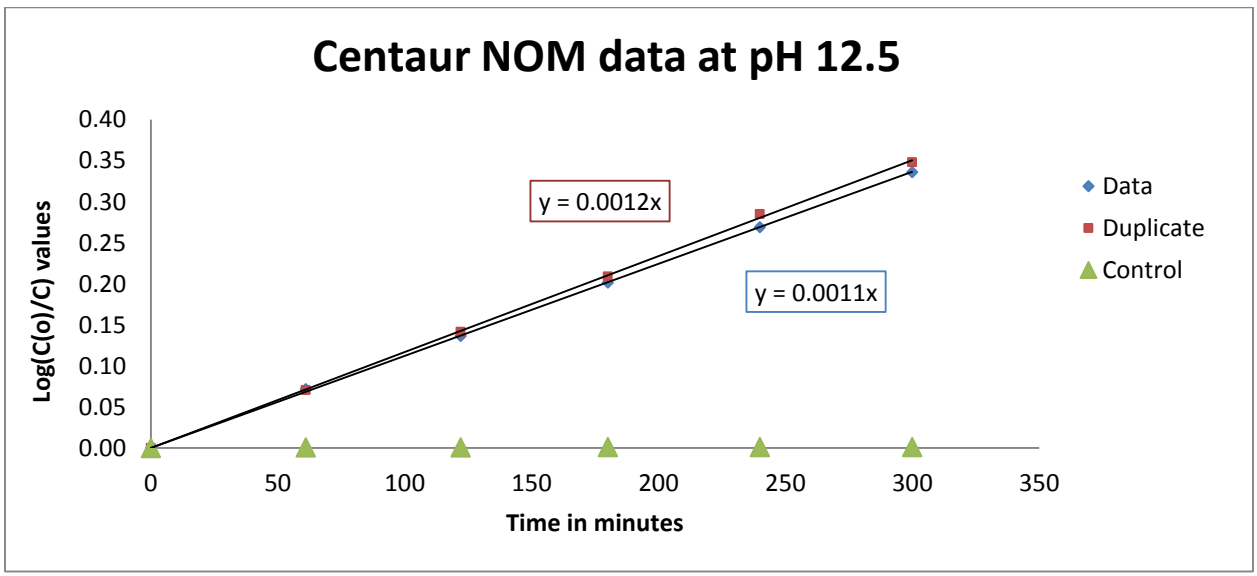
Centaur NOM data at pH 12.5
Log(C(o)/C) values
0.40
0.35
0.30
0.25
0.20
0.15
0.10
0.05
0.00
y = 0.0012x
y = 0.0011x
0
50
100
150
200
250
300
350
Time in minutes
Data
Duplicate
Control

A.2.3 K values of Centaur aged with NOM + H_2O_2

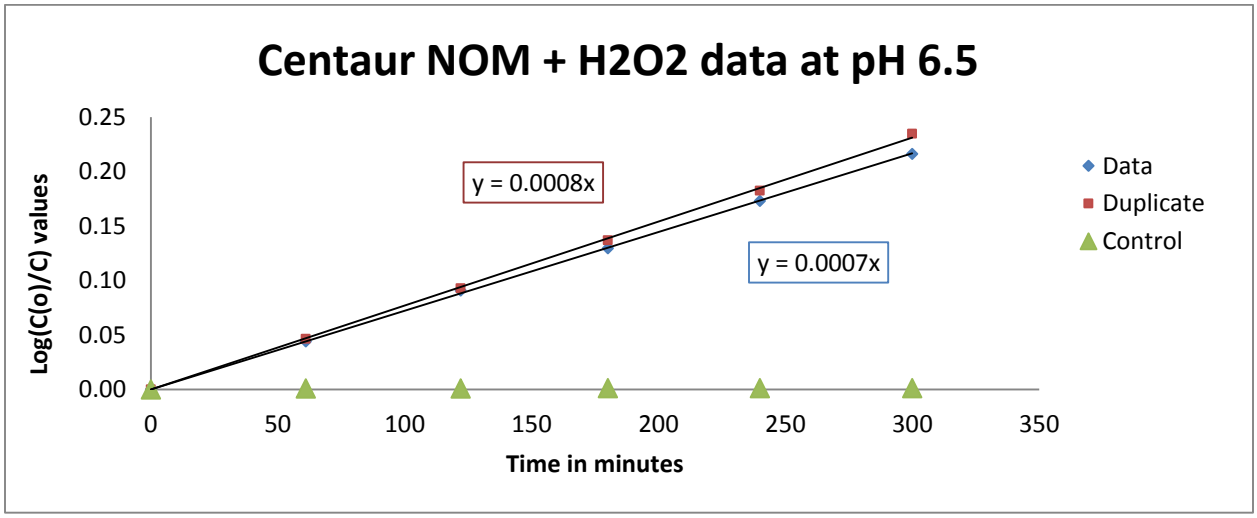

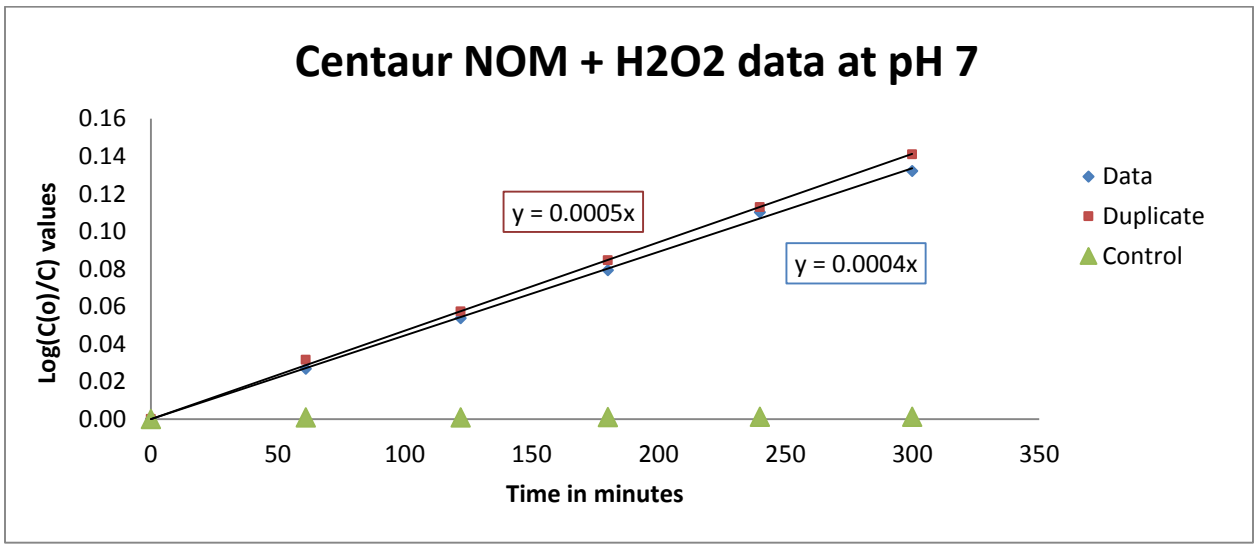

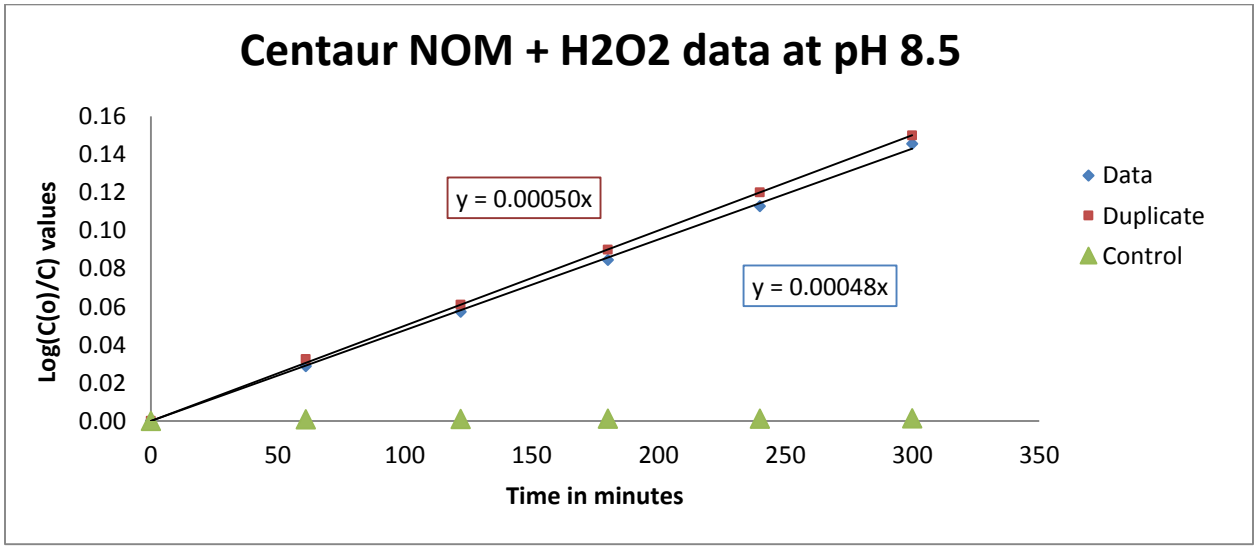

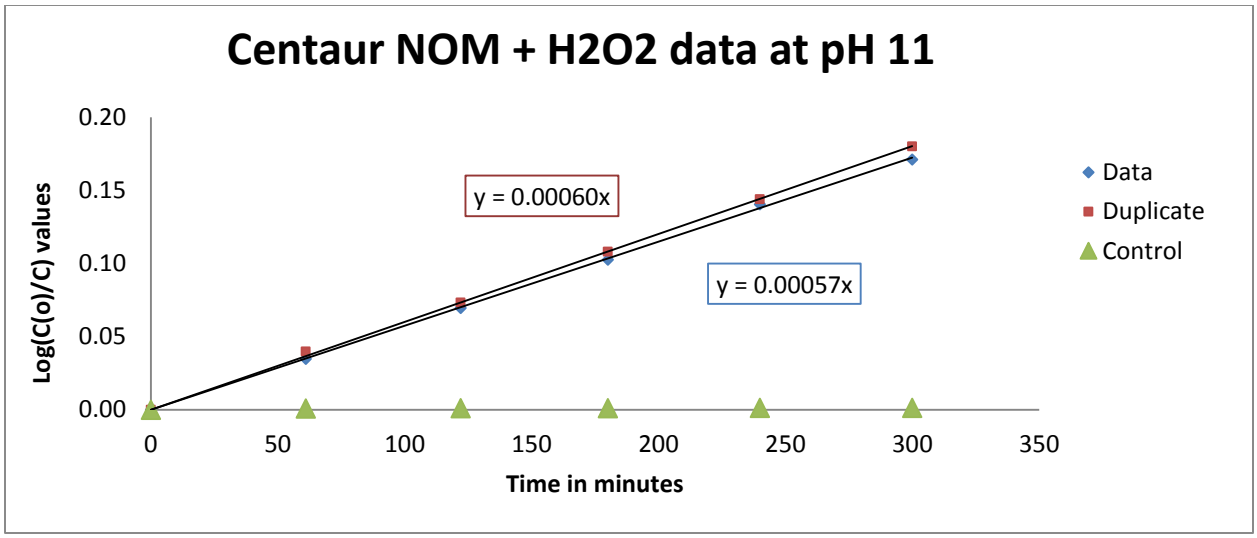
Centaur NOM + H2O2 data at pH 11
Log(C(o)/C) values
0.20
0.15
0.10
0.05
0.00
y = 0.00060x
y = 0.00057x
0
50
100
150
200
250
300
350
Time in minutes
Data
Duplicate
Control

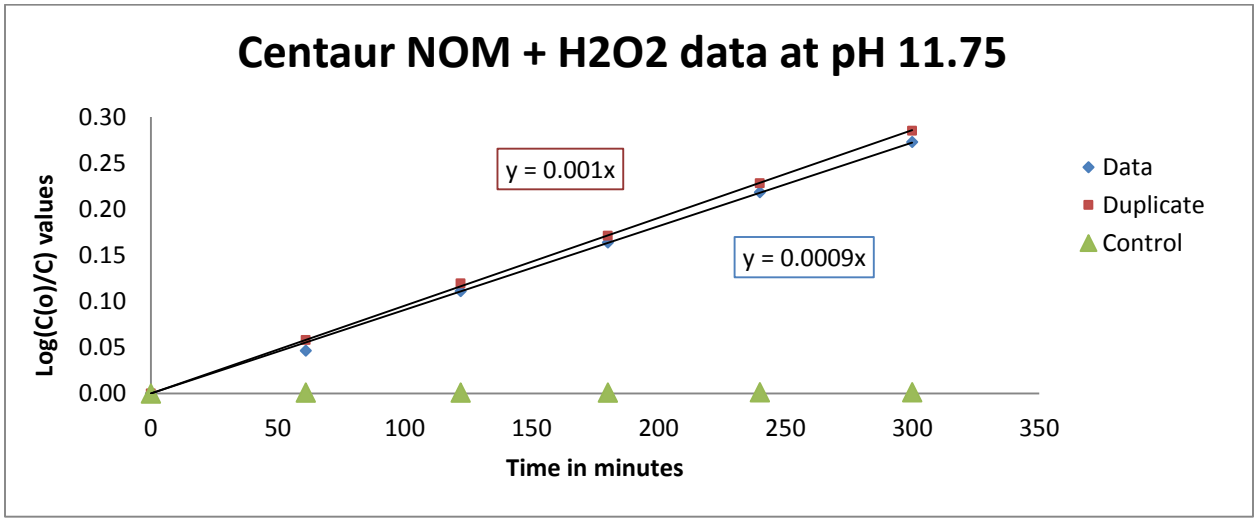
Centaur NOM + H2O2 data at pH 11.75
Log(C(o)/C) values
0.30
0.25
0.20
0.15
0.10
0.05
0.00
y = 0.001x
y = 0.0009x
0
50
100
150
200
250
300
350
Time in minutes
Data
Duplicate
Control

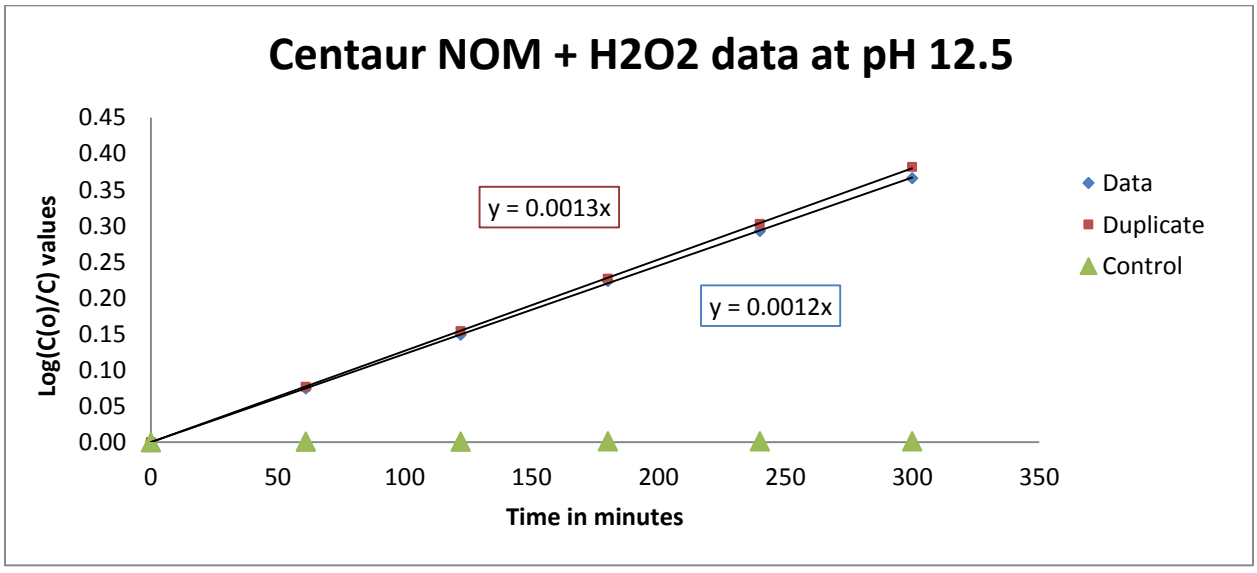
Centaur NOM + H2O2 data at pH 12.5
Log(C(o)/C) values
0.45
0.40
0.35
0.30
0.25
0.20
0.15
0.10
0.05
0.00
y = 0.0013x
y = 0.0012x
0
50
100
150
200
250
300
350
Time in minutes
Data
Duplicate
Control

A.3.1 K values of Virgin F-300

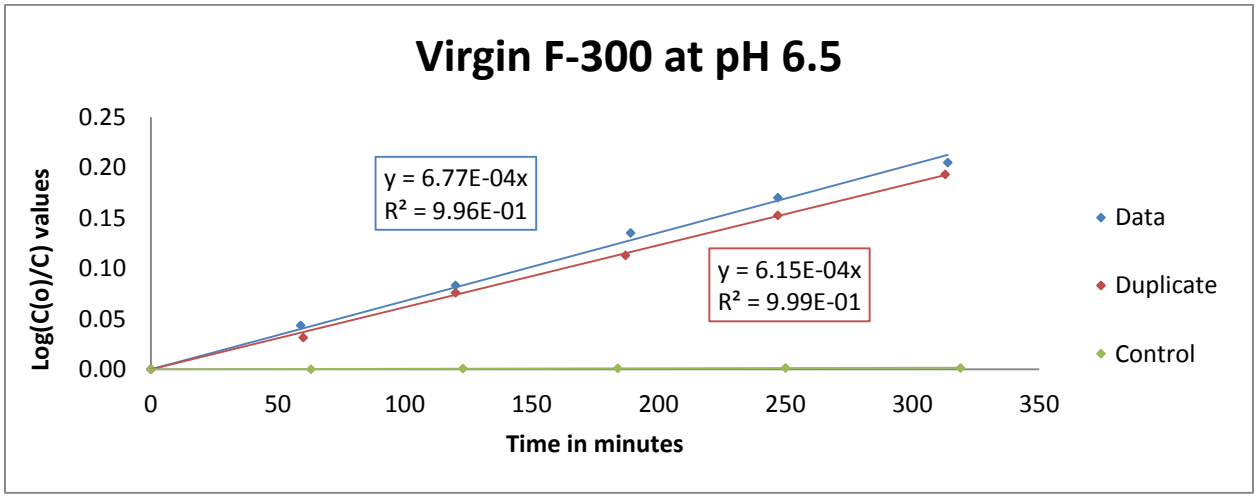

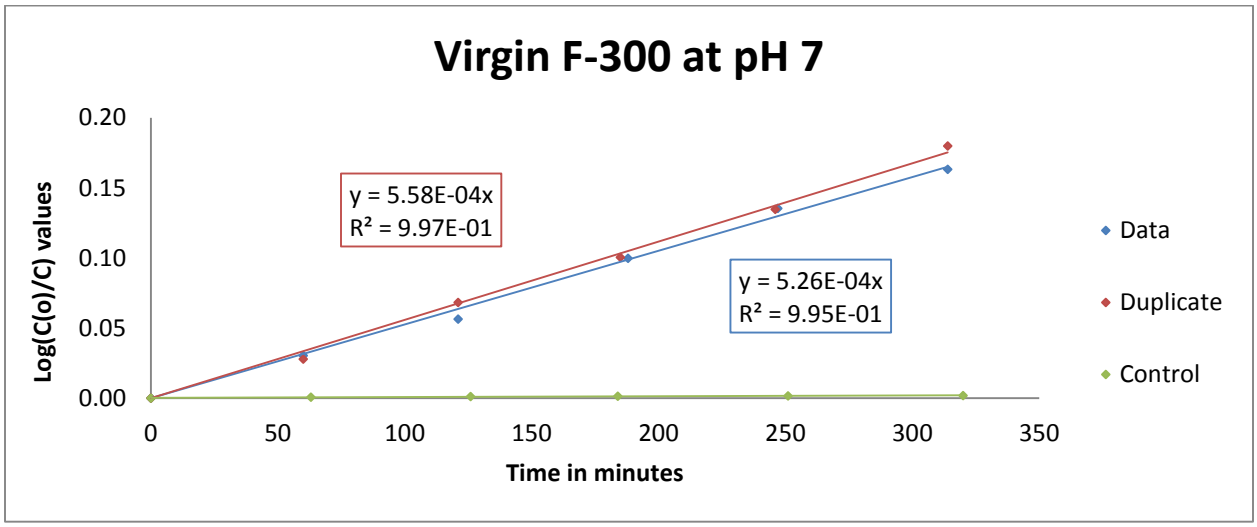

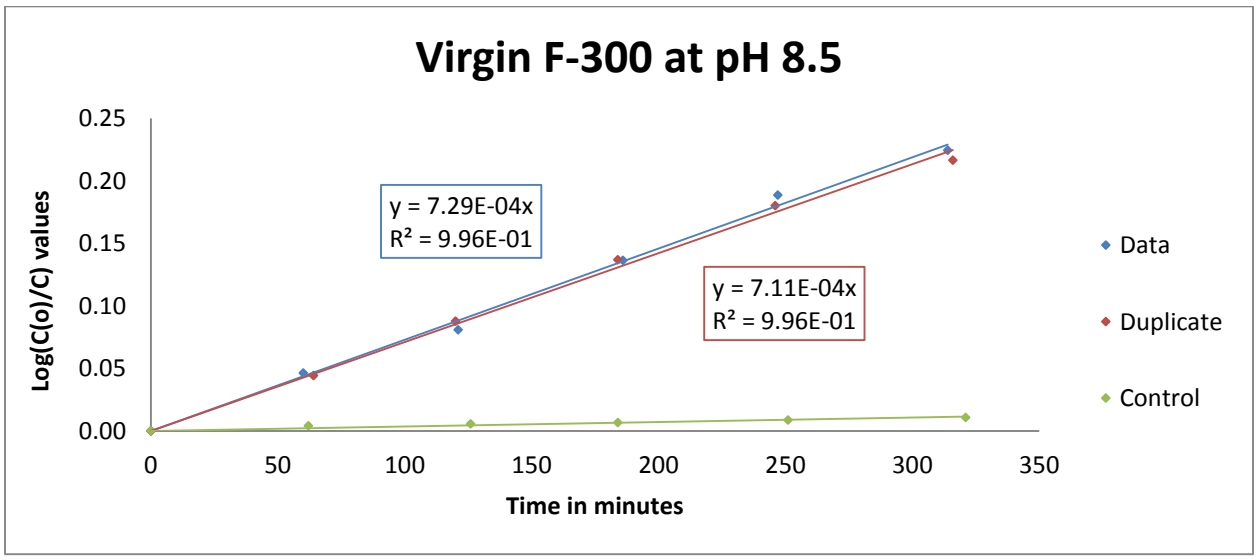

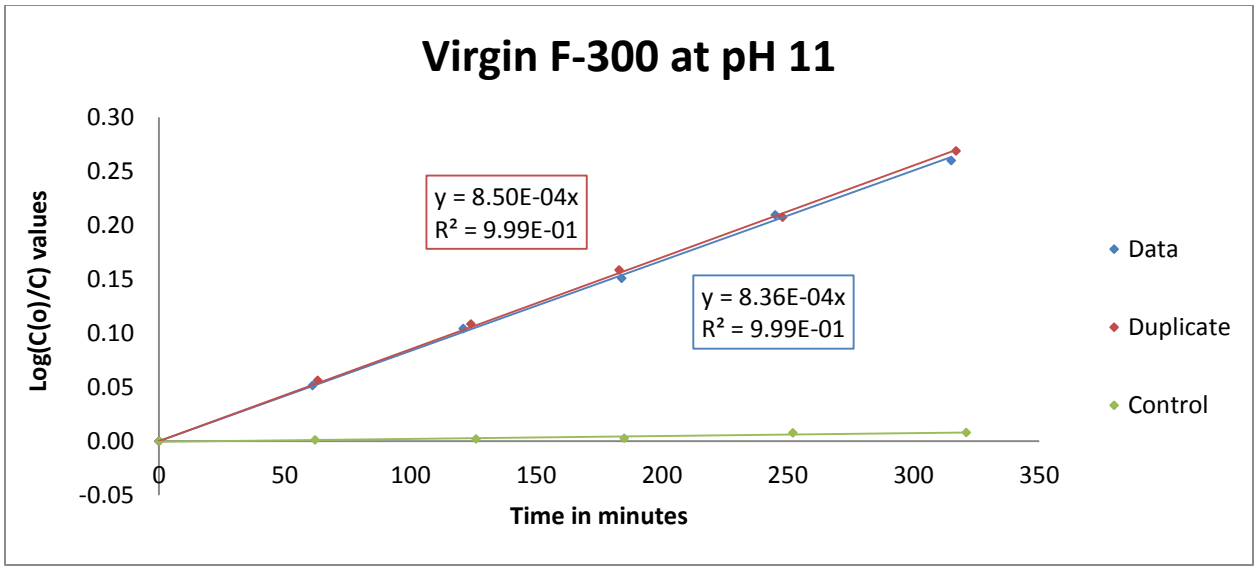
Virgin F-300 at pH 11
Log(C(o)/C) values
0.30
0.25
0.20
0.15
0.10
0.05
0.00
-0.05
0
50
100
150
200
250
300
350
Time in minutes
y = 8.50E-04x
R² = 9.99E-01
y = 8.36E-04x
R² = 9.99E-01
Data
Duplicate
Control

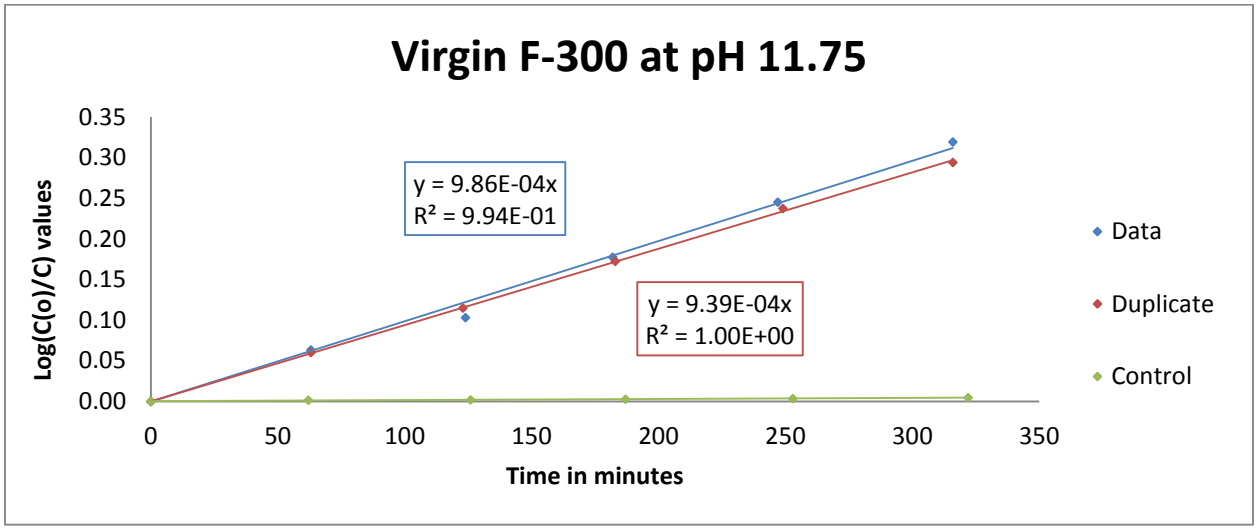
Virgin F-300 at pH 11.75
Log(C(o)/C) values
0.35
0.30
0.25
0.20
0.15
0.10
0.05
0.00
0
50
100
150
200
250
300
350
Time in minutes
y = 9.86E-04x
R² = 9.94E-01
y = 9.39E-04x
R² = 1.00E+00
Data
Duplicate
Control

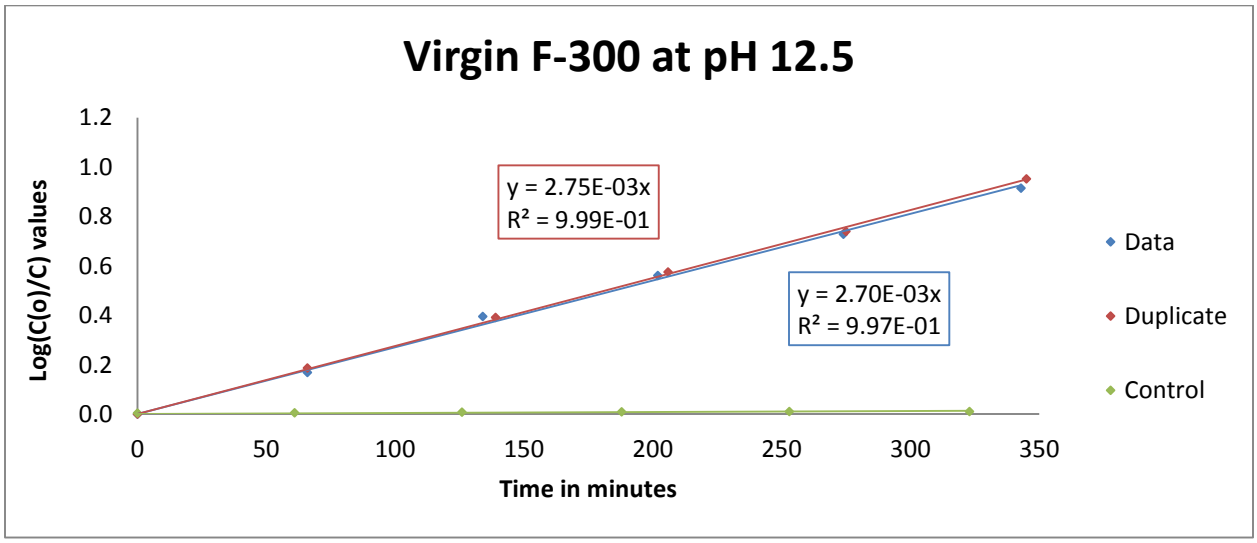
Virgin F-300 at pH 12.5
Log(C(o)/C) values
1.2
1.0
0.8
0.6
0.4
0.2
0.0
0
50
100
150
200
250
300
350
Time in minutes
y = 2.75E-03x
R² = 9.99E-01
y = 2.70E-03x
R² = 9.97E-01
Data
Duplicate
Control

A.3.2 K values of F-300 aged with NOM

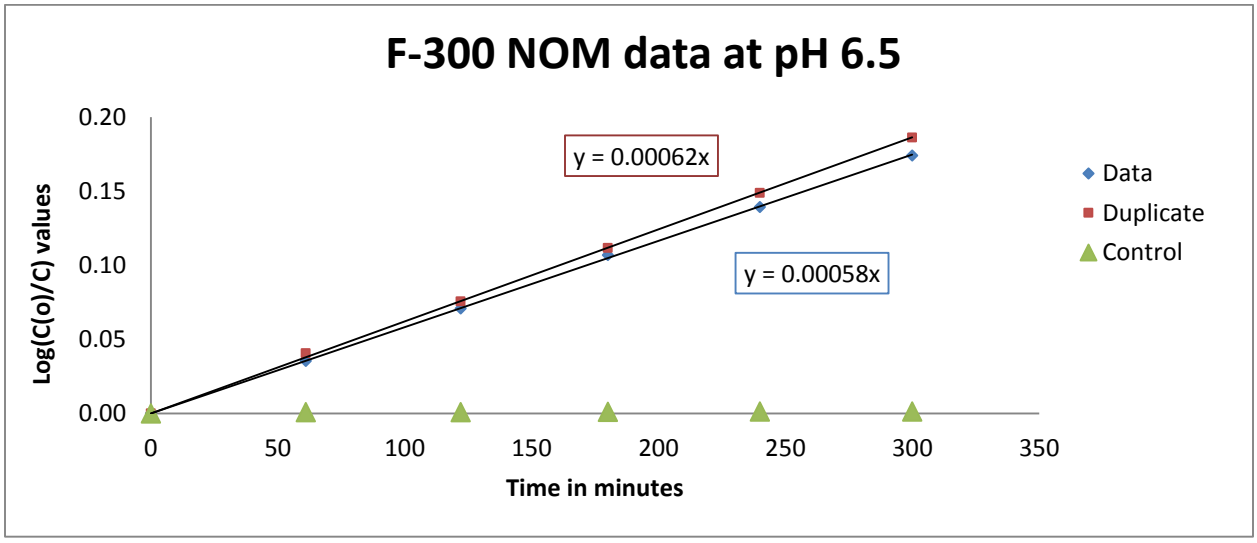

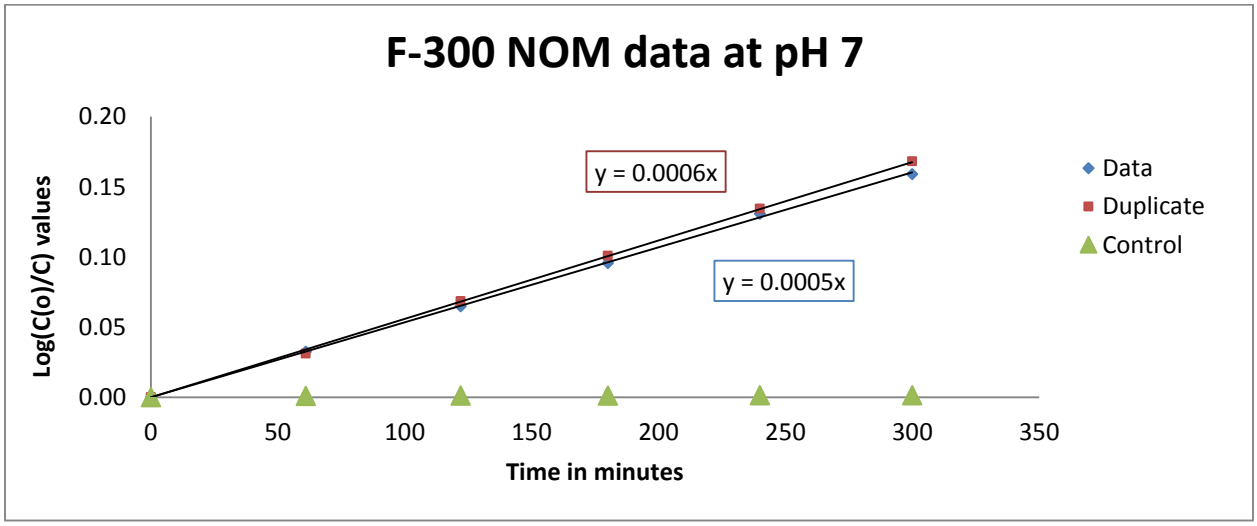

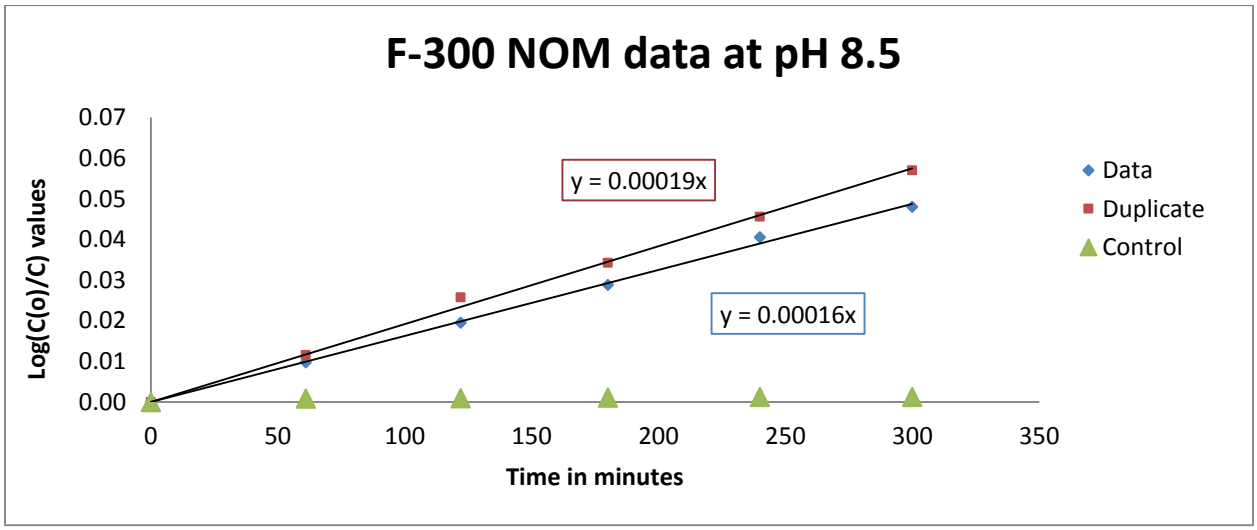

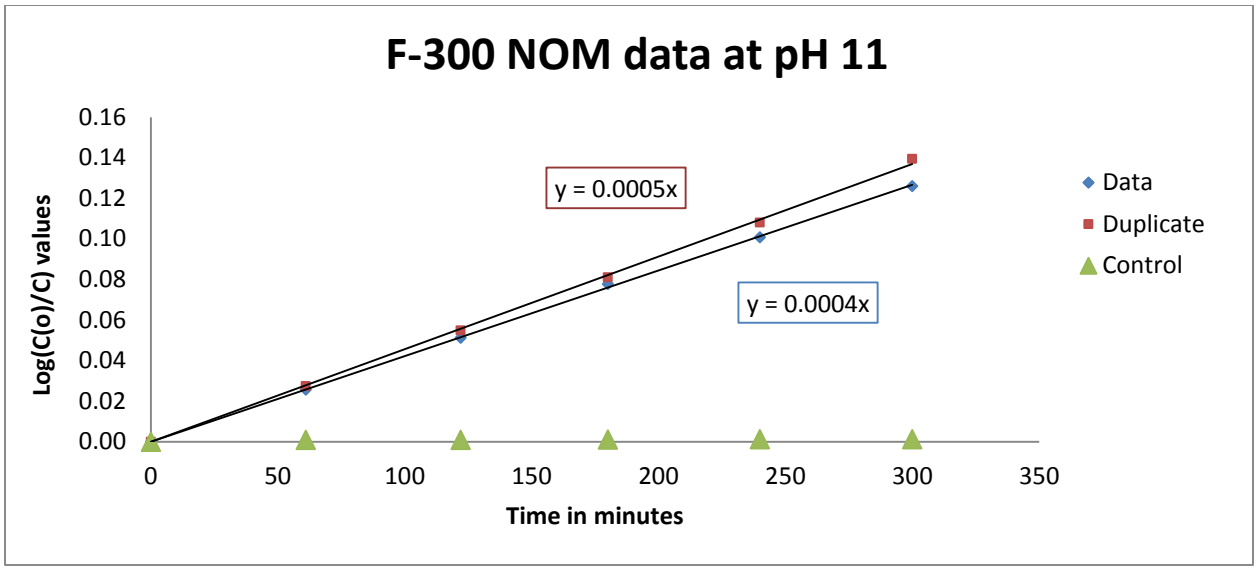
F-300 NOM data at pH 11
Log(C(o)/C) values
0.16
0.14
0.12
0.10
0.08
0.06
0.04
0.02
0.00
y = 0.0005x
y = 0.0004x
0
50
100
150
200
250
300
350
Time in minutes
Data
Duplicate
Control

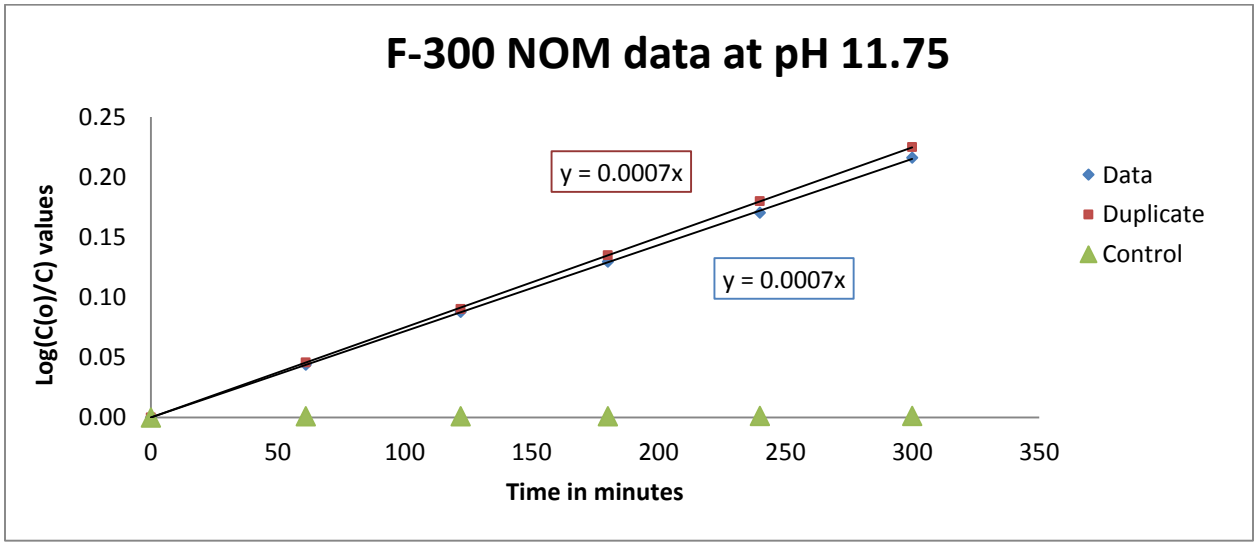
F-300 NOM data at pH 11.75
Log(C(o)/C) values
0.25
0.20
0.15
0.10
0.05
0.00
y = 0.0007x
y = 0.0007x
0
50
100
150
200
250
300
350
Time in minutes
Data
Duplicate
Control

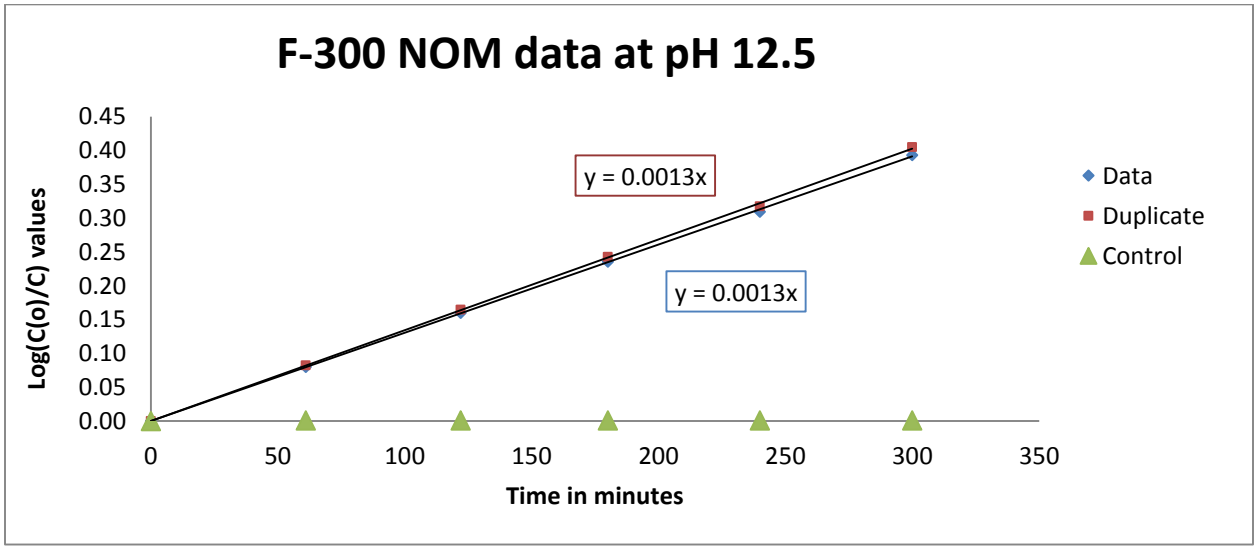
F-300 NOM data at pH 12.5
Log(C(o)/C) values
0.45
0.40
0.35
0.30
0.25
0.20
0.15
0.10
0.05
0.00
y = 0.0013x
y = 0.0013x
0
50
100
150
200
250
300
350
Time in minutes
Data
Duplicate
Control

A.3.3 K values of F-300 aged with NOM + H_2O_2

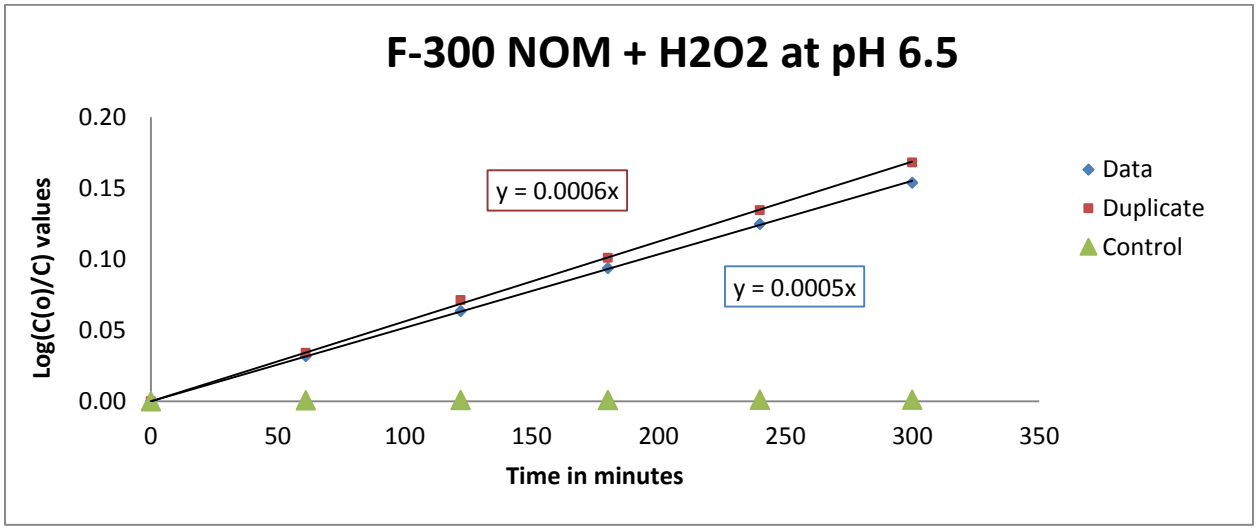

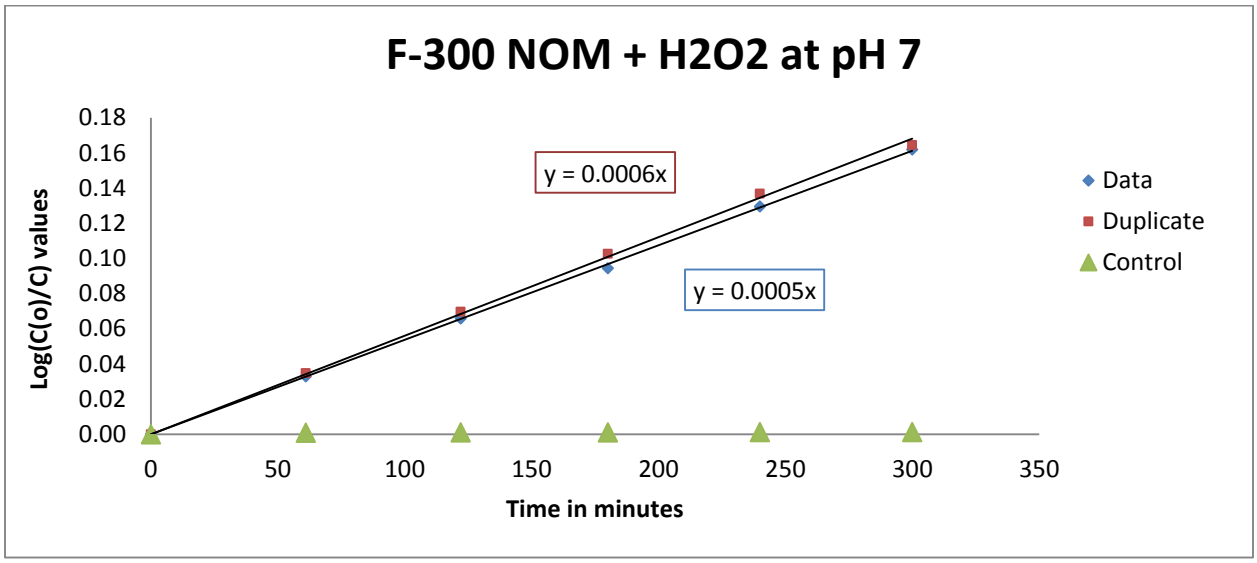

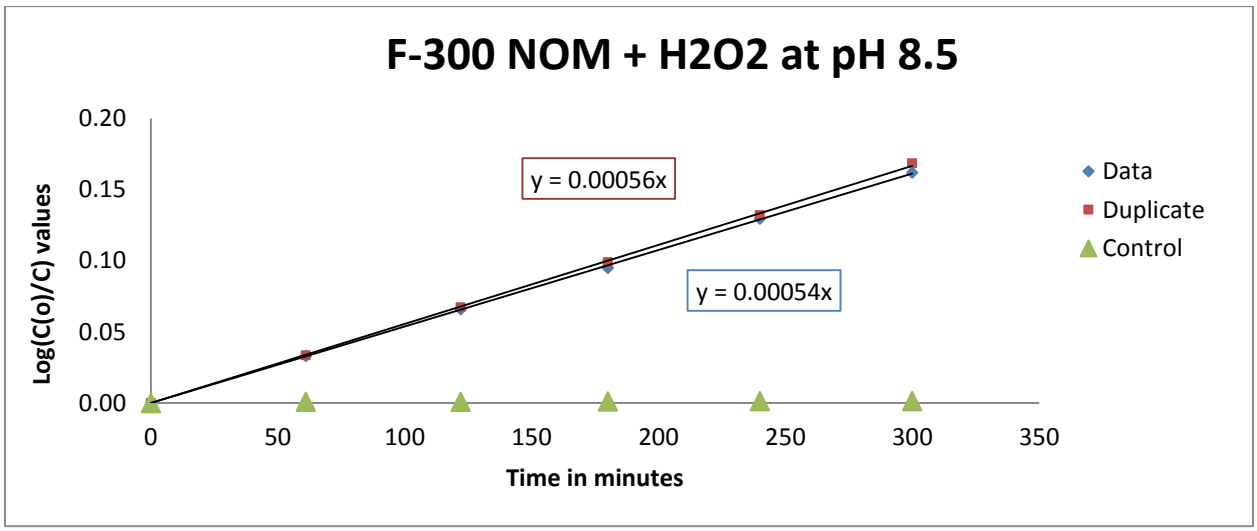

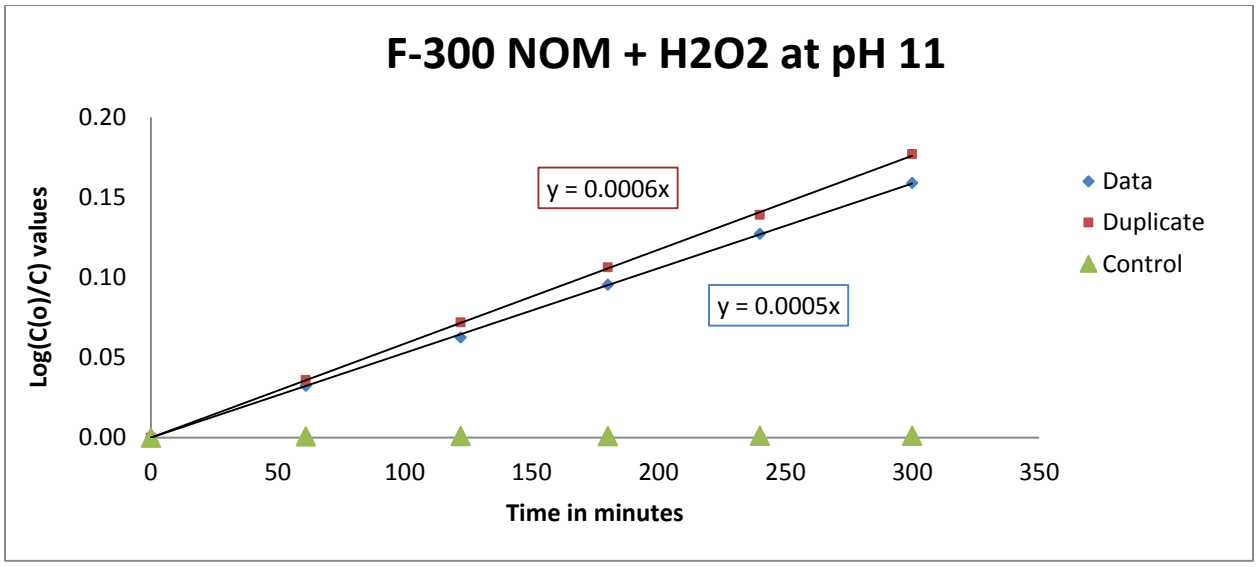
F-300 NOM + H2O2 at pH 11
Log(C(o)/C) values
0.20
0.15
0.10
0.05
0.00
y = 0.0006x
y = 0.0005x
0
50
100
150
200
250
300
350
Time in minutes
Data
Duplicate
Control

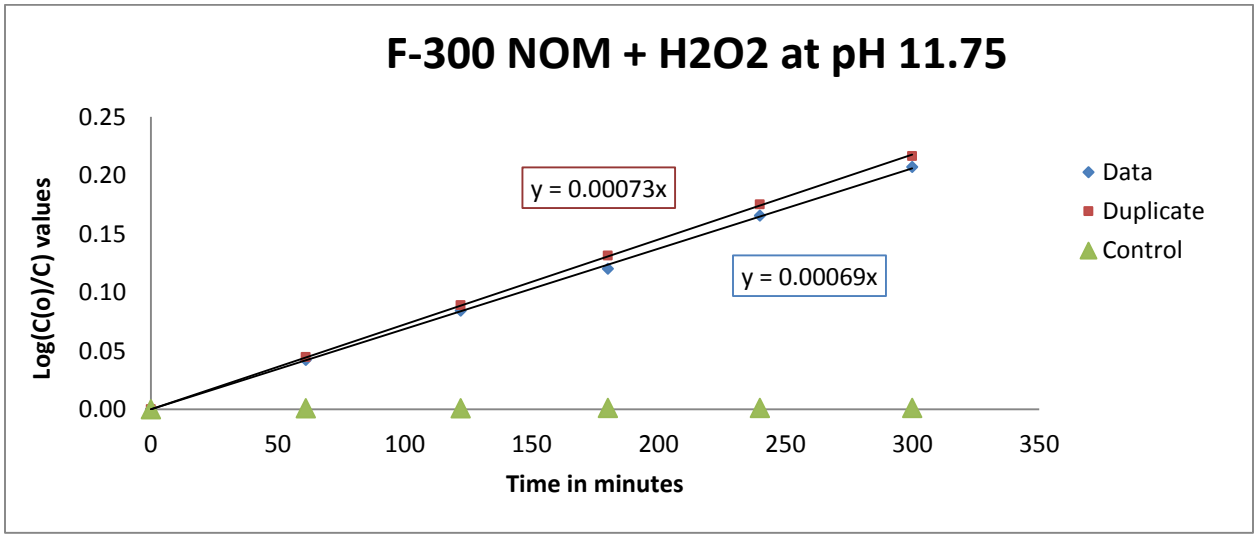
F-300 NOM + H2O2 at pH 11.75
Log(C(o)/C) values
0.25
0.20
0.15
0.10
0.05
0.00
y = 0.00073x
y = 0.00069x
0
50
100
150
200
250
300
350
Time in minutes
Data
Duplicate
Control

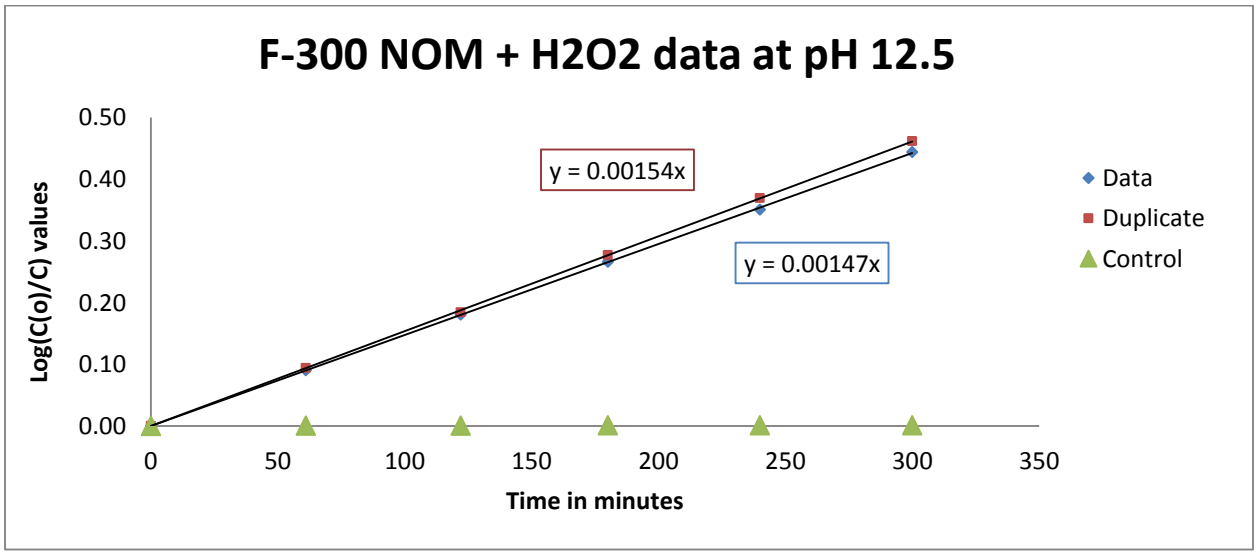
F-300 NOM + H2O2 data at pH 12.5
Log(C(o)/C) values
0.50
0.40
0.30
0.20
0.10
0.00
y = 0.00154x
y = 0.00147x
0
50
100
150
200
250
300
350
Time in minutes
Data
Duplicate
Control

A.4.1 K values of virgin GAC-300

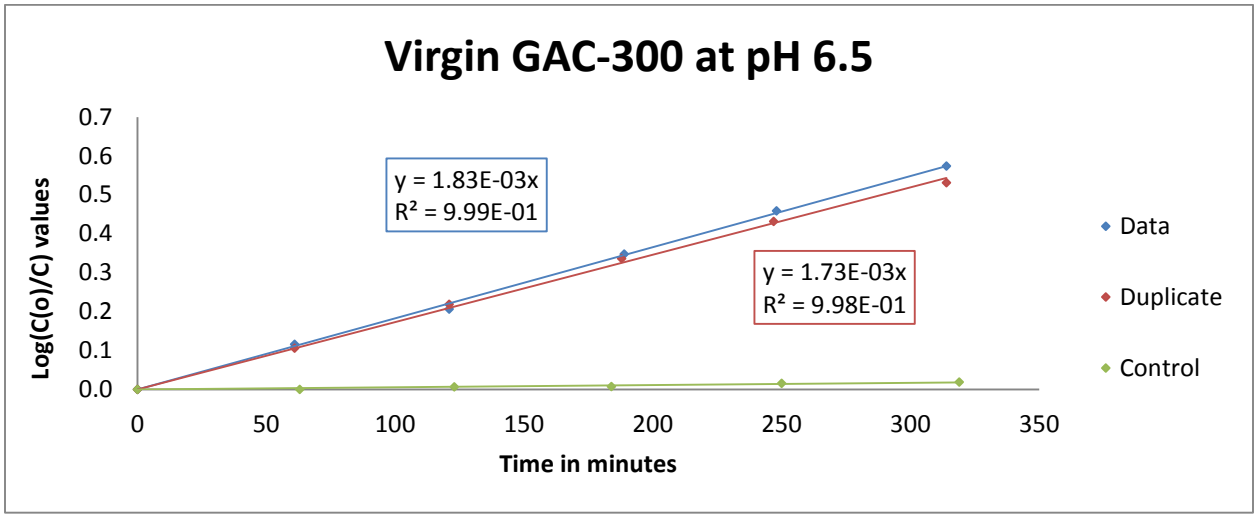

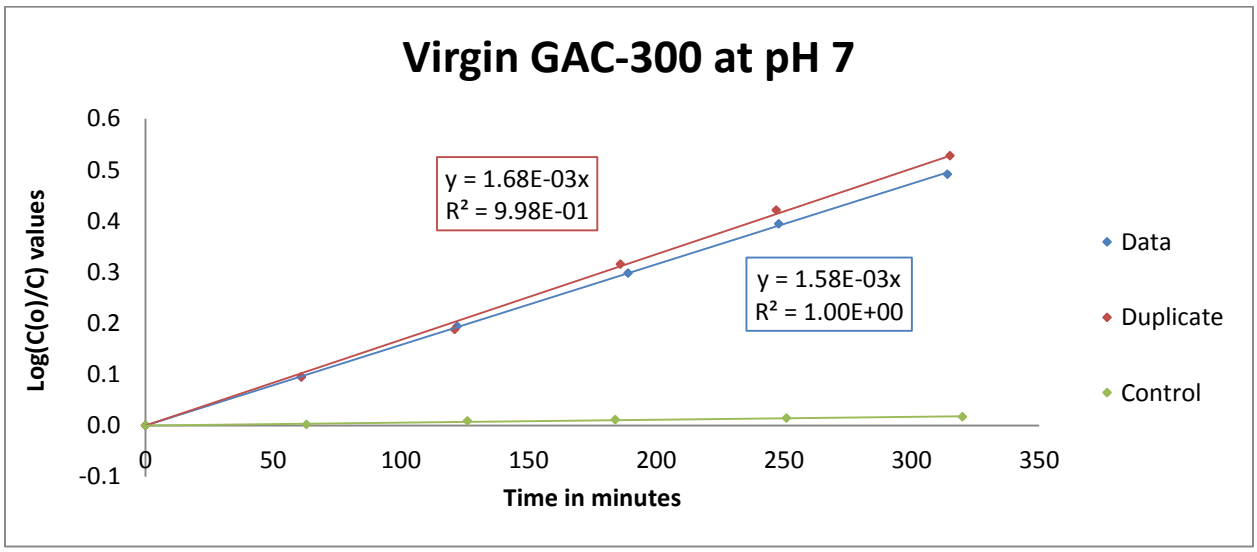

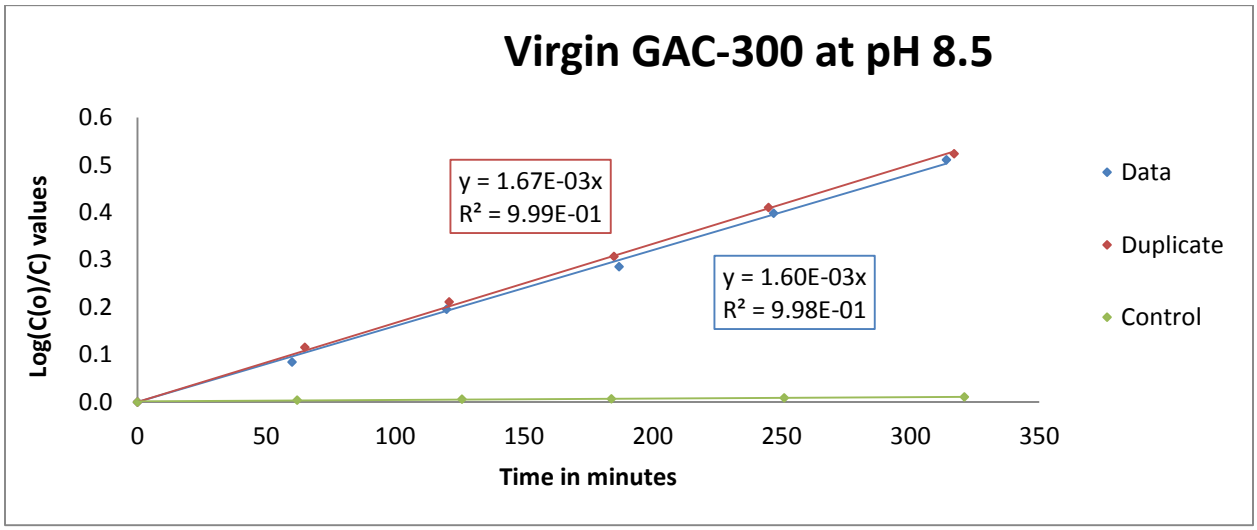

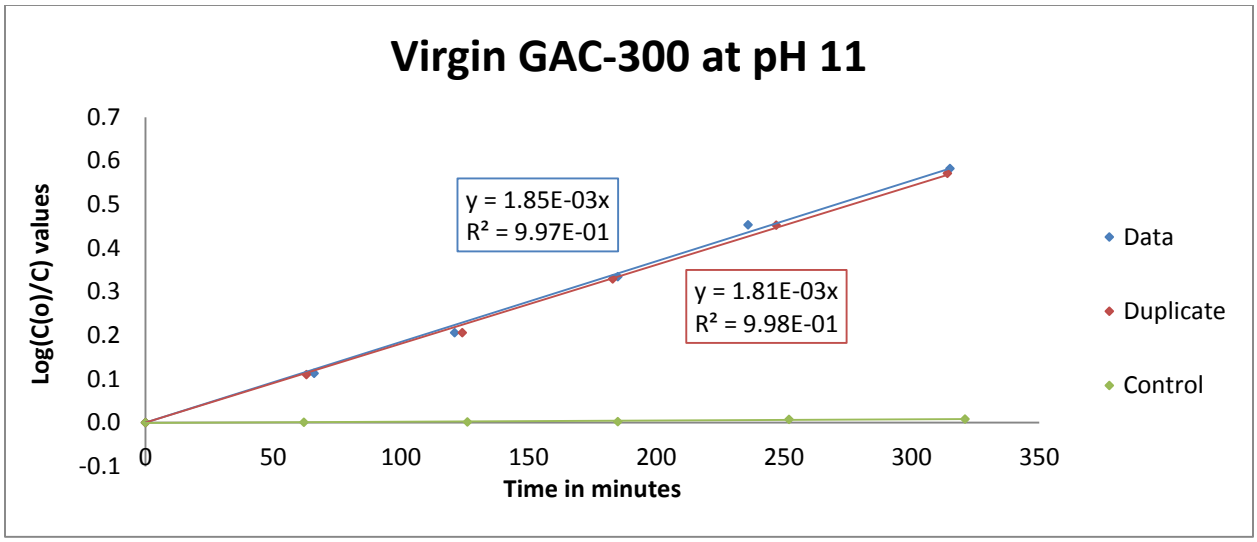
Virgin GAC-300 at pH 11
Log(C(o)/C) values
Time in minutes
y = 1.85E-03x
R² = 9.97E-01
y = 1.81E-03x
R² = 9.98E-01
Data
Duplicate
Control

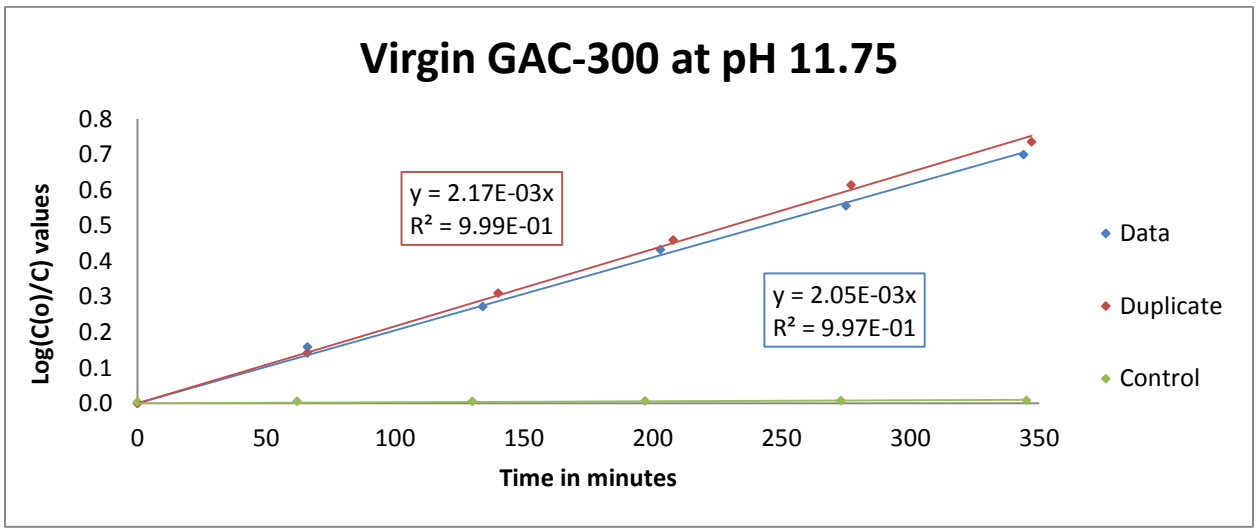
Virgin GAC-300 at pH 11.75
Log(C(o)/C) values
Time in minutes
y = 2.17E-03x
R² = 9.99E-01
y = 2.05E-03x
R² = 9.97E-01
Data
Duplicate
Control

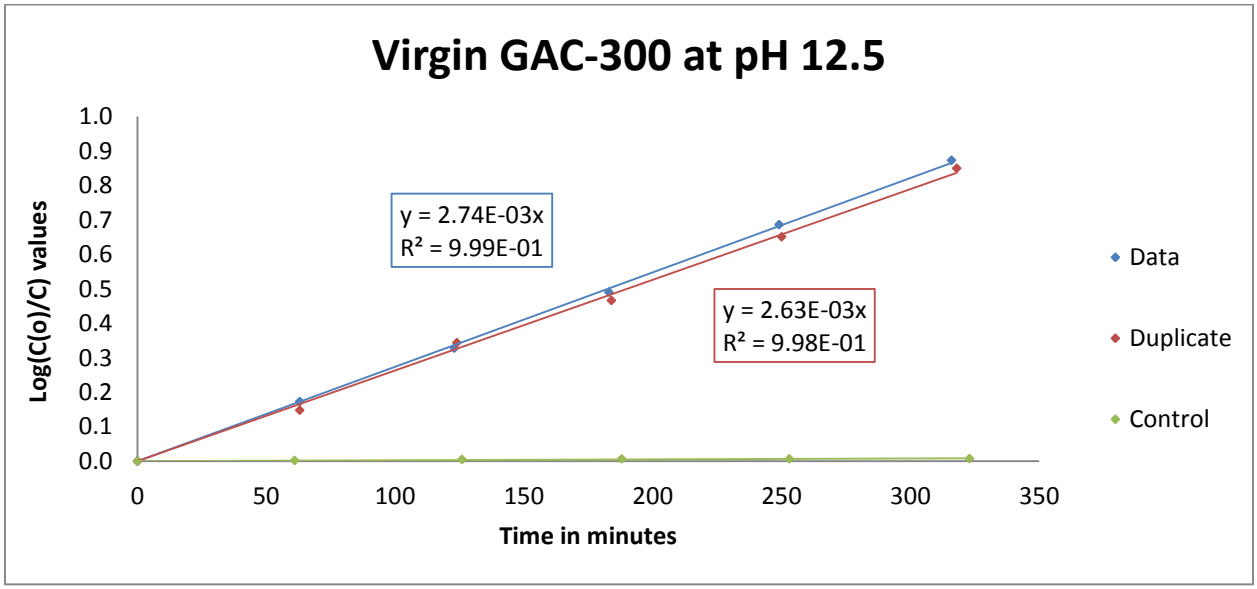
Virgin GAC-300 at pH 12.5
Log(C(o)/C) values
Time in minutes
y = 2.74E-03x
R² = 9.99E-01
y = 2.63E-03x
R² = 9.98E-01
Data
Duplicate
Control

A.4.2 K values of GAC-300 aged with NOM

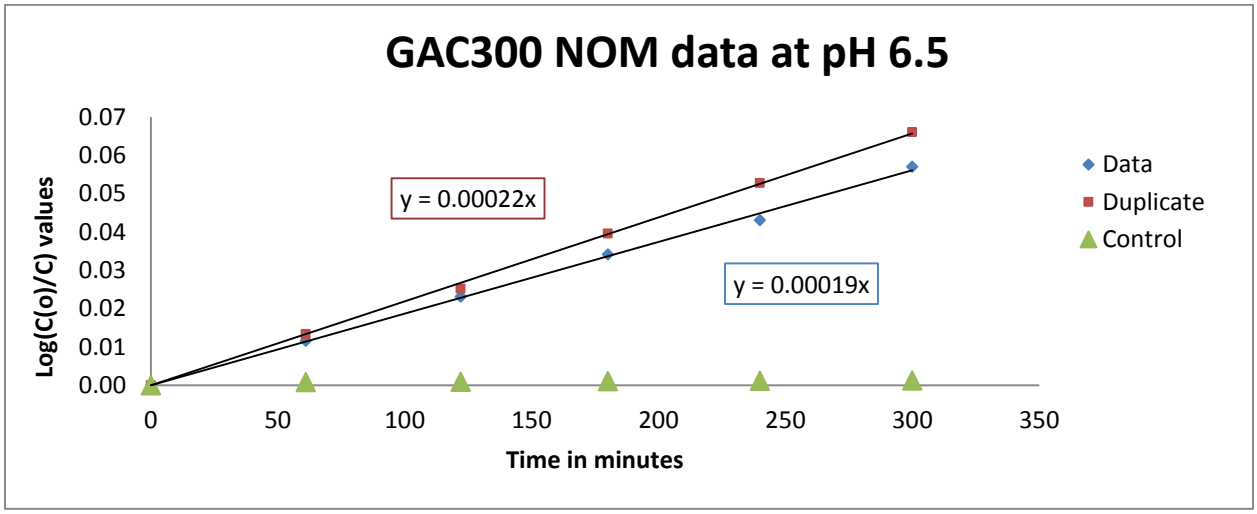

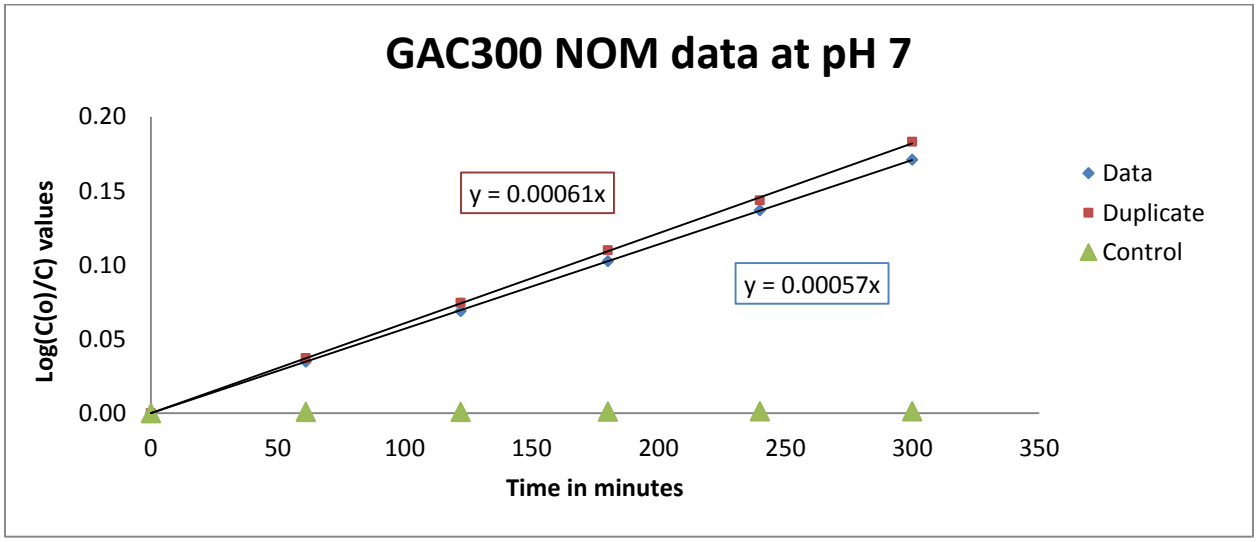

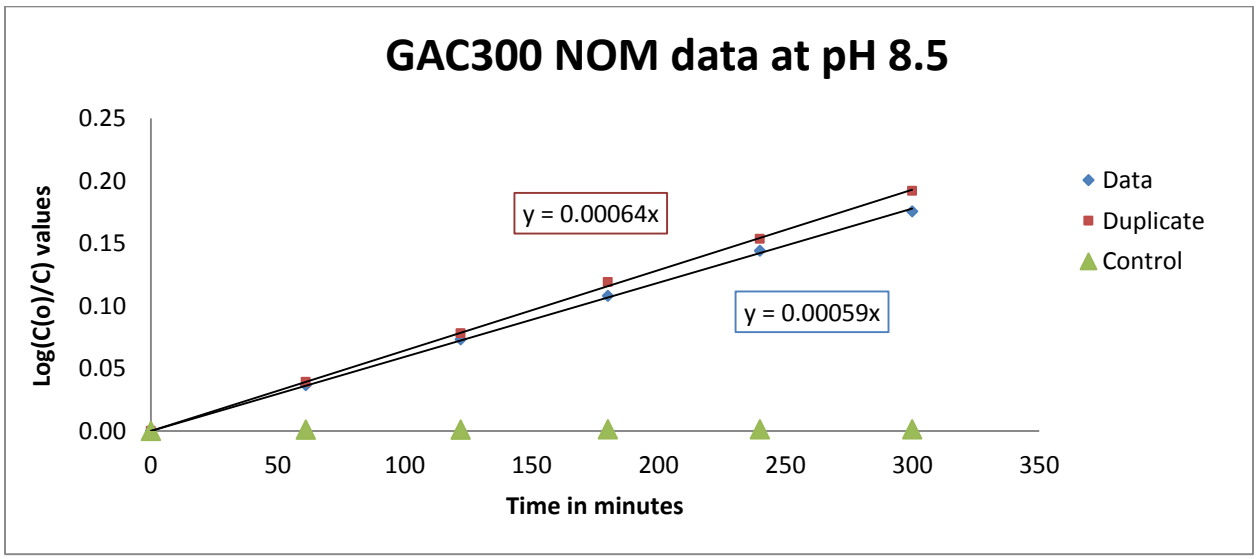

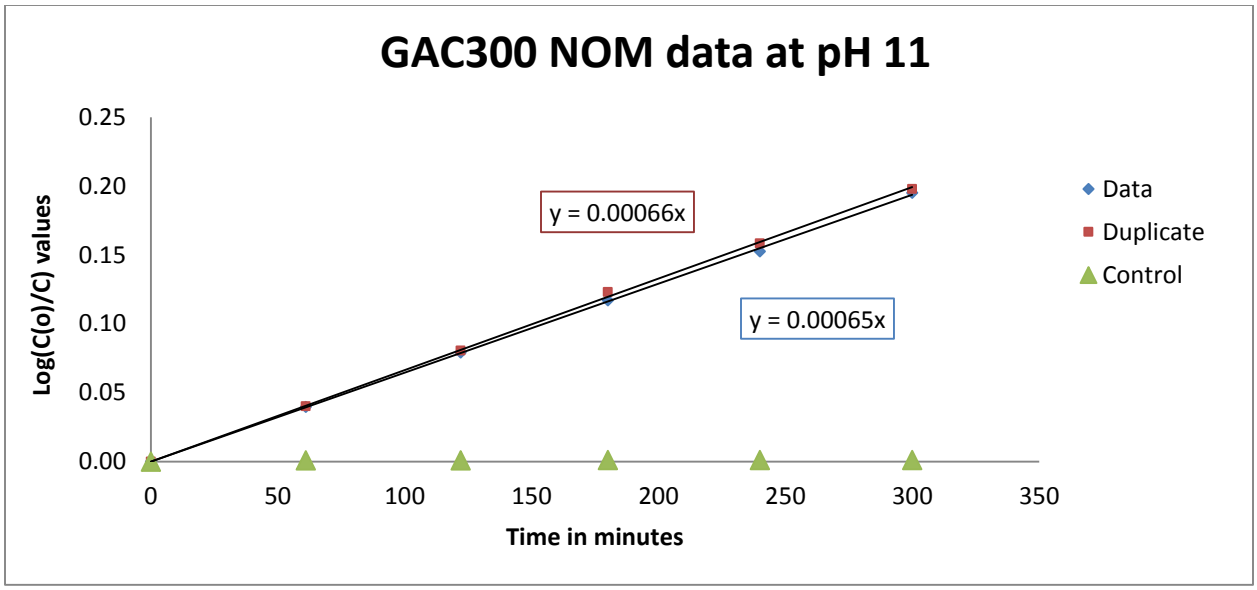
GAC300 NOM data at pH 11
Log(C(o)/C) values
0.25
0.20
0.15
0.10
0.05
0.00
y = 0.00066x
y = 0.00065x
Data
Duplicate
Control
0
50
100
150
200
250
300
350
Time in minutes

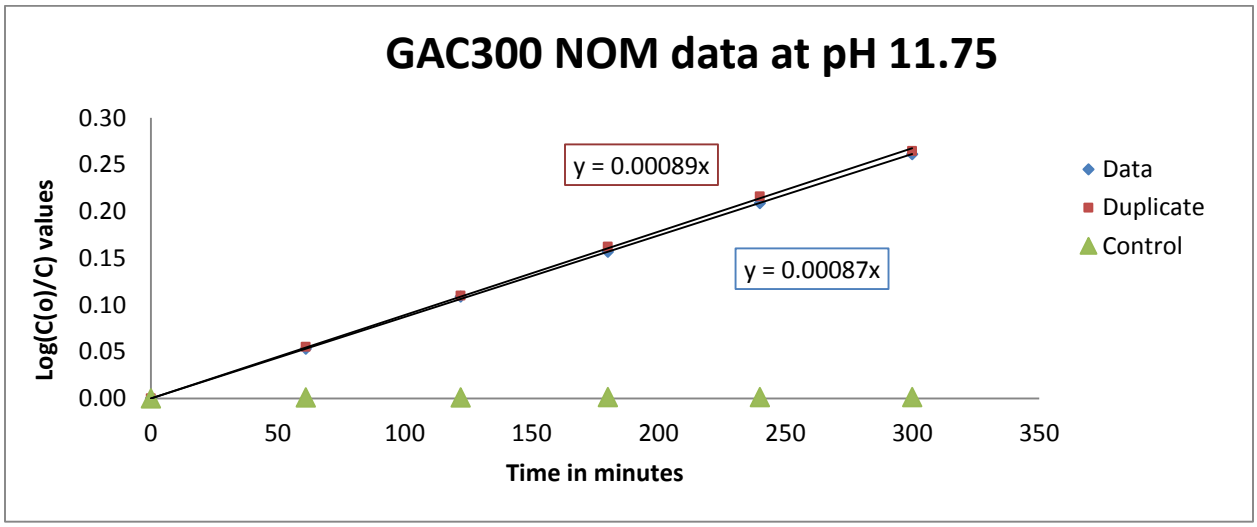
GAC300 NOM data at pH 11.75
Log(C(o)/C) values
0.30
0.25
0.20
0.15
0.10
0.05
0.00
y = 0.00089x
y = 0.00087x
Data
Duplicate
Control
0
50
100
150
200
250
300
350
Time in minutes

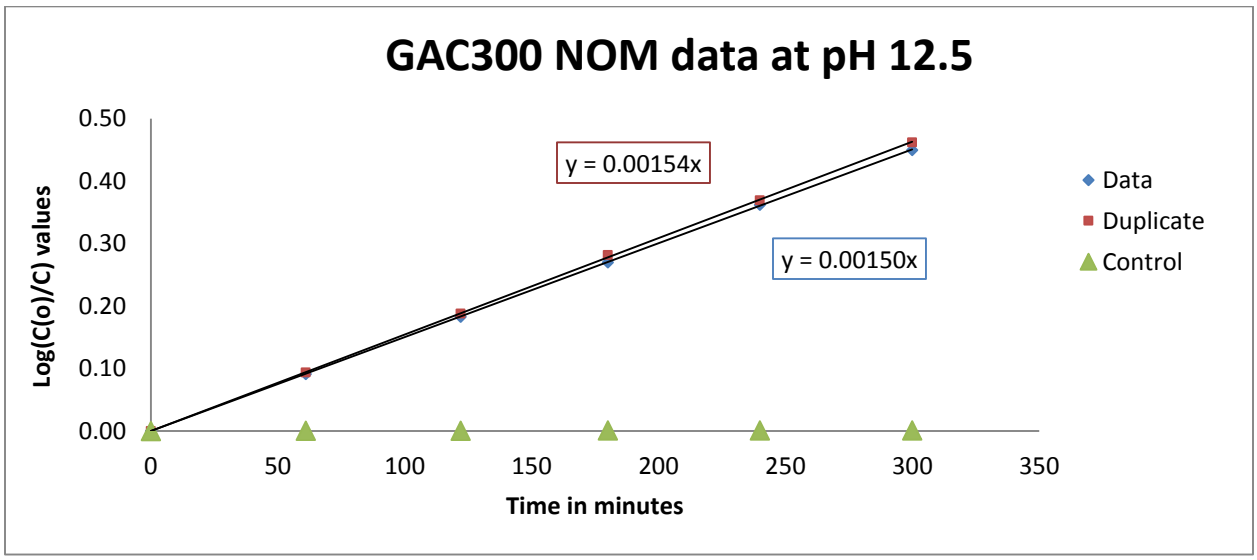
GAC300 NOM data at pH 12.5
Log(C(o)/C) values
0.50
0.40
0.30
0.20
0.10
0.00
y = 0.00154x
y = 0.00150x
Data
Duplicate
Control
0
50
100
150
200
250
300
350
Time in minutes

A.4.3 K values of GAC-300 aged with NOM + H_2O_2

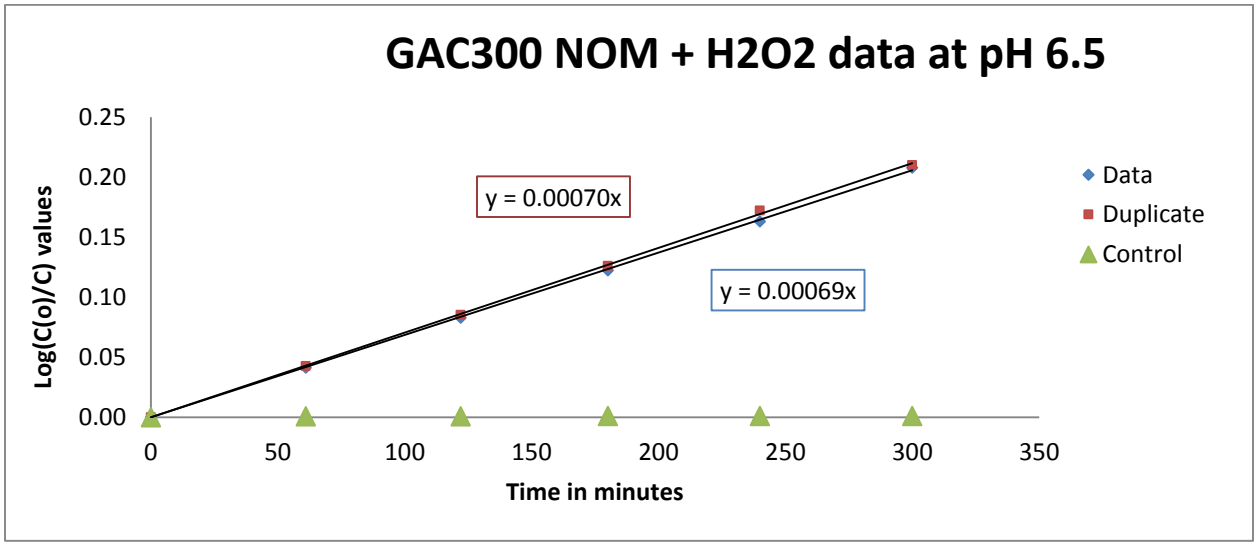

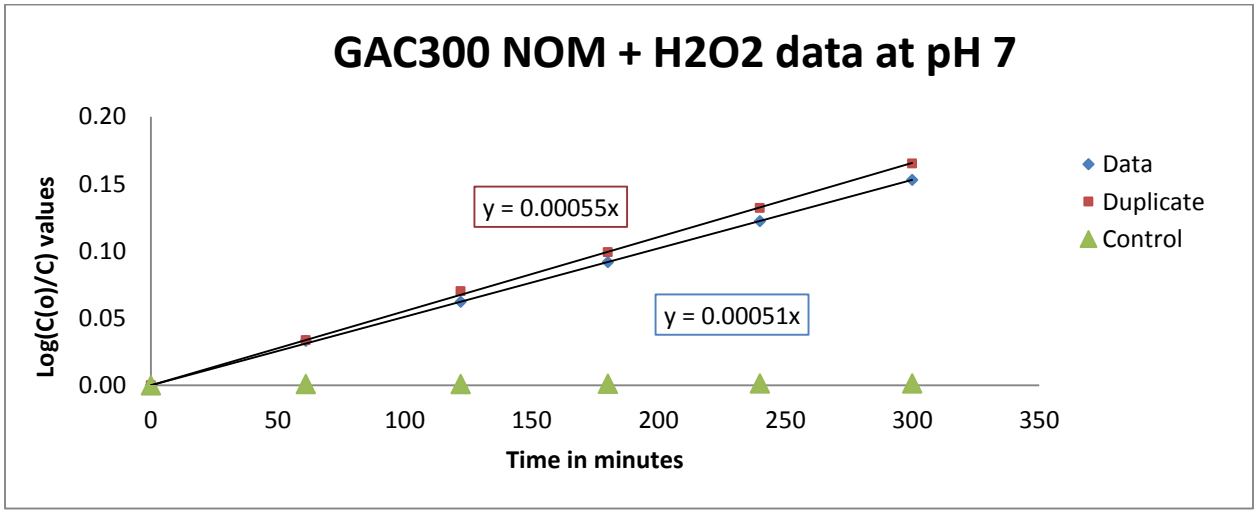

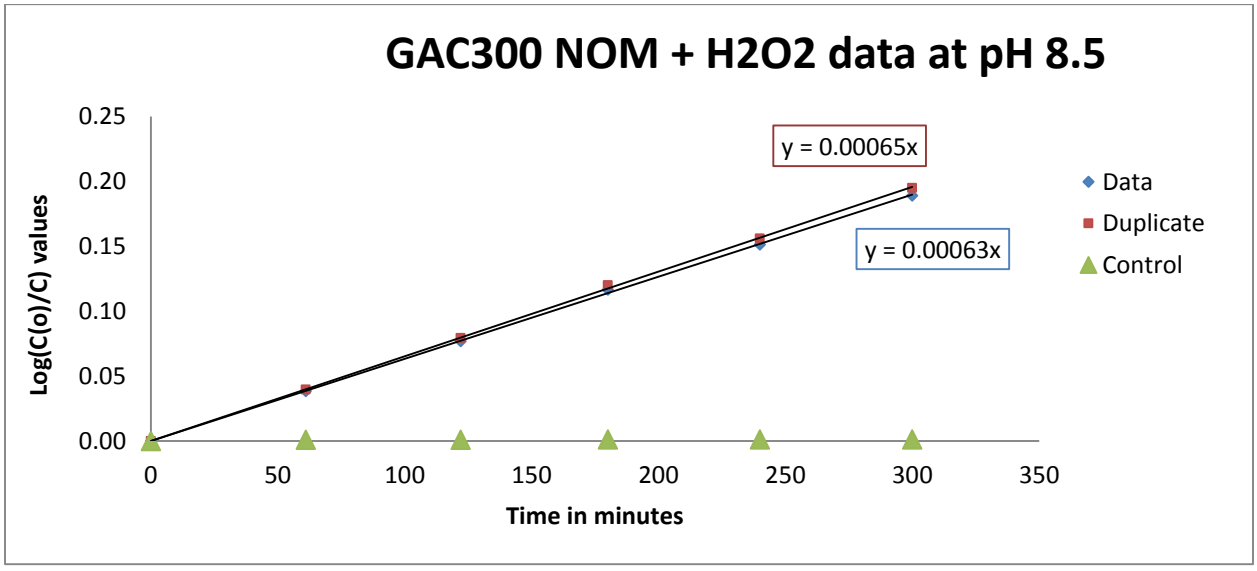

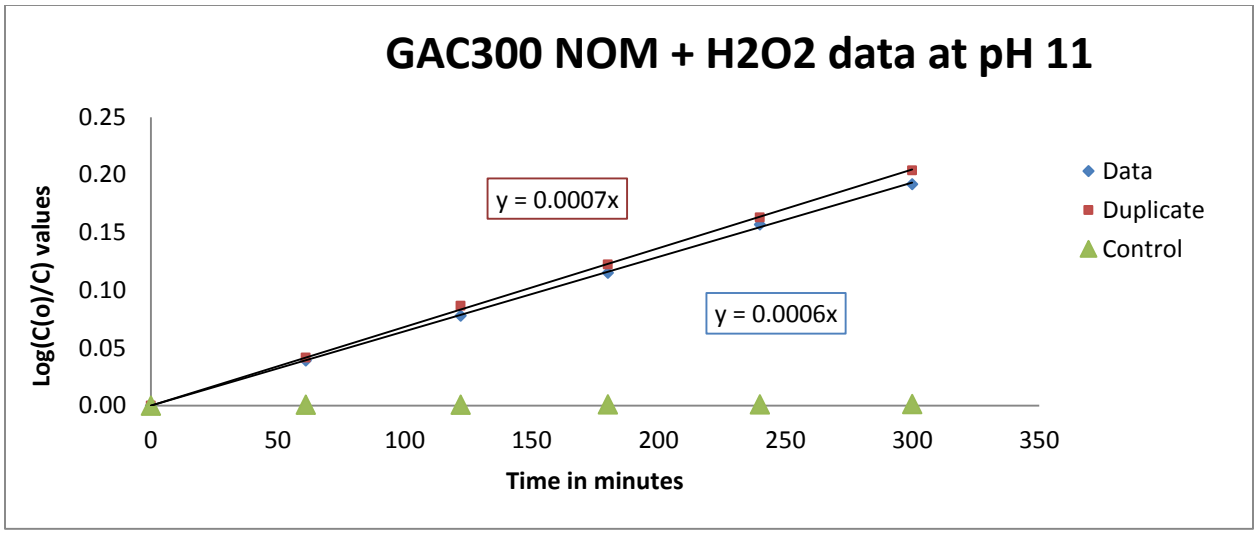
GAC300 NOM + H2O2 data at pH 11
Log(C(o)/C) values
0.25
0.20
0.15
0.10
0.05
0.00
y = 0.0007x
y = 0.0006x
0
50
100
150
200
250
300
350
Time in minutes
Data
Duplicate
Control

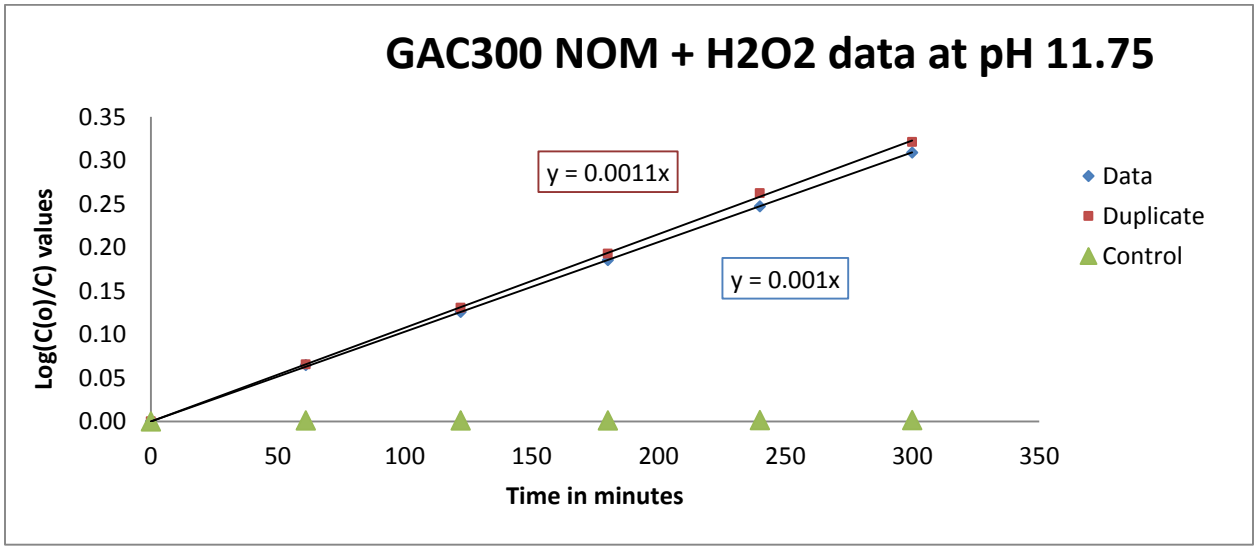
GAC300 NOM + H2O2 data at pH 11.75
Log(C(o)/C) values
0.35
0.30
0.25
0.20
0.15
0.10
0.05
0.00
y = 0.0011x
y = 0.001x
0
50
100
150
200
250
300
350
Time in minutes
Data
Duplicate
Control

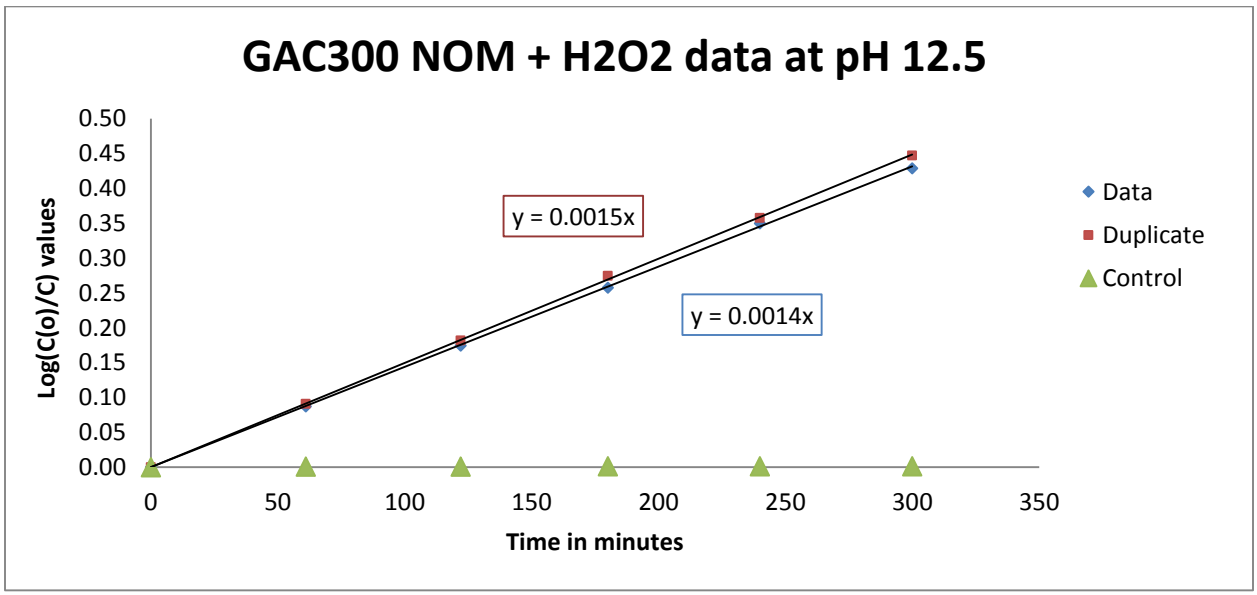
GAC300 NOM + H2O2 data at pH 12.5
Log(C(o)/C) values
0.50
0.45
0.40
0.35
0.30
0.25
0.20
0.15
0.10
0.05
0.00
y = 0.0015x
y = 0.0014x
0
50
100
150
200
250
300
350
Time in minutes
Data
Duplicate
Control

A.5.1 K values of Virgin HD-3000

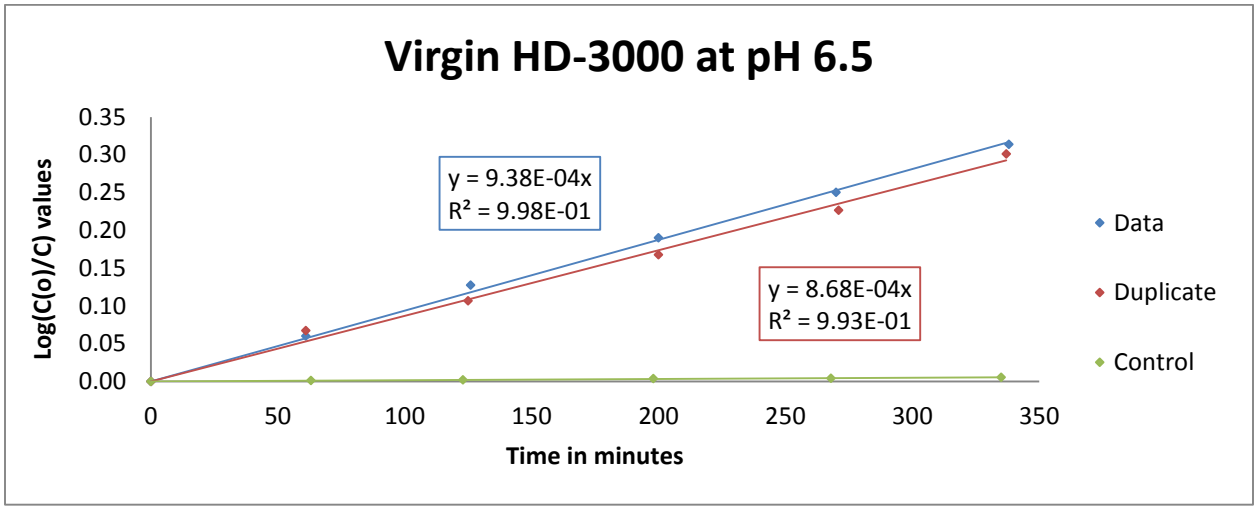

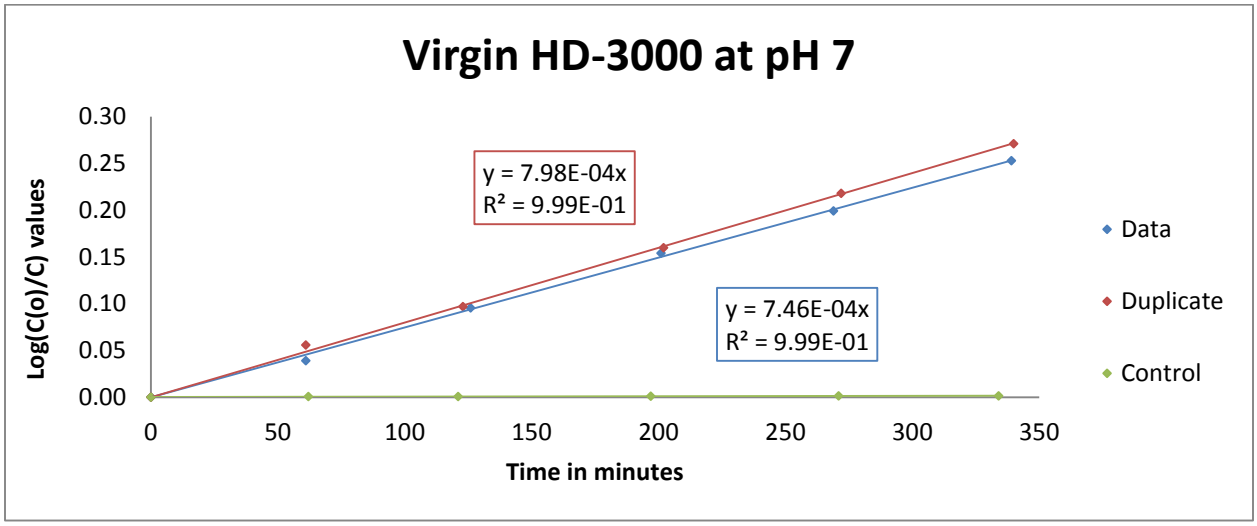

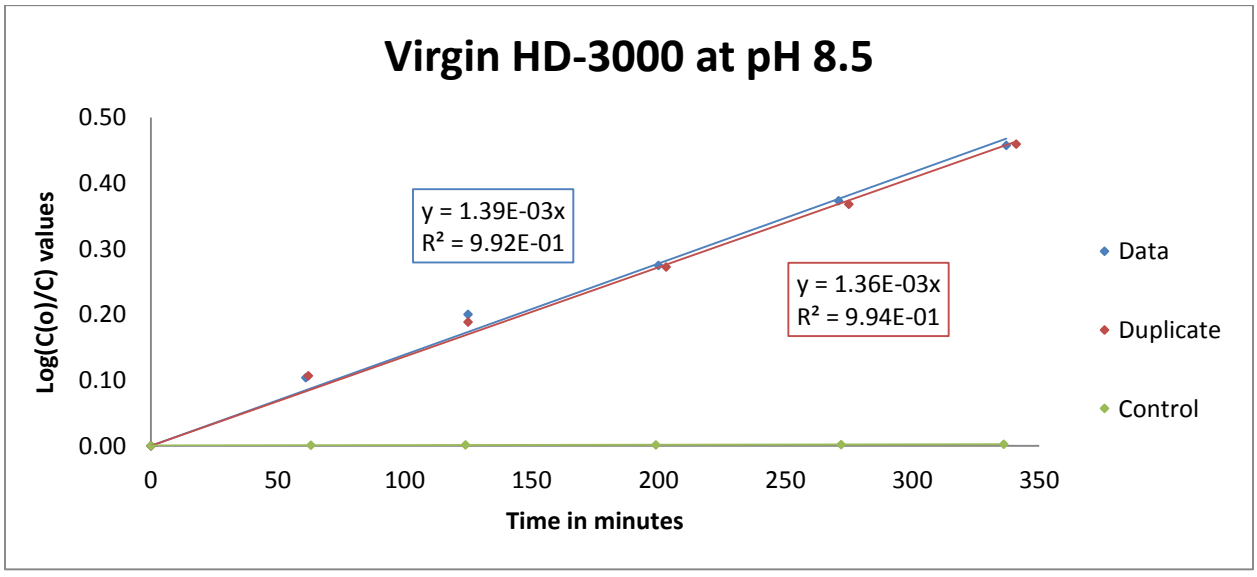

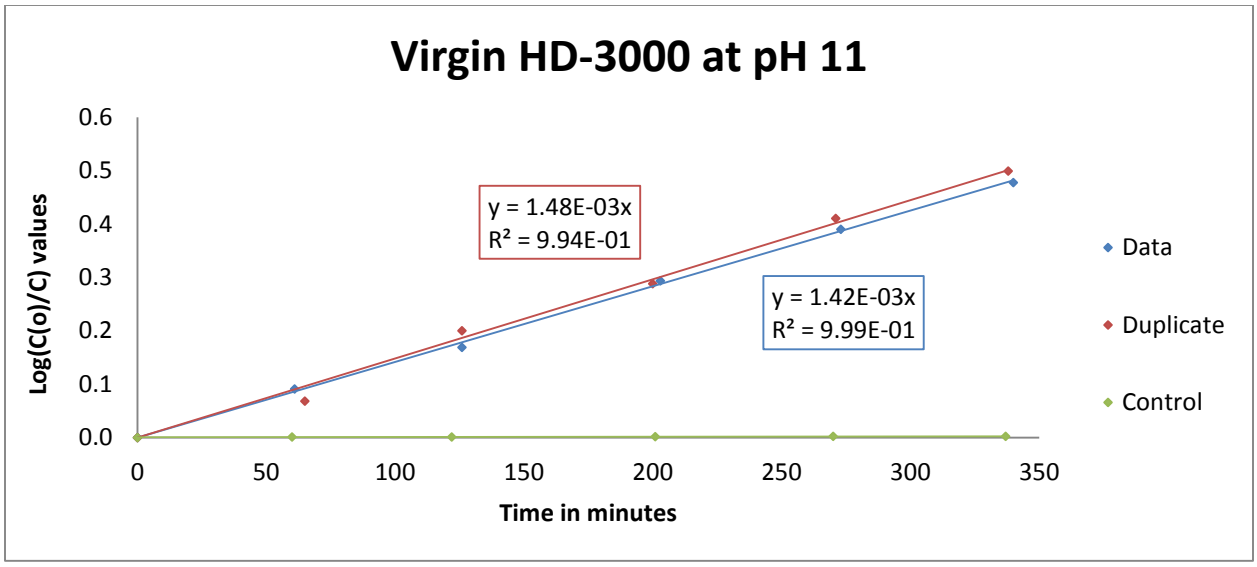
Virgin HD-3000 at pH 11
Log(C(o)/C) values
0.6
0.5
0.4
0.3
0.2
0.1
0.0
y = 1.48E-03x
R² = 9.94E-01
y = 1.42E-03x
R² = 9.99E-01
0
50
100
150
200
250
300
350
Time in minutes
Data
Duplicate
Control

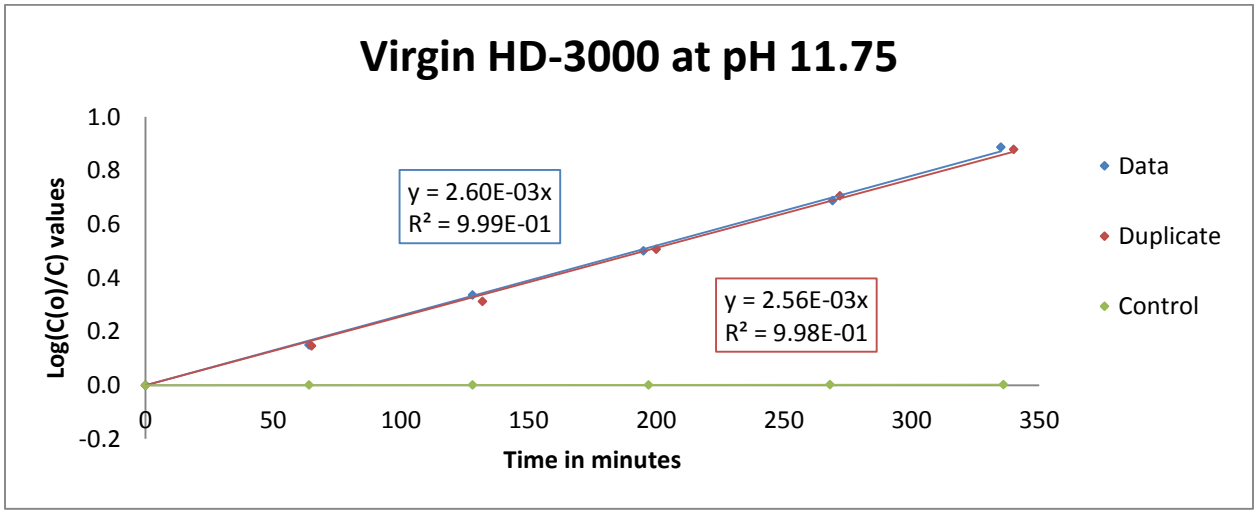
Virgin HD-3000 at pH 11.75
Log(C(o)/C) values
1.0
0.8
0.6
0.4
0.2
0.0
-0.2
y = 2.60E-03x
R² = 9.99E-01
y = 2.56E-03x
R² = 9.98E-01
0
50
100
150
200
250
300
350
Time in minutes
Data
Duplicate
Control

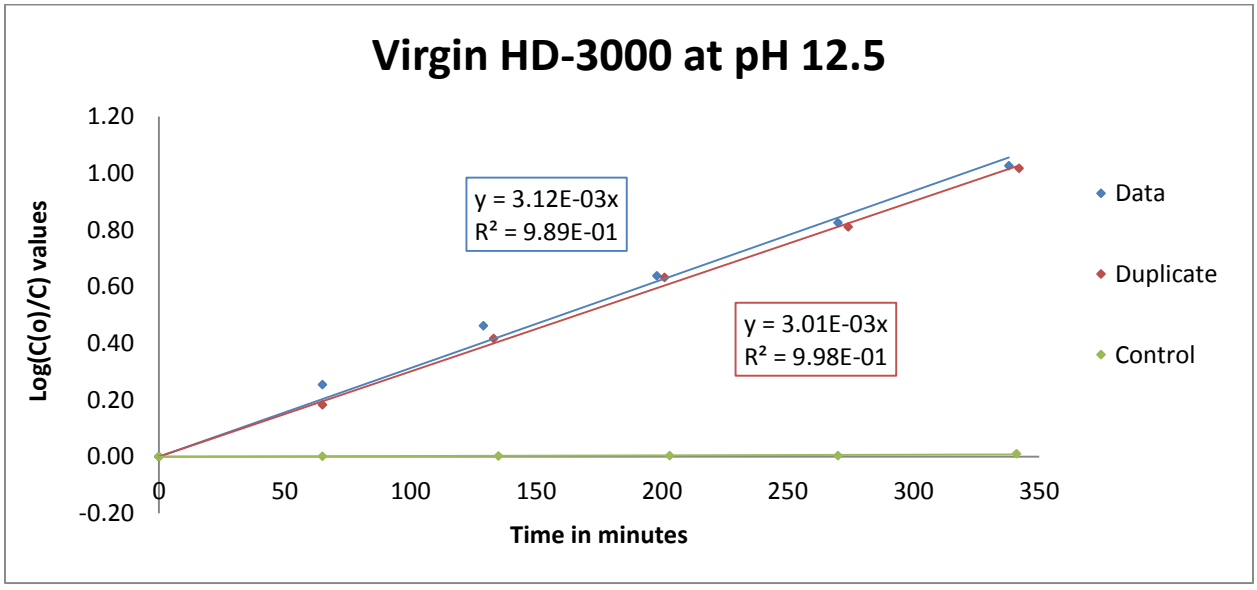
Virgin HD-3000 at pH 12.5
Log(C(o)/C) values
1.20
1.00
0.80
0.60
0.40
0.20
0.00
-0.20
y = 3.12E-03x
R² = 9.89E-01
y = 3.01E-03x
R² = 9.98E-01
0
50
100
150
200
250
300
350
Time in minutes
Data
Duplicate
Control

A.5.2 K values of HD-3000 aged with NOM

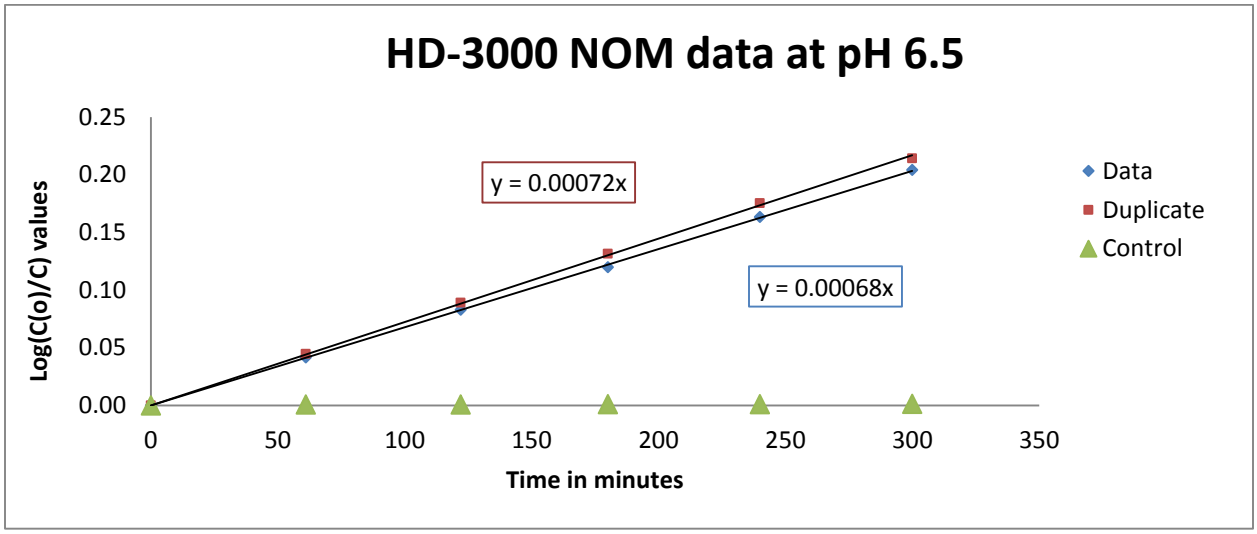

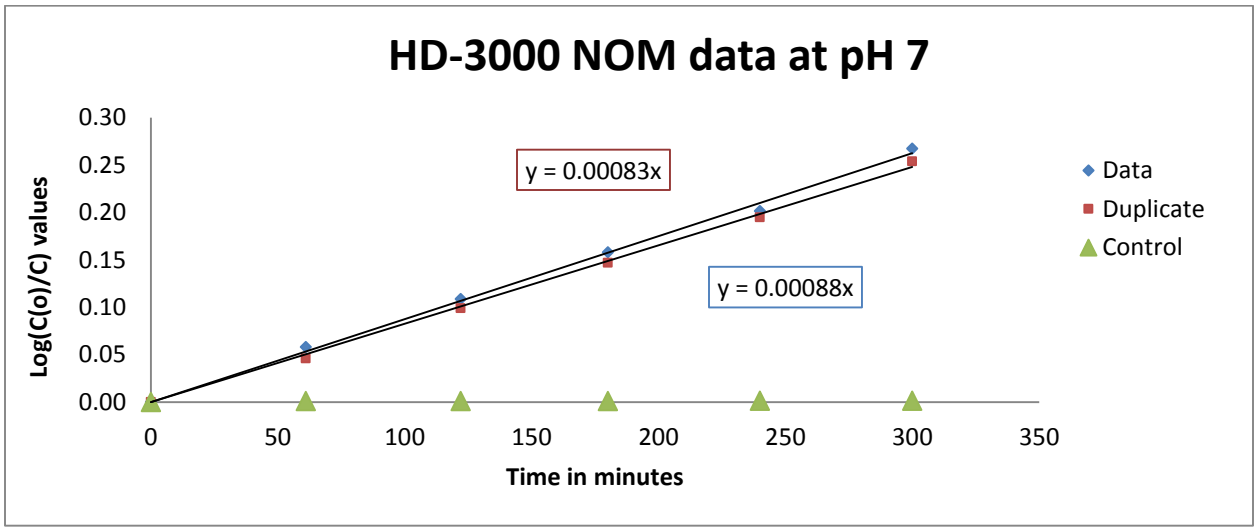

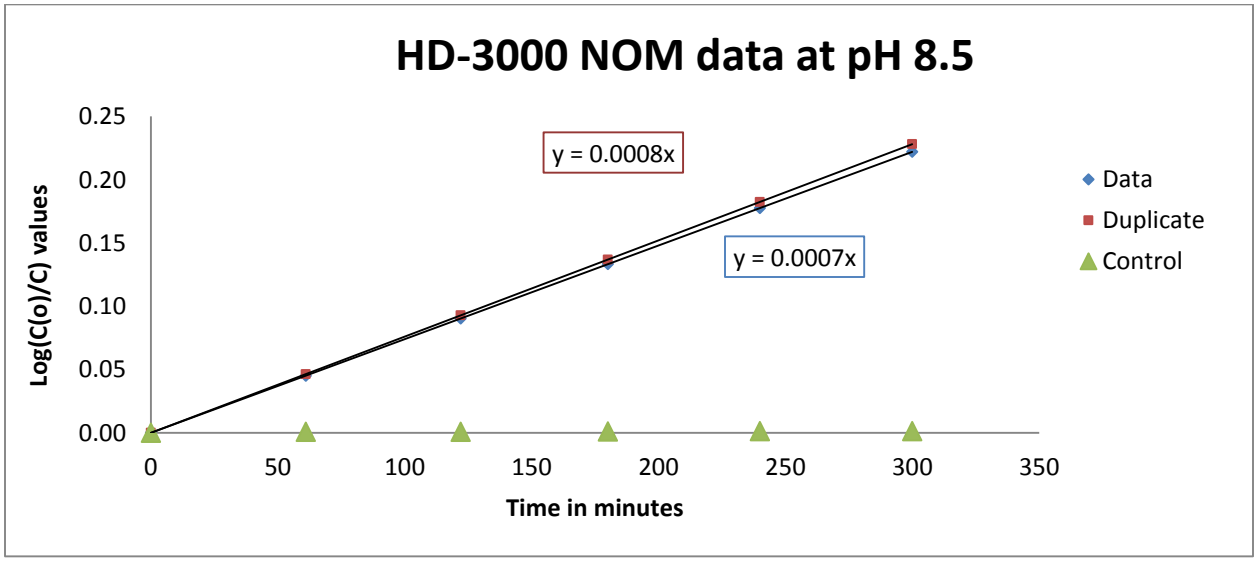

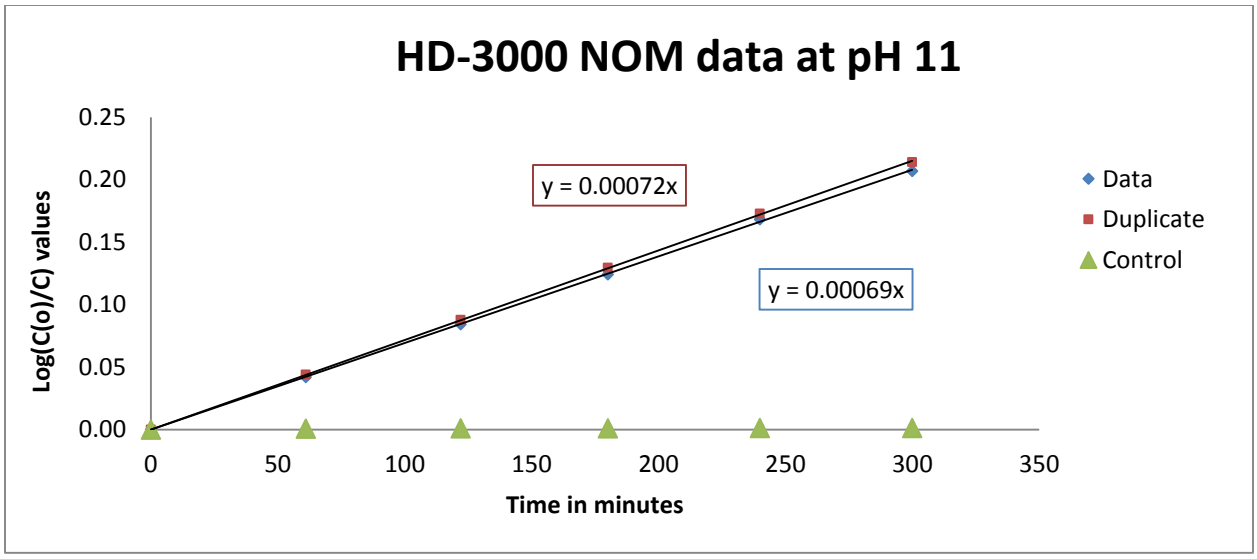
HD-3000 NOM data at pH 11
Log(C(o)/C) values
0.25
0.20
0.15
0.10
0.05
0.00
y = 0.00072x
y = 0.00069x
Data
Duplicate
Control
0
50
100
150
200
250
300
350
Time in minutes

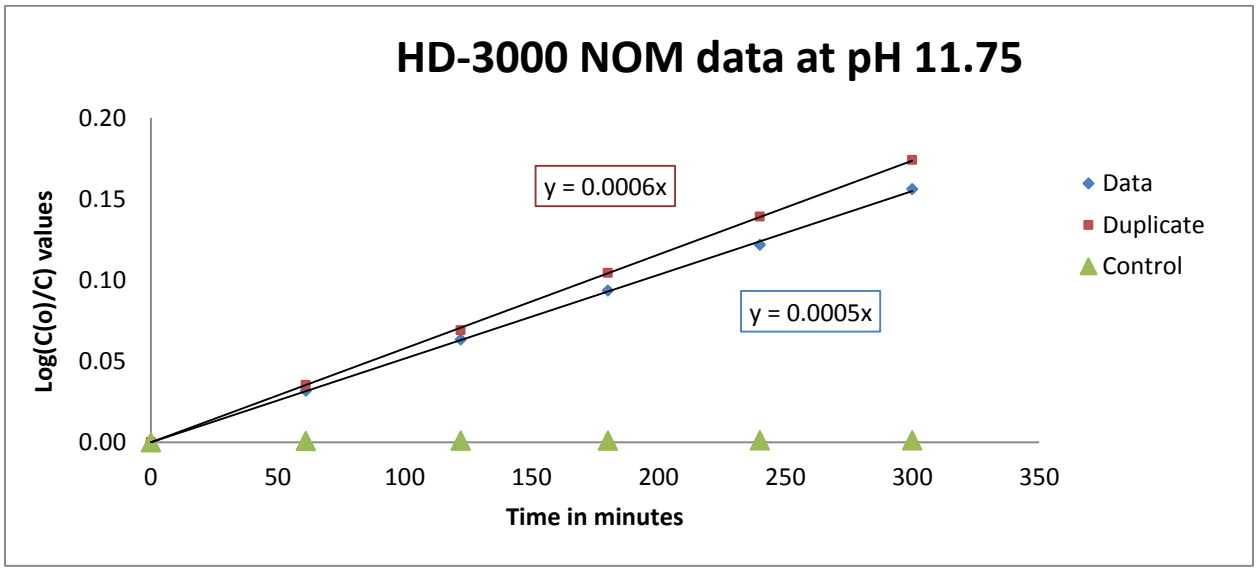
HD-3000 NOM data at pH 11.75
Log(C(o)/C) values
0.20
0.15
0.10
0.05
0.00
y = 0.0006x
y = 0.0005x
Data
Duplicate
Control
0
50
100
150
200
250
300
350
Time in minutes

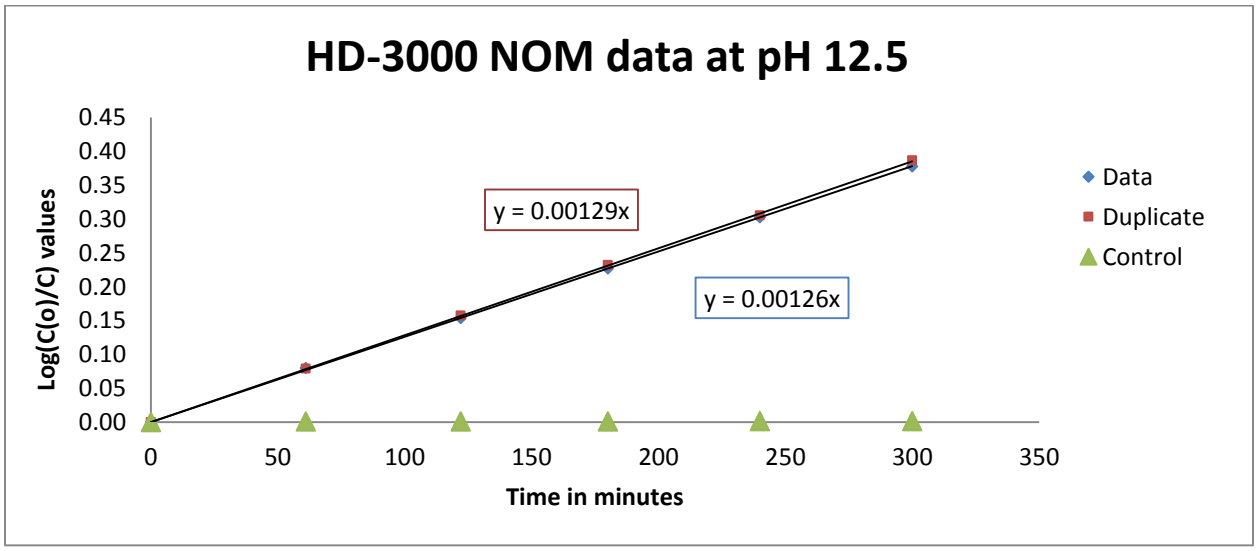
HD-3000 NOM data at pH 12.5
Log(C(o)/C) values
0.45
0.40
0.35
0.30
0.25
0.20
0.15
0.10
0.05
0.00
y = 0.00129x
y = 0.00126x
Data
Duplicate
Control
0
50
100
150
200
250
300
350
Time in minutes

A.5.3 K values of HD-3000 aged with NOM + H_2O_2

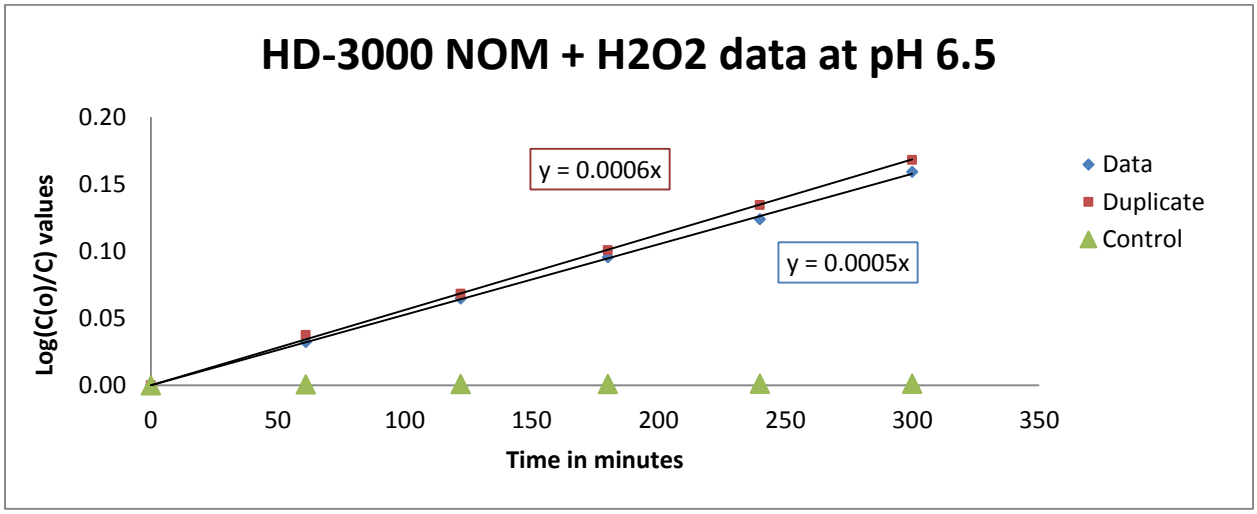

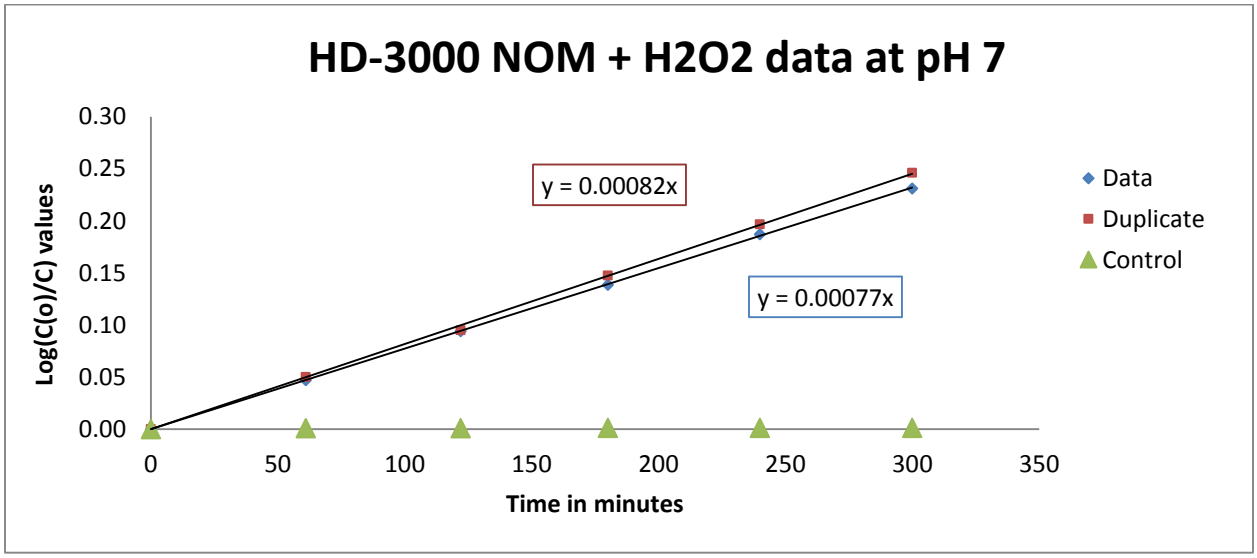

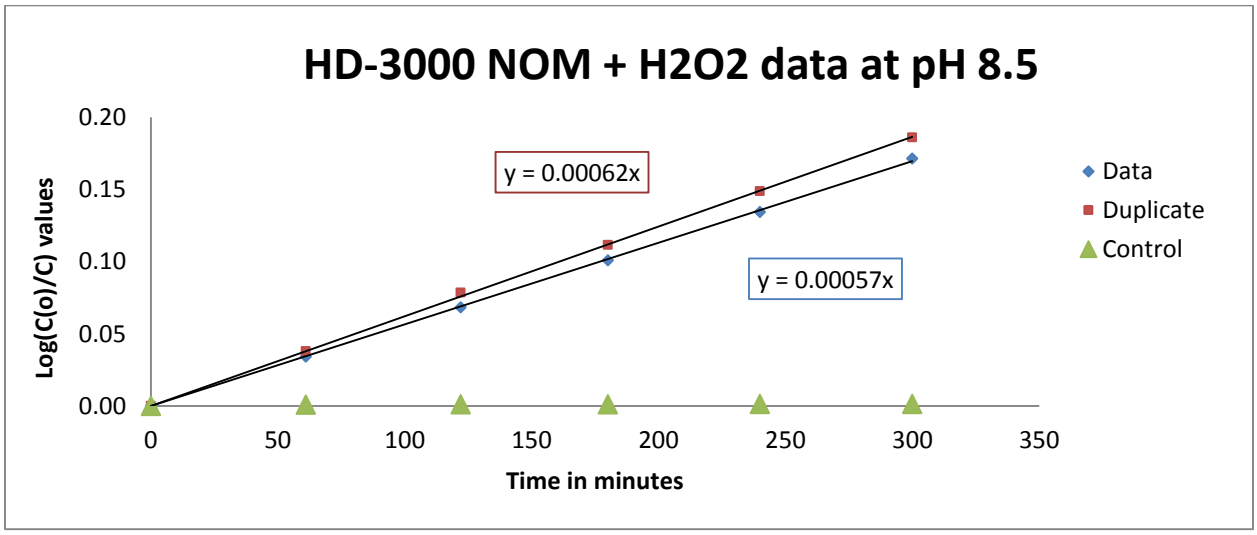

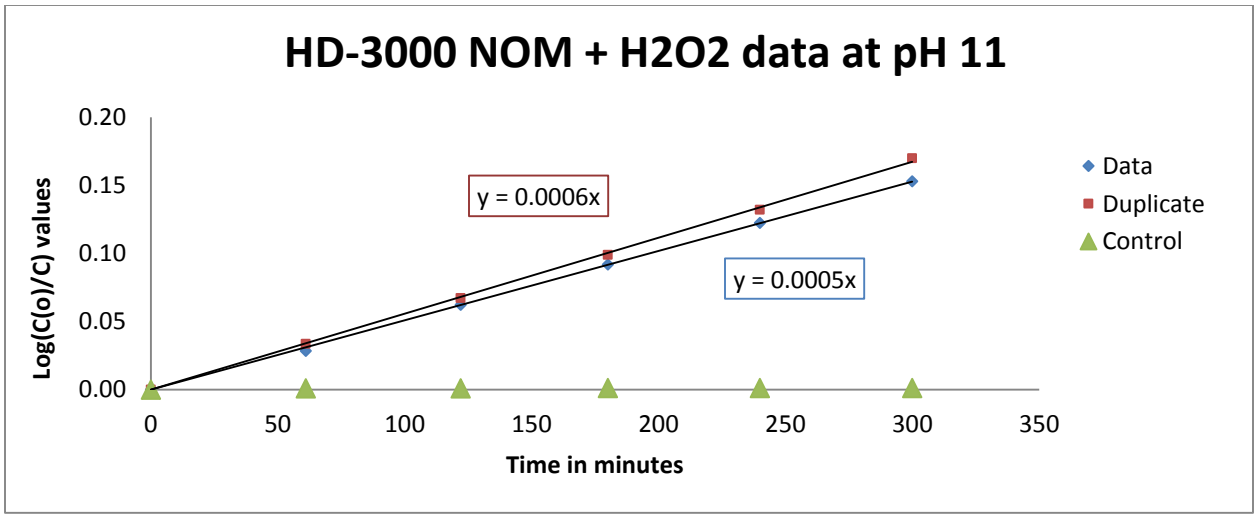
HD-3000 NOM + H2O2 data at pH 11
Log(C(o)/C) values
0.20
0.15
0.10
0.05
0.00
y = 0.0006x
y = 0.0005x
Data
Duplicate
Control
0
50
100
150
200
250
300
350
Time in minutes

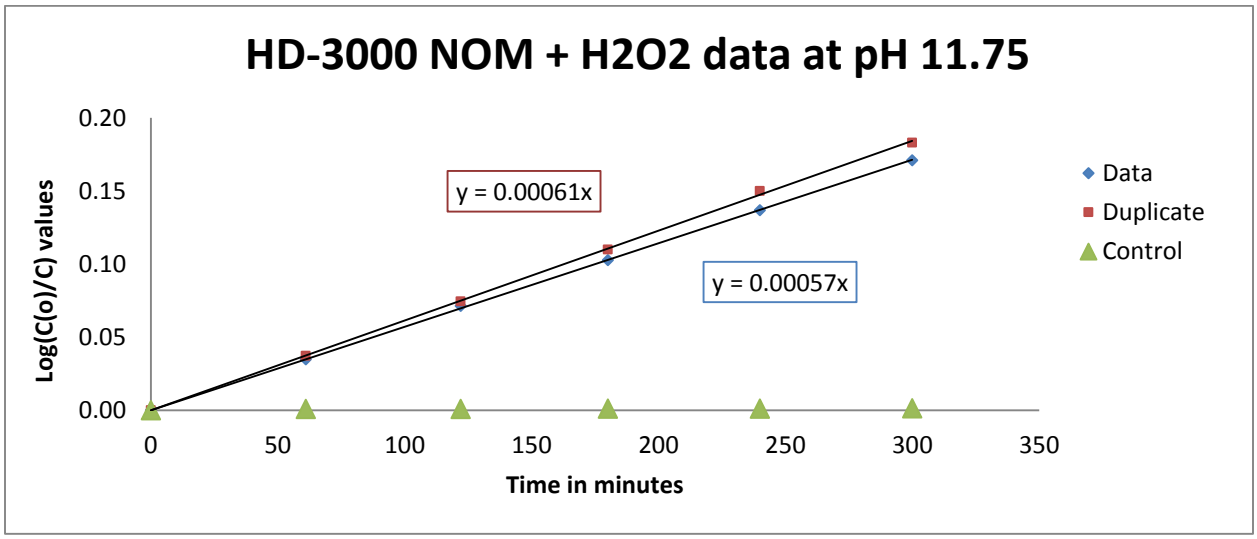
HD-3000 NOM + H2O2 data at pH 11.75
Log(C(o)/C) values
0.20
0.15
0.10
0.05
0.00
y = 0.00061x
y = 0.00057x
Data
Duplicate
Control
0
50
100
150
200
250
300
350
Time in minutes

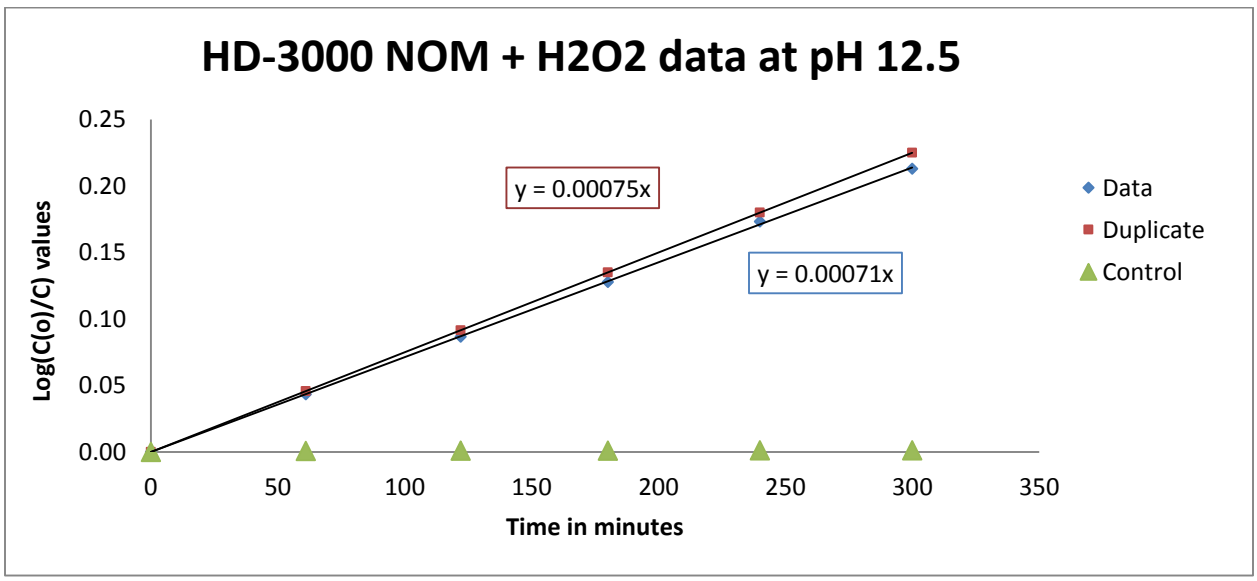
HD-3000 NOM + H2O2 data at pH 12.5
Log(C(o)/C) values
0.25
0.20
0.15
0.10
0.05
0.00
y = 0.00075x
y = 0.00071x
Data
Duplicate
Control
0
50
100
150
200
250
300
350
Time in minutes

A.6.1 K values of Virgin TN-5

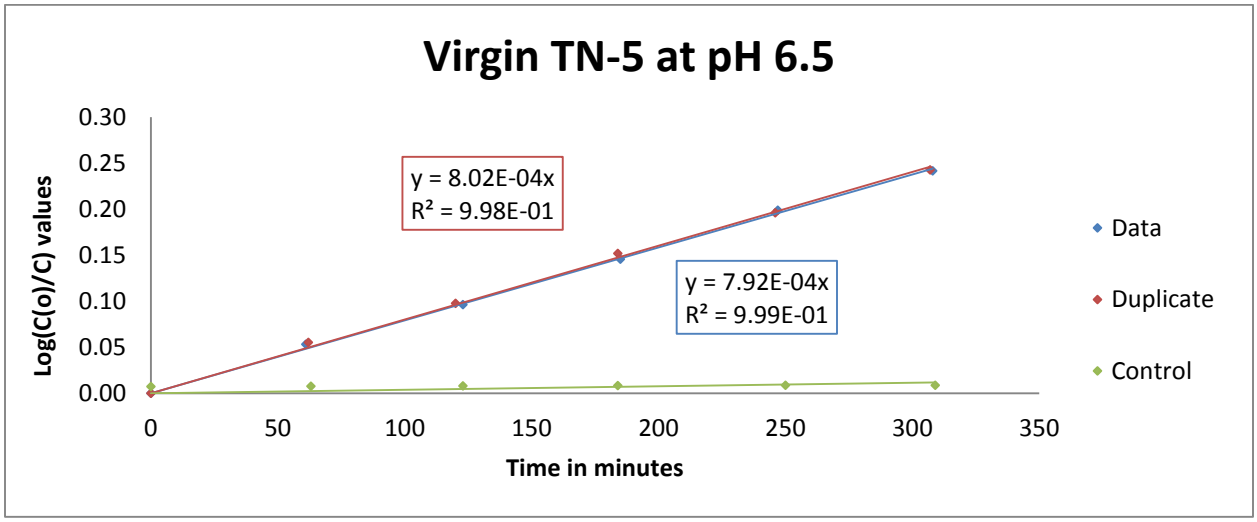

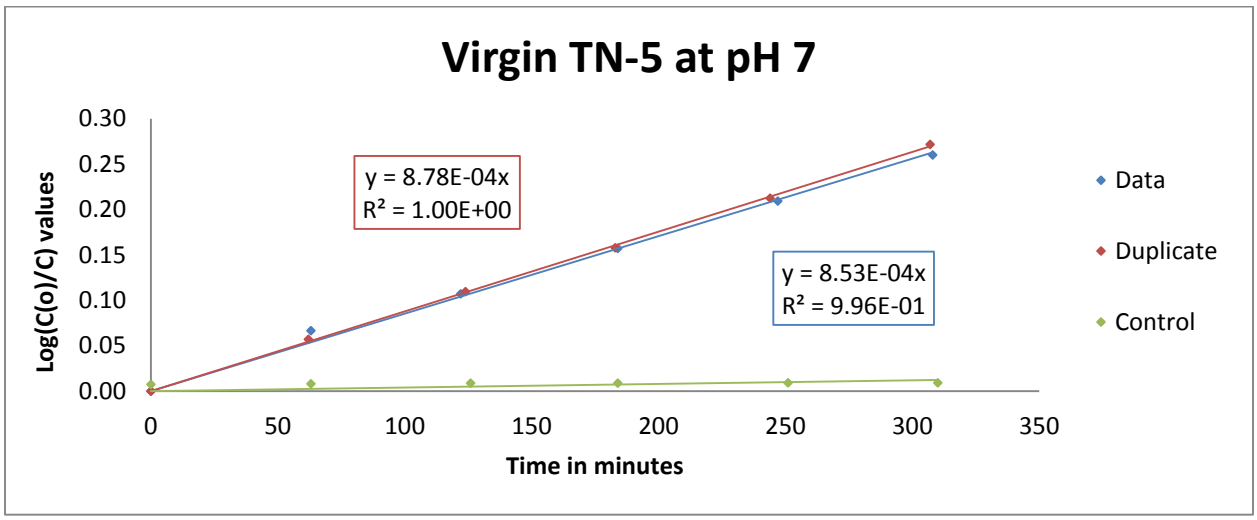

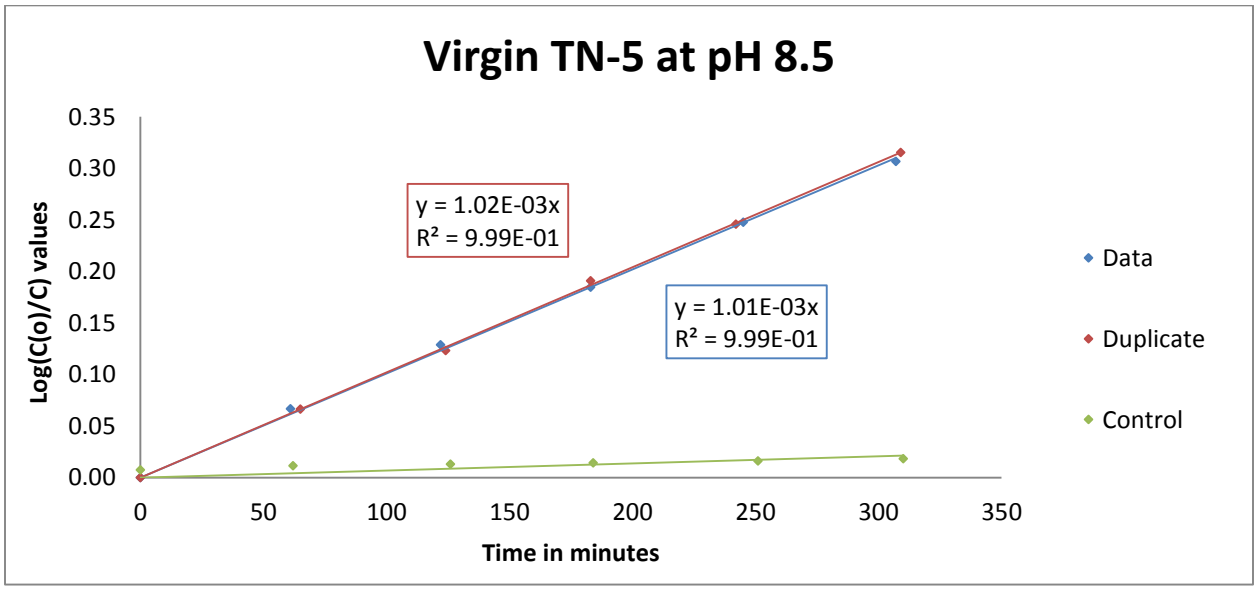

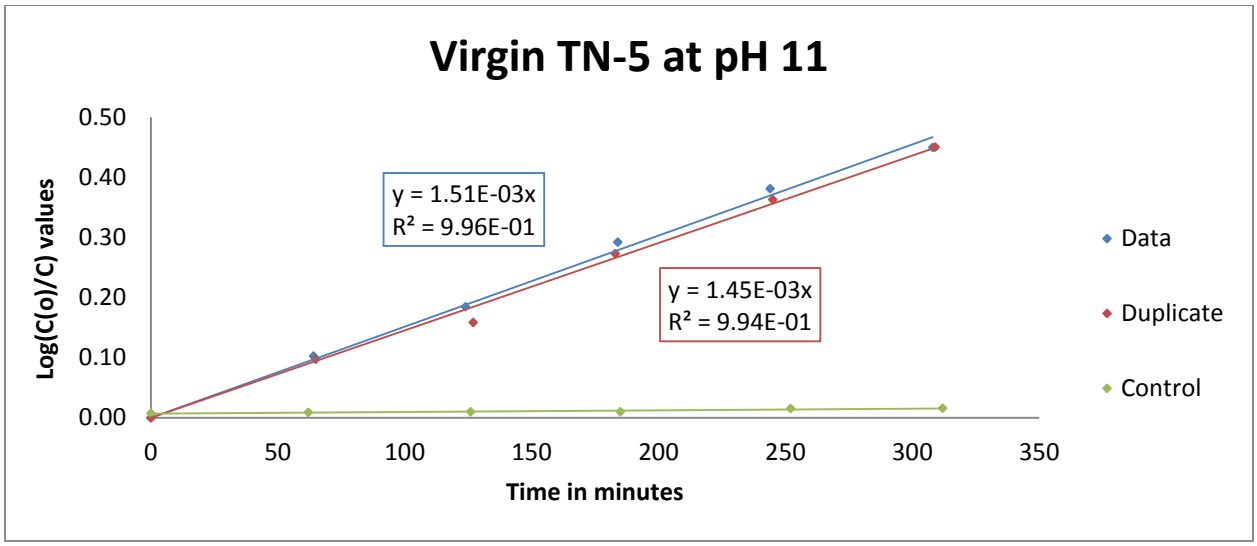
Virgin TN-5 at pH 11
Log(C(o)/C) values
0.50
0.40
0.30
0.20
0.10
0.00
y = 1.51E-03x
R² = 9.96E-01
y = 1.45E-03x
R² = 9.94E-01
0
50
100
150
200
250
300
350
Time in minutes
Data
Duplicate
Control

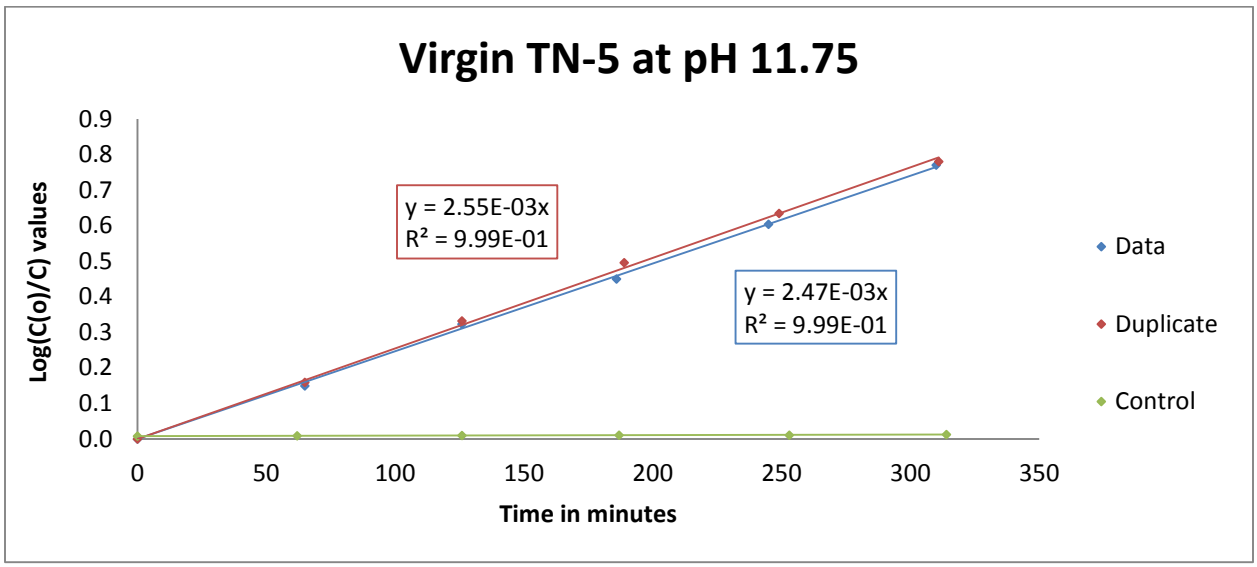
Virgin TN-5 at pH 11.75
Log(C(o)/C) values
0.9
0.8
0.7
0.6
0.5
0.4
0.3
0.2
0.1
0.0
y = 2.55E-03x
R² = 9.99E-01
y = 2.47E-03x
R² = 9.99E-01
0
50
100
150
200
250
300
350
Time in minutes
Data
Duplicate
Control

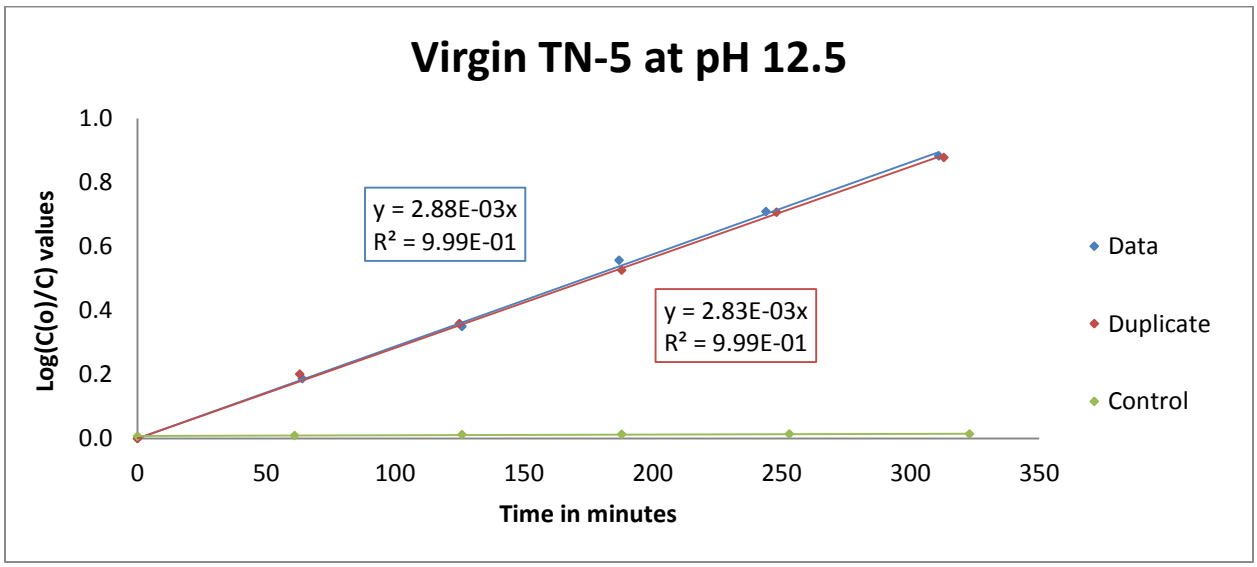
Virgin TN-5 at pH 12.5
Log(C(o)/C) values
1.0
0.8
0.6
0.4
0.2
0.0
y = 2.88E-03x
R² = 9.99E-01
y = 2.83E-03x
R² = 9.99E-01
0
50
100
150
200
250
300
350
Time in minutes
Data
Duplicate
Control

A.6.2 K values of TN-5 aged with NOM

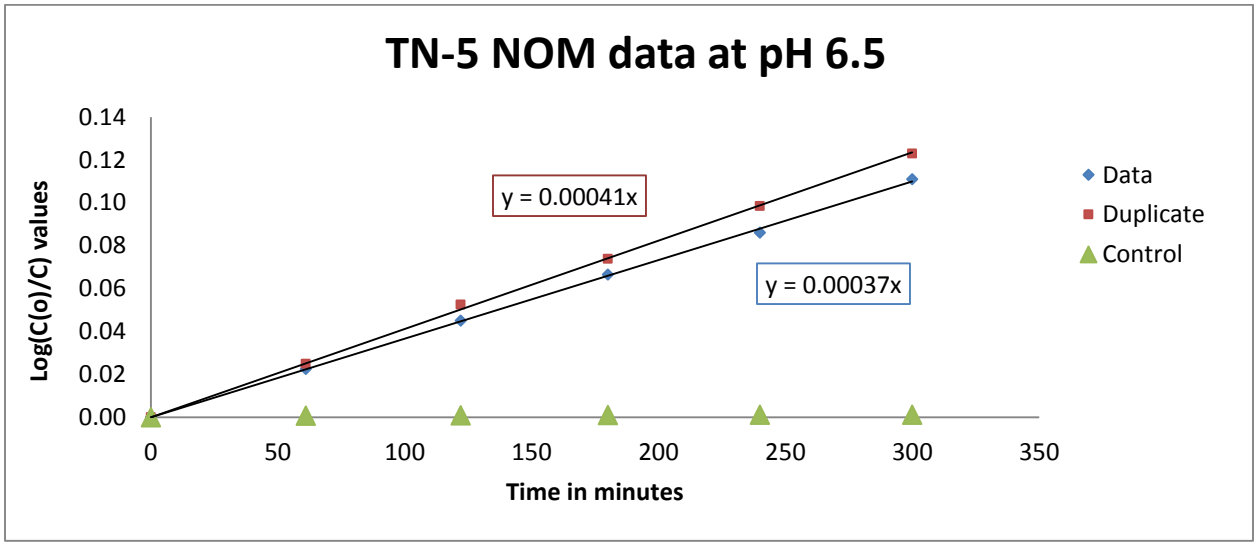

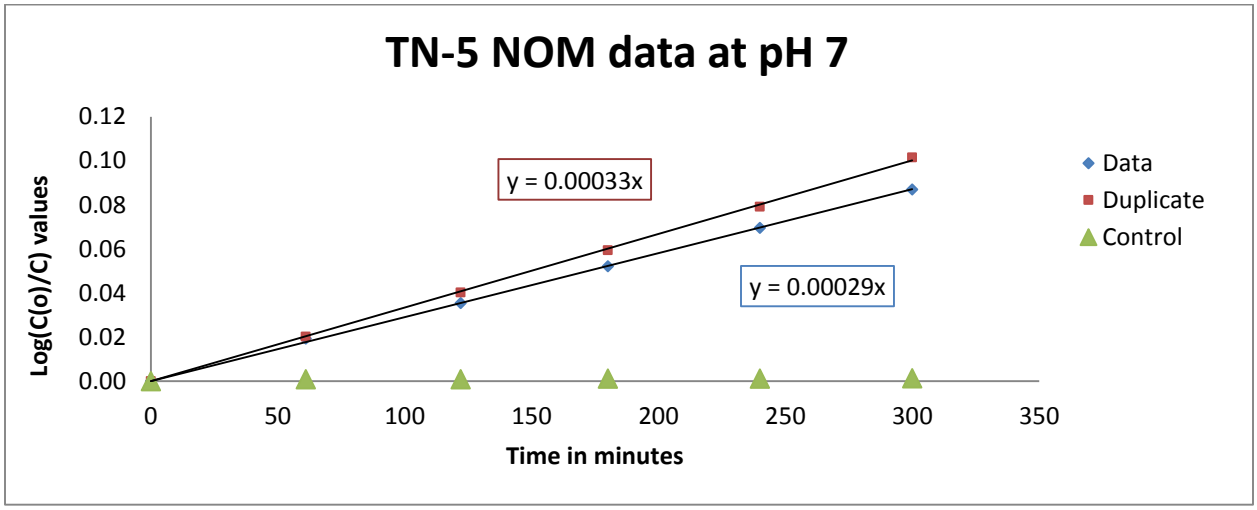

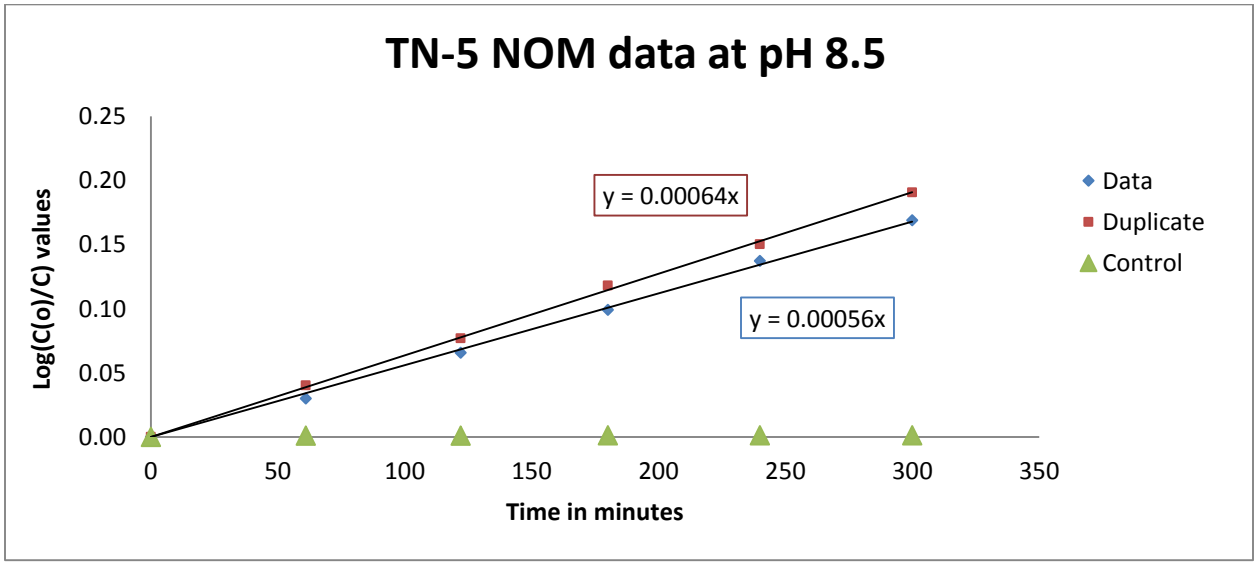

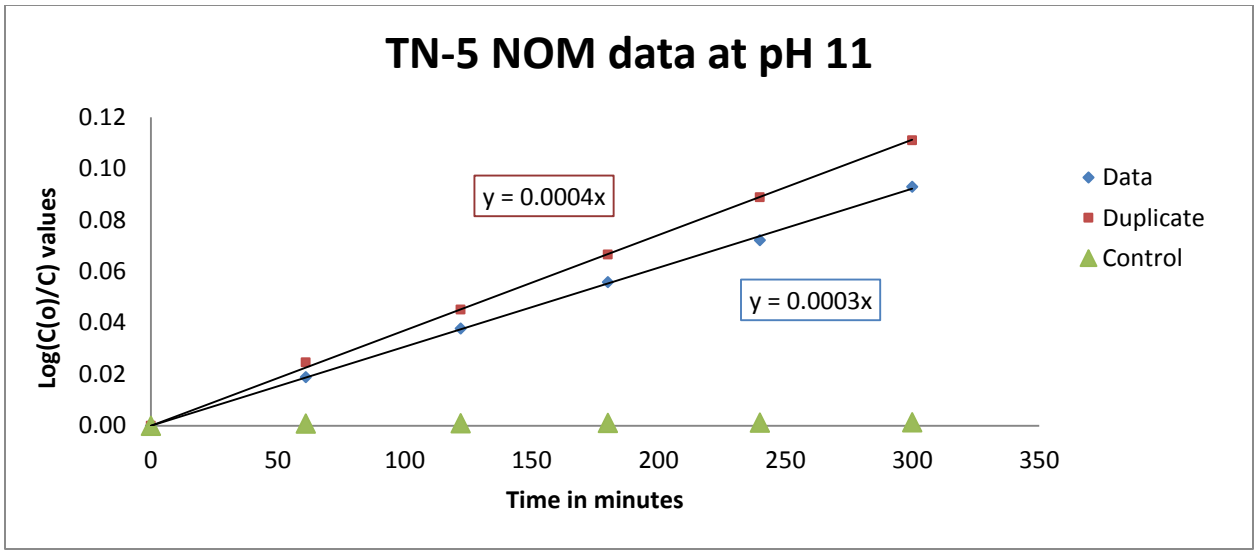
TN-5 NOM data at pH 11
Log(C(o)/C) values
0.12
0.10
0.08
0.06
0.04
0.02
0.00
y = 0.0004x
y = 0.0003x
Data
Duplicate
Control
0
50
100
150
200
250
300
350
Time in minutes

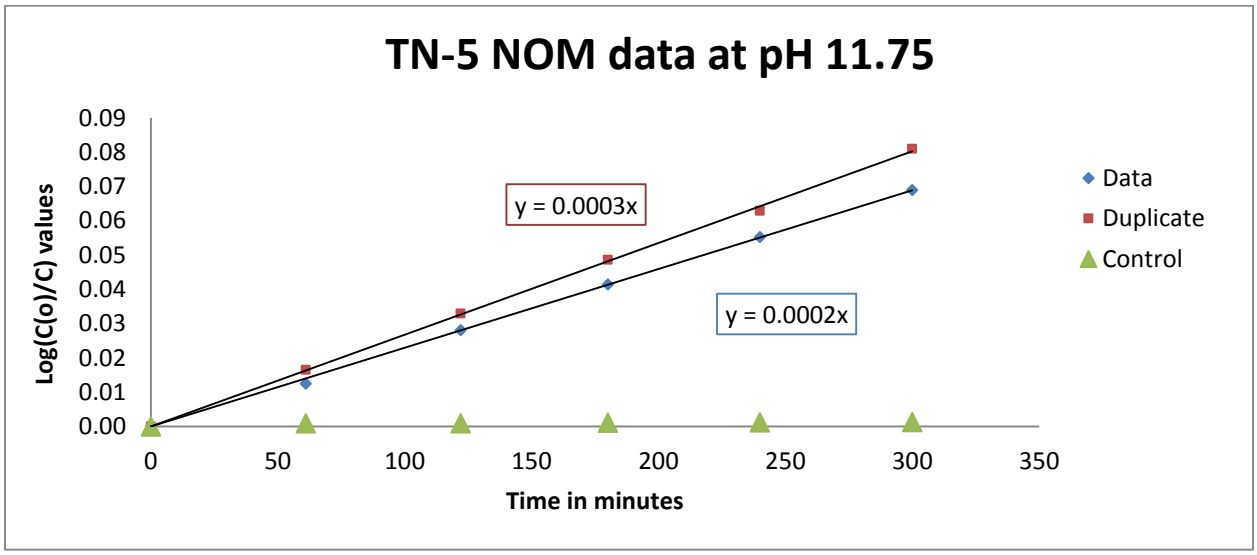
TN-5 NOM data at pH 11.75
Log(C(o)/C) values
0.09
0.08
0.07
0.06
0.05
0.04
0.03
0.02
0.01
0.00
y = 0.0003x
y = 0.0002x
Data
Duplicate
Control
0
50
100
150
200
250
300
350
Time in minutes

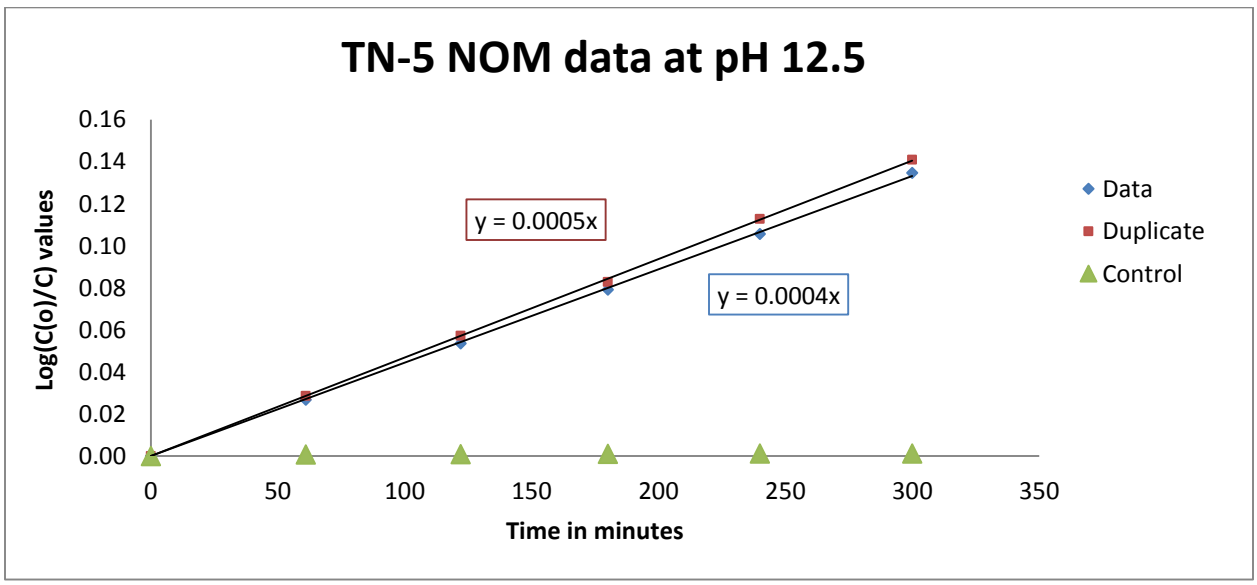
TN-5 NOM data at pH 12.5
Log(C(o)/C) values
0.16
0.14
0.12
0.10
0.08
0.06
0.04
0.02
0.00
y = 0.0005x
y = 0.0004x
Data
Duplicate
Control
0
50
100
150
200
250
300
350
Time in minutes

A.6.3 K values of TN-5 aged with NOM + H_2O_2

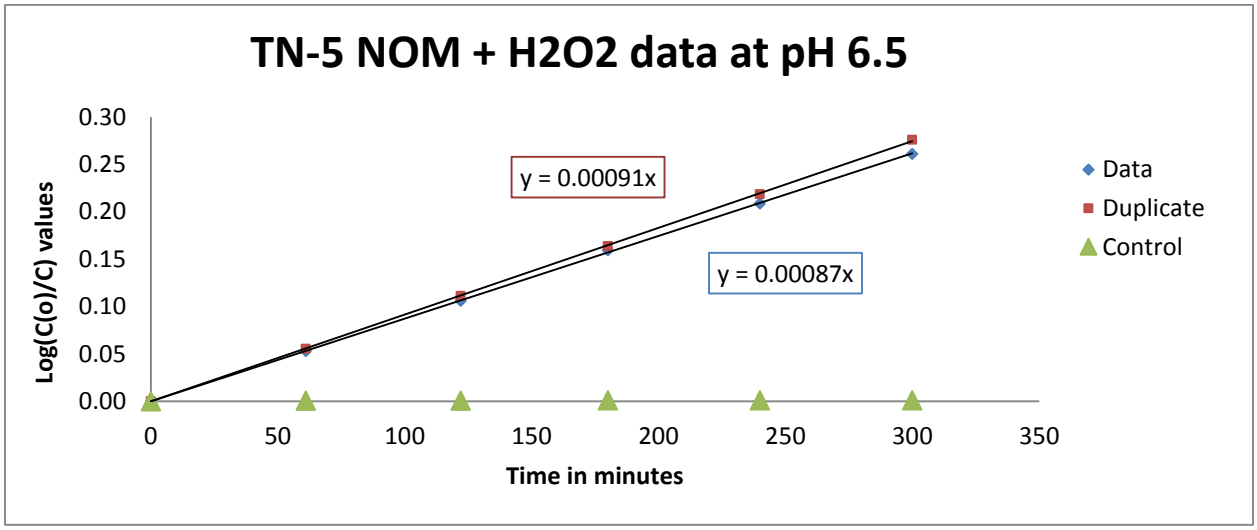

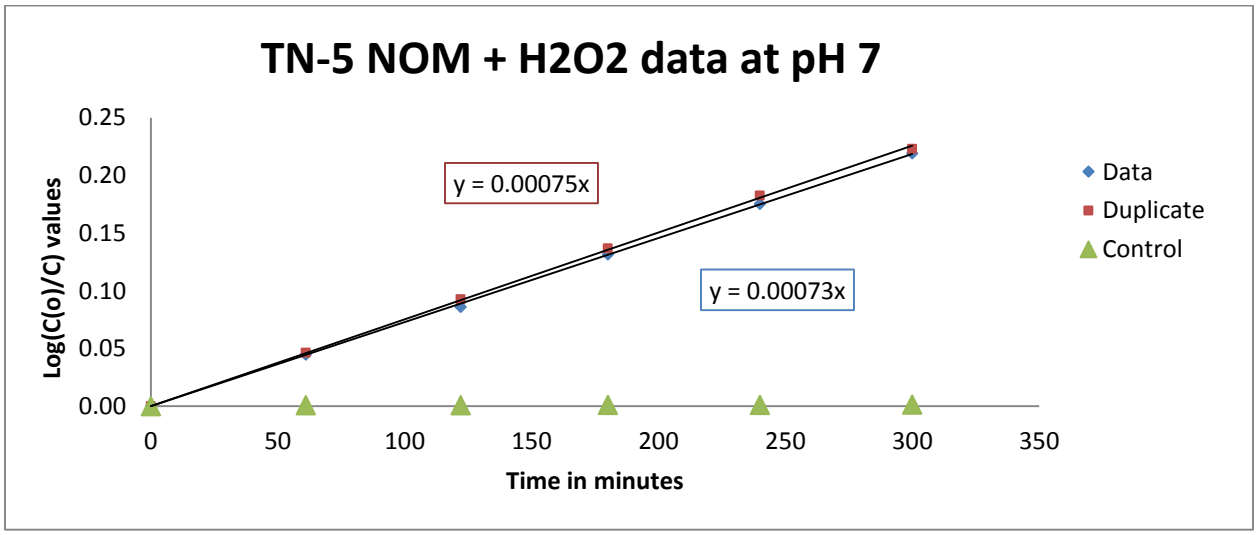

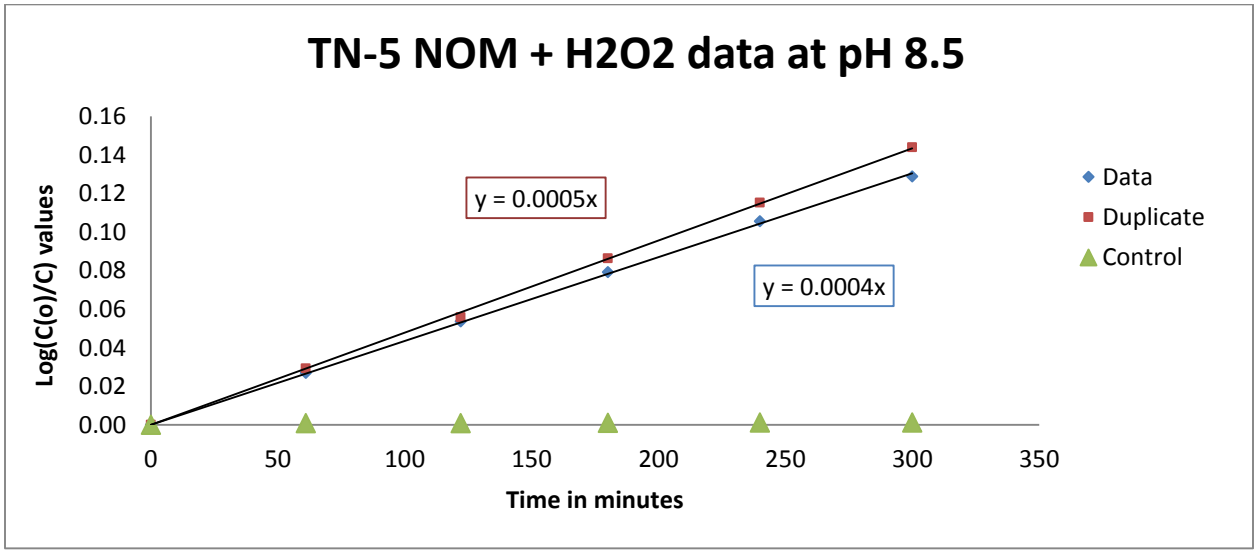

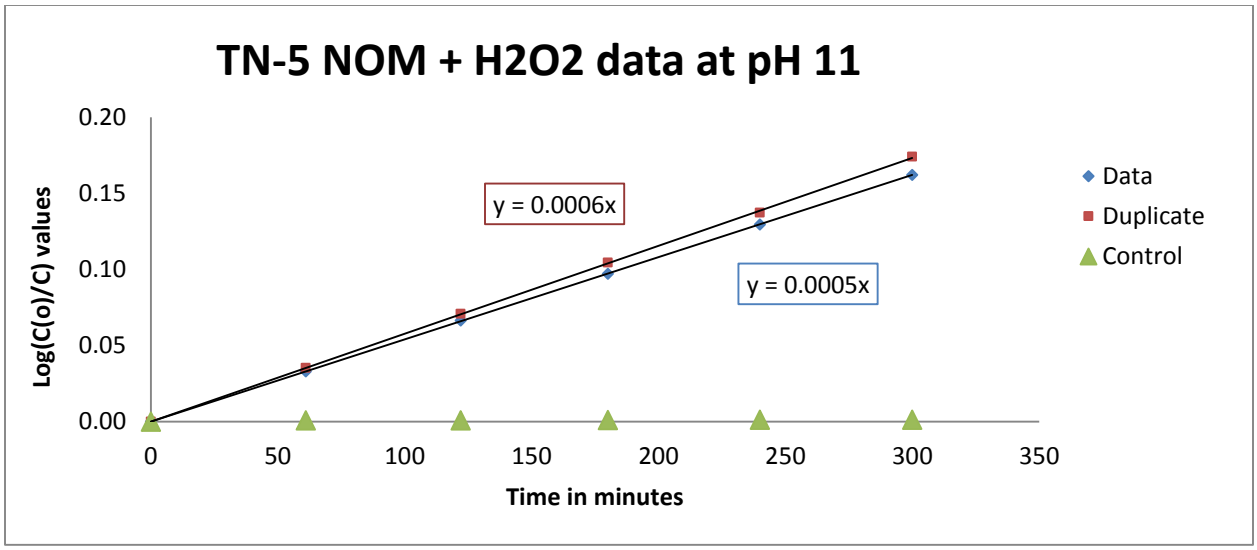
TN-5 NOM + H2O2 data at pH 11
Log(C(o)/C) values
0.20
0.15
0.10
0.05
0.00
y = 0.0006x
y = 0.0005x
Data
Duplicate
Control
0
50
100
150
200
250
300
350
Time in minutes

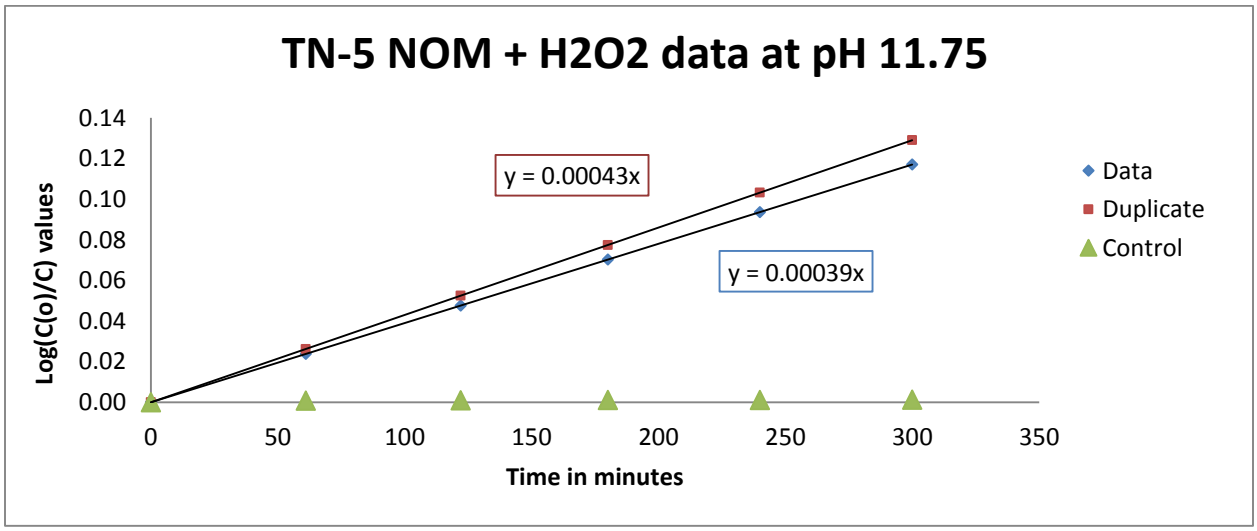
TN-5 NOM + H2O2 data at pH 11.75
Log(C(o)/C) values
0.14
0.12
0.10
0.08
0.06
0.04
0.02
0.00
y = 0.00043x
y = 0.00039x
Data
Duplicate
Control
0
50
100
150
200
250
300
350
Time in minutes

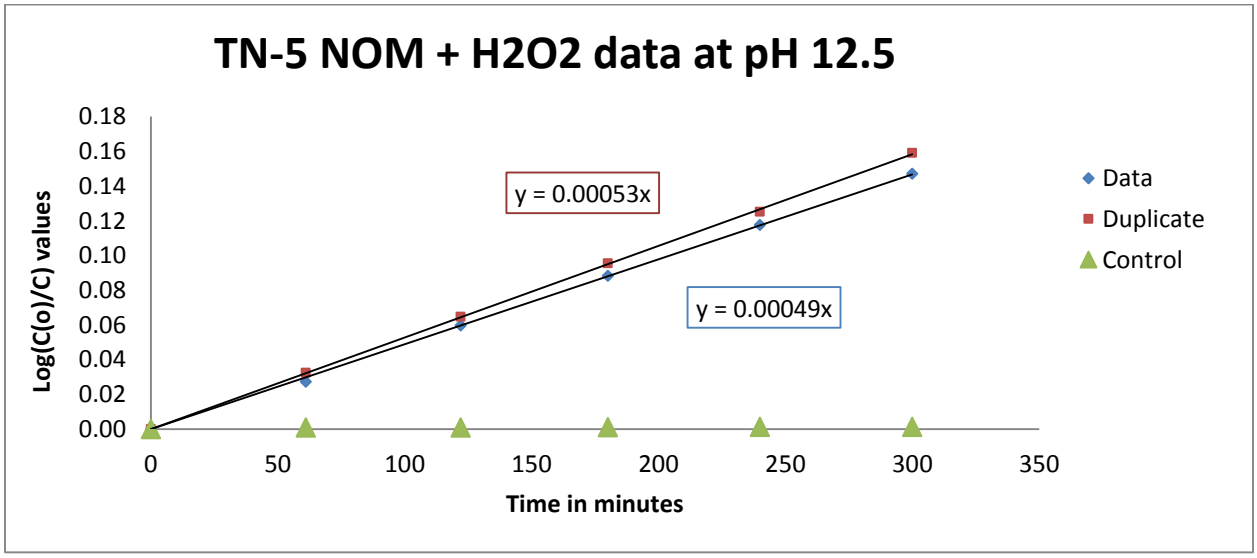
TN-5 NOM + H2O2 data at pH 12.5
Log(C(o)/C) values
0.18
0.16
0.14
0.12
0.10
0.08
0.06
0.04
0.02
0.00
y = 0.00053x
y = 0.00049x
Data
Duplicate
Control
0
50
100
150
200
250
300
350
Time in minutes

A.7.1 K values of GAC in week 3 of biofilm experiment

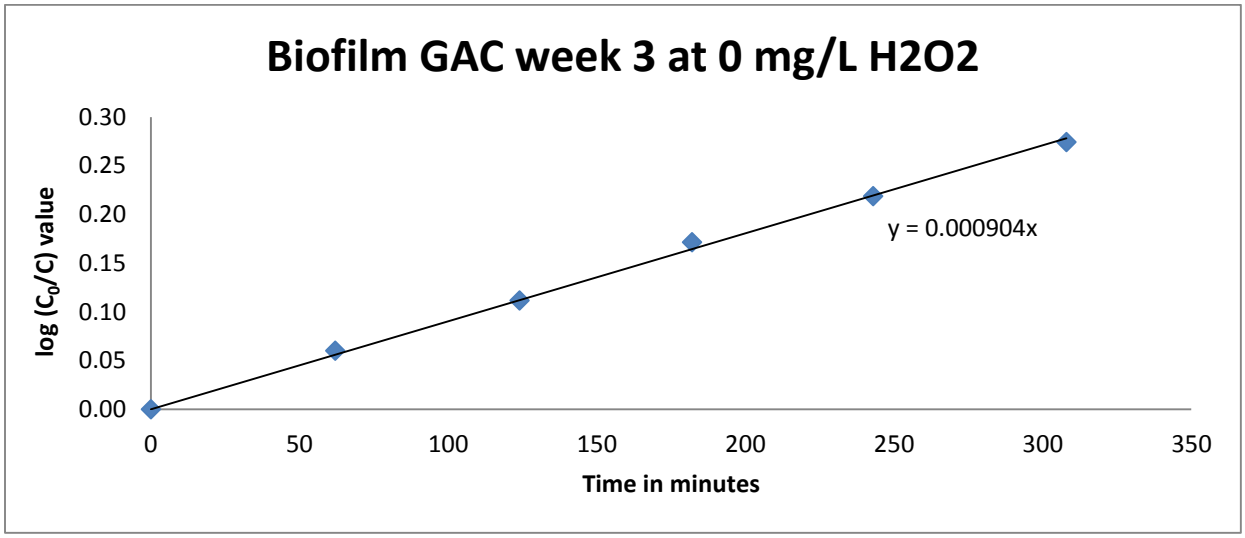

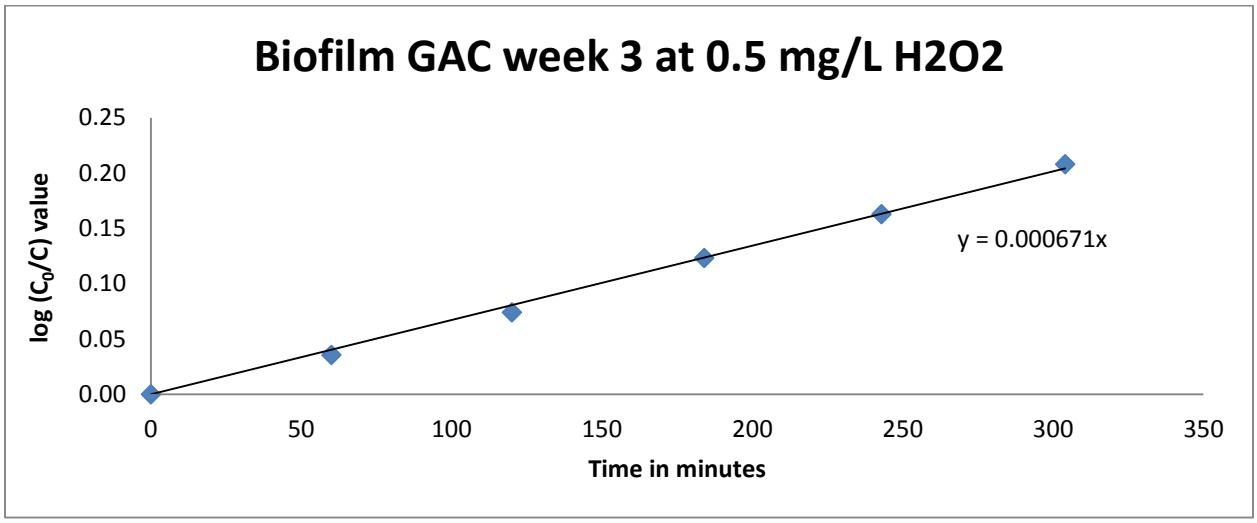

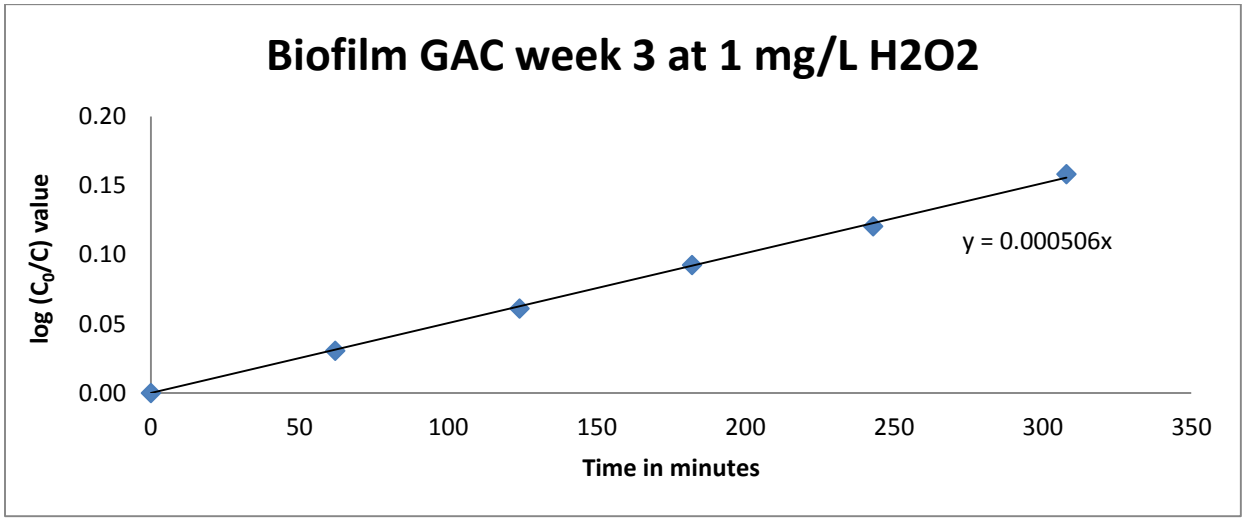

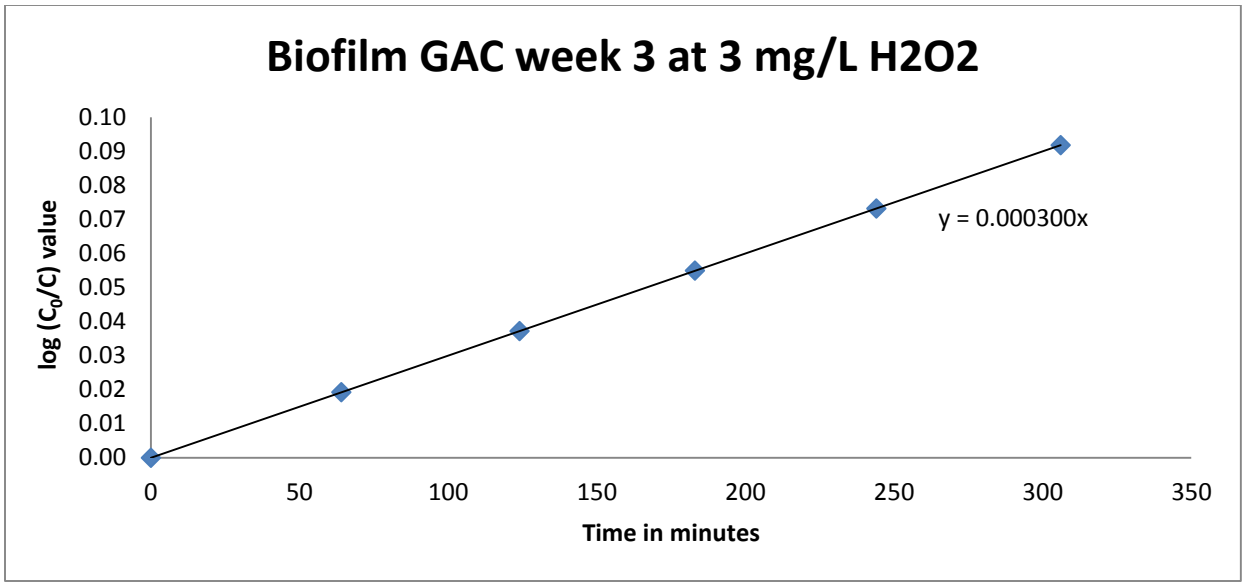
Biofilm GAC week 3 at 3 mg/L H2O2
log (C0/C) value
0.10
0.09
0.08
0.07
0.06
0.05
0.04
0.03
0.02
0.01
0.00
y = 0.000300x
0
50
100
150
200
250
300
350
Time in minutes

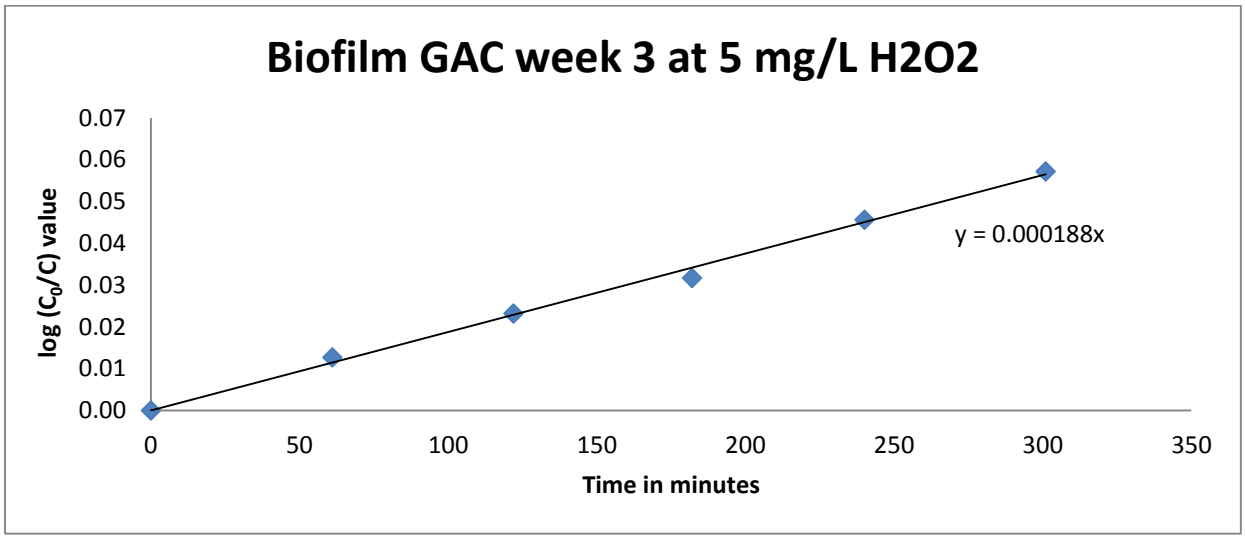
Biofilm GAC week 3 at 5 mg/L H2O2
log (C0/C) value
0.07
0.06
0.05
0.04
0.03
0.02
0.01
0.00
y = 0.000188x
0
50
100
150
200
250
300
350
Time in minutes

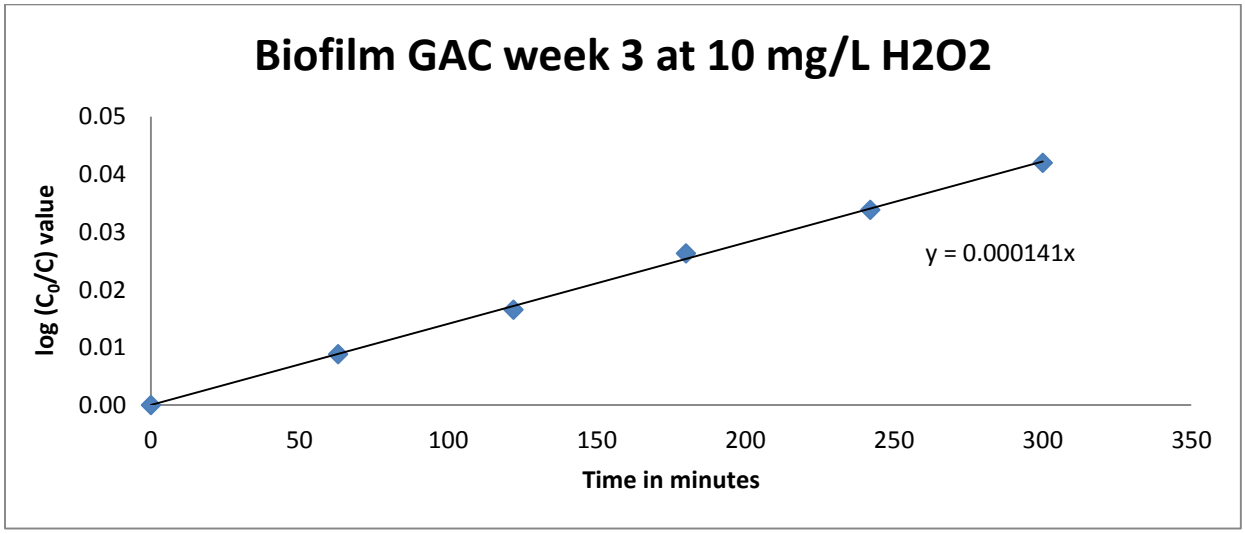
Biofilm GAC week 3 at 10 mg/L H2O2
log (C0/C) value
0.05
0.04
0.03
0.02
0.01
0.00
y = 0.000141x
0
50
100
150
200
250
300
350
Time in minutes

A.7.2 K values of GAC in week 10 of biofilm experiment

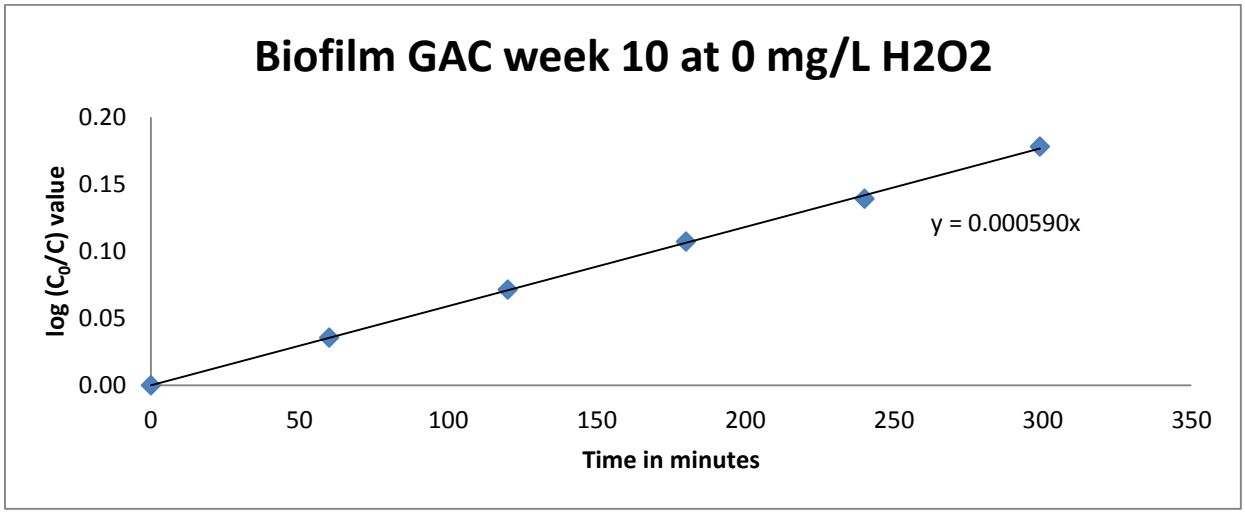

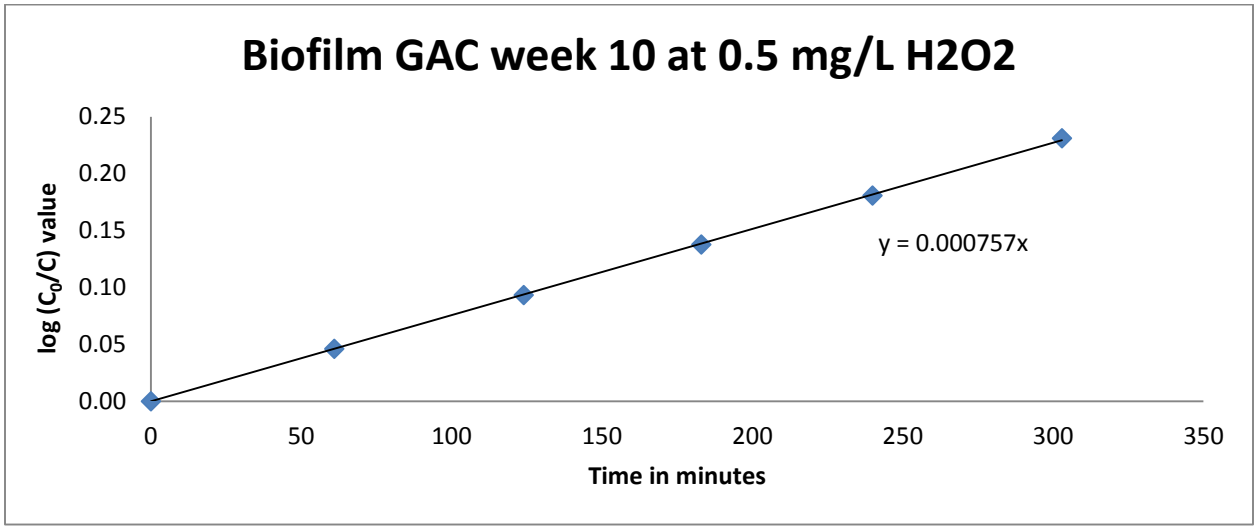

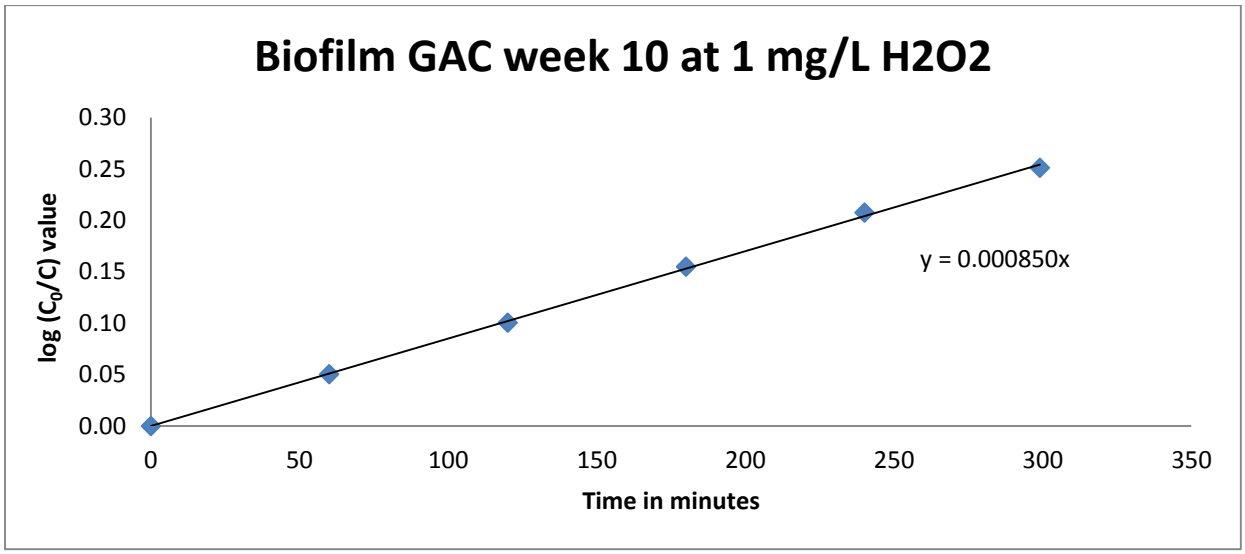

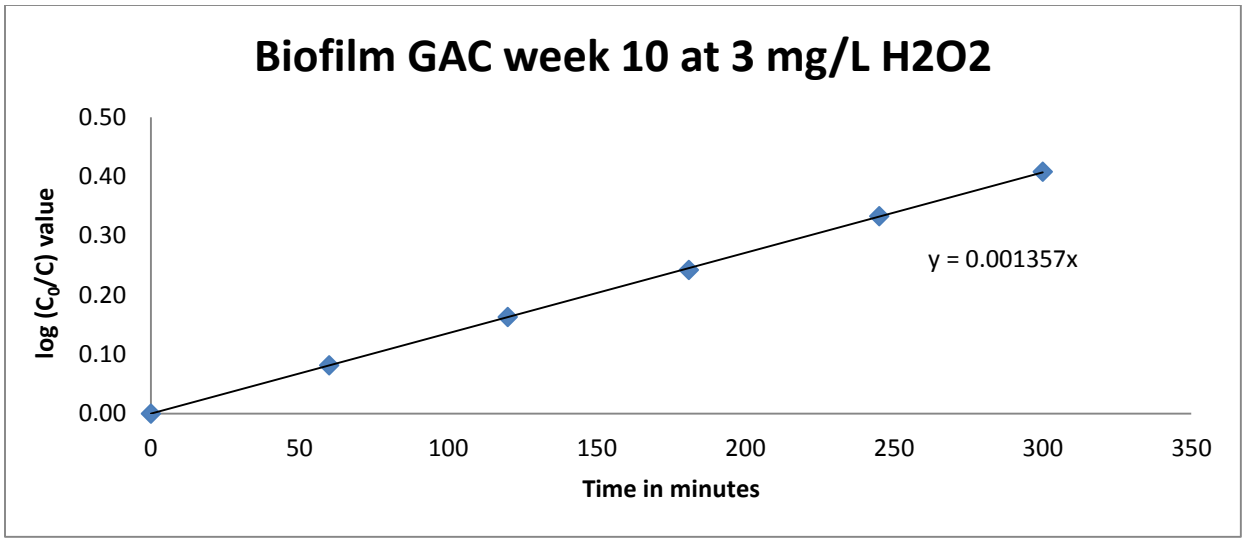
Biofilm GAC week 10 at 3 mg/L H2O2
log (C0/C) value
0.50
0.40
0.30
0.20
0.10
0.00
y = 0.001357x
0
50
100
150
200
250
300
350
Time in minutes

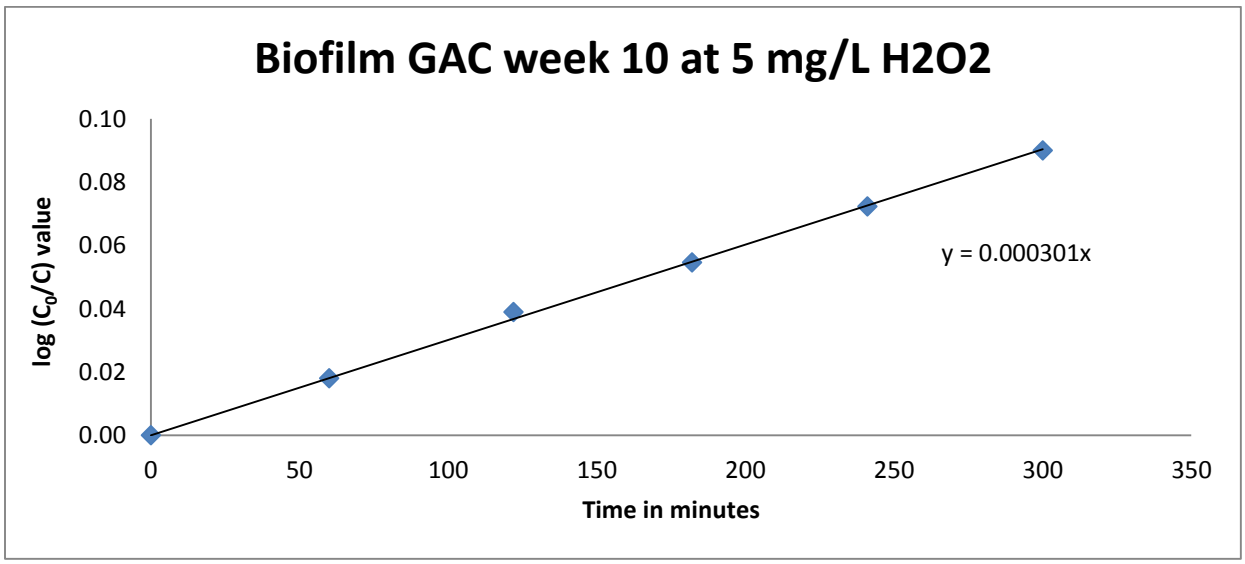
Biofilm GAC week 10 at 5 mg/L H2O2
log (C0/C) value
0.10
0.08
0.06
0.04
0.02
0.00
y = 0.000301x
0
50
100
150
200
250
300
350
Time in minutes

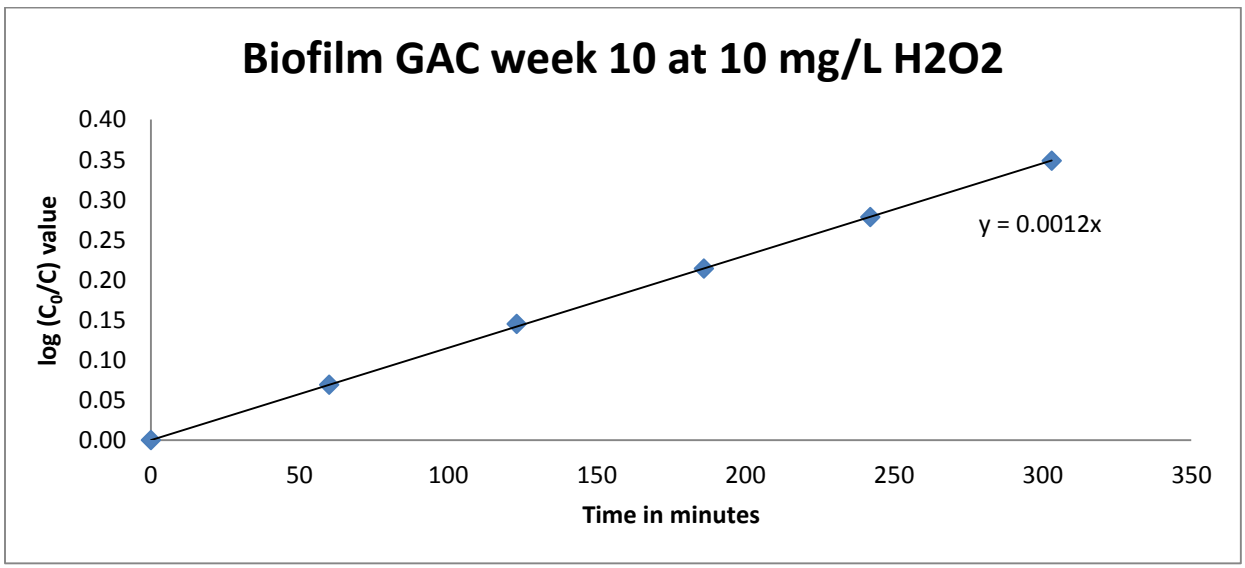
Biofilm GAC week 10 at 10 mg/L H2O2
log (C0/C) value
0.40
0.35
0.30
0.25
0.20
0.15
0.10
0.05
0.00
y = 0.0012x
0
50
100
150
200
250
300
350
Time in minutes

A.8.1 K values of Sand media in week 3 of biofilm experiment

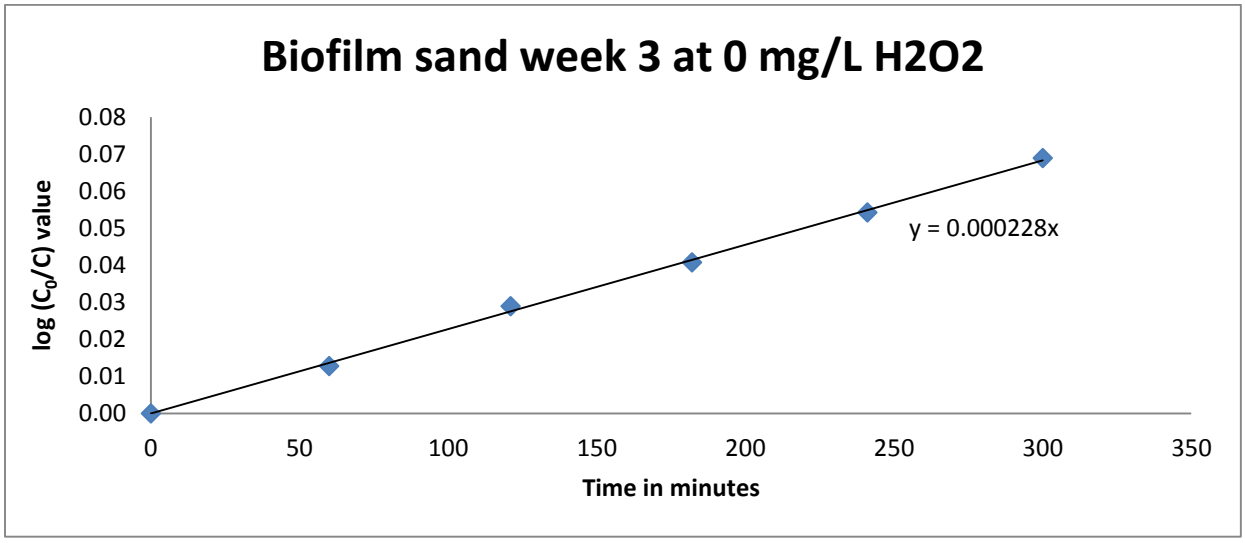

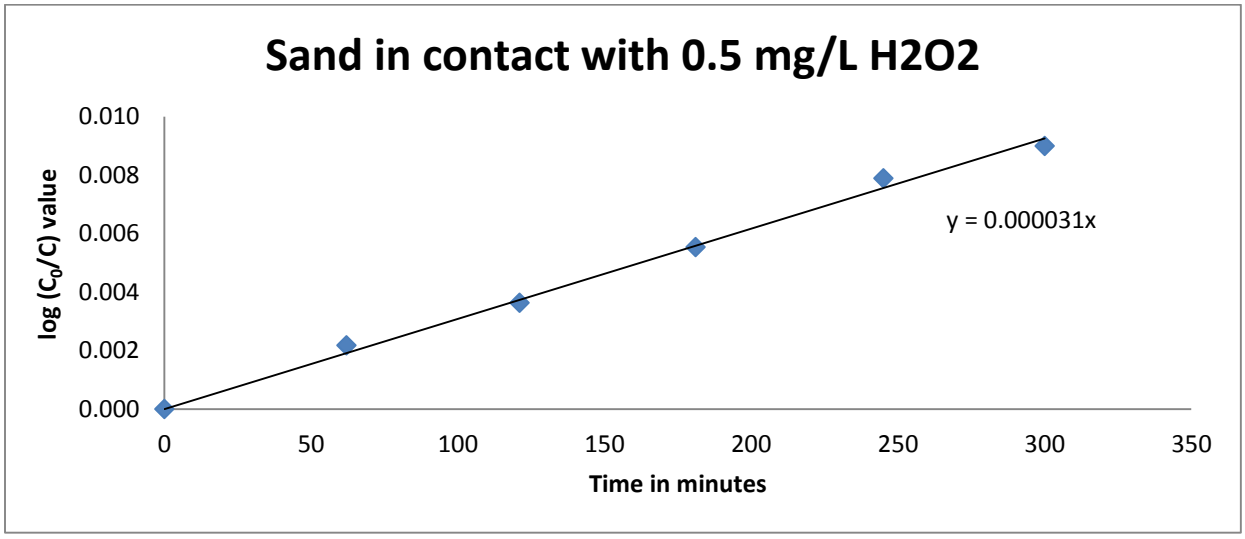

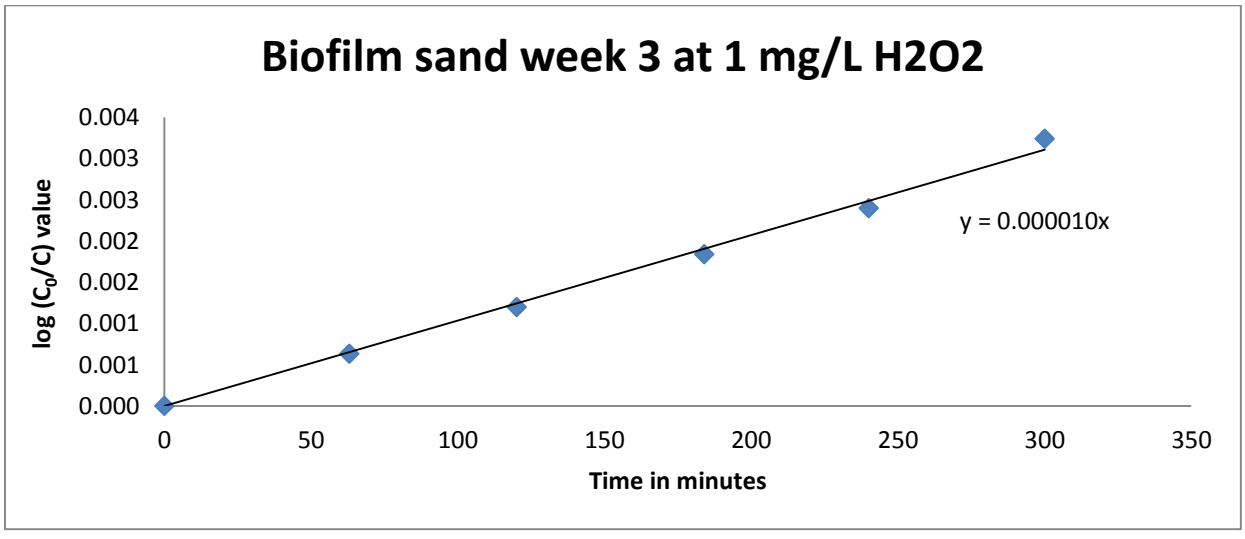

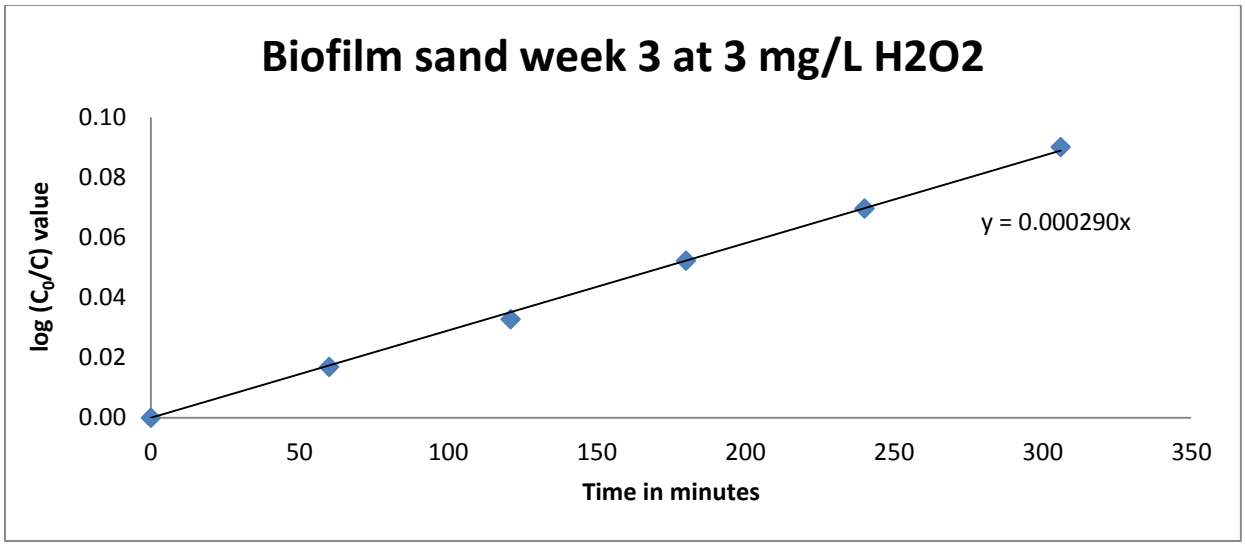
Biofilm sand week 3 at 3 mg/L H2O2
log (C0/C) value
0.10
0.08
0.06
0.04
0.02
0.00
y = 0.000290x
0
50
100
150
200
250
300
350
Time in minutes

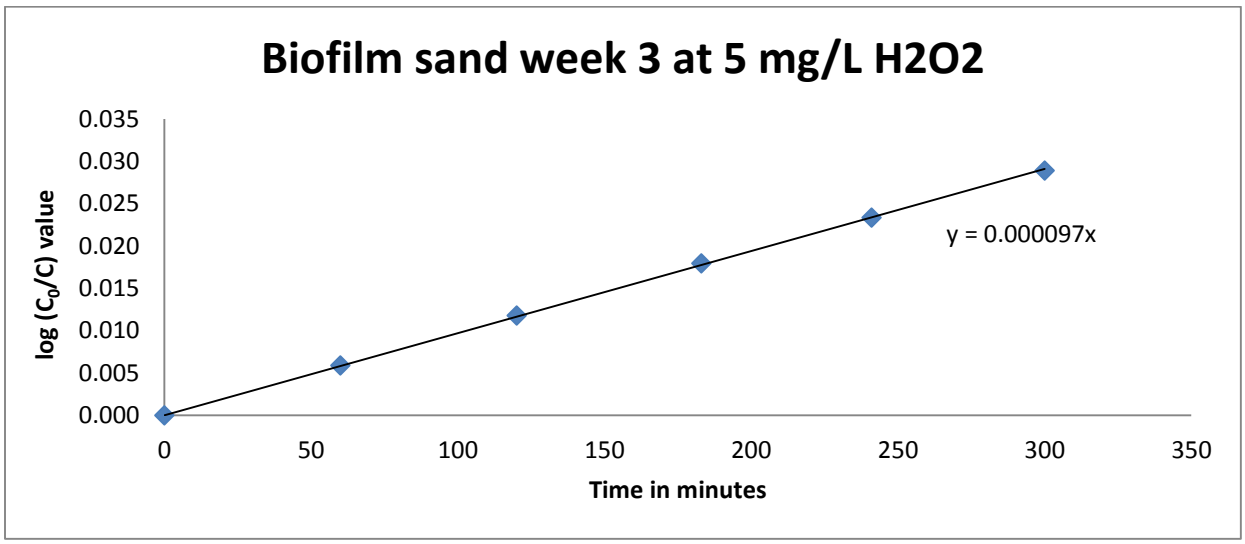
Biofilm sand week 3 at 5 mg/L H2O2
log (C0/C) value
0.035
0.030
0.025
0.020
0.015
0.010
0.005
0.000
y = 0.000097x
0
50
100
150
200
250
300
350
Time in minutes

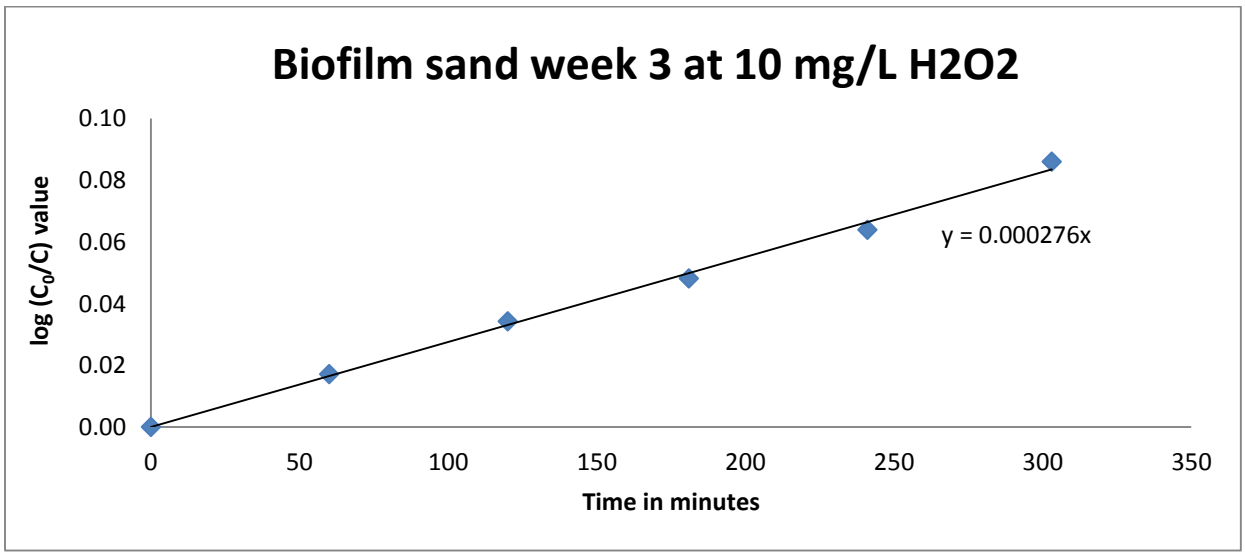
Biofilm sand week 3 at 10 mg/L H2O2
log (C0/C) value
0.10
0.08
0.06
0.04
0.02
0.00
y = 0.000276x
0
50
100
150
200
250
300
350
Time in minutes

A.8.2 K values of Sand media in week 10 of biofilm experiment

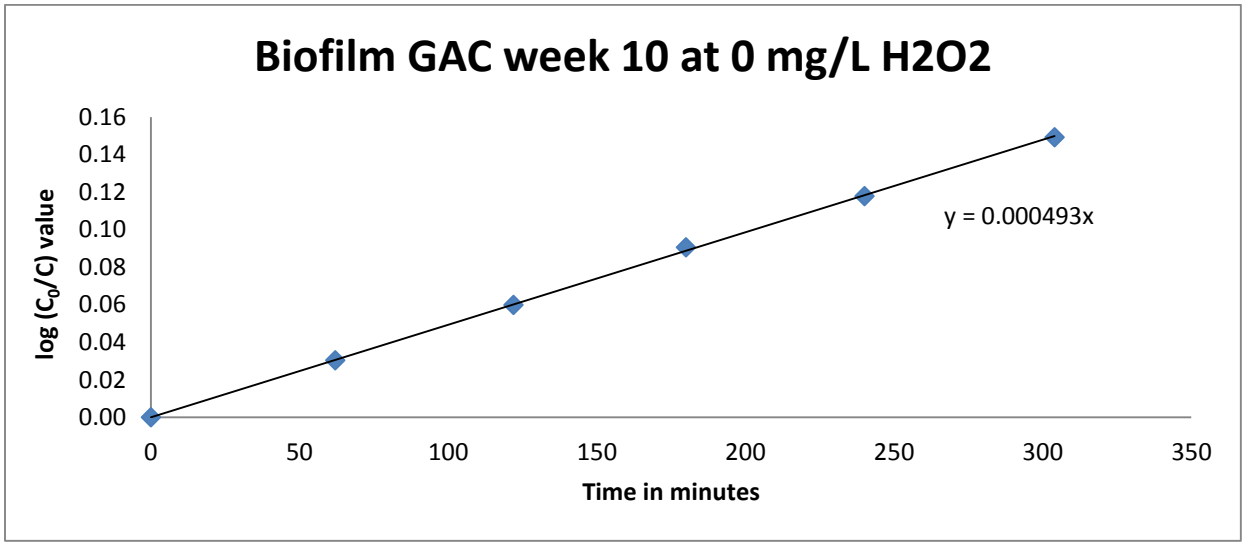

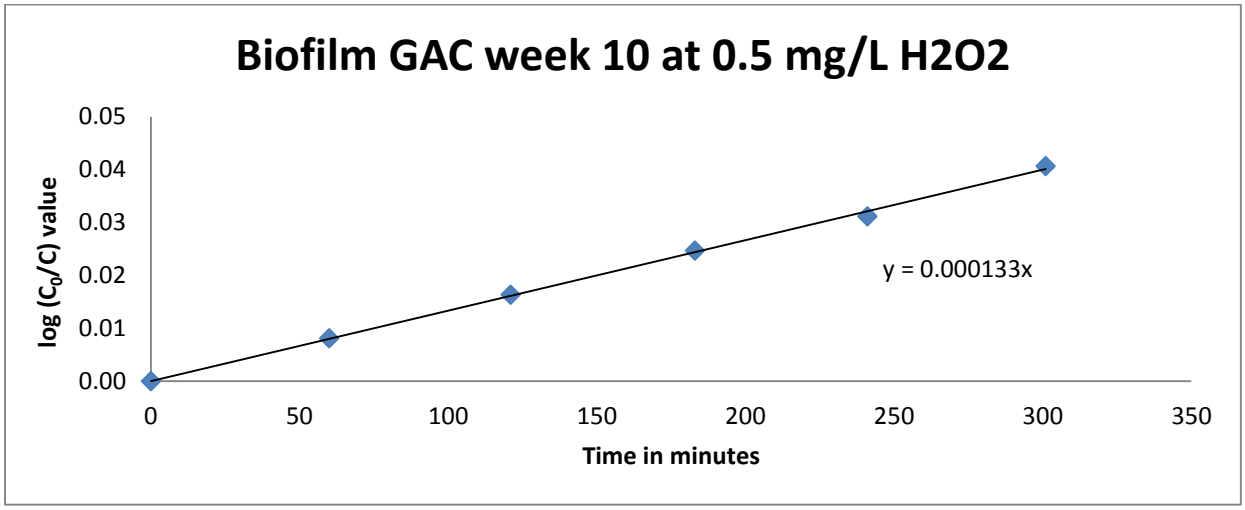

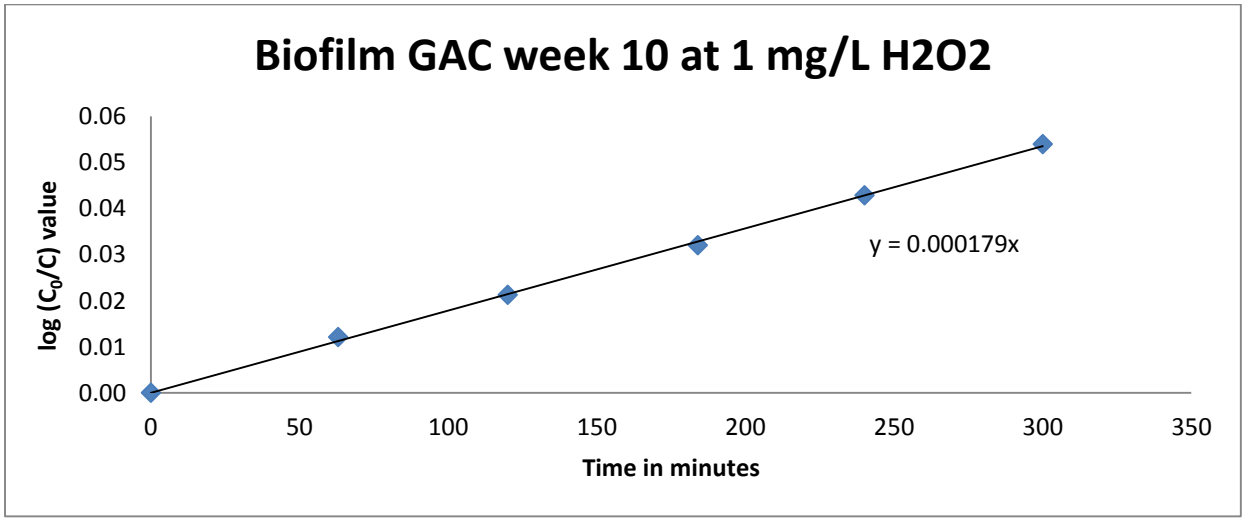

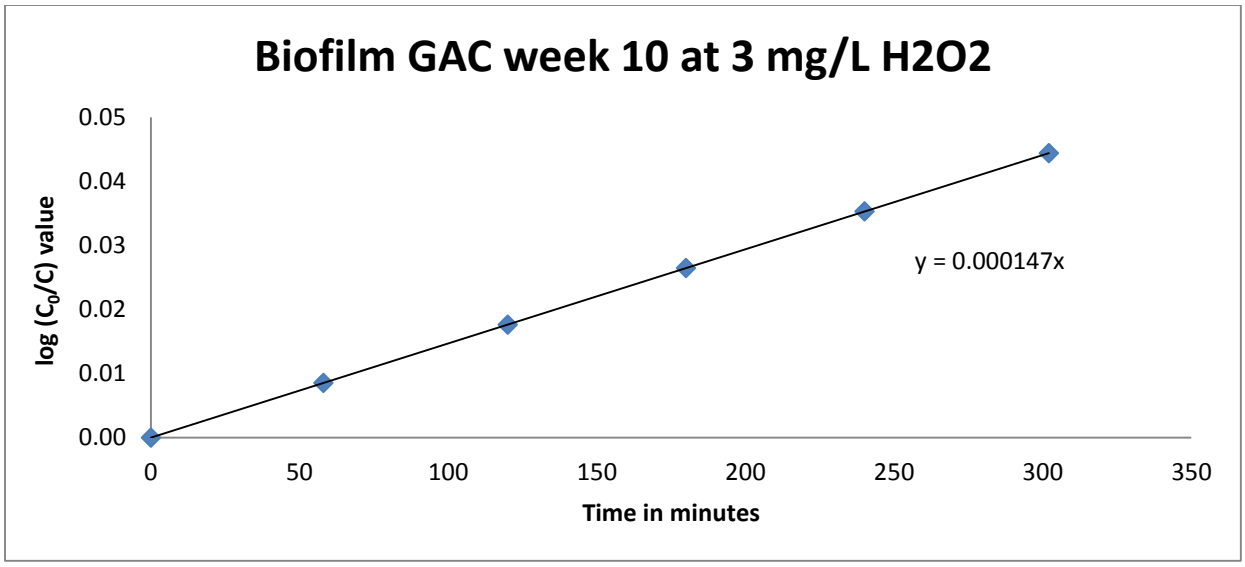
Biofilm GAC week 10 at 3 mg/L H2O2
log (C0/C) value
0.05
0.04
0.03
0.02
0.01
0.00
y = 0.000147x
0
50
100
150
200
250
300
350
Time in minutes

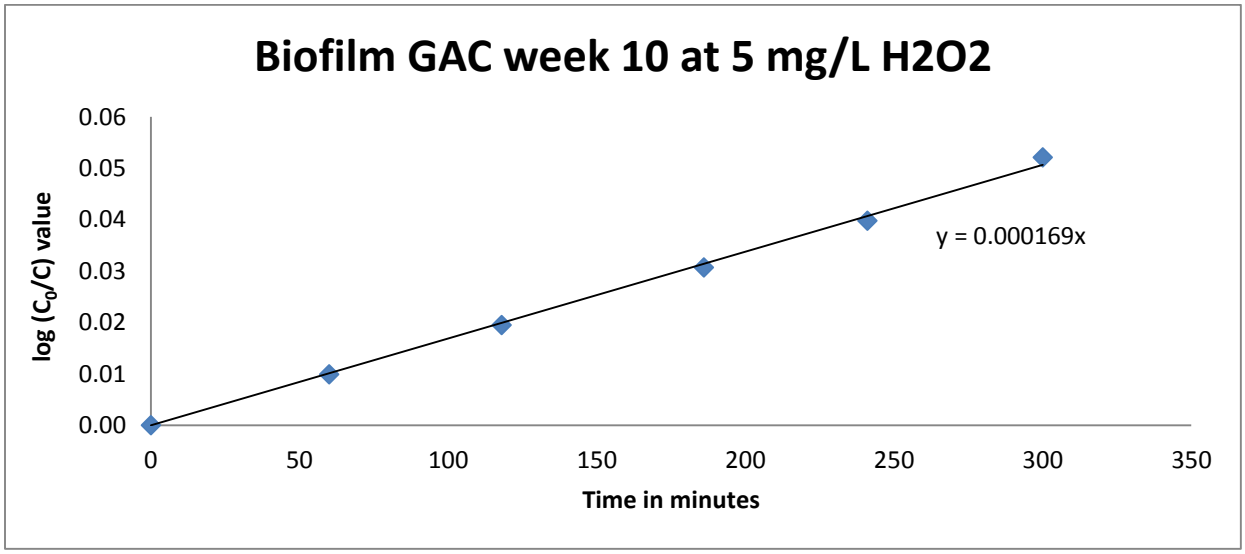
Biofilm GAC week 10 at 5 mg/L H2O2
log (C0/C) value
0.06
0.05
0.04
0.03
0.02
0.01
0.00
y = 0.000169x
0
50
100
150
200
250
300
350
Time in minutes

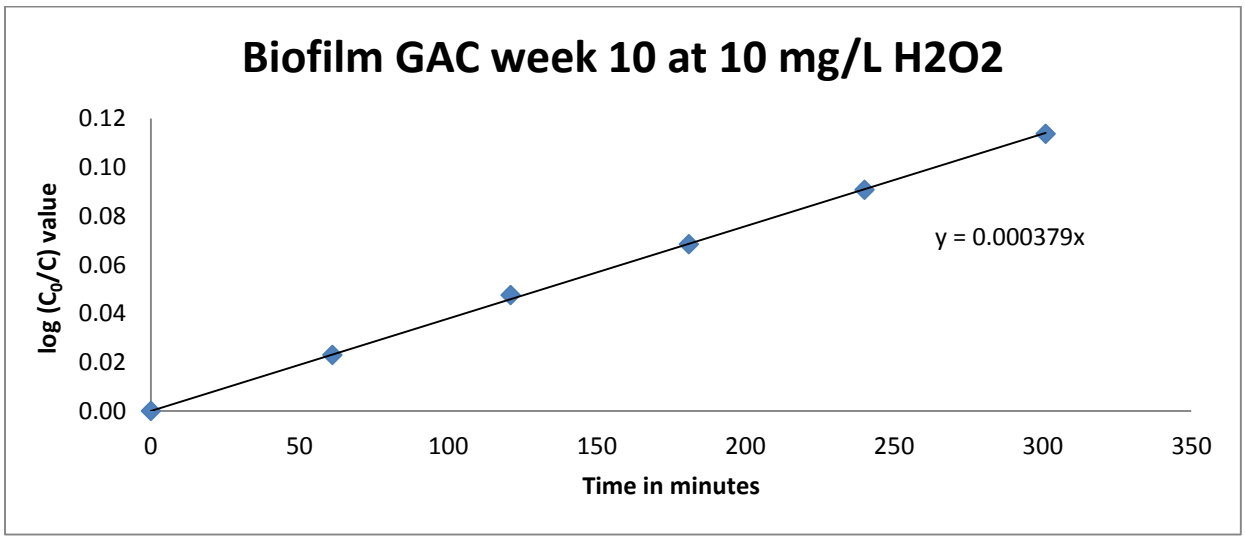
Biofilm GAC week 10 at 10 mg/L H2O2
log (C0/C) value
0.12
0.10
0.08
0.06
0.04
0.02
0.00
y = 0.000379x
0
50
100
150
200
250
300
350
Time in minutes

Appendix B

SOP for hydrogen peroxide analysis

One or more steps in this SOP (see below for specific directions) must be performed in (circle):

Fume hood biosafety cabinet

other_____

Safety Equipment Required: acid-resistant gloves (nitrile gloves)

(safety glasses) UV-filtering safety glasses

face-shield (lab coat)

other_____(Acid Gloves)_____

Biosafety Certificate Required: yes (no)

Principle:

The analysis of H_2O_2 at concentrations as low as 1 μM is conveniently done by determining the yield of I_3^- formed when H_2O_2 reacts with KI in a buffered solution containing ammonium molybdate as a catalyst. The method consists of mixing equal weights of solutions A and B, followed by the addition of the H_2O_2 solution. The absorbance of the resulting solution is measured at 351.0 nm in a 1, 2, or 4 cm cuvette, depending on the $[H_2O_2]$, to achieve an absorbance of approximately 0.9. The blank absorbance was determined by subtracting the absorbance of water from the absorbance of an equiweight mixture of A and B, assuming the difference was due to adventitious I_3^-.

Safety Notes and Operational Concerns:

Handle solutions carefully (nitrile gloves at all times).

Equipment and Materials:

Reagents:

1. Potassium iodide (KI), ACS Grade
2. Sodium Hydroxide (NaOH), ACS Grade
3. Ammonuim molybdate tetrahydrate, ACS Grade
4. Potassium hydrogen phtalate (KHP), ACS, 99.95% - 100.05%

Method Outline:

1. Prepare solution A: Dissolve 16.5 g of KI (potassium iodide), 0.5 g of NaOH, and 0.05 g of ammonium molybdate tetrahydrate in 250 mL of Milli-Q water. Store in an amber bottle in the dark to inhibit the oxidation of I^-. Stir the solution for approximately 10 minutes. Solution A should have a pH of 12.8.
2. Prepare solution B: Dissolve 5g of KHP (potassium hydrogen phthalate) in 250 mL of Milli-Q water. Solution B should have a pH of 4.03.
3. Add 2.5 mL Solution A and 2.5 mL Solution B to a 23 mL glass vial.
4. Add varying amounts of sample to obtain an absorbance of about 0.9. Example:

Concentration	Sample volume	Total volume
10 mg/L	0.5 mL	5.5 mL
5 mg/L	1.5 mL	6.5 mL
1 mg/L	2.0 mL	7.0 mL

5. Wait 1 min. Read at 351 nm using 1-cm quartz cuvette.
6. Create blank readings by adding varying amounts of Milli-Q water to reagents. Create zero readings by adding varying amounts of sample water to reagents. [NOTE: must create a blank and zero reading for each dilution used].
7. Calculate the resulting H_2O_2 concentration using:
   Mg/L H_2O_2 = [A_{351} × (total vol./sample vol.) × 34 g/mol × 1000 mg/g] / 26450 $M^{-1}m^{-1}$

Waste Disposal and Clean-up:

Samples can be disposed of down drain. Whenever flushing used reagents or chemical waste it is best to flush with cold tap water to prevent a reaction with another reagent that is subsequently flushed down the same drain.

SOP for ATP analysis (Lumin-ultra test kit instructions)

Principle:

LuminUltra's test kits are based on the measurement of ATP, which is a direct and interference-free indicator of total living biomass. ATP is measured using the firefly luciferase assay, where a sample containing ATP is introduced to a solution containing the enzyme Luciferase, which naturally occurs in the tails of fireflies, to produce light. The light is detected in a luminometer as Relative Light Units (RLU).

$$ATP + O_2 + \text{luciferin} \xrightarrow{Mg++\,Luciferase} AMP + PPi + \text{oxyluciferin light}$$

The DSA test kit utilizes a 10-minute dilution-based analysis to measure a parameter called Total ATP (tATP™). When measured on surfaces or in deposits, tATP represents the accumulation of sessile biomass on process equipment and therefore can indicate the presence of or potential for microbiological corrosion.

Equipments and Materials:

Reagents:

LuminaseTM Dropper (Lu-5mL) Luciferase Enzyme Reagent, 5mL

UltraCheckTM 1 Dropper (UC1-2.5mL) 1 ng ATP/mL Standard, 2.5mL

UltraLyseTM 7 Bottle (UL7-125mL) tATP Extraction Reagent, 125mL

UltraLuteTM Bottle (ULu-250mL) tATP Dilution Reagent, 250mL

LumiSolveTM Bottle (LS-30mL) Swab Wetting Reagent, 30mL

Method:

Step 1 – UltraCheck 1 Calibration

The UltraCheck 1 (UC1) Calibration converts luminometer RLU values into actual ATP concentrations. Perform one UltraCheck 1 calibration per day or for each set of samples analyzed at the same time. Be sure that Luminase is allowed to reach ambient temperature prior to use.
PROCEDURE: Add 2 drops (100µL) of UltraCheck 1 and 2 drops (100µL) of Luminase to a new 12x55mm test tube (the Assay Tube), swirl gently five times, immediately insert into the luminometer and measure. Record RLU-UC1 for use in final calculations.

Step 2 – Sample Preparation

The DSA test kit provides three options to collect and prepare samples:
A. Surface Swab – A measured area of the surface to be tested is swabbed to collect microbial particles. ATP is then extracted and measured from the swab.
B. Measured Deposit – A deposit is collected and a precise mass or volume is measured. ATP is then extracted and measured from the deposit.
C. Biofilm Collector – A biofilm collection device (e.g. corrosion coupon) in directly immersed into UltraLyse 7 to extract and measure ATP.
Choose from any one of methods A, B or C, and then proceed to Step 3 (tATP Analysis). In general, option B is preferred as it is the most quantitative.

Step 3 – DSA tATPTM Analysis

In this step we add 5 ml of Ultralyse 7 to the measured sample media in step 2. The DSA Total ATP (tATP) analysis measures all ATP within a sample, including ATP from living cells in addition to ATP that has been released from dead cells.
3.1 – INCUBATION
Allow at least 5 minutes for incubation of the Extraction Tube to proceeding to 3.2.

3.2 – DILUTION
Use a micropipettor to transfer 1mL from the Extraction Tube to a new 17x100mm test tube and add 9mL of UltraLute. Cap and invert three times to mix. This new tube is called the Dilution Tube.

3.3 – ASSAY
Using the micropipettor, transfer 100µL from the Dilution Tube to a new 12x55mm test tube (the Assay Tube), add 2 drops (100µL) of Luminase, swirl gently five times, immediately insert into the luminometer and measure. Record RLUtATP for use in final calculations.

Calculations:

For Deposit sample: $tATP\ (pg/g) = RLU_{tATP} / RLU_{UC1} \times 50{,}000 / m_{sample}\ (g)$

For water sample: $cATP\ (pg/g) = RLU_{cATP} / RLU_{UC1} \times 10{,}000 / v_{sample}\ (mL)$

Appendix C

Spectrophotometer details:

Agilent 8453 instrument
Light Source: Deuterium Lamp
Wavelenth Range: 370 – 1100 nm range
Wavelenth interval: 1.09 nm
Integration Time: 0.5 sec

Table 5: Lower limit of UV transmission for common solvents

Lower Limit	Solvent
180 – 195 nm	Sulfuric Acid, (96%) Water, Acetonitrile
200 – 210 nm	Cyclohexane, n-Hexane, Glycerol 2,2,4-Trimethyl Pentane, Methanol
210 - 220 nm	n-Butyl Acohol, Isopropyl alcohol, Cyclohexane, Ethyl ether
245 - 260 nm	Chloroform, Ethyl Acetate, Methyl Formate
265 - 275 nm	Carbon Terachloride, Dimethyl Sulfoxide, Dimethyl Formamide, Acetic Acid
280 – 290 nm	Benzene, Toluene, m-Xylene
300 nm	Pyridine, Acetone, Carbon disulfide